Deniss Brodņevs

ANALYSIS OF THE PERFORMANCE OF CELLULAR MOBILE NETWORKS FOR THE REMOTE-CONTROL SYSTEMS OF UNMANNED AERIAL VEHICLES

Doctoral Thesis

RIGA TECHNICAL UNIVERSITY

Faculty of Mechanical Engineering, Transport and Aeronautics
Institute of Aeronautics

Deniss Brodņevs

Doctoral Student of the Study Programme "Transport"

ANALYSIS OF THE PERFORMANCE OF CELLULAR MOBILE NETWORKS FOR THE REMOTE-CONTROL SYSTEMS OF UNMANNED AERIAL VEHICLES

Doctoral Thesis

Scientific supervisor
Professor *Dr. habil. sc. ing.*
VITĀLIJS PAVELKO

Riga 2021

Brodnevs D. Analysis of the performance of cellular mobile networks for the remote-control systems of unmanned aerial vehicles. Doctoral Thesis.

Published accordingly to the decision of Promotion Council No. P-22 of 26 February 2021, Minutes No. 04030-9.12.1/4.

DOCTORAL THESIS PROPOSED TO RIGA TECHNICAL UNIVERSITY FOR THE PROMOTION TO THE SCIENTIFIC DEGREE OF DOCTOR OF SCIENCE

To be granted the scientific degree of Doctor of Science (Ph. D.), the present Doctoral Thesis has been submitted for the defence at the open meeting of RTU Promotion Council on 17 December 2021 at 13.00 at the Faculty of Mechanical engineering, transport and aeronautics of Riga Technical University, 6B Kipsala Street, Room 204.

OFFICIAL REVIEWERS

Professor Dr. habil. sc. ing. Volodymyr Kharchenko
National Aviation University, Ukraine

Professor Dr. sc. ing. Ramunas Kikutis
Vilnius Gediminas Technical University, Lithuania

Professor Dr. habil. sc. ing. Vladimirs Šestakovs
Riga Technical University, Latvia

DECLARATION OF ACADEMIC INTEGRITY

I hereby declare that the Doctoral Thesis submitted for the review to Riga Technical University for the promotion to the scientific degree of Doctor of Science (Ph. D.) is my own. I confirm that this Doctoral Thesis had not been submitted to any other university for the promotion to a scientific degree.

Name Surname ……………………………. (signature)
Date: ………………………

The Doctoral Thesis has been written in English. It consists of an Introduction; 4 Chapters; Conclusion; 111 figures; 29 tables; 0 appendices; the total number of pages is 141 not including appendices. The Bibliography contains 103 titles.

LIST OF ABBREVIATIONS

2D – Two-dimensional

2G – Second generation mobile networks

3G – Third generation mobile networks

4G – Fourth Generation

AGL – Above Ground Level

AMC – Automatic Modulation and Coding

BS – Base Station

C2 – Command and Control

CID – Cell ID

COTS – Commercial-of-the-shelf

D2D – Device-to-Device

D2WAN – Device-to-WAN

DAN – Double Attached Node

DC-HSPA+ – Dual Carrier High Speed Packet Access protocol

DNS – Dynamic Name Server

Ec/Io – Energy per chip to interference power ratio

EDGE – Enhanced Data Rates for GSM Evolution

ETSI – European Telecommunications Standards Institute

FPV – First Person View

GCS – Ground Control Station

GPS – Global Positioning System

GSM – Global System for Mobile communications

HARQ – Hybrid Automatic ReQuest

HF – High Frequency

HSPA – High Speed Packet Access

HSPA+ – evolved High Speed Packet Access

ICAO – International Civil Aviation Organization

ICMP – Internet Control Message Protocol

IP – Internet Protocol

IPDV – IP Packet Delay Variation

IPPM –IP Performance Metrics Working Group

IPTD – IP Packet Transfer Delay

ITU – International Telecommunication Union

KPI – Key Performance Indicator

LOS – Line-of-Sight

LTE – Long Term Evolution mobile networks

LTE-A – Long Term Evolution – Advanced (4G mobile network)

MASL – Altitude above mean Sea Level

MB – Mobile Broadband

MIMO – Multiple-Input and Multiple-Output

MPTCP – Multipath TCP

OSPPt – Test based on Probability Plot of Ordered Statistics

PIFA – Planar Inverted-F Antenna

PRP – Parallel Redundancy Protocol

RC – Remote-Control

RCV – Remote-Controlled Vehicle

RPA – Remotely Piloted Aircraft

RPAS – Remotely Piloted Aircraft System

RSCP – Received Signal Code Power

RSRP – Reference Signal Received Power

RSSI – Received Signal Strength Indicator

RTT – Round-Trip Time (two-way delay)

SAN – Single Attached Node

SINR – Signal to Interference plus Noise Ratio

STDEV – Standard Deviation

TCP – Transmission Control Protocol

UE – mobile User Equipment

UHF – Ultra-High Frequency

UMTS – Universal Mobile Telecommunication System

VHF – Very High Frequency

vi – virtual instrument (LabVIEW executive file)

VLOS – Visual Line-of-Sight

WAN – Wide Area Network

SUMMARY

INTRODUCTION

Unmanned Aerial Vehicles (UAV) and Remote-Control Vehicles (RCV) require wireless communication solution to perform Remote Controlled (RC) operations. The use of airborne radio receiver in conjunction with Electronic Speed Controllers (ESCs) allows to operate UAV via remote control transmitter. The approach "ground transmitter->airborne receiver->ESC" is the most lightweight and cheap solution. However, such solution does not provide fail-safe operation of the RPA (pilot is responsible to compensate all flight conditions e.g. wind gusts), does not provide any feedback from RPA (e.g. remaining battery power, artificial horizon, etc.) and does not allow autonomous flight (by waypoints instead of manual remote piloting). To overcome above mentioned disadvantages, modern UAVs typically are equipped with flight controllers (also called "telemetry systems").

Flight controller is responsible to control ECSs according to received commands from the ground transmitter. One of the most common function of the flight controller is an automatic stabilization of the RPA with respect to wind gusts or excessively fast made commands from the ground pilot. This enables possibility to build more efficient flying vehicles by the cost of stability (copters are unstable by default). So, the primary function of the flight controller is RPA flight stabilization. The stabilization function requires information about roll, pitch and yaw. Such information usually is supplied from the build-in Accel / Gyro solid state unit (typically called Micro-Electro-Mechanical System, or MEMS). This means that the information about roll, pitch and yaw is available in the flight controller and can be supplied to the ground pilot's Ground Control Station (GCS) too. This requires additional UAV-ground radio link called "telemetry link". Usually remaining battery capacity (from dedicated battery sensor), barometric altitude (from barometric pressure sensor), GPS coordinates and compass information are also supplied in addition to the artificial horizon information via telemetry link. Finally, GPS, barometric altitude and magnetic compass can be used to ensure autonomous flight by using waypoints. This means that typical mini-RPA (takeoff weight is less than 30 kg) have two radio channels: one for the remote-piloted operations and second one for the telemetry. The telemetry channel should be bidirectional to be able not only to receive reports from, but also to specify new waypoints to the UAV.

Currently, the most common remote-control systems utilize VHF and UHF frequency bands. The use of radio frequencies is regulated by the relevant authorities. Recommendations for coordinating of the use of radio frequencies are issued by the International Telecommunication Union (ITU). Local standards are issued based on ITU recommendations. On the territory of the European Union, European Telecommunications Standards Institute (ETSI) is responsible for creating standards. At the legislative level in the territory of the European Union member states, standards are approved by local authorities. In Latvia, the responsible structure is "VAS Elektroniskie sakari". Manufacturers of radio equipment for RPAS are trying to make it universal for any part of the world. So, the most widely used frequencies are: 2.4 GHz for the RC channel, 433 MHz for the telemetry channel (the option with a frequency of 915 MHz is used in North America). Such typical approach is shown in Fig. 1.
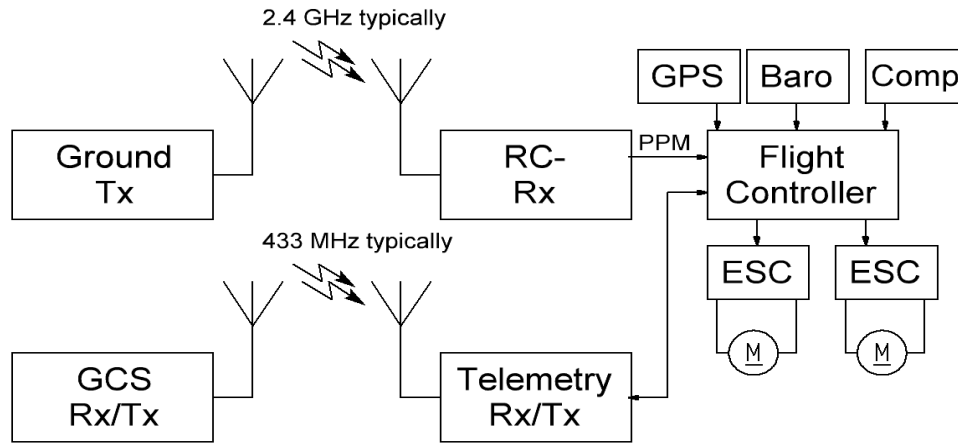
Fig. 1. Typical wireless equipment of a typical lightweight UAV.

Frequencies above 30 MHz are propagated along the line of sight (LOS). However, maximum power restrictions typically do not allow to utilize the full range of LOS. Since frequencies with a lower frequency have less free space attenuation, the telemetry channel uses a lower frequency (433 MHz). The RC channel requires lowest latencies but can actually be used only at relatively short distances with good visual control of the RPAS. For this reason, the 2.4GHz frequency is a good compromise.

Since all the above frequencies are propagated in LOS mode, the maximum communication range is usually limited to a few kilometers. This in itself makes it impossible to safely integrate RPAS into the common sky concept. ICAO highlighted the need of a reliable command and control link in their concept, called "RPAS Concept of Operations" [1]. In ICAO terminology, such a link is termed "C2 link".

One of the possible prospects for the implementation of C2 link is the use of data transmission services of mobile cellular networks. In theory, such a solution will allow remote-control of the aircraft throughout the entire territory covered by the cellular network. Since 3G and LTE networks are widely deployed, such a solution has good potential to provide C2 link functionality over continents as well as over coast regions.

Despite the promise of this idea, at the time of the start of the study (in 2016), there were practically no studies of the suitability of cellular networks for piloting and transmitting telemetry of UAVs. For this reason, it was decided to start with an experimental study of the performance of cellular networks both close to the earth's surface and at high altitudes. Obviously, other researchers have also started researching this problem, since several articles on this topic have been published in the next few years. Since the researches were carried out in parallel, there could be no mutual influence of the results presented in this dissertation with the results of research of other researchers. This made it possible not only to indirectly confirm the results obtained, but also, without being influenced by a priori knowledge, to reveal some of the nuances that were missed by other researchers.

Since there are currently many publications and reports on the vertical coverage of cellular networks available, and many solutions to the identified problems have been proposed, less attention is paid to the issue of vertical coverage of cellular networks in this dissertation. The

experimental study of the vertical coverage of 3G and LTE cellular networks was carried out only in a limited area near the city of Riga. This study was carried out because cellular network operators can change the slope of the radiation patterns of base stations depending on the average height of buildings, as well as the local terrain, which can be different depending on the country. Despite the secondary attitude to this issue in this thesis, during the experiments, the harmful effect of soft handover (which is used in 3G networks) in conditions of complex coverage was revealed. Other researchers overlooked this problem, apparently because they concentrated on LTE networks (where hard handover is used).

The second important problem associated with the analysis of the possibility of using mobile networks for C2 link data transmission is network delays. Existing publications, made by 3GPP (see short description of the 3GPP report in [2]) contains a lot of field studies about vertical coverage, whereas delays in an LTE network are only calculated (forecasted) using mesh of Base Stations (BS) and putting several drones inside each cell. In a contrast to modelled data, very little attention has been paid to the experimental evaluation of real working networks in available publications. Basically, existing publications contain experimental studies of cellular network latency, carried out on specific routes. Since the delay studies in LTE, presented in this thesis, were carried out in parallel with other researchers, after analyzing and comparing the results, a strong discrepancy was found. Obviously, the obtained latency values, as a rule, were presented by other researchers in the form averaged values (or CDF) over the entire network. This approach is not entirely correct, since the mobile user equipment operates with a specific BS, and not with the entire network at once. Apparently, this is precisely what caused the fact that the results obtained by various researchers never coincided with each other, and therefore the conclusions were always different.

To answer the question of whether the delays in the existing cellular LTE networks meet the requirements for delays in the UAV communication channel, a previously nonexistent method was proposed. The thesis uses the method of representing the delays of the entire cellular network of one operator in the form of a two-dimensional distribution function of the parameters of the distributions of delays in cells. The parameters of the distribution function are estimated from the experimentally obtained values of the delays in the cells of a particular cellular operator. This approach made it possible to analyze delays in each cell separately; in addition, it became possible to predict delays in cells that were not included in the experimental study (because it is not possible to experimentally evaluate all cells within the country).

Further, it was necessary to develop requirements for delays, which did not exist at that time. The requirements for the delays in the UAV control channel were successfully derived by analyzing the existing reports and publications on the effect of delays on the quality of piloting. Thus, it became possible to answer the question whether the delays in cellular networks meet the requirements for C2 link.

Finally, since the quality of the vertical coverage of existing LTE networks is instable and the delays in some LTE cells are too high, a parallel redundant communication link has been proposed. Two existing parallel redundant software solutions were tested, Next, a method was proposed for predicting delays in a parallel redundant network, taking into account packet loss rate.

GENERAL CHARACTERIZATION OF THE THESIS

Urgency of the Research

Today, a new industry with great economical potential starts to be created on the base of Unmanned Aerial Vehicles (UAV). The UAV operates as a part of a system called an Unmanned Aerial System (UAS). In order to be able to operate under remote control, any UAS requires a reliable command (Remote Control (RC)) and control (telemetry) link. In ICAO terminology such link is termed to as Command and Control or "C2 link" [1].

At the date, the VHF and UHF frequencies are commonly used to implement C2 link. Frequencies in these bands generally propagate in a Radio Line-of-Sight (RLOS) manner (it is worth noting here that the radio waves propagation model for UAV and RPAS differs from the traditional model, which is valid for terrestrial wireless communication, since communication occurs between equipment located on the ground and in the air). The main problem is that UAV flight takes place at a relatively low altitude (typically allowed altitude is up to 120 m above ground level (ALG), while in some populated areas the maximum altitude is set to 50 m AGL. Low altitudes, as well as the ability to quickly change altitude and speed of flight, increase the likelihood that the traditional radio link becomes obstructed. This in itself drastically reduces maximum ranges of flight where reliable operation of the C2 link can be guaranteed.

The use of the cellular data transfer services (e.g. 2G, 3G, LTE, 5G) can significantly increase the range of C2 link operation. However, cellular mobile data transfer services up to LTE incl. were originally designed for terrestrial users. The performance of these services for flying users is not guaranteed. The mission of the Thesis is the evaluation of the suitability of data transfer over mobile cellular networks for C2 link implementation for low-flying (up to 120 m) UAVs.

Mission of the Thesis

The goal of the research is the evaluation of the suitability of the data transfer over LTE mobile cellular networks for "Command and Control Link" implementation for low-flying (up to 120 m), small size (group 1) UAVs.

Tasks

1. Development of the delay requirements for the wireless "C2 Link" of low-flying UAVs.
2. Determination of the type of distribution law of delay values of the LTE mobile data transfer service.
3. Experimental estimation of delay values in various cells of cellular mobile network.
4. Analysis of the compliance of the delays of mobile data transfer to the requirements of a "C2 Link" of low-flying UAVs.
5. Experimental evaluation of the impact of the mobility of terrestrial users on the performance of 3G and LTE mobile data transfer services.
6. Experimental evaluation of the impact of flying altitude on the performance of 3G and LTE mobile data transfer services.

7. Application of the parallel redundancy to increase the reliability and reduce the delays of a "C2 Link".

Methodology

Theoretical and experimental means were used to achieve the goals and objectives.

An experimental study involves conducting field experiments within the existing operating cellular networks of Latvia. Mobile 3G/LTE dongles were used as the main means for conducting experimental evaluations of the key performance indicators (KPI) of mobile cellular network's radio links and data transfer. The evaluations were performed in the cases of stationary placed equipment on the ground, as well as mobile equipment on the ground and in the air. For this, the dongles were stationary located, or transported by a car, or lifted by the 450 mm drone with a companion computer attached to it, or flied by lightweight airplane.

The first mobile dongle was Huawei 3372h. The Huawei E3372h is equipped with two PIFA antennas (for the receiver diversity) and is a 24th category 3G device which supports 64-QAM modulation and can be operational in dual cell DC-HSPA+ mode and a LTE Cat 4 device which supports operation in LTE cells with 20 MHz bandwidth. By default, it operates in the Hi-Link mode (CdcEthernet). In this mode it operates as a NAT server and emulates a virtual network card (NDIS), and its configuration is done via the web interface. Since the indicators of a radio network performance should be logged too, the device was reprogrammed into stick mode (RAS) (firmware 21.315.01.00.143_M_01). The stick mode enables access to the set of standard serial AT-commands and reports.

The second device was Huawei ME909s-120. This is Cat 24 and LTE Cat 4 device. The main difference with the E3372h is that this module has no built-in antennas, allows to search for LTE cell (the E3372h allows search in 2G and 3G modes only) and by default operates in MB (Mobile Broadband) mode. In order to get access to its serial AT-commands and reports, the device was switched to debug mode, thus debug drivers were used too.

All the radio network parameters were reported by the 3G/LTE dongles (Huawei 3372h or Huawei ME909s-120). The travelling speed and location were obtained via the Global Sat BU-353-S4 GPS receiver.

All the experimental data as well as the speed and altitude (reported by the GPS receiver) have been captured via the virtual instrument (vi), created in the LabVIEW environment. The proposed vi performed decoding of the data and allowed export of the experimental data into MS Excel files.

The delays of data transfer service generally were evaluated via the ICMP packets to exclude the impact from the fast acknowledgement by Base Station (BS). The ICMP requests were generated by the standard utility "ping". In some special cases another type of packets were used, where data flows were generated by the Netperf and IPerf software.

The post-processing of the experimental data was performed in the MS Excel software. The data transfer KPI were evaluated in accordance with ITU recommendation T-REC-Y.1541 [2].

The theoretical background of the research is the theory of reliability. The analyses of delays and their properties were carried out via the methods of probability theory and mathematical statistics, namely: analysis of the suitability of distribution law via the probabilistic paper, as

well as using the goodness-of-fit tests; estimation of distribution parameters using the maximum likelihood method, as well as using fractals (under the accepted hypothesis of the distribution law); description of the parameters of the delays via the system of random variables; description of the delays in the redundant system via the minimum function. The majority of calculations as well as the data processing were done in the MATLAB and MS Excel environments.

Scientific Novelty

Scientific novelty lies in proving the suitability and limits to applicability of the LTE mobile data transfer for implementing wireless C2 link for low-flying, small size (group 1) UAVs. This is achieved by estimating the predicted delays based on experimental estimates of delays in the cells of mobile LTE network. The effects of specific situations arising during various kinds of mobility or flights over the earth's surface are also evaluated.

- The Thesis contains the goodness-of-fit tests of a statistical hypothesis of the delays in the LTE cells. It is proved that in order to obtain estimates of the average delay and delay jitter with satisfactory accuracy, it is possible to accept that the delays in LTE cells obey the logarithmically normal distribution law.

- A method for description the delays in an overall mobile cellular network using a multivariate distribution function of the delay distribution parameters of individual cells is proposed.

- The Thesis contains a list of factors that leads to temporary increased delays in 3G (HSPA+ and above) data transfer service, when the user equipment (UE) is moving on the ground.

- The Thesis states the problems that lead to temporary increased delays /increased packet loss rate in 3G (HSPA+ and above) data transfer service when UE is flying over the earth's surface. It has been found that the same problems are also applicable to the LTE systems and may lead to degraded performance of the LTE data transfer service too.

- The efficiency of parallel redundancy application in mobile data transfer services has been proven. A method for predicting delays in the redundant network solution with known packet loss rates is proposed. The method is applicable to various number of parallel redundant networks.

Practical Utility

Practical utility lies in providing the numerical values of the characteristics as well as the limits to applicability of the communication channel for implementing wireless C2 link via the LTE mobile data transfer for low-flying UAVs.
The Thesis contains the requirements for network delays for the wireless RC and FPV channels of lightweight UAVs.

- The Thesis contains the numerical characteristics of the delays of the Tele2-LV LTE network. The proposed characteristics of the delays are described via two-dimensional distribution function of the delay distribution parameters of individual cells, assuming that the delays in LTE cells fit with the logarithmically normal distribution. The

proposed model can be used to assess the compliance of LTE network delays with the required delays in specific cases in order to assess the appropriateness of LTE network as a communications channel solution.

- The Thesis contains the method of quick estimation of the logarithmically normal distribution parameters, based on known values of minimal RTT_{min} and average $RTT_{average}$ values. This approach is convenient, since the "ping" utility reports these statistics in ready to use manner. The recommendations on the required number of measurements in LTE networks are also provided.
- The Thesis contains the recommended de-jittering buffer sizes of FPV video channel that should be used in LTE network. The proposed values are estimated using the numerical characteristics of the delays of the Tele2-LV LTE network.
- The thesis contains the limits to applicability of the LTE network for implementing wireless C2 link for low-flying UAVs. The values of the proposed limits are established considering the developed requirements for the FPV and RC channels as well as the experimentally obtained numerical characteristics of the delays of the LTE Tele2 network.
- The Thesis contains the proposed method which allows to evaluate the coverage area of base stations in the air.
- The Thesis contains the experimental evaluation of the applicability of PRP and MPTCP redundant software solution implementations that previously were not implemented and tested in cellular mobile networks. The experimental data of the performance of PRP and MPTCP redundant solutions confirmed the effectiveness of the application of these redundant solutions in LTE networks. The recommendations on the selection of cellular data transfer services for the redundant solution are also provided.

Theses to be Defended

- The developed requirements for data transfer network delays for the RC and FPV wireless channels are applicable to low-flying, small size UAVs.
- The delay values in LTE network cells can be described by the parameter estimates of the lognormal distribution. This approach does not introduce noticeable errors in determining the average delay and delay jitter values.
- Evaluation of delays in overall cellular network should be carried out separately in each cell; the results should not be mixed.
- The application of the two-dimensional (bivariate) system of the distribution parameters of the delays of LTE cells with approximation according to the normal law is an effective solution to the description of delays of the entire LTE network.
- The delays in the LTE network allow the use of this network as a wireless solution for the RC of a UAV by a trained pilot.
- Assuming sufficient coverage of the cellular network, the UAV can be piloted through the FPV via the LTE network if video codecs can operate with a packet loss rate of 1 %. At the same time, the size of the de-jittering buffer should correspond (to be dynamically

adjusted) to the IPDV value determined at the level of 0.99. The use of a buffer with a constant size in the video channel in the LTE network does not allow to get the required delays in the video channel.

- The performance of 3G / LTE networks for flying users is subject to negative effects, such as strong interference and more frequent handovers. The use of soft handover (like in 3G networks) in case of complex aerial coverage leads to massive operation of the soft handoff function, which leads to a significant increase in delays, jitter and packet reordering.
- The vertical coverage of 2G/3G/LTE base stations can be experimentally evaluated by running the built-in search function of the communication module. Such approach allows to obtain a full coverage map instead of getting radio signal quality indicators only for the selected base station.
- The implementation of the parallel redundancy in the LTE networks is the effective solution.
- Application of a parallel redundancy in 3G / LTE networks is an efficient solution to increase the availability and the performance of a C2 Link.
- The delays in the redundant network solution can be predicted by using the proposed method. The proposed method uses the statistics from the "ping" utility and is more intuitive than the existing approach based on the Markov chain method.

Approbation of the Results

The results, proposed in the Thesis, were presented in the following scientific conferences:

1. International Scientific Practical Conference "Transport systems, logistics and engineering": Mini UAV long- range communication link challenge, Riga, Latvia: Riga Aeronautical Institute, 2016.
2. RTU 57th international scientific conference: "Transport – Aerospace and transport engineering": Experimental study of the quality of data transmission service of Latvian mobile operators, Riga, Latvia: Riga Technical University, 2016.
3. RTU 58th international scientific conference "Transport and aerospace engineering": Mobile user equipment reliable cellular data transfer service solution, Riga, Latvia: Riga Technical University, 2017.
4. "IEEE 58th International Scientific Conference on Power and Electrical Engineering (RTUCON)": High-Reliability Low-Latency Cellular Network Communication Solution for Static or Moving Ground Equipment Control, Riga, Latvia: Riga Technical University, 2017.
5. "IEEE 59th International Scientific Conference on Power and Electrical Engineering (RTUCON)": Reliable data communication link implementation via cellular LTE services for static or moving ground equipment control, Riga, Latvia: Riga Technical University, 2018.
6. RTU 60th international scientific conference "Transport": Measurements of signal coverage and quality of 3G / LTE mobile networks at high altitudes using a remotely piloted aircraft system, Riga, Latvia: Riga Technical University, 2019.

7. "IEEE 60th International Scientific Conference on Power and Electrical Engineering (RTUCON)": Method for estimating delays in parallel redundant data transfer networks, Riga, Latvia: Riga Technical University, 2019.
8. RTU 61st international scientific conference "Aviation transport": UAV Control via Mobile Cellular Networks., Riga, Latvia: Riga Technical University, 2020.
9. "IEEE Microwave Theory and Techniques in Wireless Communications (MTTW)": An Approach to Constructing a Model of Delays in Cells of a Cellular Network Based on Experimentally Obtained Data, Riga, Latvia: Riga Technical University, 2020.

The results, proposed in the Thesis, were published in the following scientific papers:

1. D. Brodnevs and A. Kutins, "An Experimental Study of Ground-Based Equipment Real Time Data Transfer Possibility by Using Cellular Networks," *Electr. Control Commun. Eng.*, vol. 12, no. 1, pp. 11–19, Jul. 2017. Indexing: Web of Science.
2. D. Brodnevs and A. Bezdel, "High-reliability low-latency cellular network communication solution for static or moving ground equipment control," in *Proc. IEEE 58th Annual International Scientific Conference on Power and Electrical Engineering of Riga Technical University (RTUCON)*, 2017, pp. 1–6. Indexing: IEEE, Scopus, Web of Science.
3. D. Brodnevs and A. Kutins, "Cellular networks selection for the remote control vehicles' control channel setup with parallel redundancy," *J. Mod. Technol. Eng.,* vol. 3, no. 1, pp. 63–74, 2018.
4. D. Brodnevs, "Development of a Flexible Software Solution for Controlling Unmanned Air Vehicles via the Internet," *Transp. Aerosp. Eng.,* vol. 6, no. 1, pp. 37–43, 2018.
5. D. Brodnevs and A. Kutins, "Reliable data communication link implementation via cellular LTE services for static or moving ground equipment control," in *Proc. IEEE 59th International Scientific Conference on Power and Electrical Engineering of Riga Technical University (RTUCON)*, 2018, pp. 1–6. Indexing: IEEE, Scopus, Web of Science.
6. D. Brodnevs and A. Kutins, "Deterioration Causes Evaluation of Third Generation Cellular LTE Services for Moving Unmanned Terrestrial and Aerial Systems," *Electr. Control Commun. Eng.*, vol. 14, no. 2, pp. 141–148, 2018. Indexing: Web of Science.
7. D. Brodnevs and M. Hauka, "Method for estimating delays in parallel redundant data transfer networks," in *Proc. IEEE 60th International Scientific Conference on Power and Electrical Engineering of Riga Technical University (RTUCON),* 2019, pp. 1–6. Indexing: IEEE, Scopus, Web of Science.
8. D. Brodnevs and A. Kutins, "An Approach to Constructing a Model of Delays in Cells of a Cellular Network Based on Experimentally Obtained Data," in *Proc. IEEE Microwave Theory and Techniques in Wireless Communications (MTTW)*, 2020, pp. 206–211. Indexing: IEEE, Scopus, Web of Science.
9. D. Brodnevs and A. Kutins, "Requirements of End-to-End Delays in Remote Control Channel for Remotely Piloted Aerial Systems," *IEEE Aerosp. Electron. Syst. Mag.*, vol. 36, no. 2, pp. 18–27, 2021. Indexing: IEEE, Scopus, Web of Science.

Structure of the Thesis

Chapter 1 contains the review of existing solutions for wireless command and control links of UAVs.

Chapter 2 contains an analysis of the delays in 3G and LTE cellular mobile networks as well as provides a review of the technological aspects of 3G and LTE cellular mobile networks that have a major impact on the data transfer quality. The experimental evaluation of the impact of mobility on the delays in 3G and LTE networks is provided. The chapter also presents the proof of application of a distribution law on delay values, which is applicable to LTE networks, as well as recommendations on the required number of measurements to estimate the parameters with the required probability of tolerance. It describes a method that allows to estimate the distribution parameters from known *RTTmin* and *RTTaverage* values, which are reported by the well-known "ping" utility. A two-dimensional system of random variables of the delays in LTE of Tele2-LV cells is also provided. The requirements of delays for C2 Link which were developed based on a literature review are provided. Finally, an analysis of the suitability of delays of real working LTE mobile network for the command and control link (C2 link) is provided.

Chapter 3 contains an analysis of limiting factors that reduce the performance of 3G and LTE at high altitudes.

Chapter 4 contains a mathematical model for estimating the delays in the resultant redundant network, as well as its experimental verification if two redundant LTE networks are used. It also contains a description of two experimental setups of redundant solutions (PRP and Multipath TCP) that has not been previously tested in cellular networks.

1. REVIEW OF EXISTING SOLUTIONS FOR WIRELESS LINK IMPLEMENTATION OF UNMANNED AERIAL SYSTEMS (UAS)

Currently, several communication technologies are used to implement a radio channel for communication with lightweight UAV.

The first logical solution is to use IEEE 802.11 equipment (which was initially developed for wireless local area networks (WLANs)). This standard implies utilization of 900 MHz frequency, as well as 2.4, 3.6, 5 and 60 GHz. The use of ready-available, well-developed Commercial Off-The-Shelf solutions (COTS) solutions allows to reduce cost and time for developing of the C2 link system. However, as the flight altitude increases, the receiver located on board the UAV receives more and more direct visibilities with many users of such systems. This leads to an increase in interference. The influence of interference from ground-based devices on the operation of the 802.11 communication system is described in [4]. A mathematical model for radio signal adaptation to a changing quality of the radio channel, based on Received Signal Strength (RSS) is described in [5]. The results of the mathematical model calculations are confirmed by the field experiments. Such approach allows to adapt the behavior of 802.11 systems to create equipment, suitable for use on RPAS. Additional information obtained experimentally for the operation of 802.11 systems on RPAS for the height range up to 110m AGL can be found in [6]. The horizontal arrangement of omnidirectional antennas of 802.11 class equipment allows to reduce the effect of the yaw angle rapid changes on the data transfer rate [7], [8]. Also, the use of devices operating at a frequency of 900 MHz can significantly increase the maximum range up to 2 km [9]. If the 802.11 device is planned to be used to create a wireless channel between two aircraft, then addition remarks can be found in [10].

The above-mentioned IEEE 802.11 devices have been designed for stationary equipment. In practice, these COTS are widely used in small RPAs for images and FPV video uplink. It should be noted that these devices require VLOS between the RPA and the Ground Control Station (GCS). The data rates of these COTS were experimentally evaluated and published in various scientific papers and reports. An overview of some of these papers is presented in the following 1.1. table.

1.1 table

Data throughput of IEEE 802.11 versus communication distance

Standard	Maximum data rate
802.11a (54 Mbps)	29 Mbps at 50 m [6], 17 Mbps at 100 m [11] 14 Mbps at 350 m [6] 10 Mbps at 500 m [11]
802.11b (11 Mbps)	1,4 Mbps at 1000 m and 1 Mbps at 3500 m [12]
802.11n (600 Mbps)	100 Mbps at 100 m, 50 Mbps at 120 m, 20 Mbps at 500 m, assuming static terminals and good signal level [11]
802.11ac (6933 Mbps)	By 25% higher than in 802.11n [11]

The second solution is IEEE 802.15 equipment, which is used to build a Wireless Personal Area Networks (WPAN). The most widely used subgroup of this standard is 802.15.4 Low Rate WPAN devices, which has a low power consumption and, consequently, a lower data transfer rate. The study of their use for RPAS needs is also reflected in scientific publications, for example, [13], [14]. Such solutions have lower power consumption but are mainly used for remote data acquisition from sensors located on the ground. Among others, IEEE 802.15.4 "Zigbee" can provide a data transfer rate of 56 kbps at a distance of 500 m with a packet loss rate of not more than 1% [15] .

The main advantages of the above-mentioned systems are their proven standards and technologies, as well as the availability of COTS. The main drawback of control channel implementations using the above standards is the limited range, which is often less than the LOS distance. The theoretical maximum range of such systems can be assumed as 15 km (if LOS visibility exists). In the field, the maximum range of a stable data transfer sometimes is only 1-2 km, especially if a high data transfer rate is required [16], [17]. The main limiting factors are: (1) low transmitter output power (due to limited power consumption on RPAS and restrictions on maximum EIRP from ETSI), as well as (2) the use of omnidirectional antennas. Due to the continuous RPAS movements, omnidirectional antennas are installed on board, which does not allow to use directional antennas in order to amplify the useful signal.

The use of directional antennas allows to amplify the useful signal and reduce the interference from other devices operating on the same frequency. The use of a directional antenna requires the use of rotary mechanism (gimbal), as well as algorithms for searching and holding the direction of the antenna in the desired position. The use of directional antennas allows to increase the maximum communication distance of 802.11 devices up to 5 km at a frequency of 2.4 GHz [18] (if LOS visibility exists).

With the appearance of the long-distance system Lora, it became possible to use lower frequencies by applying available COTS, thereby reducing free space and atmospheric attenuations. In Europe, Lora operates at a frequency of 868 MHz. Using a transmitter with a power of 14 dBm, it is possible to establish a stable connection at a distance of up to 10 km [19] in the presence of LOS visibility between transceivers. It should to be noted that LoraWAN service was originally designed for IoT devices, so it accept duty cycle of 1% only (1% is a typical value, in some circumstances ETSI allows duty cycle of 10%) that leads to very slow data rates maximum of few kilobits per second, which makes it unsuitable for RPAS needs. A good review of LoraWAN service and its limitations can be found in [20].

The use of troposcattering effect can significantly increase the maximum range. Consequently, such a communication system is over-horizon, i.e. ensuring LOS is not a requirement. For example, the use of a transmitter with a power of 0 dBW allows to obtain stable radio communication up to 150 km [21]. The main disadvantage of this system is the high transmitter power. This, in turn, requires a license to use radio frequencies. In addition, the large power consumption does not allow the use of this system on lightweight UAV.

The use of radio relay stations allows significantly decrease required transmitter power, as well higher frequencies can be used to reduce antenna dimensions. A lot of scientific papers offer to use motionless drones to use them as a radio relay station, for example [22], [23].

However, such approach is devoted for the limited time operations and cannot be used for permanent communication establishing.

It can be concluded that the use COTS, which operate in the VHF and UHF bands, leads to flight operations that are limited to VLOS (which ranges from several hundred meters during takeoff and up to several kilometers for RPAS flying at a ceiling of 115 m). The use of over-horizon solution, such as HF and satellite stations as well as radio-relaying, is expensive, impractical and in most cases is impossible (due to limitations of RPA payload and ability to supply large amount of electrical power).

It should be noted that modern RPAs are usually equipped with autoflight computers, which allow autonomous flights through predefined waypoints beyond visual line-of-sight (BVLOS) (when C2 link becomes obstructed). However, such flights become "blind" for both the pilots and all other flying machines. This problem of UAS integration has been also identified by ICAO [1]. In this document, ICAO indicates the need for reliable C2 link for safe integration for UAS and RPAS.

The use of cellular data transfer services (e.g. 2G, 3G or LTE) to transfer telemetry signal can significantly increase range of C2 link. Available field studies state that cellular networks has sufficient signal strength up to 300 m or even better that is fully enough for the UAV flight that is restricted to 115 m AGL [24]–[27].

The idea of using cellular data transfer services as a telemetry channel is not new (please note that the control RC channel typically remains on its RC equipment, since it is mature and therefore is more thrusted. Therefore, here we a not talking about a complete solution of the C2 link). In [28] is described solution that uses open source mavproxy software [29] to transmit the Pixhawk flight controller telemetry data thru the internet via cellular data transfer service to the GCS. Also, there are several projects, as well some of them are available for free. Minla HDW solution uses its own hardware to control RPA from the internet [30]. Minla HDW automatically establish connection with Minla server. The pilot should connect to the server via internet to be able to control his RPA via web interface. Similar project is caller Virt2Real [31]. Unlike Minla HDW, this project uses its own hardware. Navio2 [32] provides hardware extension for the Raspberry PI to get same functionality, as described above. All projects allow to control and get feedback from RPA and does not allow customization of the software.

The solution, described in [28] uses Raspberry PI embedded system to run open source mavproxy software in order to stream 3DR telemetry information into the internet via 3G/LTE. There is also free available project that provides ready to deploy image for the embedded computers which runs mavproxy software by default and streams 3DR Pixhawk flight controllers telemetry information [33]. However, all mentioned above projects can utilize various wireless links "as is" and does not allow to modify access methods e.g. does not allow to introduce diversity (redundancy).

It can be concluded that there is grooving interest to implement "C2 link" over a cellular mobile network. However, since the cellular services were developed and optimized for ground users, as well as extensive field studies for aerial users were not carried out, the thrusted service of 3G and LTE cellular data transfer services for aerial users is not guaranteed. The aim of this work is to evaluate the possibility of implementing a reliable C2 link via the LTE service.

2. EVALUATION OF DELAYS IN CELLULAR MOBILE NETWORKS

The growing deployment of 3G and LTE technologies and infrastructure of cellular networks enables a variety of new wireless mobile applications. For today, the most popular Latvian mobile service operators (Tele2, BITE and LMT) promise almost full coverage of the territory of Latvia [34]–[36]. While most of the traffic is non-essential data (website access, non-real-time applications such as Facebook and Twitter) which does not require near to real-time data transfer service, there is a suggestion that cellular network data transfer service can be used for critical and real-time data transmission. It is supposed that the cellular network data transfer service can be used to transmit various real-time control signals. Therefore, it is crucial to understand the performance indicators of cellular network data transfer service such as network latency and jitter, as well as network availability.

2.1. Definitions of the KPI to be used in the Thesis

There are a lot of Key Performance Indicators (KPIs), that can be used to describe performance of a data transfer network. In this thesis the following KPIs will be used.

One-way transmission time (sometimes termed latency) is the end-to-end delay from a source host to a destination host, which is expressed in time (typically in milliseconds). This metric is explained in details in RFC 7679 [37]. The latency is a Type-P metric [38], that means that the value of metric depends on IP packet type (e.g. TCP, UDP, ICMP) and size. This means that in the experimental part packet type and size, that was used, should to be identified. Since often this delay lies within the range of 0.1 to 100 ms, this leads to excessive requirements for the local time synchronization of a Source and Destination to be able to accurately measure this metric. This is the main motivation why the one-way transmission time measurements are not in wide use.

Two-way delay (usually termed Round Trip Time (RTT)) is the end-to-end delay from a source host to a destination host and back to the source host. This metric is explained in details in RFC 2681 [39].

Round trip time (RTT) is expressed by (2.1):

$$RTT = \frac{s}{C_{up} \cdot 10^{-6}} + d_{up} + \frac{s}{C_{down}} + d_{down},$$ (2.1)

where:
RTT round trip time, s;
s packet size, bits;
C_{up} upload speed, Mbps;
C_{down} download speed, Mbps;
d_{up} upload delay, s;
d_{down} download delay, s.

This approach eliminates the need of the local time synchronization of a Source and Destination, since the value of an RTT is processed in the Source. The general imperfection this metric is that the path from a source to a destination may differ from the path from the destination back to the source (so called "asymmetric paths"), therefore the RTT value indicates the performance of two paths and cannot be divided by two in order to calculate the one-way delay. Please note that in cellular networks the uplink (from User Equipment (UE)) and downlink (to UE) are always different channels, that are using different frequencies, modulation and coding schemes. The RTT is a Type-P metric [40], that means that the value of metric depends on type of IP packet and its size.

The RTT is a real number, it cannot be equal to zero. In case of RTT value is undefined (equal to infinity), this means that the packet was lost (delayed for an infinitely large time period). This means that either destination did not receive the packet, destination did not reply, or source did not receive that response packet. Typically, maximum period to wait for the response is specified during the measurement. In this case the packet is considered as lost if the waiting time is exceeded.

Typically, two values of the RTT measurement stream are shown. These are Minimum and Average values. The *average RTT* value is calculated from all the RTT values, except those that was delayed for more than the specified maximum (1 sec typically). The average RTT value one of the key performance indicators of the data transmission line. *The minimum RTT* is found from all the RTT values. None of boundaries are applied here (e.g. 3STDEV). The minimum value of this metric provides an indication of the delay due only to propagation and transmission delay. This metric provides an indication of the delay that will likely be experienced when the data transfer service is lightly loaded.

Packet delay variation (PDV) (sometimes termed Jitter) is the difference between the one-way-delay of the selected packets. It is based on a One-Way-Delay metric. The *jitter* meaning is frequently used by computer scientists and frequently (but not always) refers to variation in delay. This metric is explained in details in RFC 3393 [41]. The PDV is a Type-P metric [40], that means that the value of metric depends on type of IP packet and its size. The PDV has important use in the sizing of play-out buffers for applications requiring the regular delivery of packets (e.g. streaming video). The value of a PDV is either a real number (positive, zero or negative), expressed in milliseconds (typ.), or an undefined number of seconds (when at least one packet of a pair has been lost). The number of samples for the PDV statistics is not defined in the recommendation [41].

$$PDV = Latency_i - Latency_{i-1} \qquad (2.2)$$

where:

PDV   packet delay variation, ms;

Latency   packet one-way delay, ms;

i packet number.

Sometimes, the *jitter* is calculated as the absolute value of the PDV values in the sample (for example, here [42]).

Another representation of **jitter** is computed by taking absolute values of the PDV sequence and applying an exponential filter with parameter 1/16 to generate the estimate [43]. Such approach can be used to plot the jitter vs time.

$$J = J_{i-1} + \frac{\left(|RTT_i - RTT_{i-1}| - J(i-1)\right)}{16} \tag{2.3}$$

where:

J	packet jitter, ms;
i	packet number;
RTT_i	actual packet round-trip time, ms;
RTT_{i-1}	previous packet round-trip time, ms;
16	jitter value averaging.

Further, the ITU specify IP packet Delay Variation (IPDV) as $Latency_{upper\_0.999} - Latency_{min}$, where the upped bound of a one-way delay (latency) is taken as the $1\text{-}10^3$ quantile in the evaluation period.

Packet loss rate is the relative number, typically expressed in percent. Its shows the rate of number of lost packets with respect to total number of packets. The packet is considered as lost if it is delayed for more that the limit, that was specified during the measurement process.

2.2. Technological aspects of 3G and LTE data transfer services

3G networks are now fully deployed in Latvia. A 3G network has been introduced in third generation partnership project (3GPP) Release '99 (R99). 3G technology utilizes Wideband Code Division Multiple Access (WCDMA), requires new base stations (called NodeB, which is incompatible with 2G devices) and is called Universal Mobile Telecommunications System (UMTS). Its first improvement was done by a significant increase of UMTS network performance within existing NodeB by introducing High Speed Packet Access (HSPA) according to the Third Generation Partnership Project (3GPP) specifications Release 5 and 6 [44]. In addition to higher data rates (downlink speed up to 14.4 Mbps and uplink speed up to 5.76 Mbps), HSPA technology also provides low jitter – below 20 ms and latencies below 100 ms [45]. The primary technological features that help reduce RTT are:

- Optional short transmit time interval (TTI) of 2 ms
- Hybrid Automatic Repeat Request (HARQ) implementation in the NodeB.

High Speed Packet Access (HSPA) mode comprises two protocols: High Speed Downlink Packet Access (HSDPA) for downlink and High Speed Uplink Packet Access (HSUPA). Each received data packet in downlink is acknowledged automatically by the NodeB. Furthermore, NodeB is responsible for immediate acknowledgments of uplink packets in HSUPA. Now the NodeB HARQ mechanism is responsible for retransmission of all lost transport blocks in downlink and all lost packets in uplink. The main idea of work shift from the Radio Network Controller (RNC) to the NodeB is to speed up acknowledgement and lost transport blocks

retransmission by shifting it into hardware that is closer to the radio interface. The network Round Trip Time (RTT) is reduced dramatically as the sender receives ACK immediately from the NodeB and can continue to send the next packet because the HARQ will make retransmission of lost data.

In an active HSDPA the UE must send Acknowledgement or Non-Acknowledgment (ACK or NACK) as well as Channel Quality Indicator (CQI) to the NodeB. There is a certain AMC scheme that provides the highest data throughput at a given signal to interference ratio (SINR) [46]. However, if the SINR deteriorates, the BLock Error Rate (BLER) increases significantly (waterfall effect). The UE uses CQI to request a certain AMC scheme from the NodeB to operate at the 10 % BLER. Then the lost data packets are retransmitted by the HARQ. One resend add 10 ms typically if the cell is not used by multiple users [45]. The benefit of this approach is that the throughput can be improved by switching to better AMC while the Bit Error Rate (BER) is kept low (typically at the level of 0.1 % [47]).

Further improvement in 3G networks was done by implementing HSPA+ standard according to 3GPP Release 7 [48]. HSPA+ is sometimes referred as 3.5G network. It offers up to 28.8 Mbps downlink and up to 11.5 Mbps uplink by using higher order modulation (64QAM) with a Multiple Input Multiple Output (MIMO) antenna solution downlink. The simultaneous use of 64QAM modulation and MIMO downlink technology is not possible in Release 7. Its latency value is even more reduced: below 50 ms compared to 100 ms of HSPA. The UE must meet at least Cat 15 to be able to operate in HSPA+ mode. The simultaneous use of 64QAM modulation and MIMO downlink technology is possible starting from 3GPP Release 8 [47]. These networks are usually referred to as 3.9G networks. Here the UE must meet Cat 19 or 20 with the maximum downlink speed of 35.28 Mbps or 42.20 Mbps, respectively. The final improvement was done in Release 9 [46] by allowing Dual Cell (DC) in downlink (DC-HSDPA) and uplink (DC-HSUPA) simultaneous operation called DC-HSPA+ or 3.99G network. Here the UE can be configured with two uplink and two downlink frequencies from the same NodeB. The UE must meet Cat 25/26 or Cat 27/28 to support DC-HSPA+ operation with maximum data rates of 55.9 Mbps or 84.40 Mbps, respectively.

The Long Term Evolution (LTE) technology was also implemented in 3G networks starting from 3GPP Release 8 [49]. LTE uses the same MIMO and DC operations as described above. The key difference between conventional 3G DC-HSPA+ network and 3G LTE network is the use of scalable channel bandwidth (up to 20 MHz) and more spectrum- efficient OFDMA instead of WCDMA. This makes 3G and 3G LTE incompatible to each other: LTE requires its own eNodeB stations instead of existing NodeBs. The UE must meet "LTE Cat". LTE Cat from 1 to 5 (specified in 3GPP Release 8) does not support Carrier Aggregation (CA) and are called "LTE" devices (sometimes "3G LTE").

LTE-Advanced (LTE-A) was officially introduced in 3GPP Release 10, but finished in Release 11. The LTE-A is usually referred to as 4G (or 4G+, what is not true, because LTE-A is official acknowledged 3GPP standart) technology [50]. Both LTE (3G LTE) and LTE-A (4G) use the same eNodeBs and spectra. The LTE-A speed improvement is done by introducing CA and 8 by 8 MIMO. UE must meet at least LTE Cat 6 to be able to use CA. For today, typical

LTE Cat 6 device power consumption is higher than USB power supply limit, so the LTE Cat 6 device cannot be implemented as USB dongle.

The key differences between 3G and LTE for the end user are the following:

- UE must support "LTE Cat" to be able to operate in LTE cells;
- 3G and LTE (3G LTE and 4G LTE-A) use different cells (so typically 3G and LTE have different coverage and operating bands);
- UEs in 3G HSPA+ and above networks are operating in a low-speed channel (original UMTS) at idle and are switched in high speed channel (HSPA+) as soon as traffic exceeds threshold, which is set by the cellular operator (usually 64 bps);
- there are no low-speed channels in LTE, so its starting time is reduced;
- overall network latencies and maximum speeds of 3G and 3G LTE are comparable: LTE provides slightly lower RTT (due to different backhaul [51]) and slightly greater theoretically available maximum data rate;
- in 3G only a limited number of users can be allocated in a high-speed channel (HSPA+), so in highly loaded 3G network some users may be left in a low-speed mode (called UMTS); whereas LTE has no such mechanism and overloaded LTE cell usually cause a high number of dropped packets.

3G and LTE networks has significant differences in its terrestrial backhaul, which leads to different performance aspects of such networks. A terrestrial backhaul topology of cellular networks defines resulting data transfer network parameters, such as network RTT (or latency) and handover (switching from one cell to the next one). A 3G radio access is done thru Universal Terrestrial Radio Access Network (UTRAN). The radio access hardware is implemented in the NodeB. The Radio Network Controller (RNC) is acting as a hub for the NodeBs (typically more than one NodeB are connected to the same RNC, but there is always only one RNC for any NodeB). Each RNC takes response on the resources of its set of cells. The operation of RNC is time-critical, as it has direct effect on network latency. It should be noted, that NodeB and RNC Iub interconnection via IP link can be implemented as cable (optical) line or microwave radio-relay link. The second solution is much cheaper and is preferred. IP transport in the Iub was introduced in 3GPP Release 5. Since all UMTS air interfaces further was upgraded to HSPA+, the UE can source high speed traffic to/from the Iub backhaul. 3G network allows separate (independent) dimensioning of the Iub and HSPA air interfaces. If the Iub has not been upgraded (from low speed Ethernet interfaces) during air interface upgrade (to HSPA+), it becomes a capacity bottleneck. To minimize effect of the Iub bottleneck, a congestion control, called Radio Link Control – Acknowledged Mode (RLC AM) is still defined in HSPA. The HARQ mechanism directly retransmits corrupted blocks in the air interface, whereas packet drops due to transport congestion in Iub are handled by the RLC AM. As the RLC AM must be located at the RNC instead of NodeB to be able to cover Iub, it adds noticeable greater retransmission latency compared to retransmissions made by HARQ. Massive HARQ operations can overload the transport network causing congestion and packet drop, consequently RLC AM retransmission will be triggered in. This leads to "spikes" in the packet delays even if the signal quality is stable. Such phenomena is well known and, for

example, is shown (but not described) in [45]. Both HARQ and RLC AM retransmissions add jitter to the data flow: HARQ retransmission adds several milliseconds, whereas RLC AM retransmission can add several hundreds of milliseconds due to Iub saturation. Note that HARQ is operating for all transport blocks, whereas RLC AM is enabled only if a reliable channel is required (for example, for file transfer via TCP protocol). This confirms that the Iub performance (also called "first mile link") have a significant impact on overall network performance and must be upgraded simultaneously with air interface upgrade.

Two RNC are interconnected via IP based link called Iur. This link was introduced in 3GPP Rel. 5. This channel is required to provide seamless soft handover only (transition from one cell to the next one without data transmission interruption) by operating in macro-diversity mode with maximum ratio combining and can't be used for UE to UE direct communications.

Further, RNC is connected to the Core Network (CN) by means of two interfaces: Iu-cs for the circuit-switched traffic and Iu-ps for the packed-switched traffic. Such topology decreases terrestrial network cost and keeps network latencies at a reasonable level, but such static configuration does not allow dynamic load sharing. Also, it should be noted, that starting from introduction of the HSDPA, its traffic is transmitted over IP/Ethernet path, while other traffic remains on Asynchronous Transfer Mode (ATM).
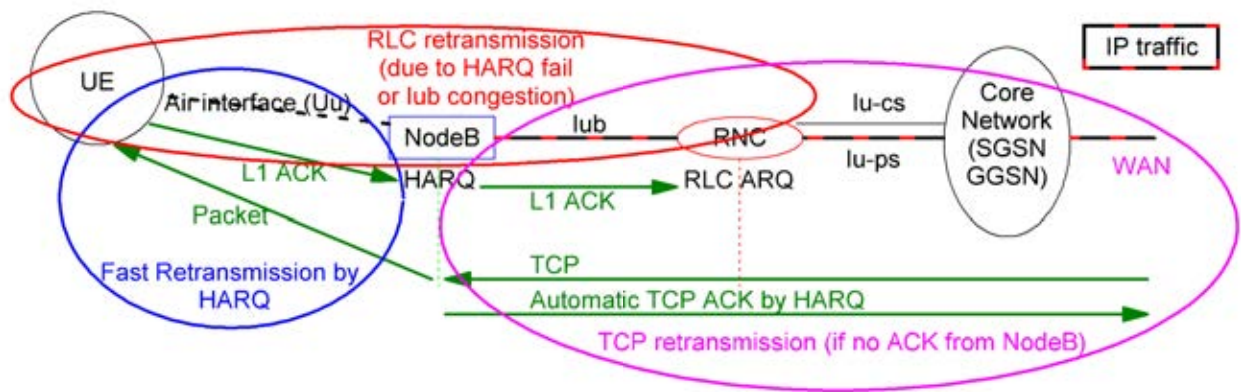
Fig. 2.1 3G packet switched traffic paths and TCP flow (3GPP Rel.5 and higher).

LTE network is a packet-switched service that supports end-to-end IP connection with defined quality of service (QoS). This means that there is no more Synchronous Digital Hierarchy (SDH), Synchronous Optical NETworking (SONET) or ATM equipment. This makes network cheaper, as well helps to reduce network latency. Its radio access is done thru Evolved UTRAN (E-UTRAN). The radio access hardware with radio resource control is implemented in the eNodeB. eNodeBs are directly interconnected with each other by means of X2 interface. However, X2 connections are used to serve soft handover function in eNodeBs coverage areas overlapping and does not provide direct traffic flow between two UEs. eNodeB is connected via S1 interfaces to its and neighbor EPCs. The EPC involves a control plane entity Mobility Management Entity (MME) and uses plane entity Serving GateWay (S-GW). The EPC also implies Packet Data Network Gateway (PDN GW), which interfaces with external network (wide area) and allocates IP addresses to the UEs. Such topology allows flexible load sharing and interference control (by means of relaying, cell handover hysteresis active control,

etc.) and even more reduced network latency. Also, there are no more controllers between base stations and core network elements. Inter-cell interference coordination on cell borders and relaying in order to enhance coverage and capacity are important topics since 3GPP Release 8 and are well-described in [50].
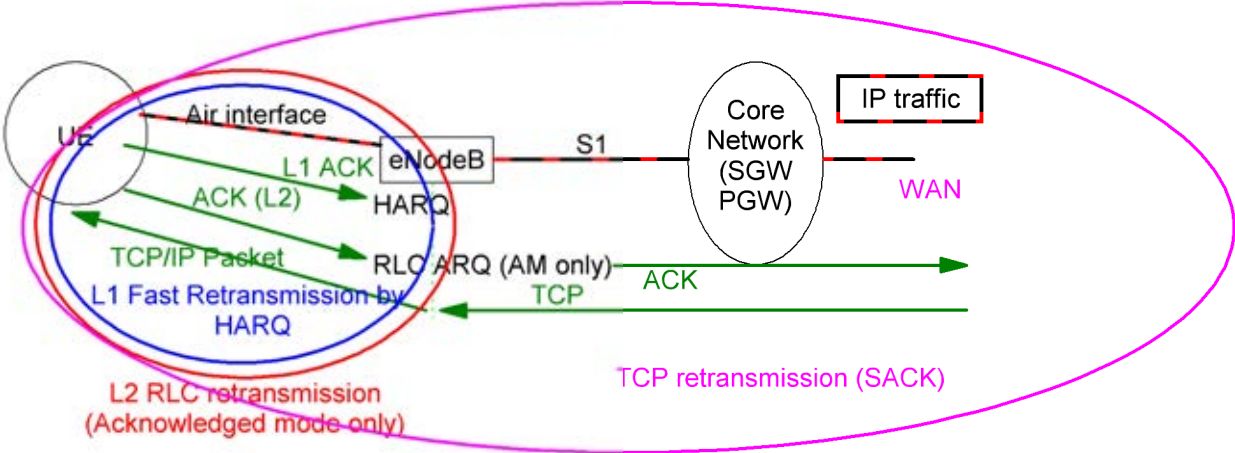

Fig. 2.2 LTE traffic paths and TCP flow (traffic is always IP packet switched.

The key differences of LTE E-UTRAN mobile backhaul compared to 3G UTRAN are:
- radio network functions implementation in the eNodeB (there are no more NodeB and RNC functions distribution, hence S1 link has no real time operation requirements);
- there is no need of RNC real-time operations (as its functions are implemented directly in the eNodeB);
- all-IP network that leads to simpler service concept (voice is also supported over IP only (VoIP)).

Interworking with different cellular operator networks (roaming) is possible over S8 interface between the EPC of home network and different operators' EPCs. This can lead to increased network latency. A more detailed explanation can be found in [12].

LTE cellular operators' EPC network supports interworking with 2G, 3G and WiMAX networks. The architecture for interworking with 3G conventional network is shown in Fig. 2.3.
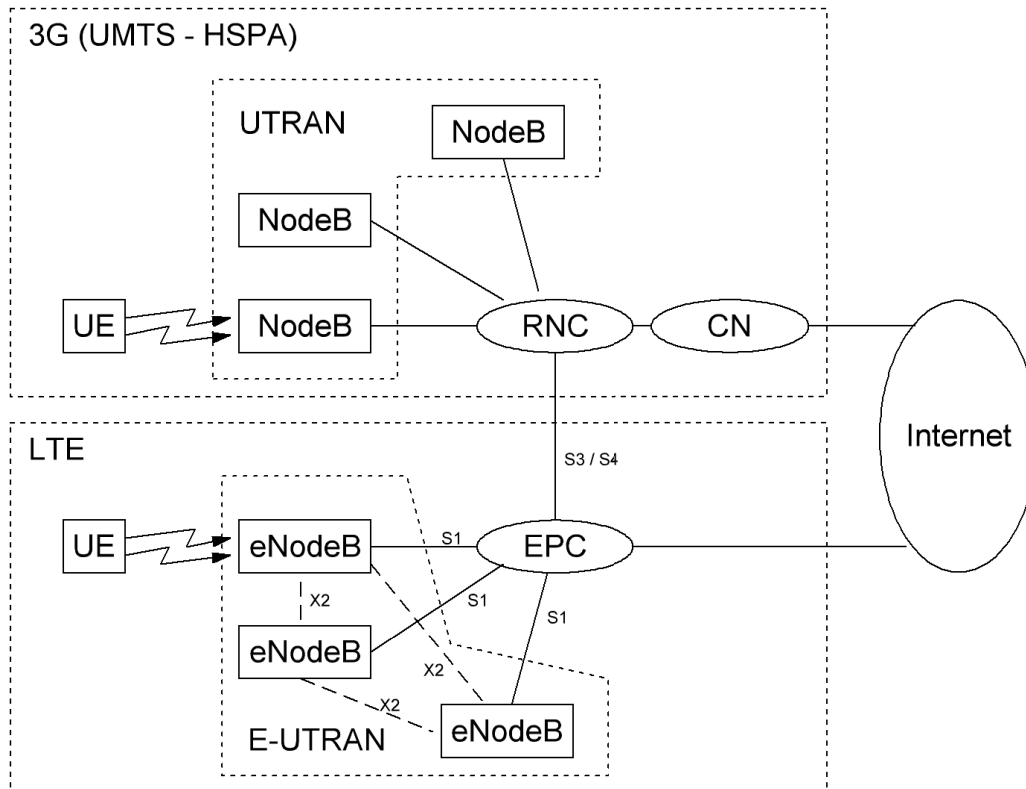
Fig. 2.3 Simplified schematic of the interworking terrestrial backhaul of LTE and 3G networks.

2.3. Evaluation of the readiness of 3G and LTE cellular networks in Latvia

The experimental testing was performed in 3G and LTE modes in Riga for Tele2, BITE and LMT cellular network operators.

The UE data packet is transmitted roughly in two stages: using cellular network operator equipment and using ground wired network segment. The cellular network operator equipment implies air interface, base station and core network. In the following description, all the above-mentioned will be referred to as "Cellular Network Operator network".

The ground wired network segment routing is done automatically, and the impact of this segment cannot be fully predicted since it depends on many factors as well as on the routing path, which is in use. This segment will be referred to as "Ground Wired network".

The Ground Wired network cannot be excluded from the testing because its infrastructure enables access to the destination servers or other equipment. On the other hand, the Ground Wired network can cause packet loss. It is not possible to identify where the packet has been lost. To exclude these kind of problems, two endpoints are used. One of them is located in Riga, the other is selected as the Google free DNS server (IP: 8.8.8.8). In this case, if one route does not respond and the other one is still operational, it is possible to conclude that the cellular

network operator service is in good condition while the data transmission error is caused by the ground wired segment network.

The use of ACK/NACK packets is usually preferred for the network latency/RTT, jitter and number of packet loss measurements [45], [52]. However, as it was already mentioned, starting with the requirements of 3GPP Release 5, the NodeB is responsible for the immediate acknowledgement of all received packets. This means that the packet retransmissions are made by HARQ. In case if they occur, these are not added to the time difference between sending a packet from the dongle and the ACK reception. This is the reason why delays, delay jitter and network availability were measured using a standard ICMP packets and well proven "ping" utility. The "ping" reported delay implies the sum of "send" and "reply" message travel time "to and back". It is known as a round trip time (RTT).

The request message was sent by the computer, which was equipped with the LTE capable mobile broadband USB dongle Huawei E3372h [53]. The Huawei E3372h is a 24th category 3G device which supports 64-QAM modulation and can be operational in dual cell DC-HSPA+ mode and a 4th category LTE device which supports full duplex operation with 20 MHz bandwidth. The dongle specification is shown in 2.1. table.

2.1. table

Characteristics of the Huawei e3372h USB dongle

Hardware	E3372h
Mode of operation	Hi-Link
Firmware	22.200.09.01.161_M_AT_01
WEBUI	17.100.13.01.03_HILINK_Mod1.2

Three dongles were used to facilitate parallel testing of all three mobile service operators simultaneously. Each mobile broadband USB dongle was attached to the dedicated computer. Computer specification is shown in 2.2. table.

2.2. table

Characteristics of the computer

Operating System	Microsoft Windows XP Professional SP3
Huawei driver	22.001.26.01.03

Three computers were working simultaneously to measure network parameters of Tele2, BITE and LMT cellular network operators.

The first selected endpoint was the server, located in the university building (IP: 213.175.90.193). The second selected endpoint was the Google free DNS server (IP: 8.8.8.8).

Operational mode of the mobile broadband USB dongles was set to Hi-Link (CdcEthernet). Then the second reported hop was made by the mobile broadband USB dongle internal NAT server. Fig. 2.4, Fig. 2.5 and Fig. 2.6 show the paths for BITE, Tele2 and LMT cellular network operators respectively.
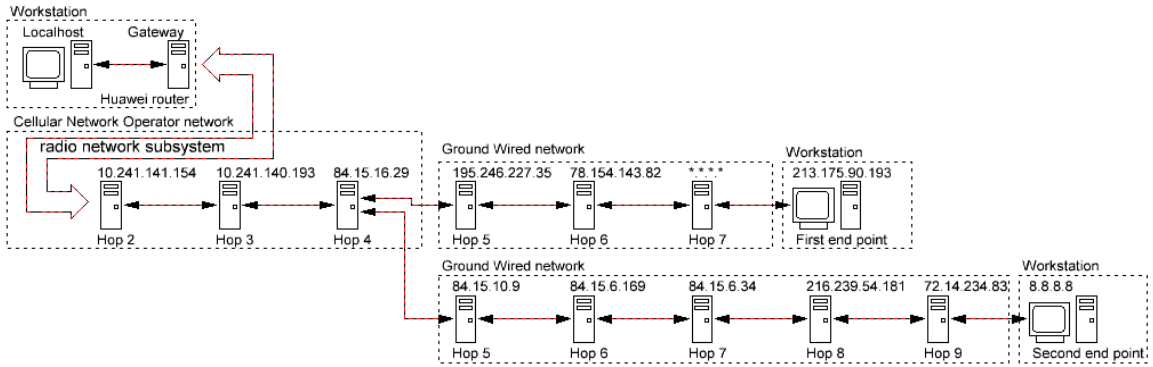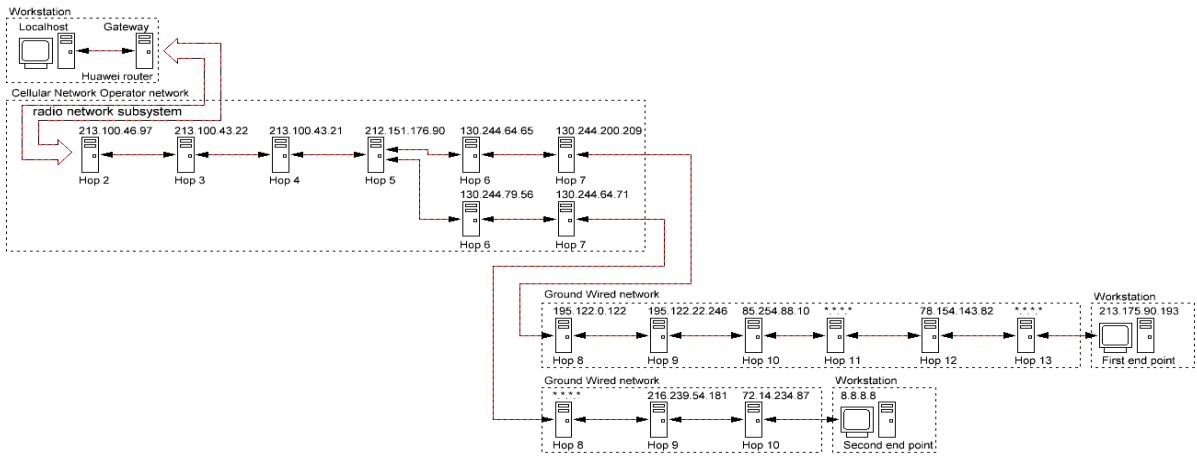
28

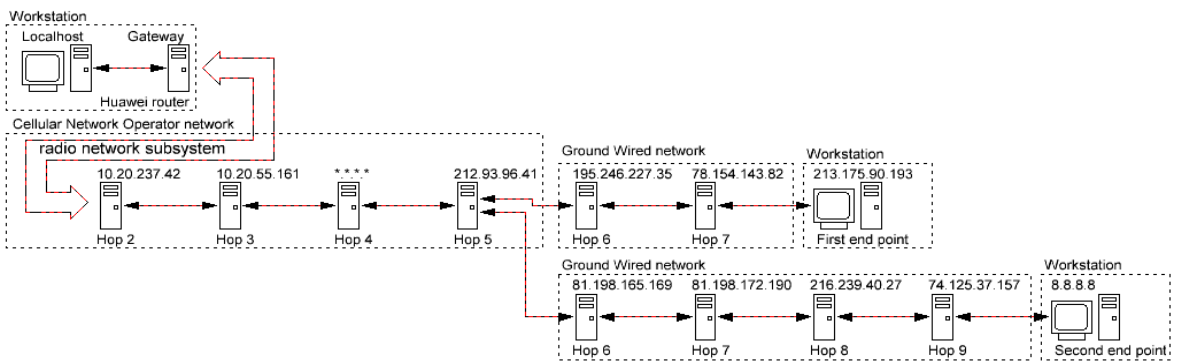Fig. 2.4 BITE-LV paths.

Fig. 2.5 Tele2-LV paths.

Fig. 2.6 LMT paths.

The RNS of all cellular network operator networks were defined as Hop 2. The end of the output networks server path, as well as the first and the second endpoint Hop numbers were individual for each operator. Table 2.3 summarizes distinctive points for the following experiments.

Distinctive points

Radio network subsystem	Operators output network servers	First endpoint	Second endpoint
BITE			
Hop 2: 10.241.141.154	Hop 4: 84.15.16.29	Hop 8: 213.175.90.93	Hop 10: 8.8.8.8
Tele2			
Hop 2: 213.100.46.97	Hop 5: 212.151.176.90	Hop 14: 213.175.90.93	Hop 11: 8.8.8.8
LMT			
Hop 2: 10.20.237.42	Hop 5: 212.93.96.41	Hop 8: 213.175.90.93	Hop 10: 8.8.8.8

The data transfer performance testing was done by running a standard Windows "ping" utility. The "ping" settings are shown in 2.4. table.

The settings of the "ping" utility

Send buffer size	32 bytes
Timeout	1 s
Period	10 s
Address	Destination IP
Logging	Text file output

The computers were located in Riga Technical University (RTU) building at Lomonosova 1, k-1. The mobile broadband USB dongles were equipped with randomly purchased SIM cards. The SIM card services are shown in 2.5. table.

Services of cellular network operators

BITE	"Bite 1": provides voice, sms and data communications (including LTE service) [54]
Tele2	"Datu plans 5": provides sms and data communications (including LTE service) [55]
LMT	"Prieksapmaksas mobilais internets": provides sms and data communications (including LTE service) [56]

The key parameters of the data transfer performance are average Round Trip Time (RTT), Jitter and network availability values.

The following LTE network performance data was obtained in July 2016. The test was performed during a one-week period. To exclude the impact of the ground wired network, the data was obtained only for the operator output network servers. The operator output network servers are shown in Table III.

The signal averaged parameters are shown in 2.6. table. Fig. 2.7, Fig. 2.8 and Fig. 2.9 show the RTT as a function of time for different distinctive points. Lost packets are shown as red rhombs on the X-axis.

2.6. table

Averaged parameters of the wireless signals in LTE mode during the experiment in 2016

	Technology	RSSI, dBm	RSRP, dBm	RSRQ, dB	SINR, dB
BITE	LTE	-57	-79	-7	17
Tele2-LV	LTE	-63	-92	-10	3
LMT	LTE	-59	-83	-7	4
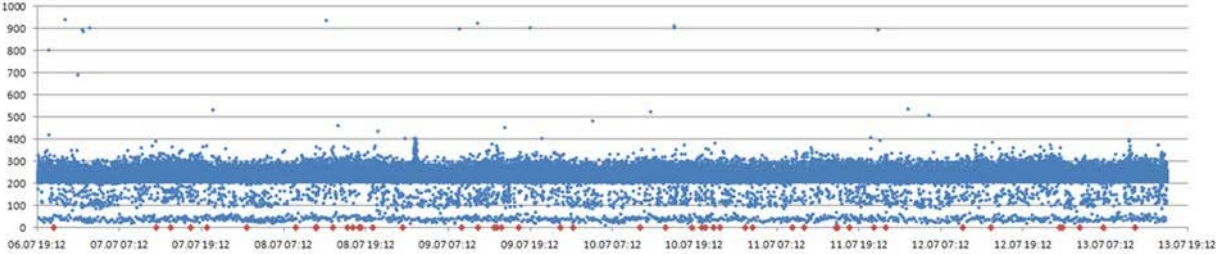
Fig. 2.7 RTT in time of Bite-LV of LTE network operator subsystem, ms.
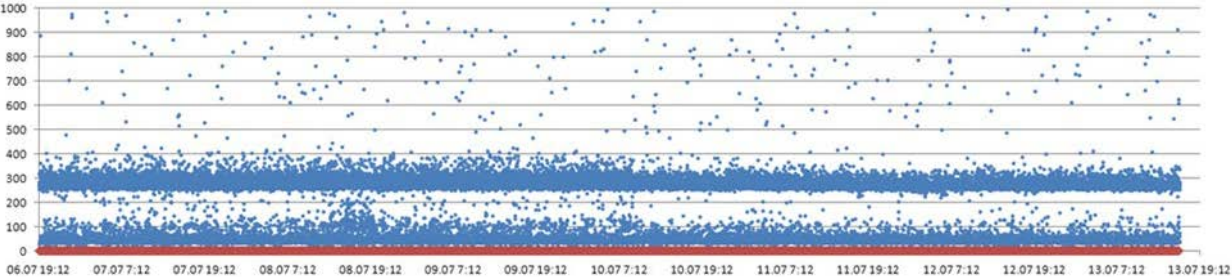
Fig. 2.8 RTT in time of Tele2-LV of LTE network operator subsystem, ms.
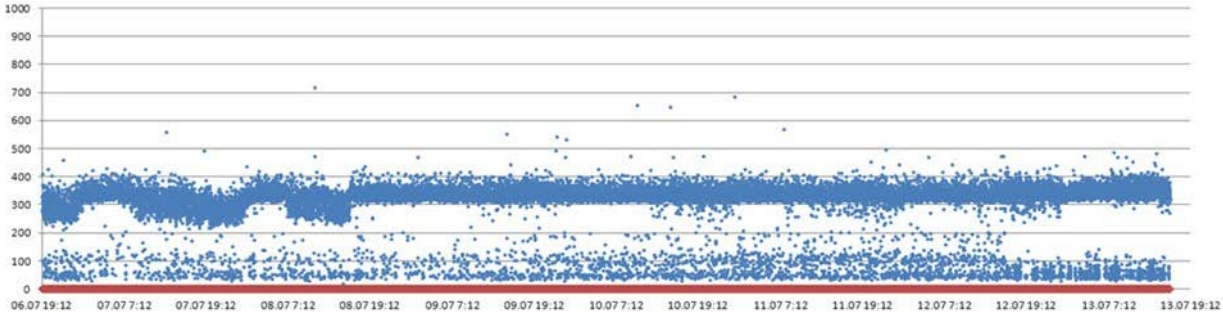
Fig. 2.9 RTT in time of LMT of LTE network operator subsystem, ms.

The summary for the performance of LTE networks in 2016 is presented in 2.7 table.

Performance of the LTE networks in 2016

	Packets Sent	Packets Lost	Average RTT, ms	Average Jitter, ms	Availability, %
Bite-LV	66 695	51	233.777	31.3756	99.9235
Tele2-LV	62 085	21 113	414.029	412.834	65.9934
LMT	61 240	25 476	520.369	334.119	58.3997

Large number of lost packets as well as high level of packet jitter show that the LTE infrastructure is overloaded in Riga and does not withstand the applied load. A typical 4G mobile broadband USB dongle typically switches to 3G mode under these conditions. The mobile broadband USB dongles were manually locked in LTE mode during the experiment. It was concluded that the quality of the LTE network service is not stable. It cannot be used for critical data transfer. Therefore, further analysis of LTE network was not performed.

3G HSPA+ network performance data was obtained in August 2016. Three computers were equipped with the Huawei 3372h mobile broadband USB dongles and were working simultaneously. The test was performed during the working days of a one-week period. The data was obtained for the operator output network servers as well as for the endpoints (RTU server and Google free DNS server). See 2.3 table for more details. Two endpoints were used to exclude the impact of the ground wired network.

The signal parameter mean values for all three mobile network operators are shown in Table 2.8.

2.8. table

Averaged parameters of the wireless signals in 3G mode during the experiment in 2016

	Technology	RSSI, dBm	RSCP, dBm	E_C/I_O, dB
BITE	DC-HSPA+	-65	-71	-6
Tele2	HSPA+	-53	-60	-7
LMT	DC-HSPA+	-60	-65	-5

Mobile broadband USB dongles of all cellular network operators automatically switch to UMTS mode if there is no data traffic. The first data packet is always sent in UMTS mode. As soon as the data traffic is detected, the dongle switches to HSPA+ or DC-HSPA+ mode (depending on cellular network operator). It is impossible to lock the dongle in HSPA+ or DC-HSPA+ modes using the local settings. If there is no traffic for 2 seconds, the dongle switches back to UMTS mode. As the ping request is being sent every 10 seconds, the mobile broadband USB dongle switches to HSPA+ or DC-HSPA+ and back to the UMTS mode. To overcome this problem, low-capacity background traffic was used: a pinging of randomly available server was done in a one-second period with 32-byte packet.

The RTT data of the less loaded 3G cellular network operator subsystem is shown in Fig. 2.10 as a function of time. Lost packets are shown as red rhombs on the *X*-axis. Their

distribution is shown in Fig. 2.11. The CDF is shown as red squares. The distribution is obtained for interval of 0 to 0.999 probabilities.

It is important to consider the impact of the ground wired network segment. The RTT for the first and the second endpoint are shown in Fig. 2.12 and Fig. 2.13 respectively as a function of time. Lost packets are shown as red rhombs on the *X*-axis.
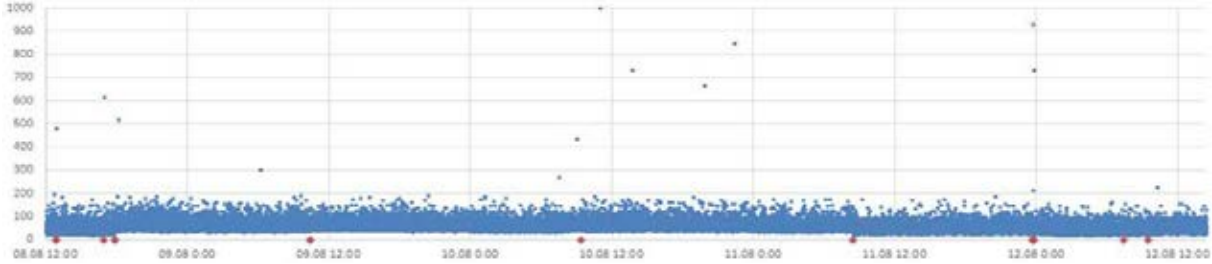

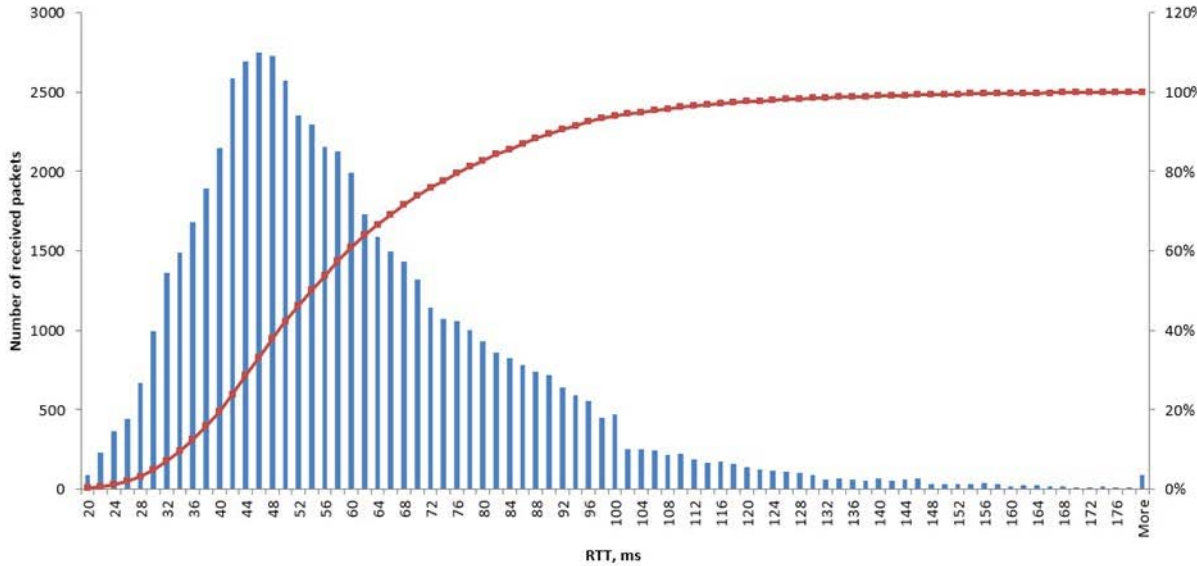Fig. 2.10 RTT in time of lightly loaded 3G network operator subsystem (LMT), ms.

Fig. 2.11 Distribution of RTT of lightly loaded 3G network operator subsystem (LMT).
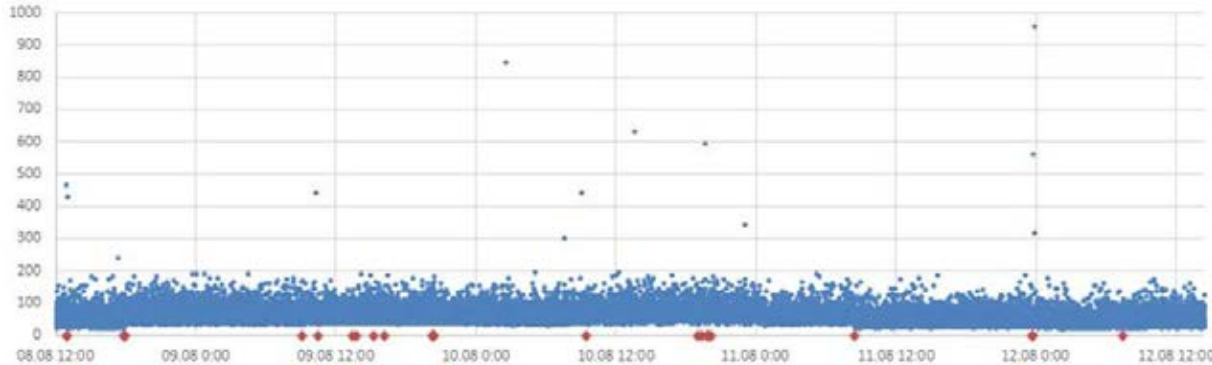
Fig. 2.12 RTT in time of lightly loaded 3G network of the first endpoint (LMT), ms.

33
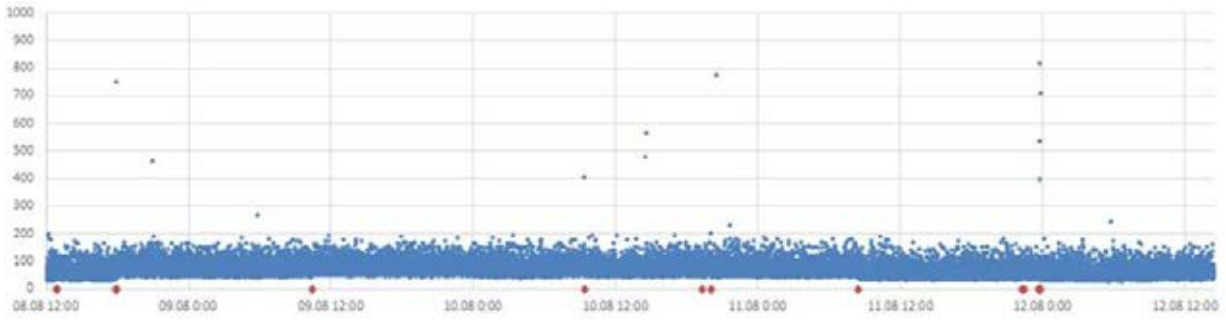
Fig. 2.13 RTT in time of lightly loaded 3G network of the second endpoint (LMT), ms.

The results for the lightly loaded 3G network are summarized in 2.9. table.

The performance of the lightly-loaded 3G service (LMT)

	Packets send	Packets lost	Averaged RTT, ms	Averaged Jitter, ms	IPDV, ms	Availability, %
LMT output network server	58 490	30	60.0174	25.3284	169	99.9487
LMT 3G to the first endpoint	58 488	36	61.1444	61.1444	164	99.9385
LMT 3G to the second endpoint	58 487	25	70.3126	25.8207	156	99.9573

The RTT of the heavily loaded 3G cellular network operator subsystem is shown in Fig. 2.14 as a function of time. The mobile broadband USB dongle is locked in 3G mode and cannot automatically switch to the 2G mode. The cellular network operator chooses 3G operation mode between HSPA+ when the network is not overloaded, and UMTS when the network is overloaded. Lost packets are shown as red rhombs on the *X*-axis.

The RTT distribution of the heavily loaded 3G cellular network operator subsystem is shown in Fig. 2.15. The CDF is shown as red squares, PDF is shown as blue columns. The distribution is obtained for 0 to 0.999 probabilities.
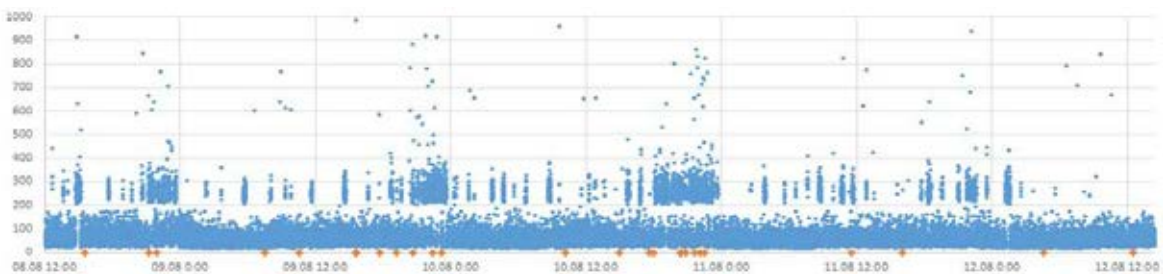

Fig. 2.14 RTT in time of heavily loaded 3G network of the operator subsystem (Tele2-LV), ms.
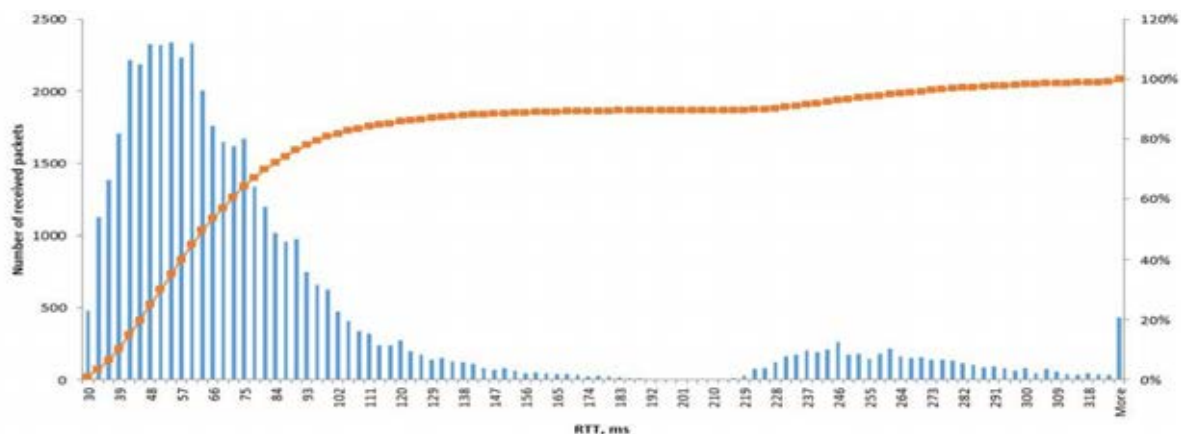
34

Fig. 2.15 RTT distribution of heavily loaded 3G network of the operator subsystem (Tele2-LV), ms.
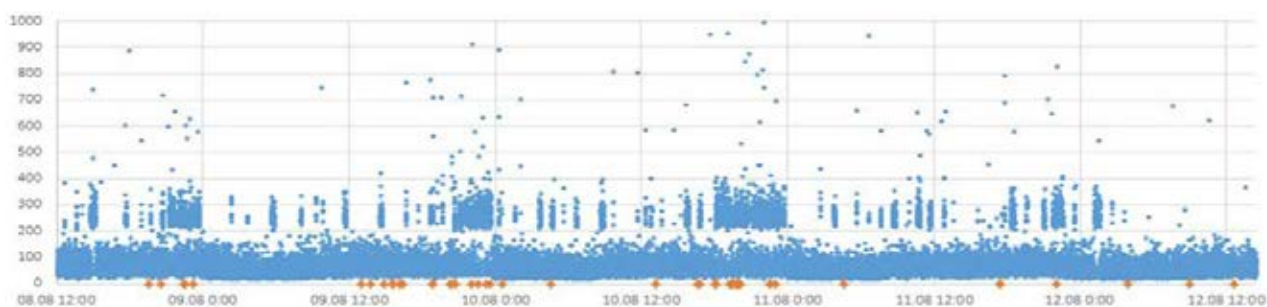

Fig. 2.16 RTT in time of heavily loaded 3G network of the first endpoint (Tele2-LV), ms.

Fig. 2.17 RTT in time of heavily loaded 3G network of the second endpoint (Tele2-LV), ms.

2.10. table

Delays of the heavily loaded 3G service (Tele2-LV)

	Packets send	Packets lost	Averaged RTT, ms	Averaged Jitter, ms	IPDV, ms	Availability, %
Tele2 output network server	45 725	33	81.0260	30.5914	707	99.9278
Tele2 3G to the first endpoint	45 712	59	82.4103	30.4748	627	99.8709
Tele2 3G to the second endpoint	45 695	58	87.9433	31.3205	725	99.8731

The results for the heavily loaded 3G mode are summarized in 2.10. table.

Typically, the switching between HSPA+ to UMTS and back can cause one packet loss. Fig. 2.18 and Fig. 2.19 show the RTT of the heavily loaded 3G cellular network as a function of time with a time delay between modes of operation switching. In this case, the number of switching events is limited. Lost packets are shown as red rhombs on the *X*-axis. Due to the 10-second ping interval, only one packet can be lost during the switching of operation mode while the other will pass. To demonstrate all the lost packets, all three results for the network operator subsystem, first and second endpoints are presented in Fig. 2.18. Zoomed-in section of Fig. 2.18 diagram is shown in Fig. 2.19.
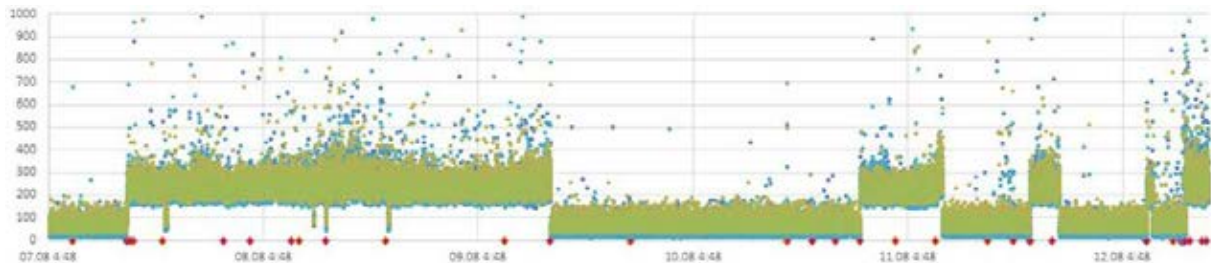

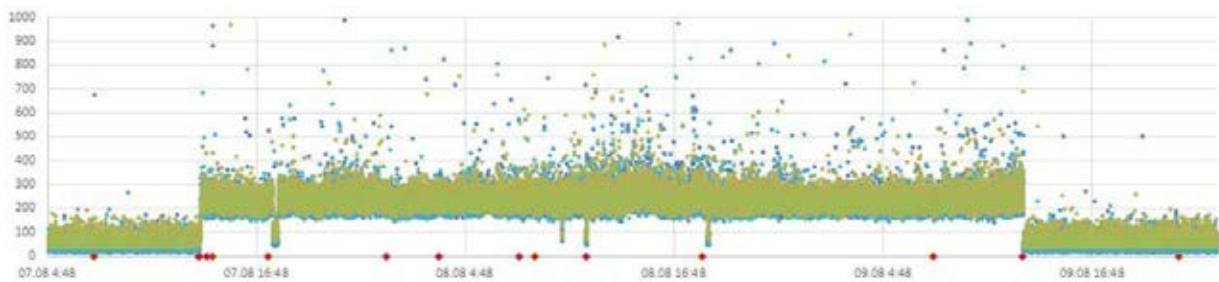Fig. 2.18 RTT in time of heavily loaded 3G network of all endpoints (Bite-LV), ms.

Fig. 2.19 Zoomed-in part of RTT in time of heavily loaded 3G network of all endpoints (Bite-LV), ms.

In 2018 LTE cellular network data transfer service testing was repeated. The test was performed in Tele2-LV during a 2,5 days period and 200'000 RTT values were obtained. A google free DNS server (IP: 8.8.8.8) was used as an endpoint. The server, located in the university building, was omitted, as it has less trusted terrestrial link. The signal averaged parameters are shown in 2.11 table.

Fig. 2.20 and Fig. 2.21 show the RTT (in ms) as a function of time for B3 (1800MHz) and B20 (800 MHz) LTE bands respectively. Packets with RTT greater than 1000 ms are considered as lost. Lost packets are shown on the X axis by the red squares. The RTT distribution of LTE B3 and LTE B20 cellular networks are shown in Fig. 2.20 and Fig. 2.21 respectively. The CDFs are shown as red squares, PDF is shown as blue columns. The distribution is built for the interval of 0 to 0.999 probabilities. The IPDV will not be calculated here, as its value depends on current cell in use. This problem will be explained in more details in Chapter 2.6

Averaged parameters of the radio signals in LTE during the experiment in 2018

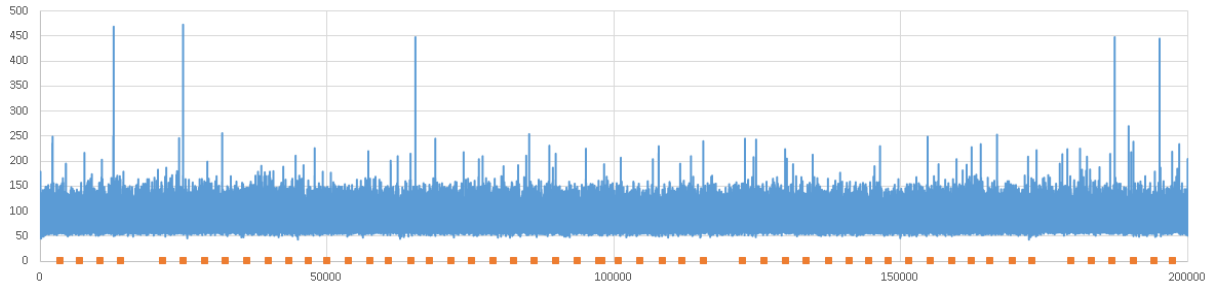| Tele2-LV	Technology	RSSI, dBm	RSRP, dBm	RSRQ, dB	SINR, dB
B3 (1800 MHz)	LTE Cat.4	-61	-90	-9	-1
B20 (800 MHz)	LTE Cat.4	-53	-78	-12	-2

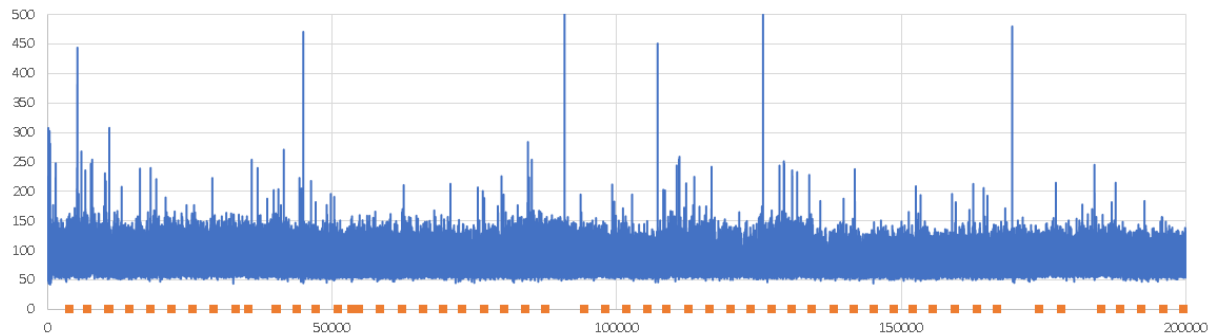Fig. 2.20 RTT in time of LTE B3, ms.
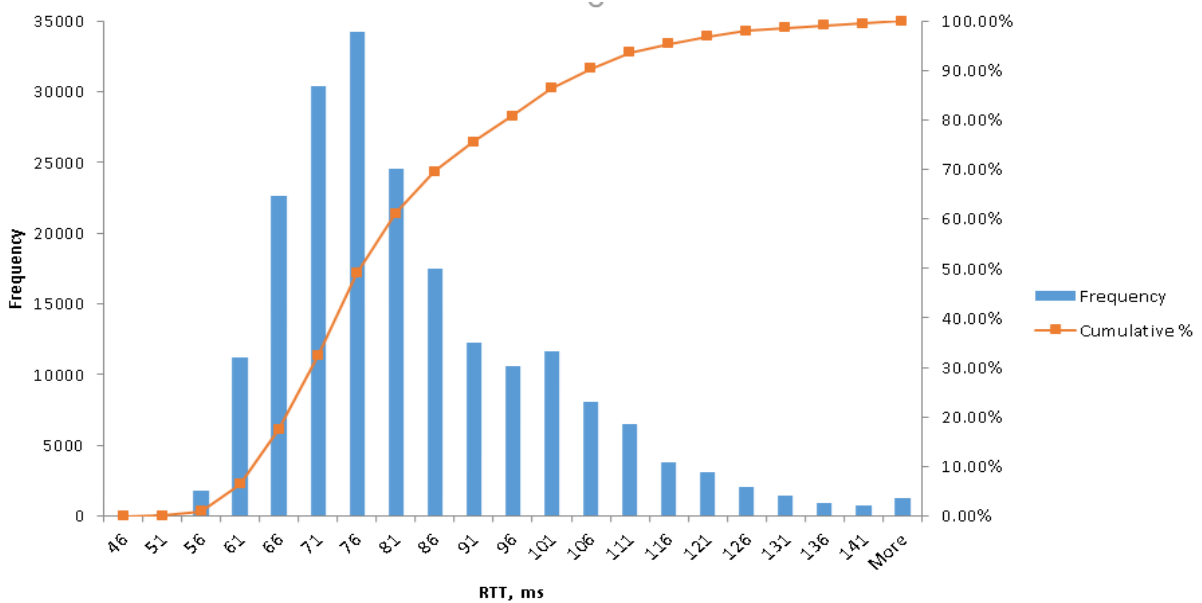

Fig. 2.21 RTT in time of LTE B20, ms.

Fig. 2.22 Distribution of RTT values in LTE B3.
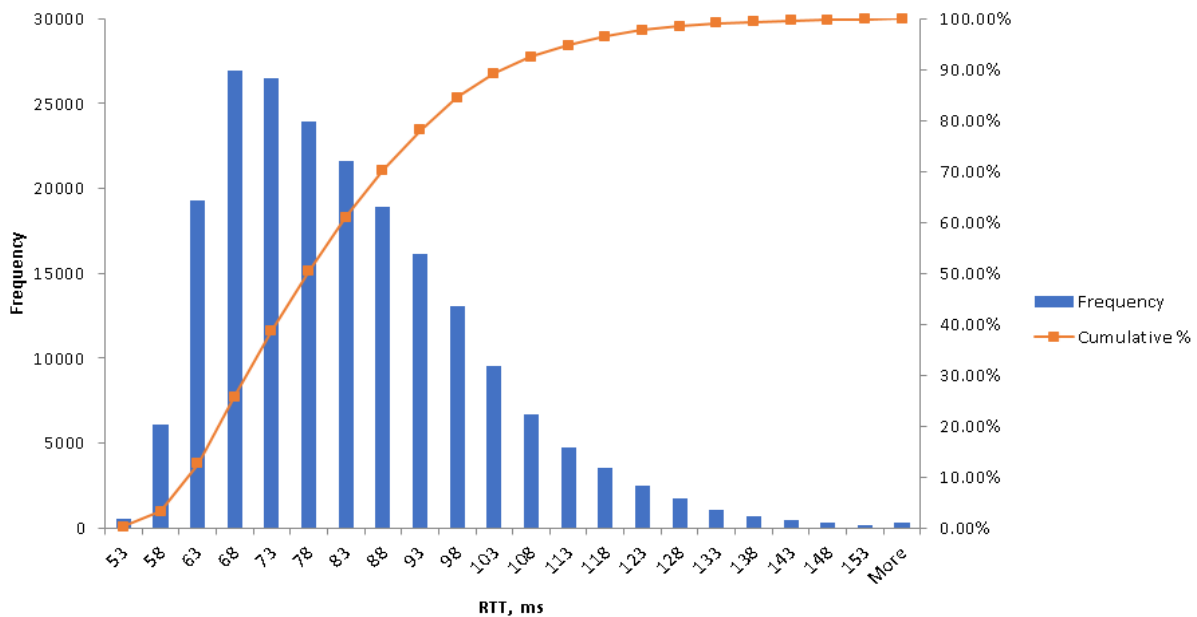
Fig. 2.23 Distribution of RTT values in LTE B20.

Network performance data of the LTE B3 and LTE B20 is shown in 2.12. table.

<div align="right">2.12. table</div>

Delays of the LTE cell in 2018 (Tele2-LV)

Tele2-LV	Technology	Averaged RTT, ms	Averaged Jitter, ms	Packet loss, %
B3 (1800 MHz)	LTE Cat.4	82	23	0.0269
B20 (800 MHz)	LTE Cat.4	81	17	0.0278

It can be concluded, that:

1. in 2016 LTE networks in Riga were overloaded and their service quality was unstable. During these experiments, the network availability of only one LTE cell is 99.95 %, while the network availabilities of two other cells are 66 % and 58 % respectively. The RTT mean value is more than 4 times bigger than in 3G HSPA+ mode.

2. A lightly loaded 3G network has excellent performance for the small packet traffic between the ground wired server and stationary computer equipped with mobile broadband USB dongle. Its RTT mean value (including ground wired network delays) is almost 70 ms and network availability (measured during a one-week period) is more than 99.95 %. However, it is desirable to keep in mind that the end service quality of data transmission also depends on the quality of service of the ground network segment, which connects servers, located in the WAN (see comparison between the google free DNS server and the server, located in the University building)..

3. When the 3G cell approaches its saturation, the mode can be switched to UMTS. Then the switching between UMTS and HSPA+ modes reduces network performance

because the switching typically comes with a loss of at least one packet (see Fig. 2.19). In addition, UMTS mode has worse performance: its RTT value is approximately 4 times greater. In the case of operation in highly loaded network (E_C/I_O drops to less than −7 dB while RSSI is stable), it is hard to foresee the parameters of the network to estimate real-time transfer mechanism of critical data.

4. Repeated experiments showed than since 2018 the performance of LTE networks in Riga becomes stable. Consequently, in further chapters, LTE network will be analyzed as the main candidate to implement wireless path of the "C2 Link". No more conclusions and comparisons about the performance of LTE network are provided here, because the performance of the cellular network should to be tested in its various cells.

2.4. Application of the distribution law to the delay values in LTE cell

Application of a distribution law on RTT sample allows to describe overall cell performance with only few distribution parameters, as well as significantly simplify various types of supplemental calculations.

First, let's perform a tentative graphical test of the applicability of the distribution law. This can be done in MATLAB application via the *Distribution Fitter* addon. In this graphical test, sample with RTT ordered data is compared with expected values of ordered statistics of gamma, lognormal and exponential distributions and is presented in Fig. 2.24.
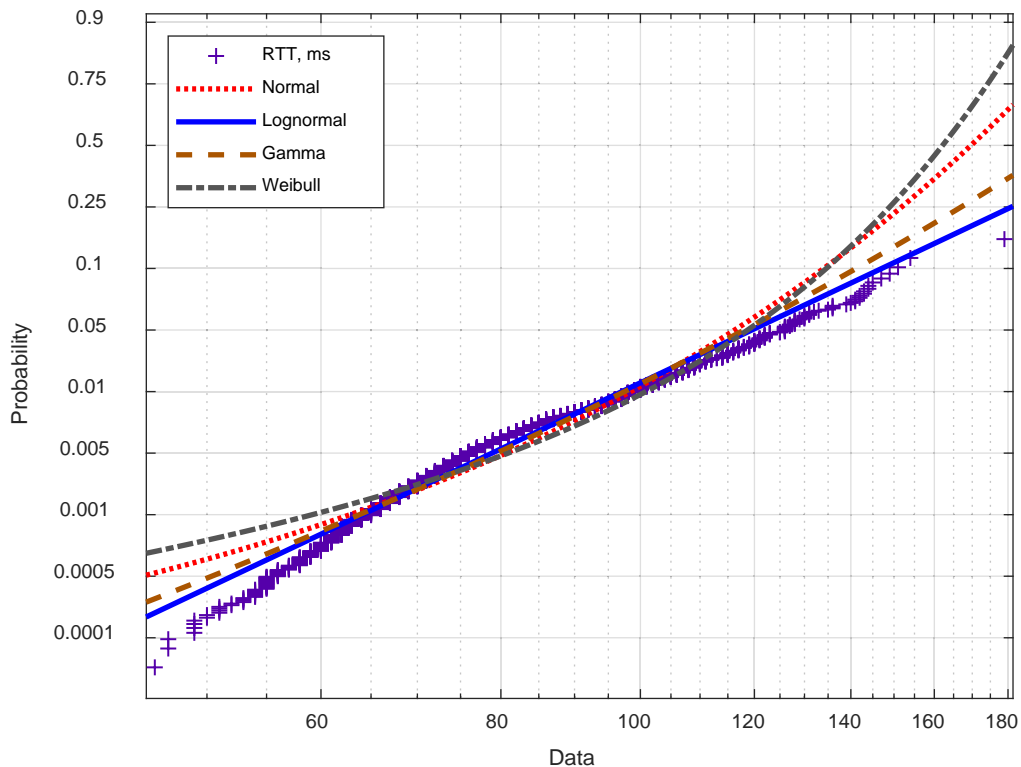

Fig. 2.24 Probability plot of the ordered RTT values, compared to gamma, log-normal and exponential distributions

This preliminary visual evaluation shows that the empirical distribution function of RTT values of the LTE cell most probably is consistent with the logarithmically normal distribution. Now, this hypothesis must be quantitatively verified. The hypothesis on type of distribution will be tested via two methods. The first one is the goodness-of-fit method, called Test based on Probability Plot of Ordered Statistics, or OSPPT, suggested by the professor of our university [57]. The value of the statistic of the goodness of fit test of the assumed distribution function is defined as follows:

$$OSPPt = \sqrt{\sum_{i=1}^{n} \frac{(\acute{x}_i - x_i)^2}{ns^2}} \tag{2.4}$$

where:
OSPPt   - is the statistic of the OSPPTest
x_i - ordered expected values $x_i = \acute{\theta}_0 + \acute{\theta}_1 E(\dot{X}_i)$
$\acute{\theta}_0$ and $\acute{\theta}_1$ - are estimates of θ_0 and θ_1 parameters
$\acute{x}_i$ - ordered observations (experimentally obtained data)
s^2 - is $s^2 = \sum_{i=1}^{n} \frac{(x_i - \bar{x})}{n}$
n - is the number of observations

The value of the *OSPPt* statistic is determined using regression analysis and is invariant to the number of samples. The expected values x_i from population of the expected CDF as well as the observations $\acute{x}_i$ forms discrete functions with the limited number of values *n*. In order to reduce the error, caused by the discrete behavior of x_i, the Monte-Carlo method is used: the expected values are generated *N_{MCorderStatistic}* times and the values of x_i for each position *i* are averaged.

The critical region of the OSPPt test of the hypothesis under consideration is defined by the inequality (3.2).

$$OSPPt = \sqrt{\sum_{i=1}^{n} \frac{(\acute{x}_i - x_i)^2}{ns^2}} > C_{alfa} \tag{2.5}$$

where:
C_{alfa} - in the boundary for the critical region
alfa   - significance level

The critical region C_{alfa} of the OSPPt test is defined as a fractal of the probability *1-alfa*, where *alfa* is the probability of the first order error, referred to as the "significance level". For this, the *C* values are ordered $C_0 \leq C_1 \leq ... \leq C_{MCalfa}$. Then, the C_{alfa} value can be found from the ordered samples by taking the value with the required sequential number as follows:

$$C_{alfa} = C_{MCalfa \cdot (1-alfa)} \tag{2.6}$$

where:
alfa   - is the required level of significance.

Typically, IP Performance Metrics Working Group (IPPM) goodness-of-fit tests are conducted using 5% significance [38]. Therefore, the value C_{alfa} is calculated as the fractal of the probability 1-0.05=0.95. Thus, if $OSPPt > C_{alfa}$, then the test of the goodness-of-fit of the assumed distribution is failed for the given confidence level *1-alfa*.

To make sure that the network load was not changed significantly, only the first 2000 samples were analyzed. A graphical representation of the RTT values (in log scale) and the statistics of deviations (scaled to 95%) for the Log-Normal hypothesis are shown in Fig. 2.25 and Fig. 2.27 respectively. Since the x scale is in logarithmic units, the *OSPPt* statistics is estimated for normal distribution.
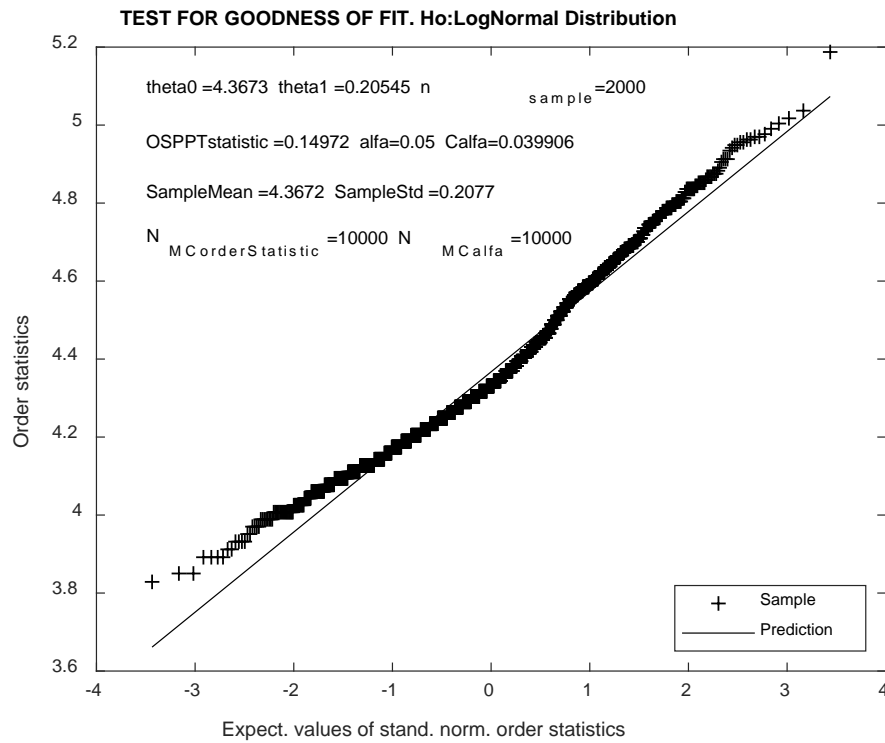

Fig. 2.25 Test for goodness of fit for the lognormal distribution hypothesis.

The value of C_{alfa} of 0.039906 is significantly less that the value of *OSPPt* statistic, therefore, the hypothesis should to be rejected. For more clarity, the histogram of *OSPPt* statistics for C_{alfa} values is shown in Fig. 2.26. Here, the value of C_{alfa} is a fractal of (1- alfa)=0.95.
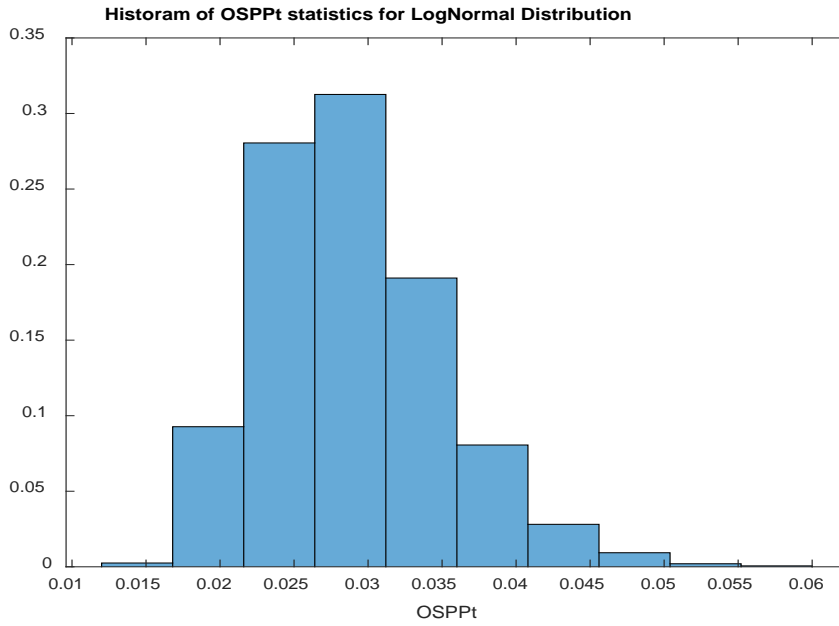
Fig. 2.26 Histogram of OSPPt statistics for C_{alfa} for the lognormal distribution hypothesis.

The histogram of deviations $\varDelta x$ of the observed data from the expected lognormal data is shown in Fig. 2.27. The values are converted back to natural scale. The x scale of the Fig. 2.27 is scaled to the level of 95% for better visual representation. As can be seen, 95% of deviations are less than 5.4892%. The deviations $\varDelta x$ of the observed data $\acute{X}_\iota$ from the expected data x_i is defined by (3.4).

$$\Delta x = abs\left(\frac{\acute{x}_i - x_i}{x_i}\right) \cdot 100\% \qquad (2.7)$$
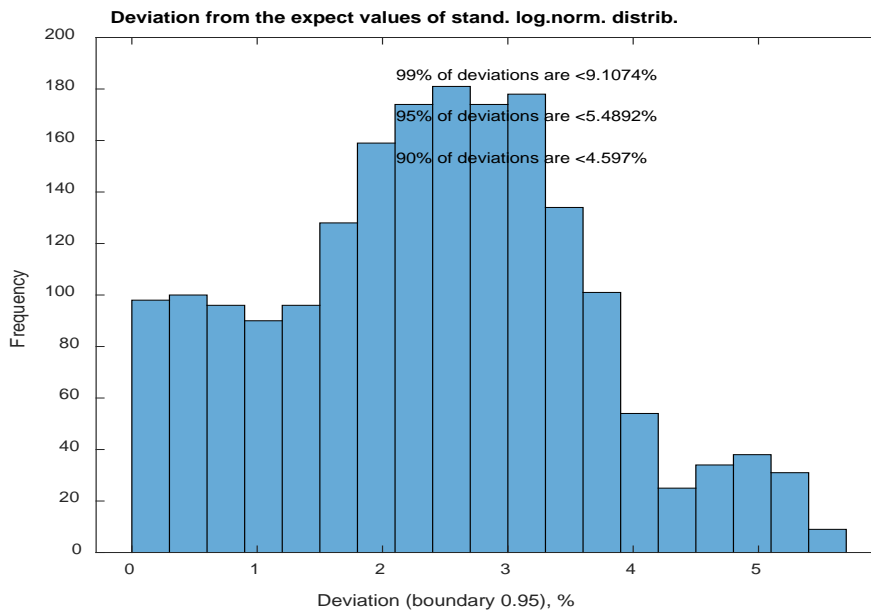

Fig. 2.27 Histogram of the observed data deviations from the expected lognormal data.

42

For the comparison, a graphical representation of the RTT values and the statistic of the gamma distribution hypothesis is shown in Fig. 2.28.
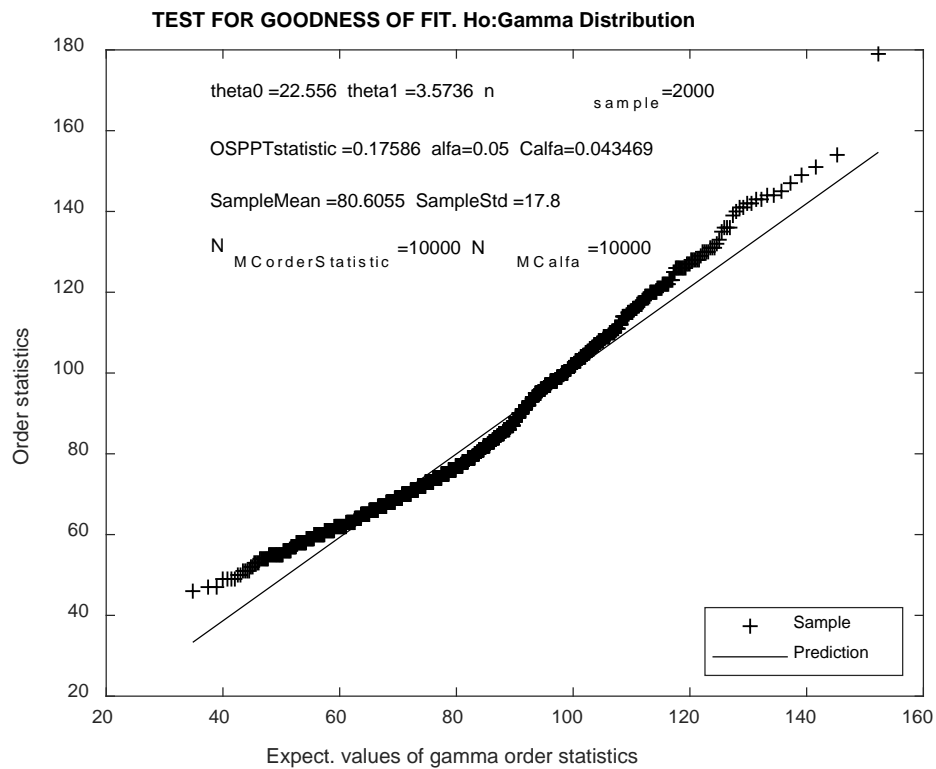

Fig. 2.28 Test for goodness of fit for the gamma distribution.
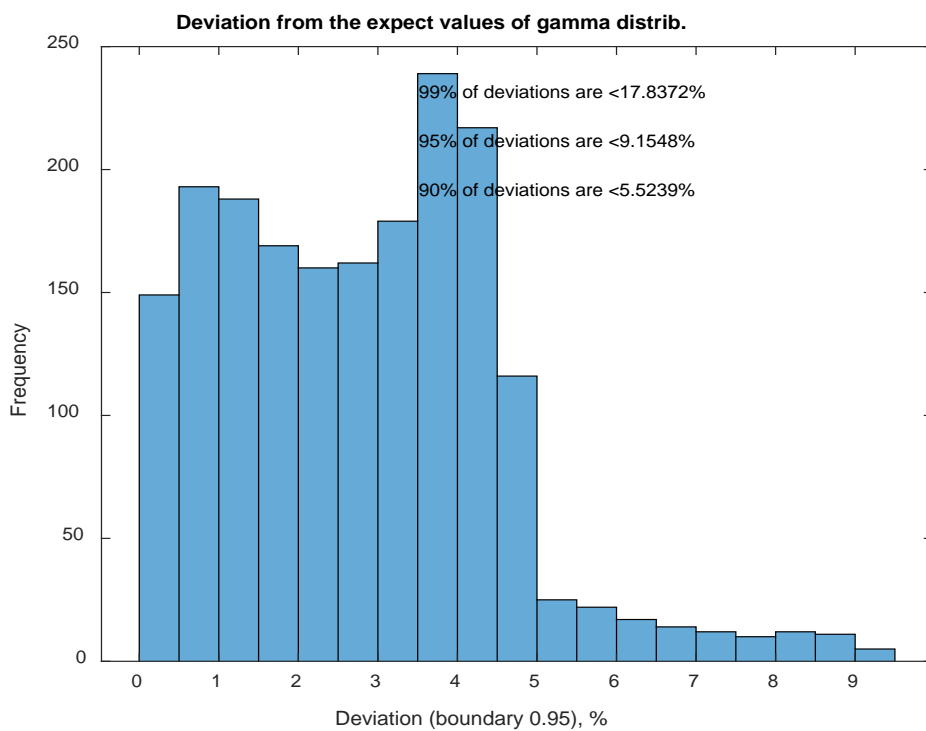

Fig. 2.29 Histogram of the observed data deviations from the expected gamma-distributed data.

The *OSPPt* statistic value of 0.17586 is greater than the value of C_{alfa} of 0.043469, therefore, the hypothesis of the gamma distribution should to be rejected to. Further, as can be seen from Fig. 2.29, 95% of deviations are less than 9.1548%.

Further illustrations are not shown to save the space. The results for the Log-normal, Gamma, Normal and Weibull hypotheses are summarized in Table 2.13.

2.13. table

Values of the OSPPt statistics for Log-normal, Gamma, Normal and Weibull distribution hypotheses

Null hypothesis	OSPPt statistic	Critical value C_{alfa}	Deviation from the expected (at the 0.90 boundary), %	Deviation from the expected (at the 0.95 boundary), %	Deviation from the expected (at the 0.99 boundary), %
Log-Normal	0.14972	0.039906	4.5970	5.4892	9.1074
Gamma	0.17586	0.043469	5.5239	9.1548	17.8372
Normal	0.26687	0.039949	8.4735	13.7242	31.8879
Weibull	0.37532	0.06546	11.0790	16.8631	28.9140

The data of the OSPPtest analysis indicates that the delays of the LTE cell does not fit to any of the distribution functions, tested with the confidence level of 95%.

Further, the delays of the LTE cell will be tested in accordance of the Anderson-Darling goodness-of-fit test, or ADT. The ADT test is suggested for various metric tests of the network performance [40], [58]. Here, the uncorrected ADT statistic A is defined by the equation:

$$A = -n - \frac{1}{n}\sum_{i=1}^{n}\left((2i-1)\left(lnF(X_i) + ln\left(1 - F(X_{n-i+1})\right)\right)\right) \tag{2.8}$$

where:
A - is the statistic of the ADTest
n - is the number of observations
$F(X_i)$ - is the CDF of the specified distribution
X_i - ordered sample data

The same $n = 2000$ samples will be tested in accordance with ADT. The level of significance also is set to 5%. The ADT will be performed for the Log-normal, Gamma, Normal and Weibull distributions in the MATLAB application via the *adtest* function. The parameters of these distributions are unknown, and their estimates are obtained via the maximum likelihood method. The results for the Log-Normal, Gamma, Normal and Weibull hypotheses are summarized in Table 3.14, where the A is the value of the statistic of ADT; P is the probability of observing an A statistic more extreme than the observed value under the null hypothesis, CV_{alpha} is the critical value for the given level of significance.

Values of the ADT statistics for Log-normal, Gamma, Normal and Weibull distribution hypotheses

Null hypothesis	P	A	$CV_{0.05}$
Log-Normal	< 0.0005	15.786	0.75161
Gamma	< 0.0005	23.001	0.75161
Normal	< 0.0005	41.833	0.75161
Weibull	< 0.0005	59.394	0.76506

The data of the ADT analysis indicates that the delays of the LTE cell does not fit to any of the distribution functions, tested with the confidence level of 95%, because in all cases $A > CV$ as well as p values are very low.

Despite on the fact, that the delays of LTE cell does not fit to any distribution law, tested with the confidence level of 95%, these are mostly fit to logarithmically normal distribution. Note that 95% of delay values deviates from the expected log-normal distributed data for less than 5.4892%. Further, in Fig. 2.24 it is shown, that the majority of deviations of the observed delay values from the expected log-normal distributed values occurs at very low and very high values. First of all, the minimum value of the delay in the network is defined by the implementation of the network backhaul and can be reached if the network is used by single user only, whereas the logarithmically-normal distribution function is a continuous probability function, therefore, has no minimum value at all. From other side, the maximum values of the delays in reality are limited to the maximum acceptable delay, after which the packet is considered lost and can be requested to be resent again. Therefore, it is not entirely correct to compare these maximum values with the continuous probability function.

2.4.1 Assuming the logarithmically normal distribution

Since the moderate values of the delays of LTE cell almost fits to log-normal distribution and only very high and low values deviates from this, let's assume that the delays of LTE cell obey the logarithmically normal distribution. Under this assumption, lets verify the accuracy of the prediction of delay average value and packet Jitter value.

First of all, let's estimate the parameters of log-normal distribution. The distribution function parameters estimation can be done via various methods, but the Maximum Likelihood Method (MLM) is recommended here because it is more applicable for processing of censored observations. Here it is possible to omit preliminary calculations and represent final equations for the $\hat{\theta}_0$ (median) and $\hat{\theta}_1$ (standard deviation) estimation, assuming lognormal distribution [59]:

$$\hat{\theta}_0 = \mu = \bar{x} \tag{2.9}$$

$$\hat{\theta}_1 = \sigma = \sqrt{\frac{\sum\left(ln(x) - ln(\bar{x})\right)^2}{n-1}} \tag{2.10}$$

First 2000 values of the experimental data, mentioned in the Chapter 2.2, now will be analyzed via the MLM. The results are $\hat{\theta}_0 = 4.367$ and $\hat{\theta}_1 = 0.20557$ respectively. Since only first 2000 values of the experimental data were analyzed, these also will be analyzed to estimate RTT mean and Jitter values. Further, 2000 values of random variables will be generated with assumption that the distribution function is log-normal and $\hat{\theta}_0$ and $\hat{\theta}_1$ are equal to estimated values $\hat{\theta}_0 = 4.367$ and $\hat{\theta}_1 = 0.20557$. The packet jitter is calculated as an average deviation from the network mean latency and is calculated using equation, described in RFC3550 [43]. The results are presented in Fig. 2.30 for visual comparison.
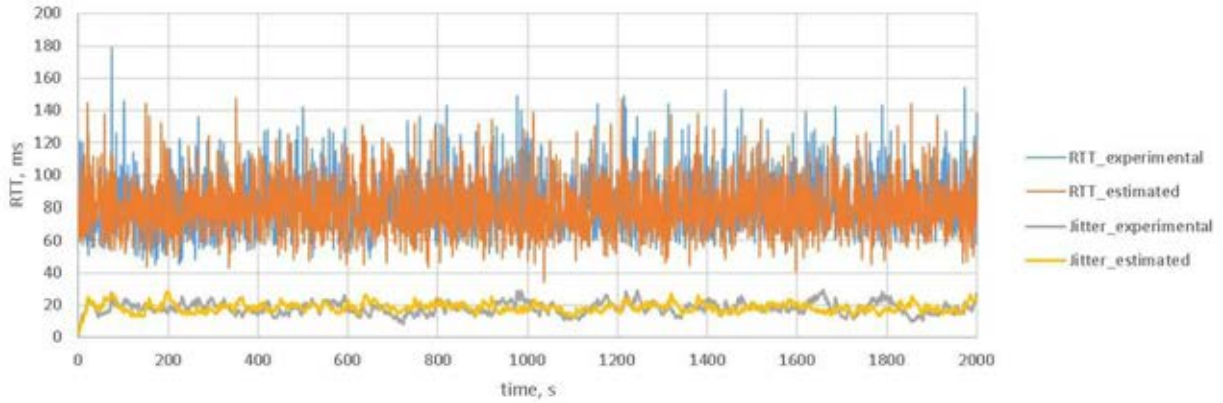

Fig. 2.30 Experimental and estimated RTT and Jitter values.

Experimental data for first 2000 RTT values is the following: average RTT=80.62 ms ; average Jitter = 18.45 ms. Estimated data for n=2000, if $\hat{\theta}_0 = 4.367$ and $\hat{\theta}_1 = 0.20557$ and assuming log-normal distribution, is the following: average RTT=80.67 ms (error=0.062%); average Jitter = 18.40 ms (error=0.27%). Errors are calculated with respect to the experimental data.

2.15. table

A comparison between experimentally obtained values as well as calculated values assuming log-normal distribution

	RTT $_{mean}$, ms	Jitter, ms
Experimentally obtained, first n=2000 values	80.62	18.45
Calculated n=2000 values, assuming log-normal distribution and estimates of $\hat{\theta}_0$ and $\hat{\theta}_1$ from first n=2000 observations	80.67	18.40
Error, %	0.062	0.27

2.4.2 Quick method for estimating the delay distribution parameters in LTE cell

In previous section it was proved that it is possible to use the lognormal distribution function in order to describe mean and jitter values of delays in LTE cells. This, by itself, allows to omit the necessity to build CDF for experimental RTT values, since it can be built for lognormal distribution function with parameters $\theta_0 = \mu = median$ and $\theta_1 = \sigma = STDEV$. The parameters can be estimated via MLM, as it is shown in previous chapter. This method requires whole set of RTT values. However, the "ping" application returns only statistical values of

minimum (*Tmin*), average (*Tavrg*) and maximum (*Tmax*) RTT values, as well number of sent and lost packets. The whole set of RTT values is not available from standard ping's interface. Here the parameters θ_0 and θ_1 can be estimated from known *Tmin* and *Tavrg*. First of all, let's suppose that RTT random value of LTE network $= F_T(t)$ is logarithmically normal distributed. Then, in natural scale, the distribution function can be written as follow:

$$P(t) = \int_{-\infty}^{\ln(t)} \frac{1}{\sigma\sqrt{2\pi}} e^{-\frac{1}{2}\left(\frac{\ln(t)-\mu}{\sigma}\right)^2} d(\ln(t)) \tag{2.11}$$

where:

ln(t)   - RTT values in natural scale;

μ - median of *ln(t)* random value;

σ - standard deviation of random value ln(t).

If RTT values are logarithmically normal distributed, then its average and fractal can be defined as:

$$Tavrg = e^{\mu+\frac{\sigma^2}{2}} \tag{2.12}$$

$$\chi_p = \frac{\ln(Tmin) - \mu}{\sigma} \tag{2.13}$$

Now let's define probability of *Tmin* in natural scale as p. Then its expression will be:

$$p = \int_{-\infty}^{\ln(Tmin)} \frac{1}{\sigma\sqrt{2\pi}} e^{-\frac{1}{2}\left(\frac{\ln(t)-\mu}{\sigma}\right)^2} d(\ln(t)) \tag{2.14}$$

Next, let's transpose from lognormal distribution law to normal distribution law. Then *p* will be equal to:

$$p = \int_{-\infty}^{\frac{\ln(Tmin)-\mu}{\sigma}} \frac{1}{\sqrt{2\pi}} e^{-\frac{1}{2}\left(\frac{\ln(t)-\mu}{\sigma}\right)^2} d(\frac{\ln(t) - \mu}{\sigma}) \tag{2.15}$$

Then, the fractal χ for the probability p will be defined as follow:

$$\chi_p = \frac{\ln(Tmin) - \mu}{\sigma} \tag{2.16}$$

So, the *Tmin* in natural scale can be expressed as follow:

$$\ln(Tmin) = \chi_p\sigma + \mu \tag{2.17}$$

Now, if average value of the random value *T* is known (*Tavrg*) as well if minimal value of the random value *T* is also known (*Tmin*), then parameters of the logarithmically normal distribution can be estimated by solving the set of equations:

$$\begin{cases} Tavrg = e^{\mu+\frac{\sigma^2}{2}} \\ Tmin = e^{\mu+\chi_p\sigma} \end{cases} \Rightarrow \begin{cases} \ln(Tavrg) = \mu + \dfrac{\sigma^2}{2} \\ \ln(Tmin) = \mu + \chi_p\sigma \end{cases}$$

$$\Rightarrow \begin{cases} \dfrac{\sigma^2}{\mu} - \chi_p\sigma = \ln(Tavrg) - \ln(Tmin) \\ \mu = \ln(Tmin) - \chi_p\sigma \end{cases}$$

$$\Rightarrow \begin{cases} \sigma^2 - 2\chi_p\sigma - 2\ln\left(\dfrac{Tavrg}{Tmin}\right) \\ \mu = \ln(Tmin) - \chi_p\sigma \end{cases}$$

$$\Rightarrow \begin{cases} \sigma = \chi_p + \sqrt{\chi_p{}^2 \pm 2\ln\left(\dfrac{Tavrg}{Tmin}\right)} \\ \mu = \ln(Tmin) - \chi_p\sigma \end{cases}$$

(2.18)

Since σ value can be only positive, then the final result is:

$$\begin{cases} \sigma = \chi_p + \sqrt{\chi_p{}^2 + 2\ln\left(\dfrac{Tavrg}{Tmin}\right)} \\ \mu = \ln(Tmin) - \chi_p\sigma \end{cases}$$

(2.19)

Now, to solve this set of equations, the probability p should be calculated. This requires a whole set of RTT values. However, the ping utility shows only statistical values of the minimum, average and maximum RTT, as well packet loss rate. To overcome this problem, let's assume that the *Tmin* is equal to fractal with the probability $p = 0.0014$ (at minus three standard deviations $\Phi^{-1}(-3\sigma)$). Next, let's utilize standard normal distribution. In this case the fractal at the probability of $\Phi^{-1}(-3\sigma)$ will be equal to $\chi_p = \chi_{0.0014} = -3$.

Finally, to estimate lognormal distribution parameters $\theta_0 = \mu$ (median) and $\theta_1 = \sigma$ (standard deviation) it is necessary to solve the following set of equations:

$$\begin{cases} \sigma = \chi_p + \sqrt{\chi_p{}^2 \pm 2\ln\left(\dfrac{Tavrg}{Tmin}\right)} \\ \mu = \ln(Tmin) - \chi_p\sigma \end{cases} \Rightarrow \begin{cases} \sigma = -3 + \sqrt{9 + 2\ln\left(\dfrac{Tavrg}{Tmin}\right)} \\ \mu = \ln(Tmin) + 3\sigma \end{cases}$$

(2.20)

2.4.2.1   Recommendations on the required number of measurements

There are two factors that affect the required number of RTT measurements: for the lognormal parameters estimation and for the packet loss rate calculations.

At first, let's specify required amount of measurements to get trusted results of lognormal distribution parameters estimation, if equation (2.20) is used. This can be done via binomial distributions. In general, if the probability of event is equal to $p = p_1$, then in n experiments the probability R_m of m events will be equal to:

$$R_m = P(X \geq m) = 1 - P(X < m)$$
(2.21)

In case if at least one event should occur (*m*=1), then this equation can be written as follow:

$$R_m = P(X \geq 1) = 1 - P(X < 1) = 1 - (1 - p_1)^n$$
(2.22)

Now, if required probability $p*$ of at least one event is known, then required number of experiments n can be found as follow:

$$p^* = R_m = 1 - (1 - p_1)^n \Rightarrow n = \frac{\ln(1 - p^*)}{\ln(1 - p_1)} \tag{2.23}$$

Now it is possible to define required amount of measurements for lognormal distribution parameters estimation thru *Tmin* and *Tavrg*. Let's define number of measurements to get at least one value *Tmin* (p_1=0.0014). At the probability of 99% (p^*=0.99) number of measurements should to be at least:

$$n = \frac{\ln(1 - p^*)}{\ln(1 - p_1)} = \frac{\ln(1 - 0.99)}{\ln(1 - 0.0014)} \cong 3289 \tag{2.24}$$

At the probability of 99.9% (p*=0.999) it is necessary to perform measurements, at least:

$$n = \frac{\ln(1 - p^*)}{\ln(1 - p_1)} = \frac{\ln(1 - 0.999)}{\ln(1 - 0.0014)} \cong 4931 \tag{2.25}$$

Hence, if number of measurements $n \geq 3287$, then will return correct values with probability of at least 99%; as well if number of measurements is $n \geq 4931$, then correct values will be returned with the probability of 99.9%.

Now let's find required number of measurements to calculate packet loss rate. This can be done by applying confidence limits (CI).

First, let's calculate unknown probability *p* of packets loss via its frequency *p** if *n* independent measurements are available. As was already mentioned, the RTT values are independent because each RTT value measurement sends its own request (ICMP packet), hence all following measurements does not depend on previous results.

Let's define packet loss event as *X* and number of lost packets as *N*. Then the packet loss frequency will be defined as follow:

$$p^* = \frac{\sum_{i=1}^{n} X_i}{n} = \frac{N}{n} \tag{2.26}$$

Since packet loss events *Xi* are independent and uniformly distributed, then in accordance with Central Limit Theorem (CLT), their sum *N* will be normally distributed in case if number of *Xi* large. Then the random variable's *X* median can be defined as:

$$\mu_{p^*} = p \tag{2.27}$$

As well the standard deviation can be defined as:

$$\sigma_{p^*} = \sqrt{\frac{p \cdot (1 - p)}{n}} \tag{2.28}$$

Let's define the probability belief as β. Next, let's find interval $\left(p - \varepsilon_\beta, p + \varepsilon_\beta\right)$, in which value *p** hits with probability β:

$$P\left(|p^* - p| < \varepsilon_\beta\right) = \beta \tag{2.29}$$

Since *p** is normally distributed, then:

$$P\left(|p^* - p| < \varepsilon_\beta\right) = 2\Phi\left(\frac{\varepsilon_\beta}{\sigma_{p^*}}\right) - 1 = \beta \tag{2.30}$$

Next, it can be transformed to:

$$\varepsilon_\beta = \sigma_{p^*} \cdot \Phi^{-1} \cdot \left(\frac{1 + \beta}{2}\right) = 2\Phi\left(\frac{\varepsilon_\beta}{\sigma_{p^*}}\right) - 1 = \beta \tag{2.31}$$

where Φ^{-1} is inverse of the normal distribution function.

Next, let's define CI boundaries as t_β:

$$t_\beta = \Phi^{-1} \cdot \left(\frac{1 + \beta}{2}\right) \tag{2.32}$$

Then:

$$\varepsilon_\beta = t_\beta \cdot \sigma_{p^*} \tag{2.33}$$

t_β value can be defined for typical probability belief β (see 2.16. table):

Definition of the $t\beta$ value for the probability belief β

β	0.9	0.95	0.99	0.9973	0.999
$t\beta$	1.643	1.960	2.576	3.000	3.290

Now, the inequality with probability β can be defined for large number of n:

$$|p^* - p| < t_\beta \sqrt{\frac{p \cdot (1 - p)}{n}} \tag{2.34}$$

Let's find CI I_β for the probability of p. To do this it is necessary to transform this equation in the quadratic form and to find the roots of the equation.

$$(p^* - p)^2 < \frac{t_\beta{}^2 \cdot p \cdot (1 - p)}{n} \tag{2.35}$$

$$p_1 = \frac{p^* + \dfrac{1}{2}\dfrac{t_\beta^2}{n} - t_\beta \sqrt{\dfrac{p^* \cdot (1 - p^*)}{n} + \dfrac{1}{4}\dfrac{t_\beta^2}{n^2}}}{1 + \dfrac{t_\beta^2}{n}} \tag{2.36}$$

$$p_2 = \frac{p^* + \dfrac{1}{2}\dfrac{t_\beta^2}{n} + t_\beta \sqrt{\dfrac{p^* \cdot (1 - p^*)}{n} + \dfrac{1}{4}\dfrac{t_\beta^2}{n^2}}}{1 + \dfrac{t_\beta^2}{n}} \tag{2.37}$$

Then the CI I_β for the probability p will be equal to:

$$I_\beta = (p_1, p_2)$$

Now it is possible to find required number of measurements n for the wanted CI with the probability β to hit into it. Let's define allowed deviation from the packet loss frequency as $p^*=kp$. Then we will have:

$$(p^* - p)^2 < \frac{t_\beta{}^2 \cdot p \cdot (1 - p)}{n} \Rightarrow n = \frac{t_\beta^2 \cdot (1 - p)}{(k - 1)^2} \tag{2.38}$$

Then, for the typical packet loss rate $p=10^{-4}$, for the CI of $\pm 30\%$ and probability to hit in $\beta=0.9$ we will have:

$$n = \frac{t_\beta^2 \cdot (1 - p)}{p \cdot (k - 1)^2} = \frac{2.576^2 \cdot (1 - 0.0001)}{0.0001 \cdot (1.3 - 1)^2} = 299909 \tag{2.39}$$

Or for the typical packet loss rate $p=10^{-4}$, for the CI of $\pm 10\%$ and probability to hit in $\beta=0.9$ we will have:

$$n = \frac{t_\beta^2 \cdot (1-p)}{p \cdot (k-1)^2} = \frac{1.643^2 \cdot (1 - 0.0001)}{0.0001 \cdot (1.1 - 1)^2} = 2699179 \qquad (2.40)$$

Therefore, $\cong$300000 measurements are required to calculate packet loss rate with CI up to 30% and 0.9 probability to hit in or $\cong$2700000 measurements to calculate packet loss rate with CI up to 10% and probability to hit in of 0.9. Also, it should to be note, that least four packets loss should to be observed to estimate trusted packet loss rate [60]. However, if RTT measurements are performed to estimate lognormal distribution parameters only, then $\cong$3300 measurements are enough to get correct results from equation (2.20) with probability of at least 99%.

It can be concluded, that:

1. In order to obtain values of the average delay and delay jitter with satisfactory accuracy, it is possible to accept that the delay values in LTE cells obey the logarithmically normal distribution law.
2. The estimates of parameters of the logarithmically normal distribution function of RTT values can also be calculated via the proposed method using known minimum and average RTT values, reported by the "ping" application. In this case a statistic of at least 3300 measurements should to be taken. If the packet loss rate should be estimated too, the number of measurements should be several millions (e.g. more than 2.7 million). This guarantee that the statistics for the estimation of parameters of the logarithmically normal distribution function always will be sufficient.

2.5. Experimental evaluation of the impact of mobility on delays in the 3G and LTE cellular networks

The impact of various types of mobility on the cellular mobile data transfer service performance will be evaluated in the following section. 3G (HSPA+ and above) and LTE (LTE Cat. 4) networks will be evaluated separately.

Moving UE data transfer service mainly depends on rapidly changed environment. This means that the network latency and number of lost packets must be logged together with various network performance indicators, as well geographic location and ground speed must be registered too. During the following experiments the request messages are sent by the portable computer which is equipped with mobile broadband USB dongle Huawei E3372h. It uses its own PIFA antennas; external antennas were not connected. By default, its operational mode is HiLink (CdcEthernet). In this mode, the device operates as a NAT server and emulates a virtual network card (NDIS) on the local computer. All configurations as well as network information can be displayed by accessing a gateway address (default gateway IP: 192.168.8.1) via web browser. It makes network information logging task complicated. The device has been reprogrammed into Stick mode (RAS) (firmware 21.315.01.00.143_M_01). The Stick mode enables access to the set of standard serial AT-commands and reports. Under the Stick mode, the device operates as a standard PPP modem, emulates two virtual serial ports and uses local computer resources (by means of modem running software) to operate. The modem software blocks any further access to the serial ports because serial ports can be accessed only

individually. The access problem can be solved by using MS Windows 8 operation system, which has built-in driver (Huawei 1.0.17.0) and allows access to the internet without installing the Huawei modem software. This retains internet access and allows access to the serial port for control and monitoring purposes simultaneously. The internet connection on the MS Windows 8 remains available even if the HUAWEI Modem 3.5 software is not running. It is necessary to manually suspend the Huawei software (that installs automatically from the Huawei ROM autorun), otherwise PC UI Interface serial port will be busy and cannot be accessed.

The following data has been captured:
- network performance indicators, reported by dongle:
  - RSSI, RSCP, Ec/Io in 3G
  - or RSSI, RSRP, SINR and RSRQ in LTE mode);
- ground speed, GPS coordinates and altitude (from the Global Sat BU-353-S4 GPS receiver)
- network RTT (based on ping report).

As base station is responsible for immediate acknowledgments of TCP packets (see introduction for more details), the time interval between sending a TCP packet from the dongle and receiving a corresponding ACK message cannot be used as RTT measurement [47]. This is the main motivation why the standard utility "ping" was chosen.

To simplify simultaneous data capturing from the USB dongle and GPS receiver NMEA messages, as well as to perform data decoding and real-time visualization, a virtual instrument (vi) was developed in the LabVIEW environment. A vi generated report can be exported into MS Excel.
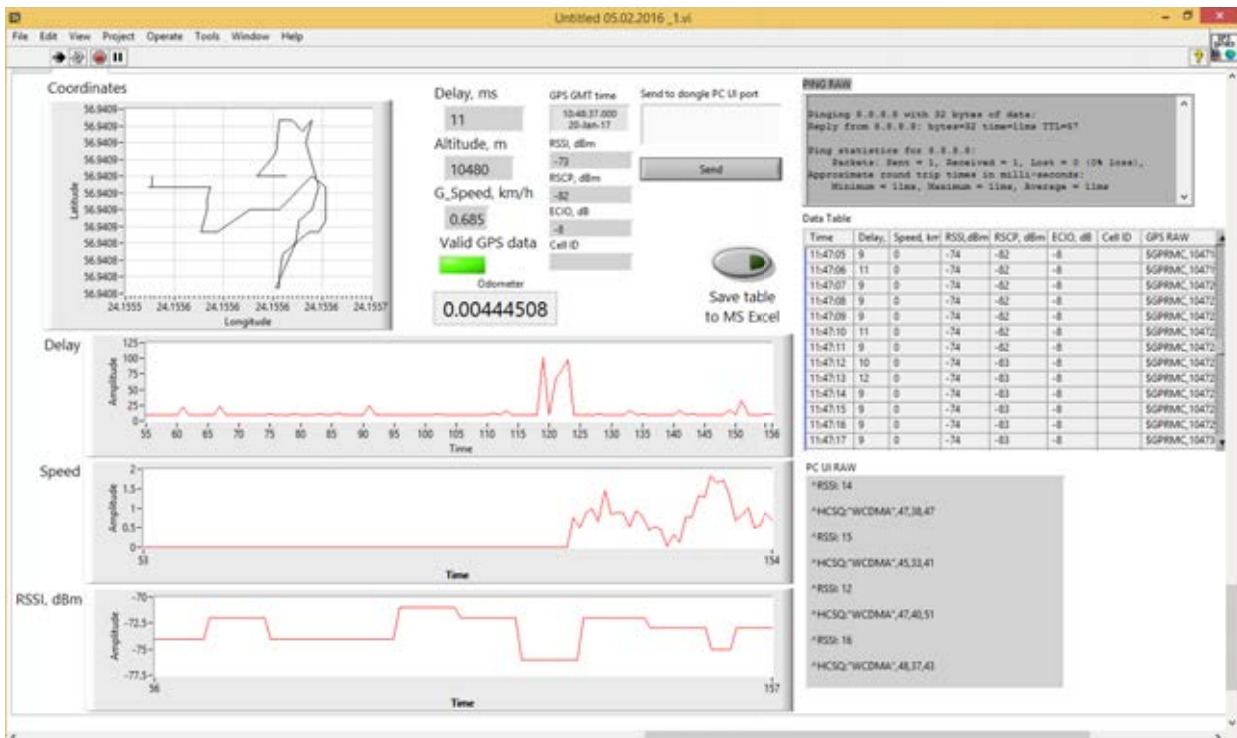

Fig. 2.31 Interface of the virtual instrument (vi).

Fig. 2.32 Data acquisition system.

Cellular operator and ground server selection: from previous section it can be concluded that the LMT cellular network operator has the least loaded cellular network in Latvia. The LMT cellular network operators' cellular data transfer service is used to reduce (or even exclude) data transfer quality deterioration due to cellular network overload. Also, from previous section can be concluded that the google free DNS server (IP: 8.8.8.8) is more trusted than the server hosted at RTU building (IP: 213.175.90.193). The use of google free DNS server helps avoid limitations that can be caused by the ground wired network segment service quality.

The first experiment is made to check network performance for the movable UE when the signal level drops significantly. All the following data were obtained in October of 2016.

The experimental results are shown in Fig. 2.33. The first plot shows RTT (an either-direction, in msec) in time (left Y axis and blue curve); ground speed in km/h (right Y axis and green curve); cell in use is shown by orange, green and violet horizontal lines. The second plot shows network performance indicators: RSSI in dBm (blue curve) and RSCP in dBm (green curve) (left Y axis, in dBm); Ec/Io in dB (right Y axis and red curve). Time marks and lost packets are shown by the red squares on the X axis.
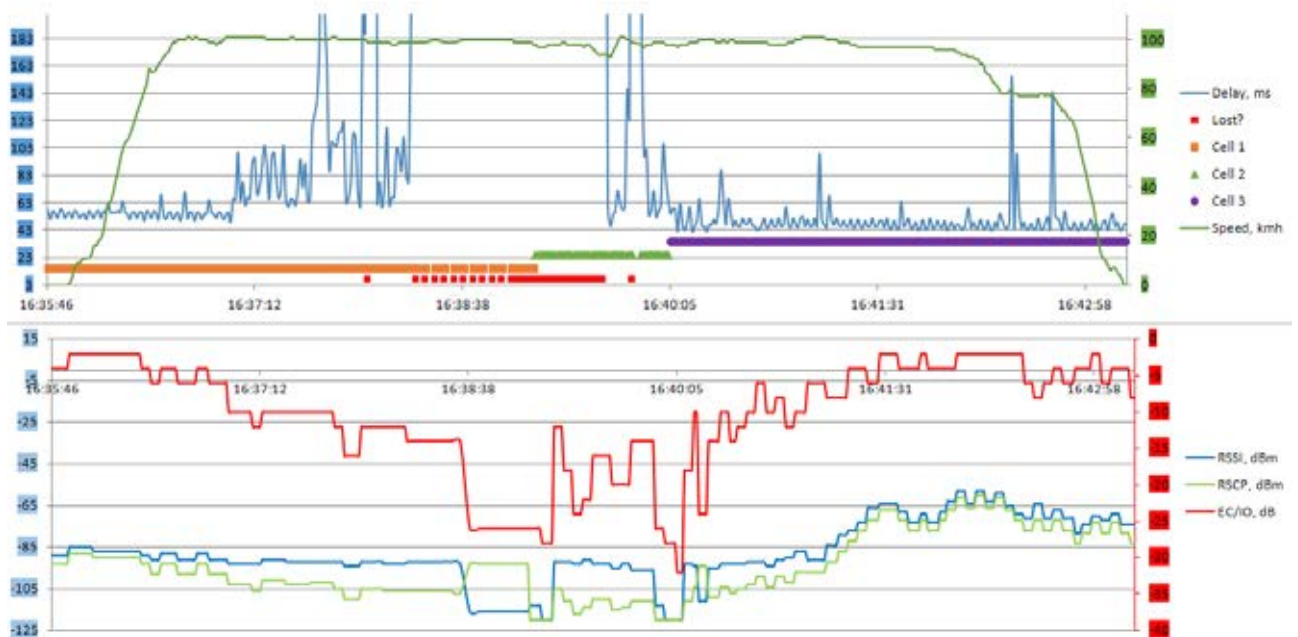
Fig. 2.33 Network performance for the moving UE in the poor signal environment.

Initial RSSI level is satisfactory: -85 dBm; Ec/Io is perfect – to – good: -2 ... -5 dB. Then the UE is accelerated up to 100 km/h. The RTT value is approximately same for both immovable and movable UE states. At 16:37:00 the RSSI drops below -90 dBm and the broadband USB dongle Huawei E3372h approaches its receiver noise floor. It causes Ec/Io value also to reduce. The data transmission aborts when the Ec/Io value falls to -15 dB and RSSI -93 dBm at 16:38:10. At 16:39:15 the second cell power level increases up to recognizable level of -92 dBm and UE switches to it. The second cell Ec/Io value is near to miss: -12 … -22 dB because RSSI value of -92 dBm is slightly above receiver noise floor value. 30 sec were taken to reestablish data transfer service. The RTT value increases and becomes unstable when the RSSI value drops to -95 dBm at 16:39:50. Then the UE switches to the third cell with RSSI -93, Ec/Io -18 dB. The data transfer service does not interrupt, but the RTT value is slightly increased and is not stable. The RTT value becomes stable when RSSI increases more than -93 dBm. The receiver noise floor is exceeded and the Ec/Io starts to increase its value up to perfect-to-good level of -5 .. -2 dB. Simultaneously the RTT decrease its value and becomes more stable.

The second experiment is been made to check network performance at the UE acceleration and deceleration. All the following data were obtained in October of 2016.

The experimental results are shown in Fig. 2.34. The first plot shows RTT (an either-direction, in ms) in time (left Y axis and blue curve); ground speed in km/h (right Y axis and green curve); cell was not changed and is shown by orange horizontal line. The second plot

shows network performance indicators: RSSI in dBm (blue curve) and RSCP in dBm (green curve) (left Y axis, in dBm); Ec/Io in dB (right Y axis and red curve). Time marks are shown on the X axis.
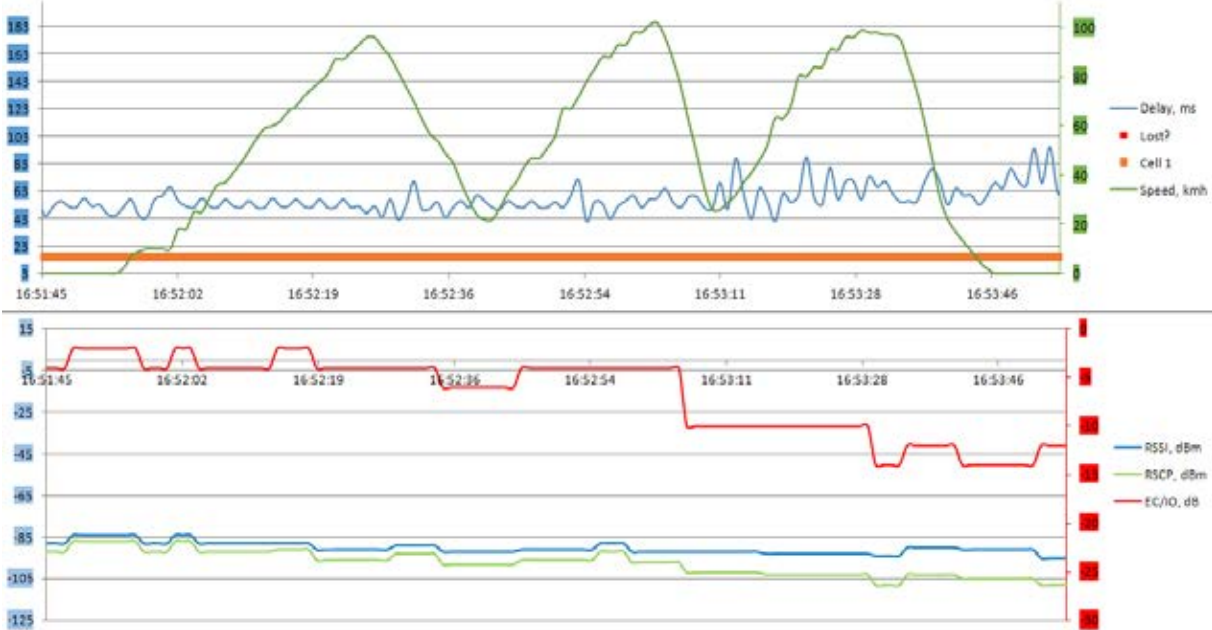

Fig. 2.34 Network performance for the moving UE during acceleration and deceleration.

It may be concluded, that the RTT does not depend on speed, acceleration or deceleration in the linear motion of the UE.

The third experiment is been made to check network performance if a short signal loss occurs. The situation has been simulated when the UE was moved under the bridge. All the following data were obtained in October of 2016.

The experimental results are shown in Fig. 2.35. The first plot shows RTT (an either-direction, in ms) in time (left Y axis and blue curve); ground speed in km/h (right Y axis and green curve); cell in use is shown by orange and green horizontal lines. The second plot shows network performance indicators: RSSI in dBm (blue curve) and RSCP in dBm (green curve) (left Y axis, in dBm); Ec/Io in dB (right Y axis and red curve). Time marks and lost packets are shown by the red squares on the X axis.
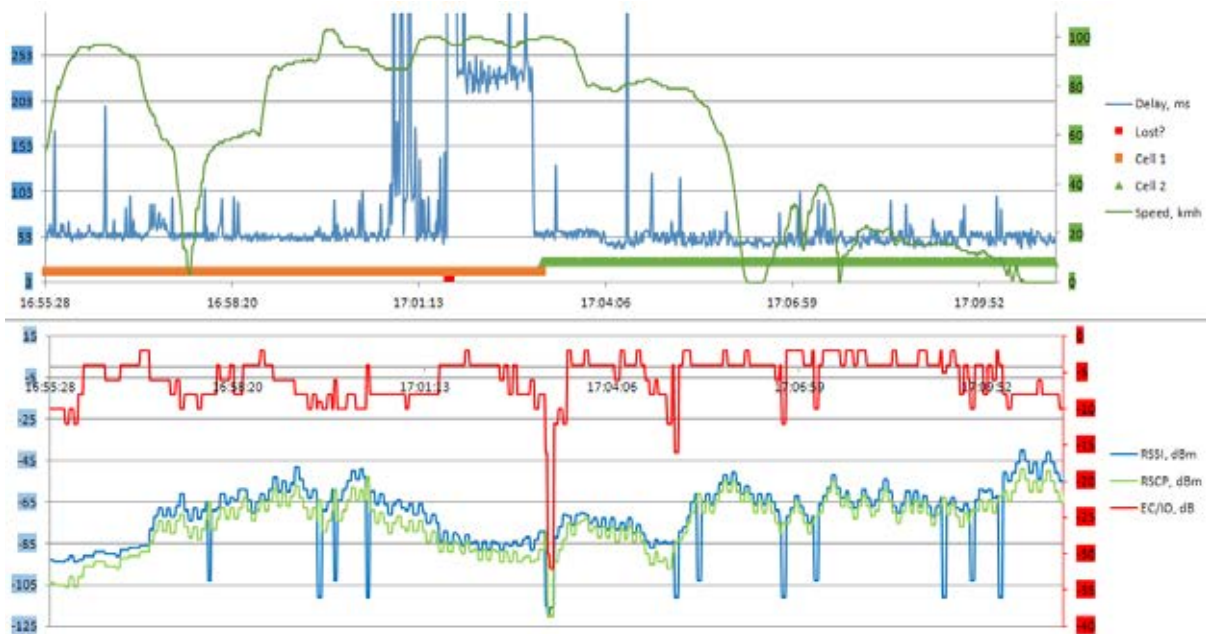
Fig. 2.35 Network performance for the moving UE during short time signal loss.

A short interruption of signal occurs when car with the UE is moved under the bridge at 17:02:10. It cause a 2 packets loss. Note that one packet is sent at 1 sec period and 2 lost packets means 2 second period. The RSSI, RSCP and Ec/Io reported values are reported approximately once per 5 sec and there is no indication of RSSI level drop. It may be concluded that short time signal level drop was not noticed by the mobile broadband USB dongle and was not reported.

Note that the cellular network usually forces UMTS mode if more than 1 sec data traffic delay occurs. A 2 sec delay cause mode switching from DC-HSPA+ to UMTS. When the bridge is over, the RSSI level becomes satisfactory and the data transmission is reestablished. Small traffic (32 bytes per second) remains unnoticed and mode of operation remains UMTS. The RTT value becomes five times increased.

When the RSSI level drops sufficiently the UE switches to the next cell at 17:03:00. The next cell detects data traffic and switches to the DC-HSPA+. The RTT value than is decreased five times. An urban area begins from 17:06:20 time mark. The RSSI value becomes less predictable and fluctuating. The RTT value also becomes less stable.

It may be concluded that the short time signal loss can cause network mode change to the UMTS. It will cause approximately 5 times higher RTT values. Note that the data transfer interruption even if signal strength has satisfactory level also cause network mode change to the UMTS. The mode change time delay depends on cellular network operator settings and usually is in 1 … 5 sec limits.

The fourth experiment is made to check network performance in urban area. The build-up area consists of 5 to 12 storeyed buildings. All the following data were obtained in October of 2016.

Fig. 2.36 Network performance in urban area.

The lightly-loaded 3G network RTT does not depends on ground speed or acceleration / deceleration rates. Also Fung Po Tso et al. [61] experimental results show that the downlink and uplink throughput performance is not affected by the ground speed.

2.5.2   Evaluation of LTE network

In the 2018 the LTE network was completely deployed in Latvia (see Chapter 2.3). This allows to take the measurements of its performance versus UE ground movements. The following experiment was performed in the beginning of 2018. A Huawei 3372h dongle was used as a UE equipment and the google free DNS server (IP: 8.8.8.8) was a destination. The experiment was performed in rural area in Sigulda's district to reduce the possibility that the cellular network will be overloaded. A path between Inciems and Kirzu lake was travelled. The modem was securely fixed in car to prevent its PIFA antennas angular rotations. The mode of operation was locked on LTE; the band was locket on B20 (800 MHz). Huawei dongle was locked in B20 band. Radio network performance indicators (such as RSSI, RSRP, SINR, RSRQ, as well cell in use) was reported by the dongle. These parameters were captured together with the RTT and travelling speed via the virtual instrument (vi), that was created in the LabVIEW environment. The RTT was measured by sending 32 bytes long ICMP packets via ping application; the speed was obtained from the Global Sat BU-353-S4 GPS receiver.

The first part of the following illustration shows RTT in time (blue dots and left scale, in ms), speed (orange line, right scale, in km/h), the transition from one sell to the next one is indicated by the green squared markers; RSSI and RSRP are shown in the second part of the Fig. 2.37, blue and orange dots respectively; SINR and RSRQ are show in the final part of the illustration, blue and orange dots respectively.
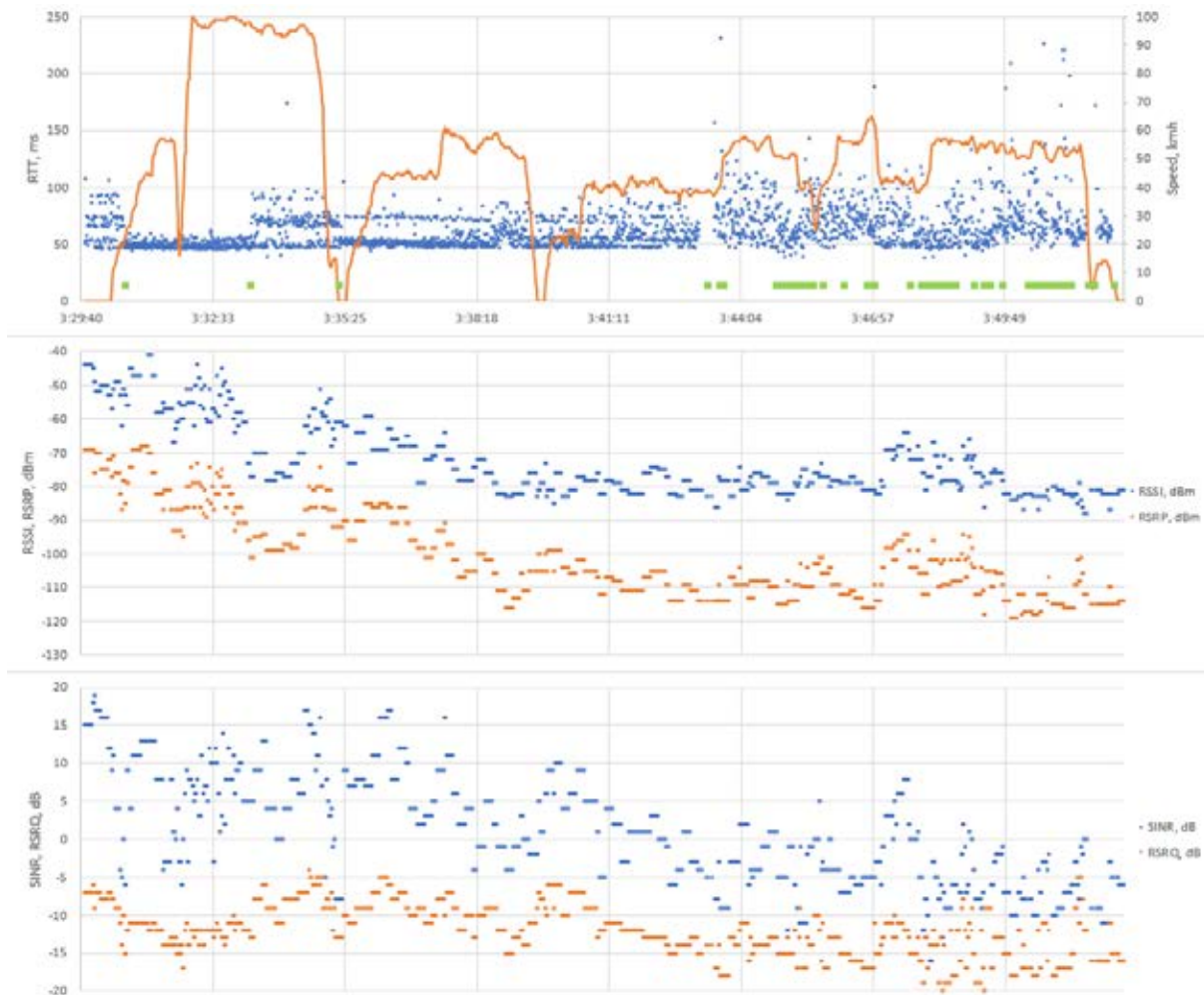
Fig. 2.37 Performance of the LTE network in rural area.

It is possible to conclude:

1. The performance of 3G HSPA+ as well LTE (LTE Cat. 4) networks do not depends on the travelling speed (proved up to 100 km/h), as well acceleration/deceleration at the reasonable rate (typical car acceleration / deceleration rates).

2. During the handover (transition from one cell to the next one) delays are not increased (at least these changes are not noticeable for a typical end user). However, in 3G HSPA+ networks the packet delays become noticeable increased during the handover if the signal strength is low (in our experiments RSSI below -86 dBm). In LTE networks such phenomena have not been noticed.

3. There is no escaping the fact that different cells have different delays. Since these are stable all the time when the UE stays within the same cell, then it is possible to assume

that such difference depends on the terrestrial backhaul of 3G and LTE networks. This phenomenon will be quantitatively evaluated in further experiments.

4. After a short-time loss of a signal, for the small data traffic, the HSPA+ networks can be switched to low speed mode (UMTS) and remain there until the transition to the next cell. This leads to degraded performance of the data transfer service. LTE does not have such behavior, since there are no low speed channels in LTE.

5. It was observed that in 3G (HSPA+ and above) RTT becomes increased if UE antennas have angular rotations. Such behavior in LTE mode was not observed.

6. Finally, it should be mentioned here, that in 3G HSPA+ spikes in latency was observed during turns or ground altitude changes. The occurrence of these locally increased latencies has no dependence on other network performance parameters (such as signal strength and interference), also these cannot be fully repeated. A deeper analysis is required here. It should be noted that such phenomenon was not observed in LTE network operation.

2.6. Evaluation of delays in the cellular network of a particular cellular operator

The use of cellular 3G/LTE data transfer services allows remote operations, which are theoretically limited only by cellular network coverage. As well, such solutions utilize low power lightweight radio interfaces, that helps to save the battery power and reduce overall mass.

With so much at stake, there are doubts about cellular 3G / LTE mobile services quality for moving RPAS control channel implementation. Rc-model's designers usually avoid 3G / LTE usage in their implementations, but whoever tries using such implementations, usually limits operating range to stay within same cell. These concerns are compounded by the fact that in the cellular data transmission service all traffic is routed from the Base Stations (BS) to the remote sites. This means that the cellular data transfer backhaul is optimized to connect User Equipment (UE) with the wide area network (internet), whereas UE to UE connections are not developed, since typical cellular mobile users does not use such connections.

The key differences of LTE E-UTRAN mobile backhaul in comparison with 3G UTRAN are: implementation of radio network functions in eNodeB (there is no more NodeB and RNC functions distribution, therefore S1 link has no real time operation requirements); there is no need for real-time RNC operations (since its functions are implemented directly in the eNodeB); all-IP network which leads to a simpler service concept (voice is also supported over ip only (VoIP)). Finally, the LTE network has not been gradually upgraded, therefore, in general, there are no capacity bottlenecks in the terrestrial backhaul.
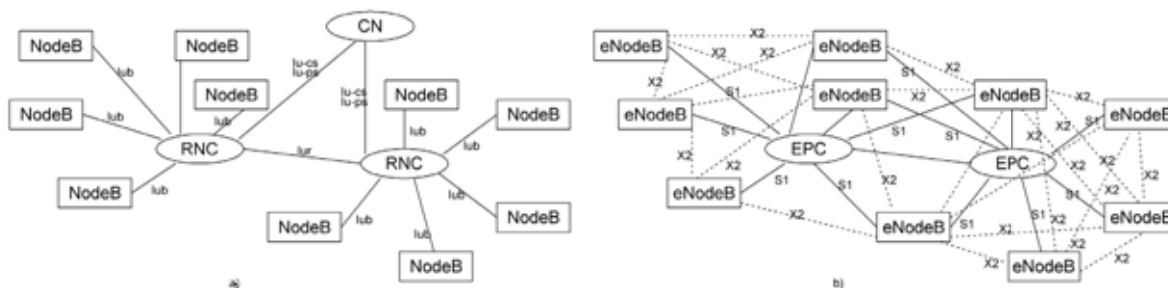
Interworking with various cellular operator networks (roaming) is possible via the S8 interface between the EPC of the home network and the EPC of different operators. This can lead to increased network latency. A more detailed explanation can be found in [62].

Therefore, traffic in 3G or LTE always goes through the RNC (in 3G) or EPC (in LTE). This means that cellular network performance mainly depends on the implementation of the first mile link. Also, it can be concluded that the implementation of the first mile link has an impact on the latency for any type of scenarios, such as Cellular-to-WAN or Cellular-to-Cellular. This consideration will be proved in the first set of experiments. Further, in the second set of experiments, statistical data on the RTT of LTE cells will be provided.

2.6.1 Evaluation of the impact of the "first mile link"

Now let's make a field testing of the first mile link performance and its impact on the overall data transfer service's RTT. As was already stated, in 3G or LTE cellular networks, data traffic always passes through the RNC (in 3G) or EPC (in LTE). This occurs in both cases: if a connection is established between the UE and a server in the WAN or if the connection is established between two UEs. In addition, the data always passes through the RNC or EPS, even if both UEs are within the same cell. This means that the delay of the cellular data transfer service mainly depends on the first mile link Iub (in 3G) or S1 (in LTE). To prove this, the following experiments were carried out.

Portable and stationary computers was equipped with 3G/LTE Huawei 3372h dongles. The portable computer was running Windows 8 with Huawei driver 1.0.17.0 and Huawei E3372h dongle connected to it. The portable computer was transported by car, starting from relatively unloaded cell located in urbans' industrial district. The traffic route first enters in a dense urban district and then goes to underpopulated rural area. The stationary computer is in the relatively unloaded cell in urbans' industrial district. The total length of the path is 20 km, including 10 km in the rural area. RTT was measured from the portable computer to two destinations simultaneously: stationary computer with the 3G/LTE dongle (called Dongle-to-Dongle or D2D) and wired WAN server (google free DNS server, ip:8.8.8.8). All of the above mentioned is summarized in Fig. 2.39.
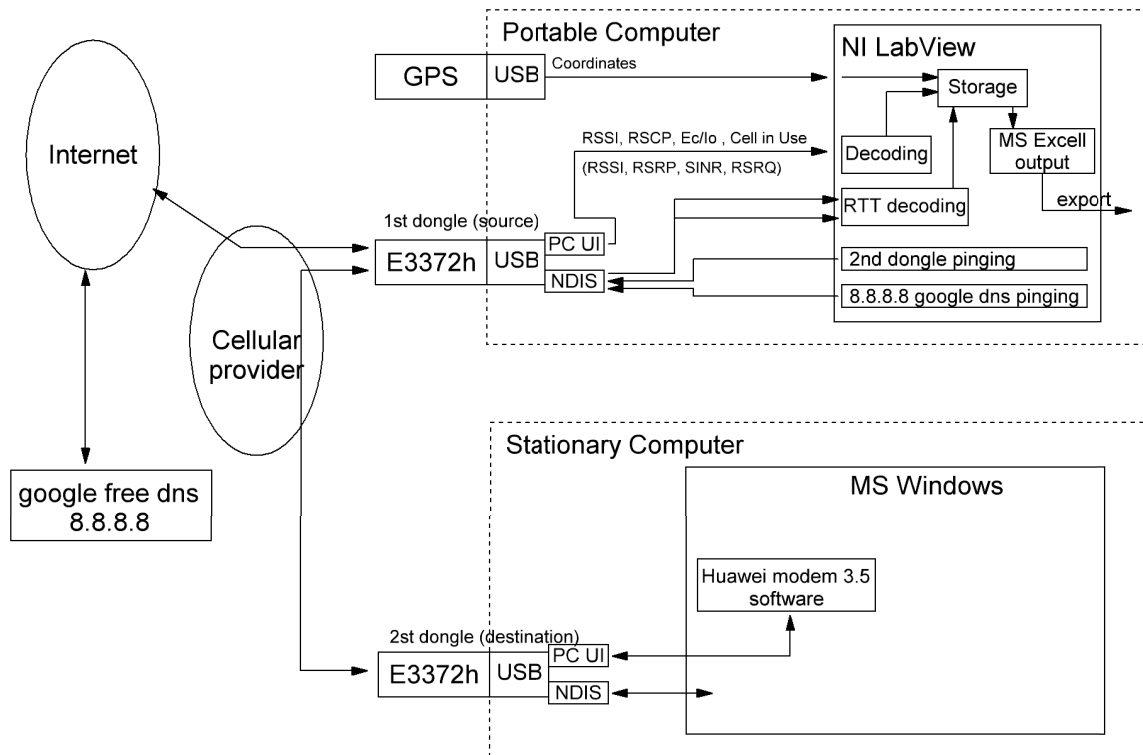
The first experiment is conducted to test network performance if the portable computer and stationary computer are operating in 3G DC-HSPA+ mode. The stationary computer is located in a relatively unloaded cell in an industrial district. The portable computer terminal is initially located at a distance of 10 meters from the stationary computer and operates in the same cell with the stationary computer. The signal RSSI is -51 dBm, RSCP is -55 dBm and Ec/Io is -4 dB.
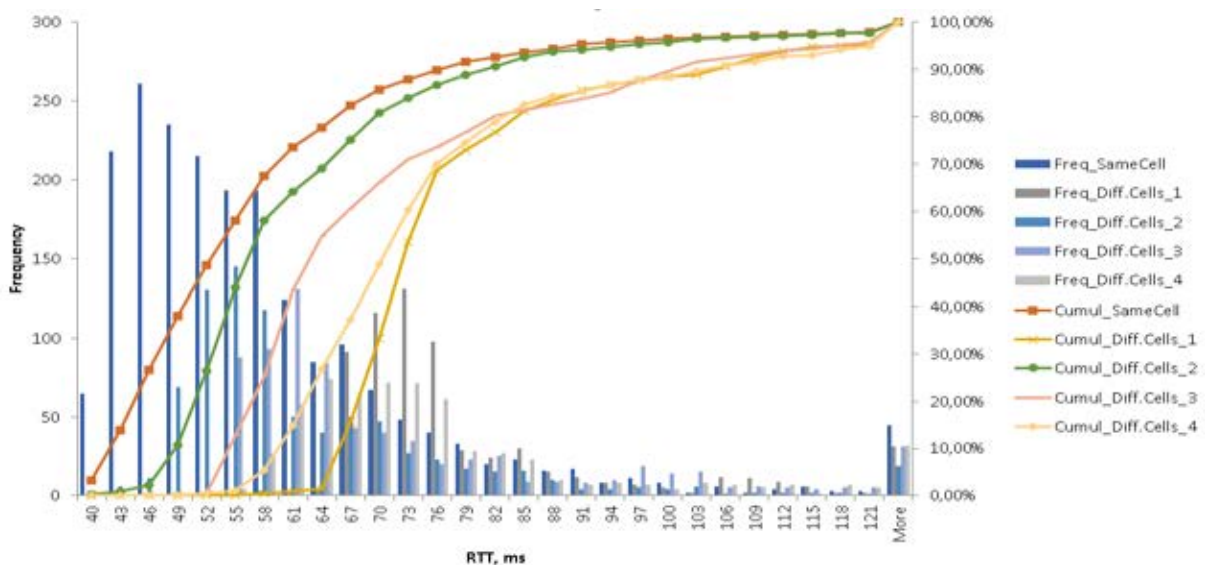
The RTT's PDFs and CDFs of the Dongle-to-Dongle (D2D) data service are shown in Fig. 2.40. The first cell in which the dongles operates simultaneously (in same cell) is called Cell-0. Then, when the car is moving, the RCV dongle switches to the next cell, called Cell-1, then to the Cell-2, etc. The RTT's PDFs and CDFs of the Dongle-to-WAN data service are shown in Fig. 2.41.

Since the 3G network has been gradually upgraded, some NodeBs have old, low-speed terrestrial links, while the recently installed NodeBs typically have modern high-speed terrestrial links. This leads to different network performance, which varies from cell to cell. To be able to distinguish between the causes of network performance changes (due to same/different cells operation or due to NodeB old/new Iub terrestrial link), RTT's PDFs and CDFs dongle-to-WAN also was measured and are shown in Fig. 2.41.
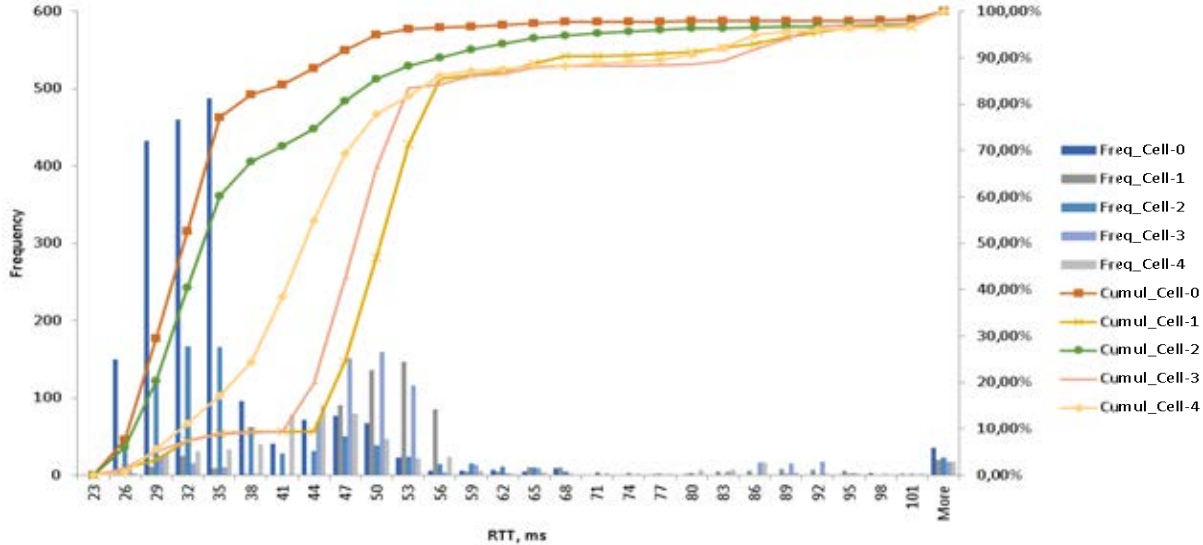
If network performance simultaneously decreases for the dongle-to-dongle and for the dongle-to-WAN connections, it can be concluded that the terrestrial Iub interface is the cause of the problem. The data is summarized in 2.17. table.

2.17. table

Summarized results for 3G HSPA+ networks

	RTT$_{avrg}$, ms (Dongle-to-Dongle)	difference, % (with respect to Cell-0)	RTT$_{avrg}$, ms (Dongle-to-WAN)	difference, % (with respect to Cell-0)
Cell-0	63.66	-	43.48	-
Cell-1	80.63	26.66	55.16	26.87
Cell-2	69.57	9.29	46.45	6.83
Cell-3	73.88	16.05	53.54	23.15
Cell-4	90.00	41.38	61.70	41.92

In the Cell-1 RTT (D2D) increases by 27% compared to Cell-0. However, since RTT of Dongle-to-WAN also increases by 27%, it can be concluded that the difference in performance is caused by the terrestrial Iub link, and not by the fact that the dongles are operate in different cells. A similar situation occurs with the 2nd cell: its RTT for Dongle-to-Dongle increases by 9% (with respect to the Cell-0), as well RTT for Dongle-to-WAN connection increases by 7%; 3rd cell: RTT increases by 16% and 23% respectively; 4th cell: 41% and 42% respectively.

The second experiment is made to test network RTT, if the stationary computer and the portable computer are operating in LTE mode (LTE Cat.4). The stationary computer is located in a relatively unloaded cell in urban industrial district. The RCV terminal is initially located at a distance of 10 meters from the portable computer and operates in the same cell with the stationary computer, which is called "Cell-0".

The RTT's PDFs and CDFs of the Dongle-to-Dongle data service are shown in Fig. 2.42. The RTT's PDFs and CDFs of the Dongle-to-WAN data service are shown in Fig. 2.43 to be able to identify cause of the RTT degradation (terrestrial S1 link or operation in same/different cells). The performance of an eNodeB significantly depends on the terrestrial S1 link implementation and its load. If the average RTT values of the cell changes simultaneously both for the Dongle-to-Dongle and Dongle-to-WAN connections, then the case is in the S1 link and not in the fact that dongles are operated in different sells. The data is summarized in
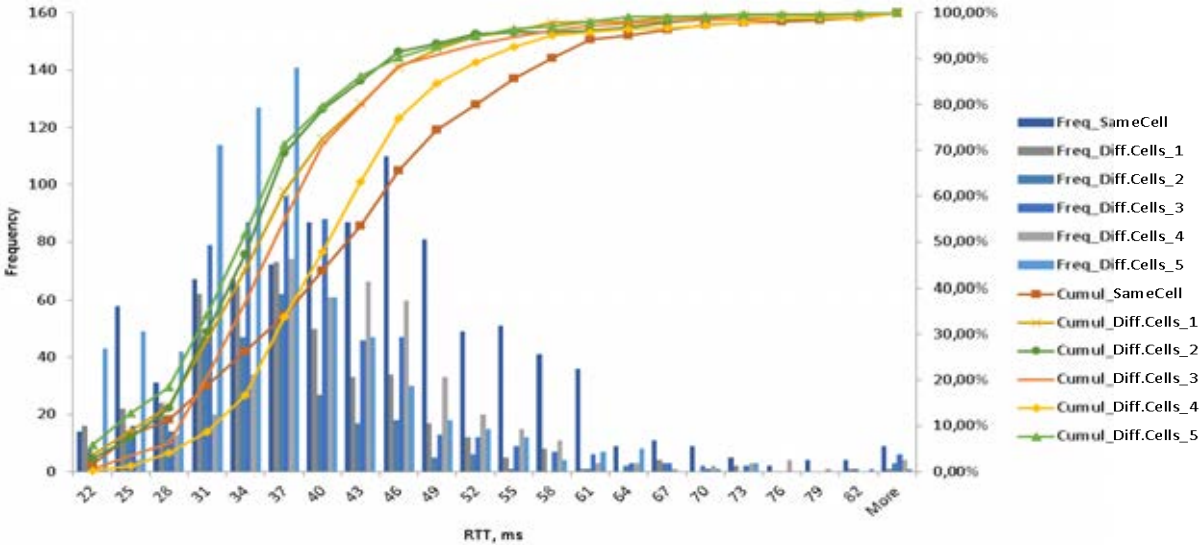
2.18. table.

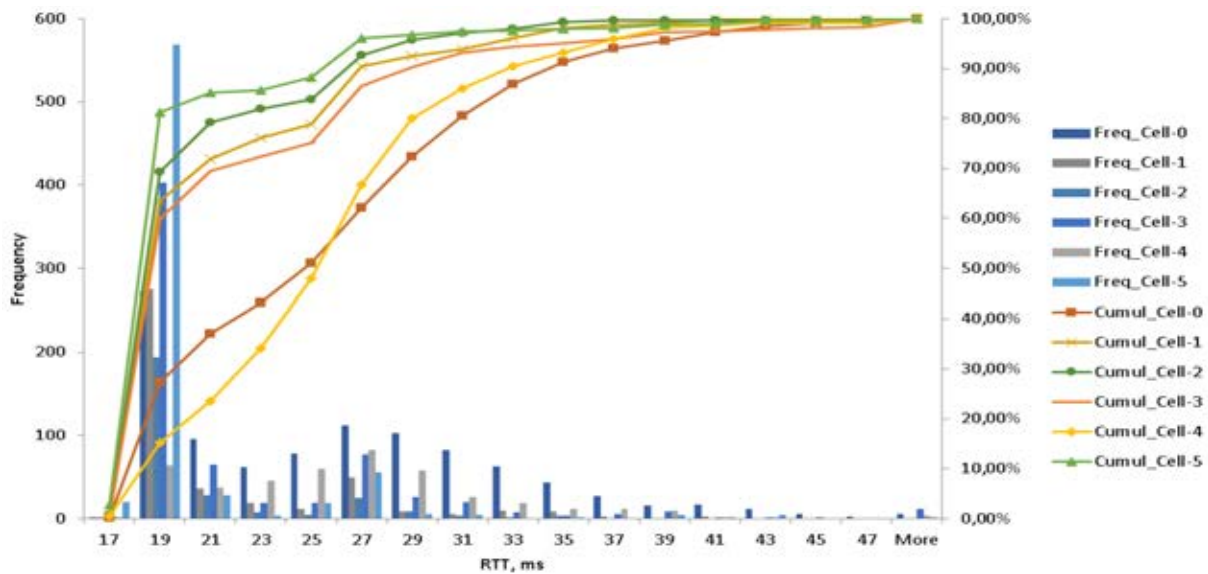Fig. 2.42 RTT of the LTE to LTE (Dongle-to-Dongle) connection.

Fig. 2.43 RTT of the LTE to WAN connection.

The RTT for the Dongle-to-Dongle is decreased by -15% when RCV dongle is operating in the Cell-1, RTT for the Dongle-to-WAN is decreased by -18% respectively; for the Cell-2 -15% and -23% respectively; for the Cell-3 -10% and -13% respectively; for the Cell-4 -2% and 0.6% respectively; for the Cell-5 -18% and -24% respectively. Therefore, it can be concluded that the difference in performance is caused by the terrestrial S1 link, and not by the fact that the dongles are operate in different cells.

2.18. table

Summarized results for LTE network

	RTT_{avrg}, ms (Dongle-to-Dongle)	difference, % (with respect to Cell-0)	RTT_{avrg}, ms (Dongle-to-WAN)	difference, % (with respect to Cell-0)
Cell-0	43.31	-	25.80	-
Cell-1	36.70	-15.28	21.17	-17.94
Cell-2	36.89	-14.83	20.85	-23.76
Cell-3	38.68	-10.71	20.53	-12.65
Cell-4	42.28	-2.41	20.96	0.62
Cell-5	35.29	-18.53	19.72	-23.55

2.6.2 Development of a model of delays in the LTE cellular network based on experimentally obtained data

In previous experiments, it was proved that the delays in 3G and LTE cells mainly depends on the implementation of the first mile link. The experimental results clearly indicate that LTE cells (as well as 3G cells) have a large variation in their latencies. Since UE is operating with

only one BS at a time (both in 3G, LTE as well as in rel-15 5G), the delays of cellular network should be evaluated separately for each cell.

The following experiments were performed to collect the delays in the LTE network of Tele2-LV cellular operator. Experimental data were obtained from a 230 km long path two times (for B3 and B20 LTE bands). The travel speed did not exceed 100 km/h, which is lower than the stated maximum travel speed for LTE devices. Two Huawei 3372h dongles were attached to the portable computer, which was located in the car. Both modems were equally oriented in space to reduce the influence of the built-in PIFA antenna patterns. The experimental data was received for B3 (1800MHz) and B20 (800MHz) LTE frequency bands. The mode of operation of both modems was locked on the same band. Also, both modems were equipped with SIM cards of the same cellular operator, with fixed IP addresses. From the first Huawei 3372h dongle, RTT to two destinations were measured simultaneously: to the server connected to the global Internet network (WAN server) and to the second Huawei 3372h dongle. As a server connected to the global network, a free Google DNS server was used (ip: 8.8.8.8). Signal parameters (RSSI, RSRP, SINR, RSRQ) were recorded from each dongle, as well as a cell ID. In addition, GPS coordinates and vehicle speed were recorded. All of the above mentioned is summarized in Fig. 2.44.
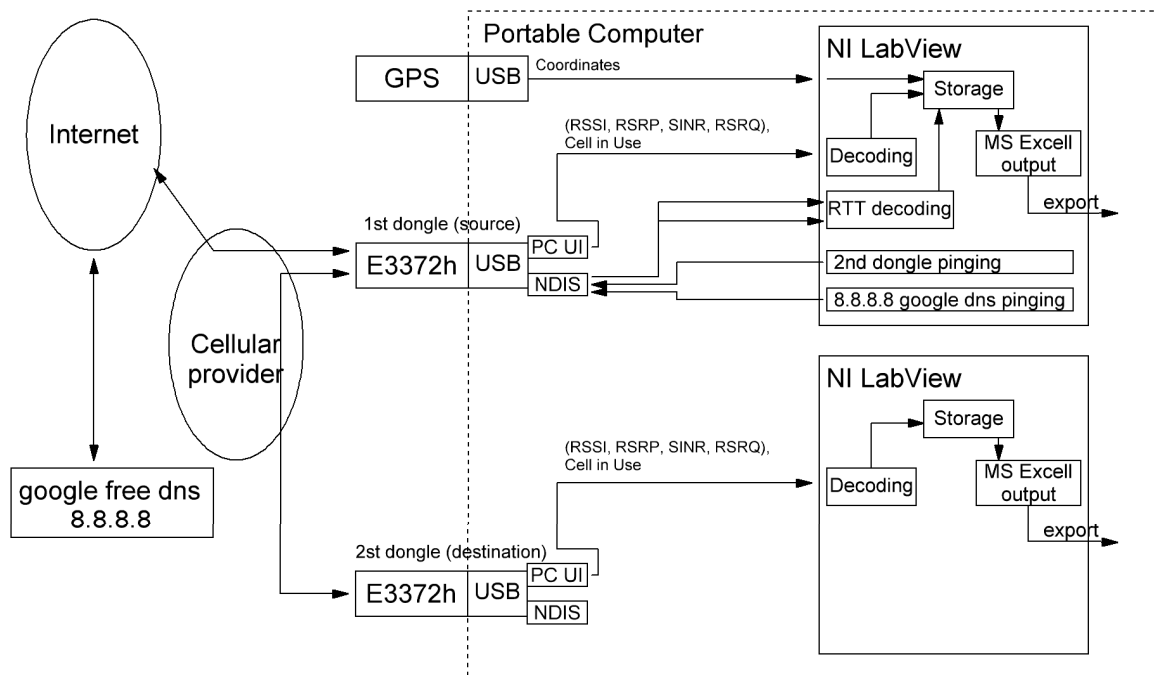

Fig. 2.44 Functions and interworking of the stationary and portable computers for the evaluation of the performance of various LTE cells.

The raw experimental data are shown below. The RTT measured between the first dongle and the server connected to the global Internet will be referred to as "D2wan" (Device-to-WAN). The RTT measured between the first and second dongles (which use the same operator's LTE network, the same frequency band and the same cell) will be referred to as "D2D" (Device-to-Device or Dongle-to-Dongle). The green bar is shown when both dongles were registered within the same cell.
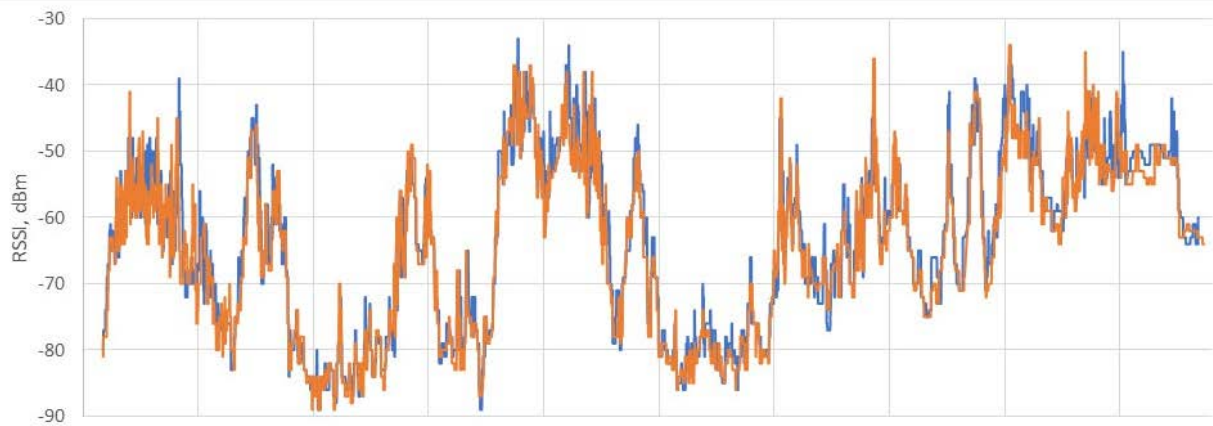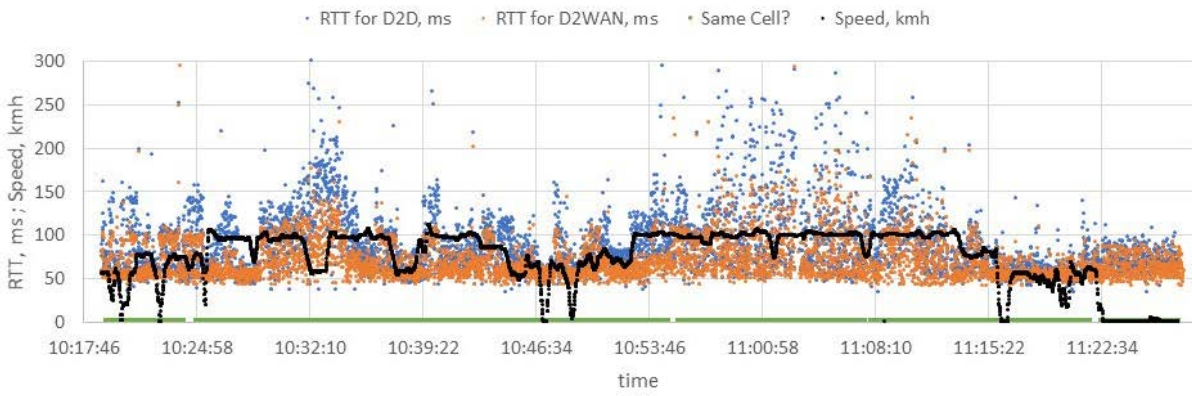
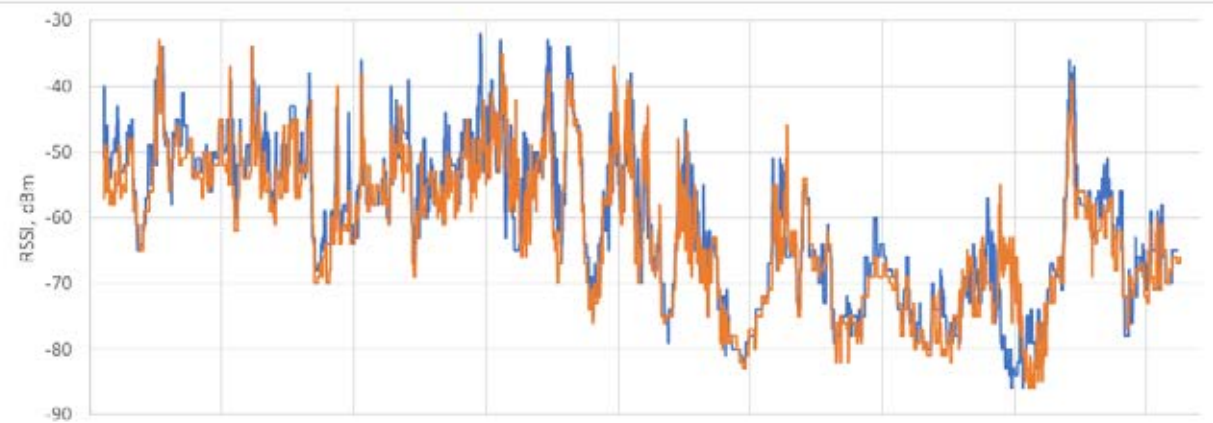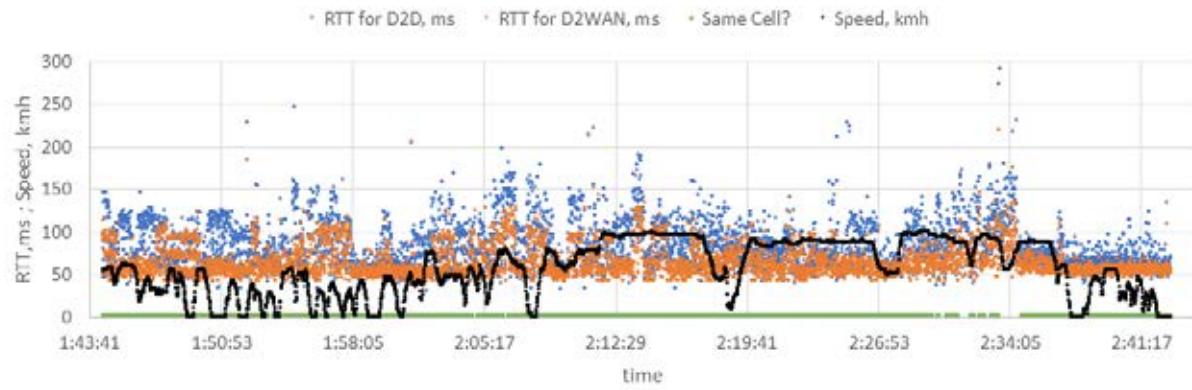Fig. 2.45 Experimental data of the LTE B3, path Cesis - Riga.

Fig. 2.46 Experimental data of the LTE B3, path Riga-Kemeri.
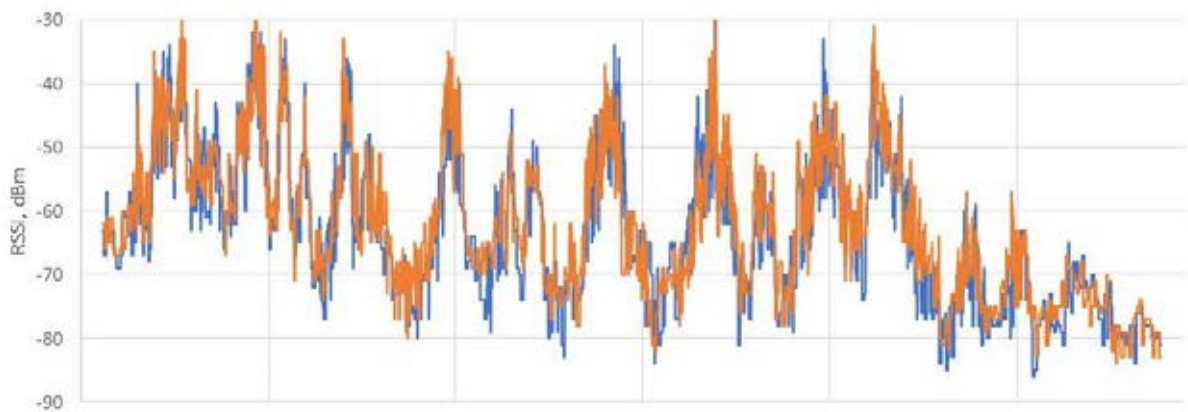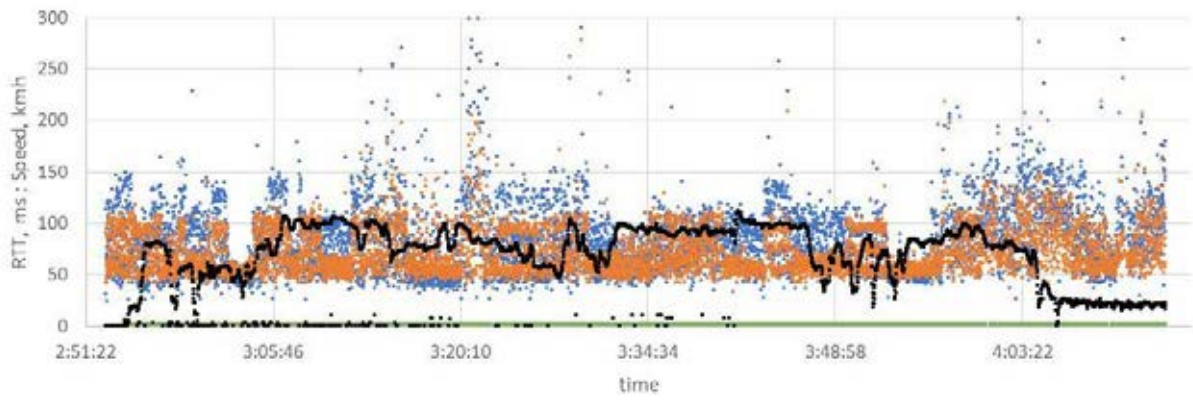
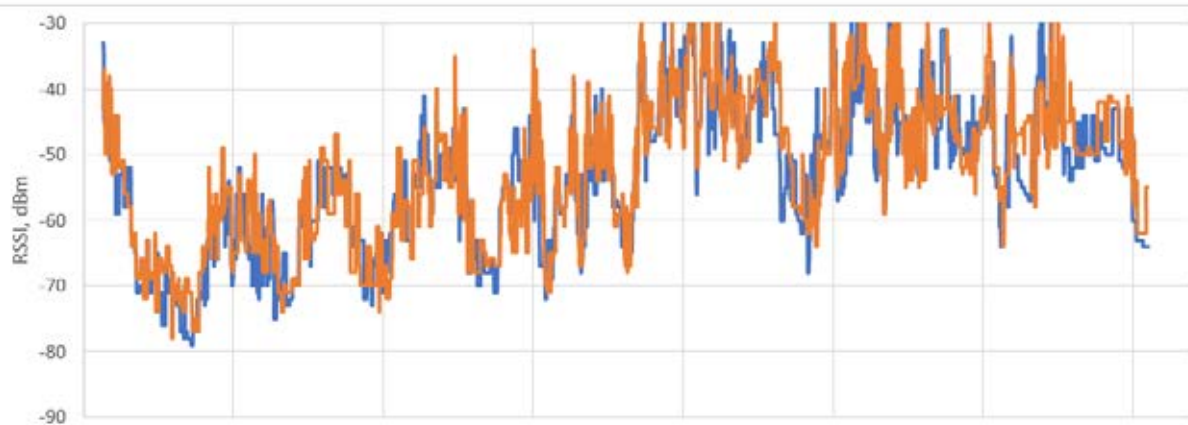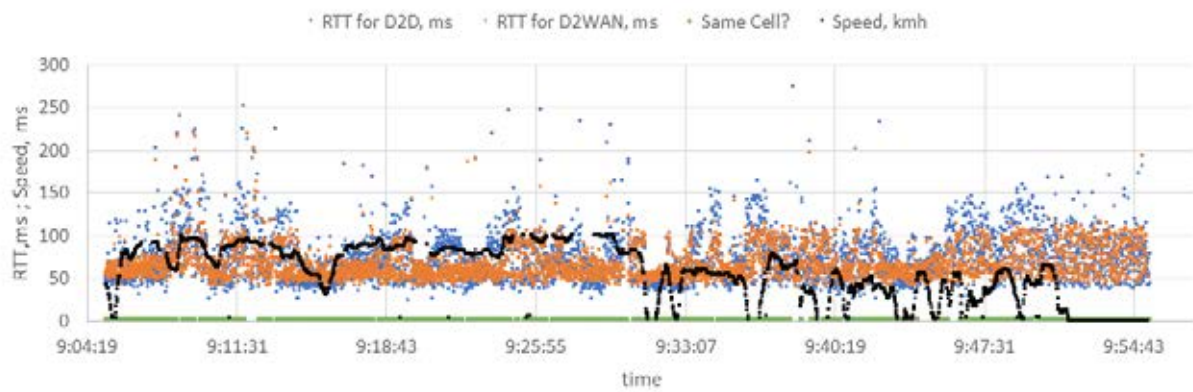Fig. 2.47 Experimental data of the LTE B20, path Riga-Cesis.

Fig. 2.48 Experimental data of the LTE B20, path Kemeri- Riga.

Further, in preliminary processing of the experimental data, all the unusable data were removed:

1. the data was used in the analysis only when both modems were registered within the same cell;
2. to eliminate the effect of a low signal level on the network RTT, experimental data obtained with the signal level RSSI < -80dBm (based on Cisco recommendations [63]) was rejected;
3. packets with a delay of more than 1 sec are considered lost and are discarded from further analysis.

Now it is necessary to evaluate the experimental data. As was already stated, the RTT of the LTE network obey a lognormal distribution law. Let us estimate the parameters of the log-normal distribution for each base station, in cases when both modems are connected to the same base station. Estimations of distribution parameters were carried out using the equations (2.9) and (2.10). Calculations were carried out only if the number of experimental data of delays $n \geq 100$. Estimates of distribution parameters for each BS (for each cell) are shown in Fig. 2.49 to Fig. 2.52, where the X axis is $\hat{\theta}_1 = \hat{\mu}$ (estimates of median), the Y axis is $\hat{\theta}_2 = \hat{\sigma}$ (estimates of standard deviation).

Fig. 2.49 Lognormal distribution parameter estimates for Device-to-Device scenario, operating in LTE B3 band.

Fig. 2.50 Lognormal distribution parameter estimates for Device-to-WAN scenario, operating in LTE B3 band.

Fig. 2.51 Lognormal distribution parameter estimates for Device-to-Device scenario, operating in LTE B20 band.
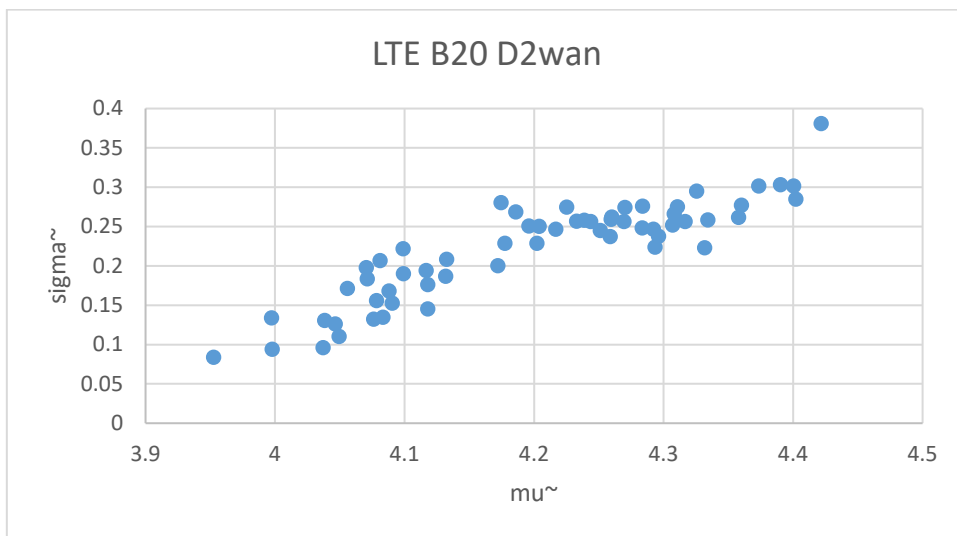
Fig. 2.52 Lognormal distribution parameter estimates for Device-to-WAN scenario, operating in LTE B20 band.

For clarity, let's also provide two-dimensional histograms of estimates of distribution parameters for BS in Fig. 2.53 to Fig. 2.56, where X is $\hat{\theta}_1 = \hat{\mu}$ and Y is $\hat{\theta}_2 = \hat{\sigma}$.
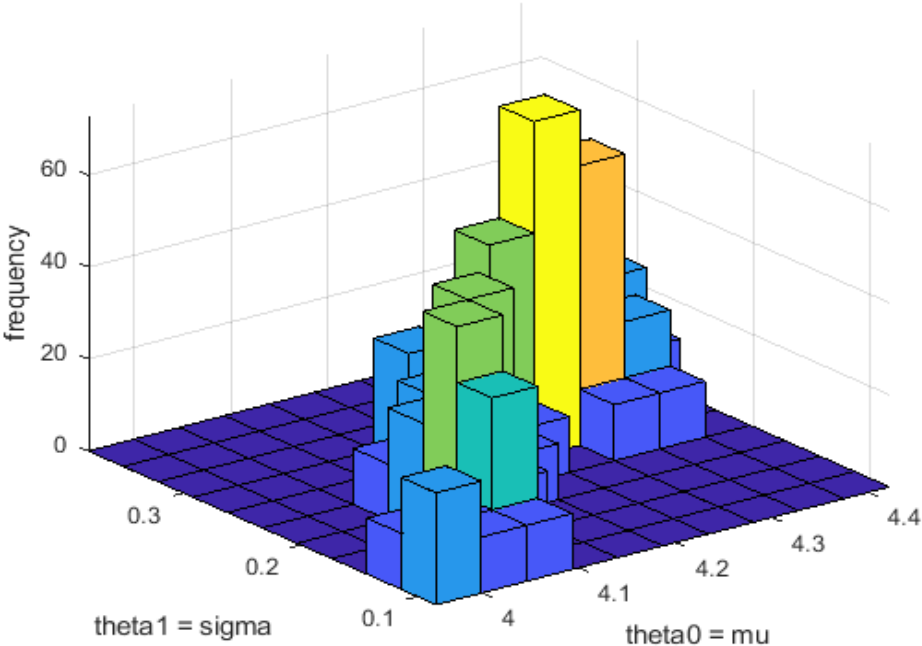
Fig. 2.53 Lognormal distribution parameter estimates for Device-to-Device scenario, operating in LTE B3 band.
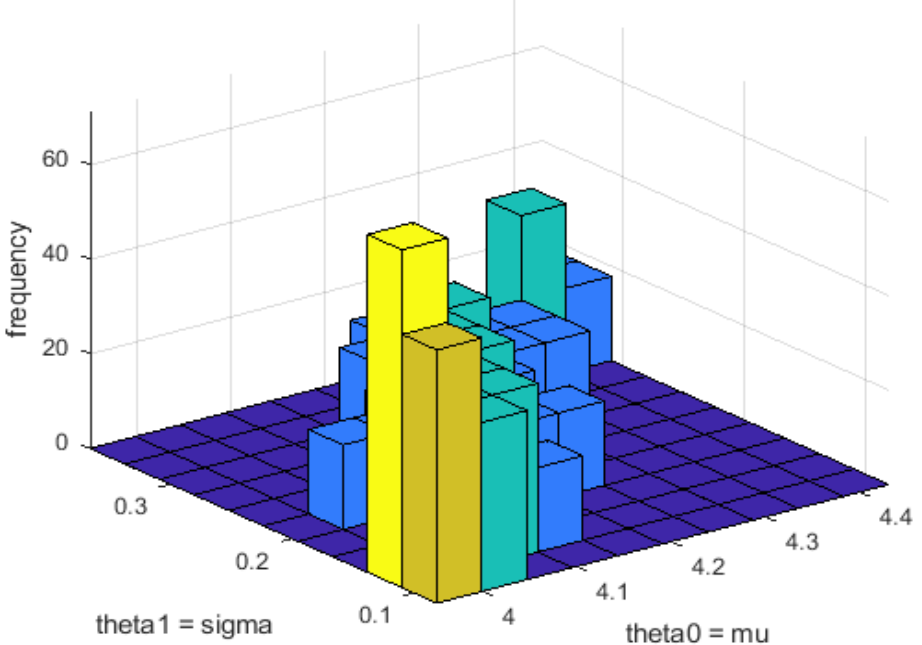
Fig. 2.54 Lognormal distribution parameter estimates for Device-to-WAN scenario, operating in LTE B3 band.
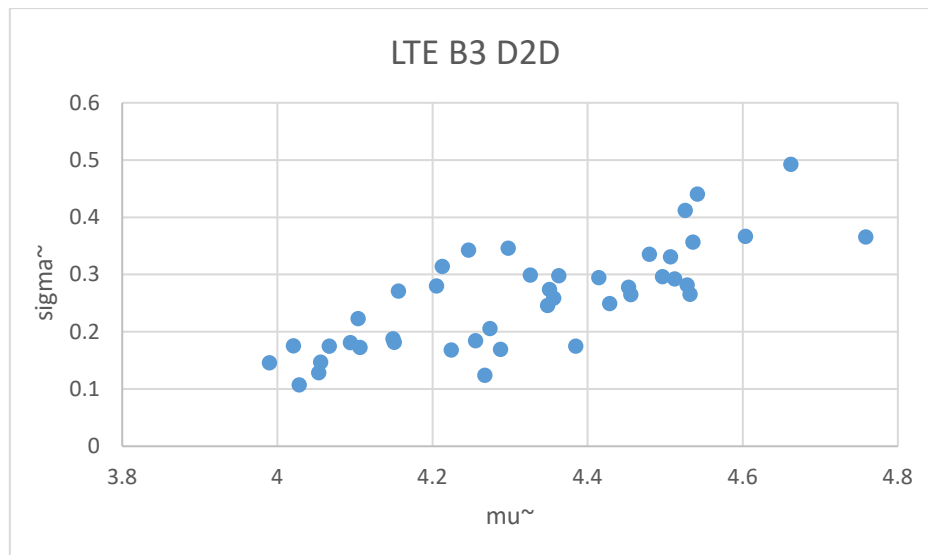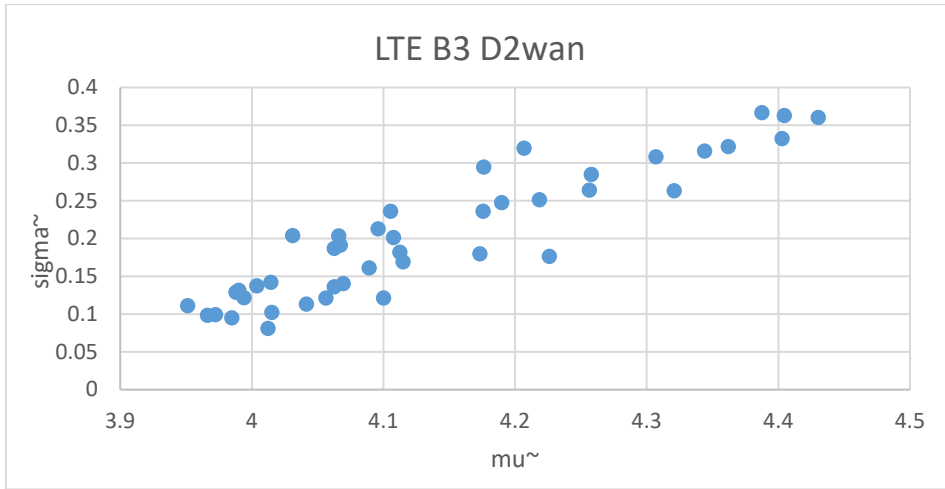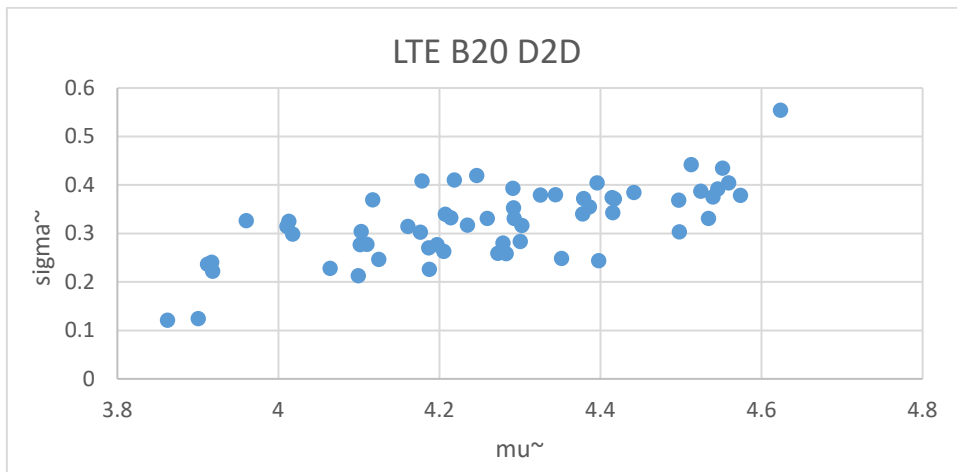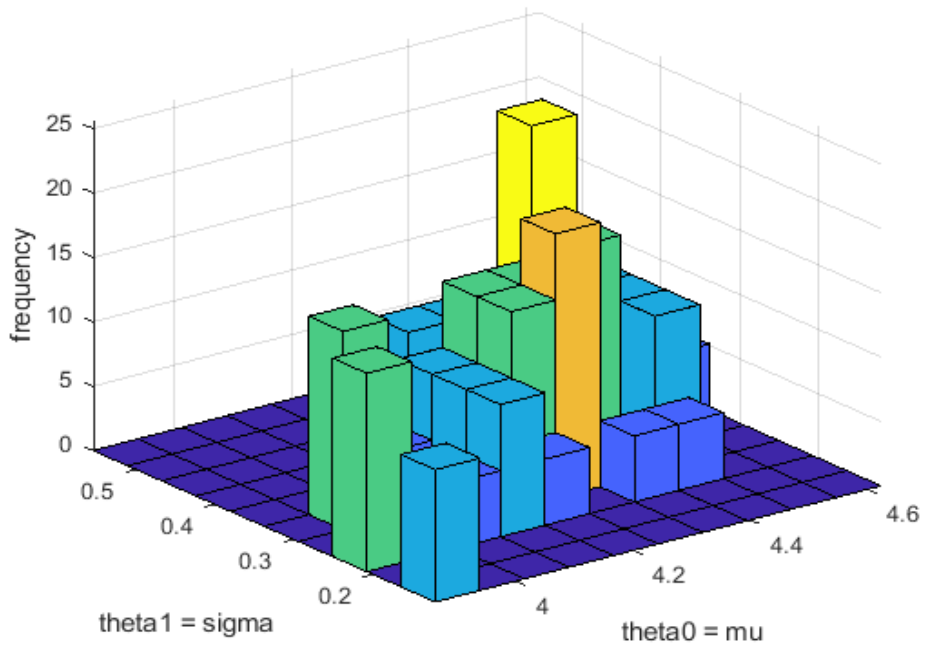
Fig. 2.55 Lognormal distribution parameter estimates for Device-to-Device scenario, operating in LTE B20 band.
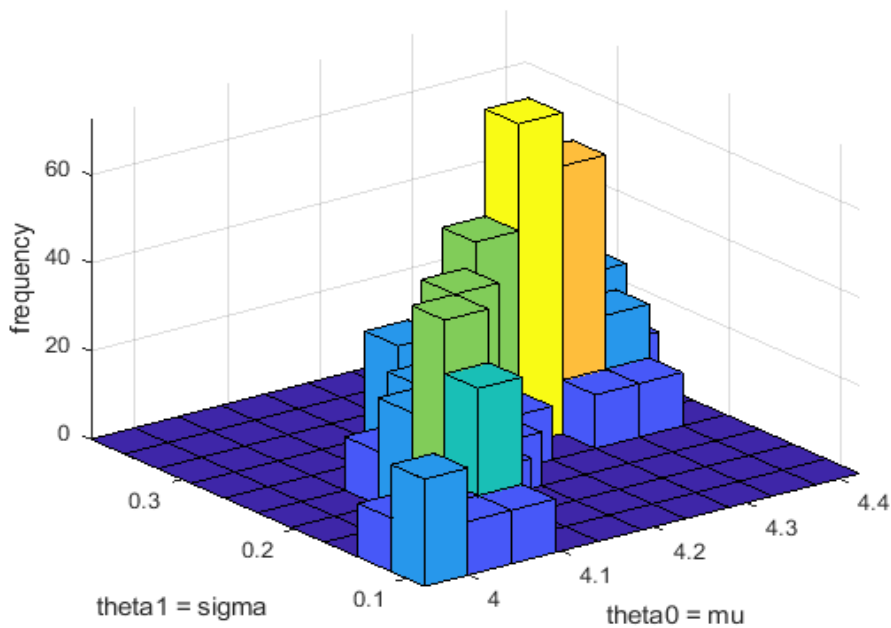
Fig. 2.56 Lognormal distribution parameter estimates for Device-to-WAN scenario, operating in LTE B20 band.

The location of the points in the graphs indicates a positive correlation between the distribution parameters of delays estimated for different LTE base stations. Now let's assume that obtained parameter estimates are equal to parameters $\hat{\mu} = \mu$ and $\hat{\sigma} = \sigma$ and let's obtain estimates for the numerical characteristics of a systems of random variables of parameters of

lognormal distributions μ and σ. Note that the values of random variables are given in natural scale, as well as these are independent. In this case, unbiased estimates of mathematical expectations (median) $\widehat{m}_\mu$ and $\widehat{m}_\sigma$ can be calculated using the arithmetic average:

$$\widehat{m}_\mu = \frac{\sum_{i=1}^n \mu_i}{n} \tag{2.41}$$

$$\widehat{m}_\sigma = \frac{\sum_{i=1}^n \sigma_i}{n} \tag{2.42}$$

The unbiased estimates of variance $\widehat{D}_\mu$ и $\widehat{D}_\sigma$ can be found by the following formulas:

$$\widehat{D}_\mu = \frac{\sum_{i=1}^n (\mu_i - \widehat{m}_\mu)^2}{n-1} \tag{2.43}$$

$$\widehat{D}_\sigma = \frac{\sum_{i=1}^n (\sigma_i - \widehat{m}_\sigma)^2}{n-1} \tag{2.44}$$

Hence, standard deviations will be equal to:

$$\widehat{\sigma}_\mu = \sqrt{\widehat{D}_\mu} \tag{2.45}$$

$$\widehat{\sigma}_\sigma = \sqrt{\widehat{D}_\sigma} \tag{2.46}$$

To find an estimate of the correlation coefficient, it is necessary to determine the statistical initial moment:

$$\alpha_{1,1}^*[\mu, \sigma] = \frac{\sum_{i=1}^n \mu_i \sigma_i}{n} \tag{2.47}$$

It is also required to find the statistical correlation moment:

$$K_{\mu\sigma}^* = \alpha_{1,1}^*[\mu, \sigma] - \widehat{m}_\mu \widehat{m}_\sigma \tag{2.48}$$

Now let's define the unbiased estimate of the statistical correlation moment:

$$\widehat{K}_{\mu\sigma} = K_{\mu\sigma}^* \cdot \frac{n}{n-1} \tag{2.49}$$

Then, the estimate for the correlation coefficient will be equal to:

$$\hat{r}_{\mu\sigma} = \frac{\widehat{K}_{\mu\sigma}}{\widehat{\sigma}_\mu \widehat{\sigma}_\mu} \tag{2.50}$$

The parameters of the system of random variables for the B3 and B20 bands both for the Device-to-Device and Device-to-wan connections are shown in the 2.19. table:

2.19. table

Parameter estimates of the system of random variables of the delays in the Tele2-LV LTE network

Mode	LTE B3		LTE B20	
Scenario	D2D	D2wan	D2D	D2wan
$\widehat{m}_\mu$	4.321111854	4.137481307	4.263534974	4.200827382
$\widehat{m}_\sigma$	0.258320572	0.202567894	0.322766576	0.221865836
$\widehat{D}_\mu$	0.037543165	0.019163568	0.037950614	0.014353549
$\widehat{D}_\sigma$	0.008008621	0.007172750	0.005791700	0.003842329
$\widehat{\sigma}_\mu$	0.193760587	0.138432539	0.194809174	0.119806296
$\widehat{\sigma}_\sigma$	0.089490898	0.084692087	0.076103222	0.061986520
$\hat{r}_{\mu\sigma}$	0.777179594	0.920297543	0.691265663	0.894327522

It should be noted that, in general, all the bands should provide similar performance (assuming similar received signal power and interference level and used bandwidth). The differences in the parameters of the system of random variables occurs due to inequality of these factors.

It can be concluded, that:

1. Traffic in 3G or LTE always goes through the core network of a cellular operator (even if the sender and the destination are within the same cell). This means that the implementation of the "first mile link" has an impact on the latency for any type of scenarios, such as Cellular-to-WAN or Cellular-to-Cellular.

2. Since UE operates with a particular BS and not with several BSs simultaneously, the delays in 3G or LTE networks should be evaluated separately for each cell; the results should not be combined, averaged, etc.

3. The difference in delays when mobile UE switches from one cell to the next one is caused by the differences in the terrestrial S1 link (also called "first mile link"), and not by the fact that the dongles are operate in different cells.

4. The assumption (myth) that the transmitter and receiver must be within the same cell to get the best performance, is not truth.

2.7. Development of delay requirements for the "C2 link"

As already mentioned, "C2 link" is a command and control link (the terminology and definition is provided in ICAO document [1]). Unfortunately, ICAO does not provide exact KPI values for a C2 link.

In order to specify the requirements for the delay for C2 link operations, at first it is necessary to review already existing requirements.

The real time network services comprise conversational and streaming services. These services are defined in the "End-to-end Quality of Service (QoS) concept and architecture" document of the European Telecommunications Standards Institute (ETSI), ETSI TS 123 207 V15.0.0 [64].

The first, well-known conversational network service is conversational voice, or VoIP (voice over IP network). The recommendations for the one-way transmission time for the international telephone connections and circuits are provided in the recommendation G.114 of the ITU [65]. The recommendation provides one-way delay limits of the average value in the so-called "E-model". The e-model helps to estimate the effect of one-way delay on voice communication service. This model shows that almost all users are satisfied with the quality if the one-way delay is below 150 ms. This model shows that with the delay of 400 ms only 70% of users are satisfied. The one-way delay of 400 ms is considered as the upper limit for the average value of the delay. It should be notes, that recommended one-way delay represents overall delay, in other words – implies the processing time too. Typical delay values of the individual parts and codecs of a transmission system are also provided in the recommendation [65]. The requirements of a PDV (or jitter) are not provided in the [65]. The main motivation to exclude this requirement is that the human ear is highly intolerant of it. In order to make the

voice service acceptable for the human ear, the variability in incoming packet arrival times is removed via the "de-jittering buffers" in all types of the voice services. The use of de-jittering buffer, by itself, add additional delays. This introduces jitter limits as < 1 ms. The human ear is more tolerant to some distortions of the audio information. These distortions typically are introduced by lost data packets, that leads to increased distortions in audio from the audio codecs. To eliminate the impact of the lost packets onto audio quality, the packet loss requirement in modern cellular networks for the voice transmission is set to $\leq 10^{-3}$, but in any cases not more than 3%, even if good audio codec is used.

The conversational video (videophone) also requires similar low-latency cervices. Typically, it requires that the average one-way delay should be less than 150 milliseconds, with the limit of 400 ms (similar to conversational audio). The main problem here is that the video signal should be transmitted with the voice, that leads to increased requirements for the video and audio streaming sync in order to provide "lip-synch". It is worth noting that latest MPEG-4 video codecs will provide acceptable video quality with frame loss rates up to about 1% [66].

The third conversational service is the control command transmission. Since these commands are entered by the operator, the operator must verify that the command was completely executed. This means that in the command transmission the operator will see a two-way delay (or RTT). For a typical operator, the RTT of a command transmission should not be greater than 250 milliseconds. Also, the command transmission, in a contrast with the voice transmission, is not tolerated to the lost packets [66].

The telnet service is also one of the conversational command transmission tools. However, it requires very short delay in order to provide character echo-back for the operator. The mean RTT value should to be < 200 milliseconds [66].

The remote-desktop connection also requires feedback from the remote-controlled computer, hence two-way delay again is significant. The available study indicates that a typical user tolerates with the mean RTT of 200 ms [67].

The authors in [68] state that the command and control link should be with the delay of 50-100 ms.

Finally, the last one conversation service is the interactive games. Such type of games requires short delays in order to be really "interactive". The author in the [69] states that different types of interactive games may tolerate with different RTTs. The third person avatar games (Role Playing Games (RPG) and Massively Multiplayer Online Role-Playing Games (MMORPG)) tolerates with the mean RTT up to 500 ms, whereas < 120 ms is recommended [70]. The first-person avatar (e.g. shooters) tolerates with the mean RTT up to 100 milliseconds only.

Next, it is possible to analyze already existing requirements based on IP network QoS classes and its network performance objectives. Y.1541 The numerical objectives of a data transfer network performance are organized in sets, called network Quality of Service (QoS) classes. The number of classes is small, so each class must satisfy the needs of various applications. The network QoS classes are listed in the following table 2.20, in accordance with [3]. Note that these requirements apply to public End-to-End IP network (excluding processing time in the source and destination).

IP network QOS class definitions and network performance objectives

Network performance parameter	Nature of network performance objective	QoS classes				
		Class 0	Class 1	Class 2	Class 3	Class 4
IP packet Transfer Delay, one-way (IPTD)	Mean IPTD	100 ms	400 ms	100 ms	400 ms	1 s
IP packet Delay Variation (IPDV) (* 2-point IP packet delay variation)	Upper bound on the $1-10^3$ fractal of IPTD minus the minimum IPTD	50 ms	50 ms	Undefined	Undefined	Undefined
IP packet Loss Ratio (IPLR)	Upper bound	1×10^{-3} (based on high-quality voice applications requirements)	1×10^{-3} (based on high-quality voice applications requirements)	1×10^{-3}	1×10^{-3}	1×10^{-3}
IP packet Error Ratio (IPER)	Upper bound	1×10^{-4}	1×10^{-4}	1×10^{-4}	1×10^{-4}	1×10^{-4}

Note that a sample of a minimum of 1000 packets [3] is required to evaluate the $1-10^3$ bound of the IPDV.

The performance parameters of the data transfer network are mostly affected by the packet size. A fixed information field size of 160 or 1500 octets is recommended in [3].

The following table gives guidance for the applicability of QoS classes. These recommendations are provided in [3].

IP Guidance for IP QOS classes

QoS class	Applications	Node mechanisms	Network techniques
0	Real-time, jitter sensitive, high interaction (VoIP, VTC)	Separate queue with preferential servicing, traffic grooming	Constrained routing and distance
1	Real-time, jitter sensitive, interactive (VoIP, VTC)		Less constrained routing and distances
2	Transaction data, highly interactive (Signaling)	Separate queue, drop priority	Constrained routing and distance
3	Transaction data, interactive		Less constrained routing and distances
4	Low loss only (short transactions, bulk data, video streaming)	Long queue, drop priority	Any route/path

Some results, based on field experiments, that are related to controlled flights, also can be found. Since the time-delay in RPAS refers to time period between sending command input from the GCS and displaying feedback in GCS after response of aircraft, this delay is a two-way delay. This means that the two-way delay in RPAS systems imply not only latencies of uplink and downlink data transfer channels, but also flight control computer delay (doubled, because it should give a command to actuator or ESC and process a feedback from sensors), as well actuator or ECS delay. Based on experimental data, provided in [71], it is possible to conclude that the overall time delay in the control channel and its feedback for a manned flight should not to be more than 310 ms. Starting from 360 ms the piloting tasks still are possible, but these requires more mental effort; as well with the delays more than 410 ms controlled landings becomes problematic. It should be noted that none of techniques to reduce the impact of the delay was not used. Similar results are obtained in [72]. The authors investigate the impact of the communication delay on the flock in order to prevent an oscillatory behavior. They found that the communication delay must be below 200 ms, otherwise the feedback becomes too slow in order to eliminate the oscillations in maneuvers. It should to be noted, that the research implies only communication delay, without other delays, included in [71].

Now let's specify KPI for a typical command and control link.

At first, the RC operation is one of the conversational network services. It implies sending the command from GCS, its delay in uplink channel, it's processing in the flight computer and actuator, as well the delay in feedback, that also implies the delay in downlink channel. As can be seen from the voice conversation services, typical human can tolerate with the latency (one-way delay) < 150 ms (PDV is compensated via the de-jittering buffer). Under ITU recommendations the RC application apply to QoS Class 0, that requires mean latency (one-way delay) of ≤ 100 ms and the IPDV of ≤ 50 ms (that gives almost the same requirements, compared to voice service). The conversation service of the command transmission requires

RTT (two-way delay) ≤ 250 ms. It should be noted that this delay also implies processing time in the target machine. The first-person avatar games, where the environment changes very rapidly, requires RTT of ≤ 100 ms.

The RC operations require bi-directional communications. In case if the feedback is provided via the video channel (so-called First-Person View (FPV)), the overall one-way delay for a video channel (including processing time of the codecs) must be ≤ 150 ms. Similar requirements come from the machine-to-machine (M2M) data link: not more than 200 ms one-way delay in order to illuminate the oscillations in their activity's coordination.

As can be seen from the experimental studies, the experienced pilot can tolerate with the overall delay of the control system + feedback of 310 ms, whereas higher delays require more mental effort and may result in oscillations of the airplane.

The required data rate is another source of concern. These requirements should be based on the proposed application, e.g. telemetry, video broadcast, image transfer, etc.

The 3GPP introduces the generalized requirements for uplink/downlink data rates for command-and-control traffic of 60-100 Kbps. This was done in the 3GPP Release 15 [73], [74]. However, it should be noted that particular requirements for command-and-control traffic depends on data amount that should be sent, e.g. GPS coordinates, altitude feedback, etc., since the amount of data can be different for various implementations.

The authors in [68] with the reference to [75] specify generalized requirements for the image transfer as 1 Mbps with the delay of 50-100 ms. Further, similar generalized recommendations, with the reference on [76] are provided for the video streaming: 2 Mbps with delay on 50-100 ms. The term "delay" here should be understood as latency (one-way delay), since here the streaming services are discussed.

It can be concluded, that:

1. The "ideal" overall two-way delay (from the command input and to the feedback display) should be ≤ 150 ms for a <u>typical pilot</u>; and not more than 200 ms to prevent oscillations (if none of helping technologies (e.g. PID controllers) are used).
2. The "ideal" overall two-way delay (from the command input and to the feedback display) should be ≤ 310 ms for an <u>experienced pilot</u>; with the limit of 400 ms (will require more mental effort from the pilot).
3. In case if FPV is used as feedback, the <u>video channel</u> overall (including processing time of video codecs) one-way delay should be ≤ 150 ms (assuming 0 latency in the command data transfer line for a typical pilot!).

2.8. Analysis of compliance of delays in the LTE cellular network with the "C2 link" requirements

In this chapter the delays of various LTE cells will be analyzed for the suitability to the RC and FPV needs. The RC operation implies sending the control command, its processing by the remote equipment, the reaction of this equipment and finally the feedback to the pilot.

Based on the review of different requirements, that has been shown in the Chapter 2.7 of the thesis, the requirements for the RC operations are as follow:

- ≤ 150 ms is recommended for a typical pilot (with the limit at 200 ms)
- ≤ 310 ms is recommended for an experienced pilot (with the limit at 400 ms)

Since the delay in RC operations also imply feedback, then the RTT value should be used. Assuming that no PID controllers are used, as well that the onboard equipment has negligible processing time (which is not true if the control data transfer bus in not synchronized with the processes in the autopilot), the overall delay in RC operations mainly consists of network RTT.

Based on the review of available requirements that has been shown in the beginning of the thesis, the requirements for the conversational video (in our case this is the FPV are as follow:

- overall one-way delay should be ≤ 150 ms (this implies the impact of the de-jittering buffer, as well codec's processing time)

Assuming that "zerolatency" codecs are used (like H.264, when one packet is processed at a time), the overall delay will consist of a data transfer line delay plus de-jittering buffer delay. Let's assume that the de-jittering buffer delay is equal to IPDV value. The IPDV value states the difference between the upper bound on the 0.999 fractal of IPTD minus the minimum IPTD (see introduction for more details in metrics).

To obtain the results, let's utilize the system of random variables of the Tele2-LV LTE network, operating in B20 band in D2D scenario. The expectations will be made based on the assumption, that RTT values of LTE cells obeys the lognormal distribution. The following Fig. 2.57 shows simulated (blue dots) and experimental (yellow markers) parameters of lognormal distributions. The simulation results consist of 50'000 simulated distribution parameters. The simulation is done using normal distribution law. approximation of the system of random variables and the experimental data, listed in 2.19. table.
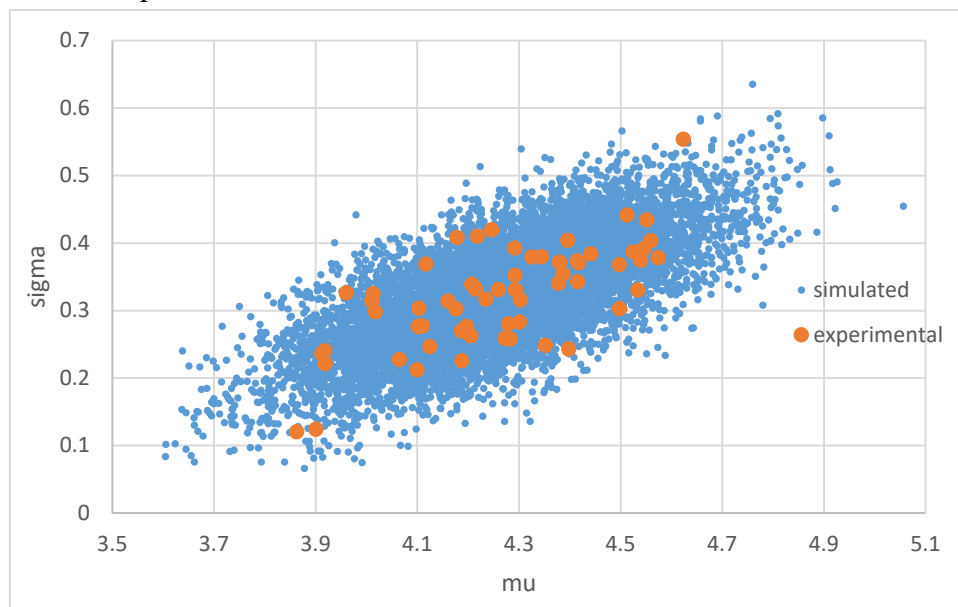

Fig. 2.57 Parameters of lognormal distributions of RTTs of different LTE cells (D2D scenario of LTE-to-LTE in the band B20, Tele2-LV).

The RTT for RC-operations will be expressed from the simulated data, related to the performance of individual cells. The RTT will be expressed as the 0.999 fractal (with the aim to show that the RTT in 99.9% will not be greater than value specified). The estimation of the

0.999 fractal $\Phi^{-1}(0.999)$ will be done assuming that RTT values of LTE cells are logarithmically normal distributed. The following illustration Fig. 2.58 shows the PDF and CDF of the 0.999 fractal of RTT.
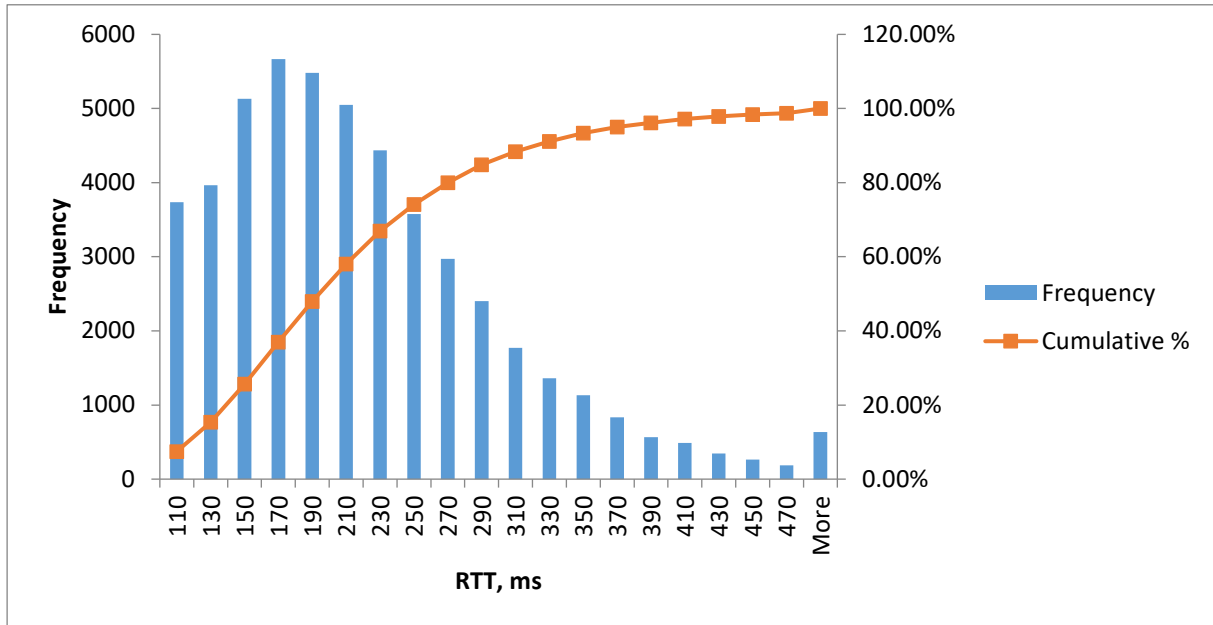

Fig. 2.58 The 0.999 fractal of RTT (D2D scenario of LTE-to-LTE in the band B20, Tele2-LV).

The results show that the performance of only 25 % of LTE cells guarantee that at least 99.9% of RTT will be below 150 ms and only 53 % of LTE cells guarantee that at least 99.9% of RTT will be below 200 ms. Therefore, the delays of LTE networks in many cases are not suitable for the RC operations for a typical pilot.

The results show that the performance 88 % of LTE cells guarantee that at least 99.9% of RTT will be below 310 ms and 97 % of LTE cells guarantee that at least 99.9% of RTT will be below 400 ms (which is the maximum allowed RTT for an experience pilot). This indicates that the experienced pilot can perform RC operations via the LTE network (note that sometimes an experienced pilot will have to provide more mental effort, as RTT will be greater than 310 ms).

Finally, it should be noted, that the experimental results for different cells operation were analyzed only if a signal quality was "good" (as specified in the recommendation [63]).

Next, it is necessary to evaluate the delays for an FPV video channel. The FPV is unidirectional data transfer, hence here we are interested in latency (one-way delay). The problem is that the experimental data as well as the simulated data contain only RTT (two-way delays), whereas one-way delay measurements are complicated due to precise time synchronization problem on both ends. If the uplink and downlink channels are identical, then the network latency can be estimated by dividing the RTT by two. Unfortunately, the uplink and downlink channels in HSPA+ and LTE networks have different performance (more detailed information about the performance of uplink and downlink channels in HSPA and LTE can be found in [77]). However, in D2D scenario, when LTE UE is connected to another UE, the RTT implies two uplink and two downlink channels. Also, since both UE are within same cell (as it was in the experiment), they should operate with same modulation and coding scheme. This

79

leads to similar performance of both uplink channels and similar performance of both downlink channels. This, by itself, makes possible to estimate the latency of D2D channel by dividing the RTT by two.

Considering all the above mentioned, the distribution parameters for latency estimation in D2D scenario (assuming lognormal distribution) will be calculated as follow:

$$\theta_{0\ RTT} = \mu_{RTT} = \ln(2) + \theta_{0\ latency} = \ln(2) + \mu_{latency} \qquad (2.51)$$

$$\theta_{1\ RTT} = \sigma_{RTT} = \theta_{1\ latency} = \sigma_{latency} \qquad (2.52)$$

Next, the overall latency in conversational video transfer should imply the delay in de-jittering buffer. In the following evaluation it will be assumed that the de-jittering buffer length is equal exactly with the IPDV (IPDV is defined as the difference between 0.999 fractal and the minimum value of latencies). The illustration Fig. 2.59 shows the length of required de-jittering buffers (that are equal to IPDV values), depending on the cell in use.
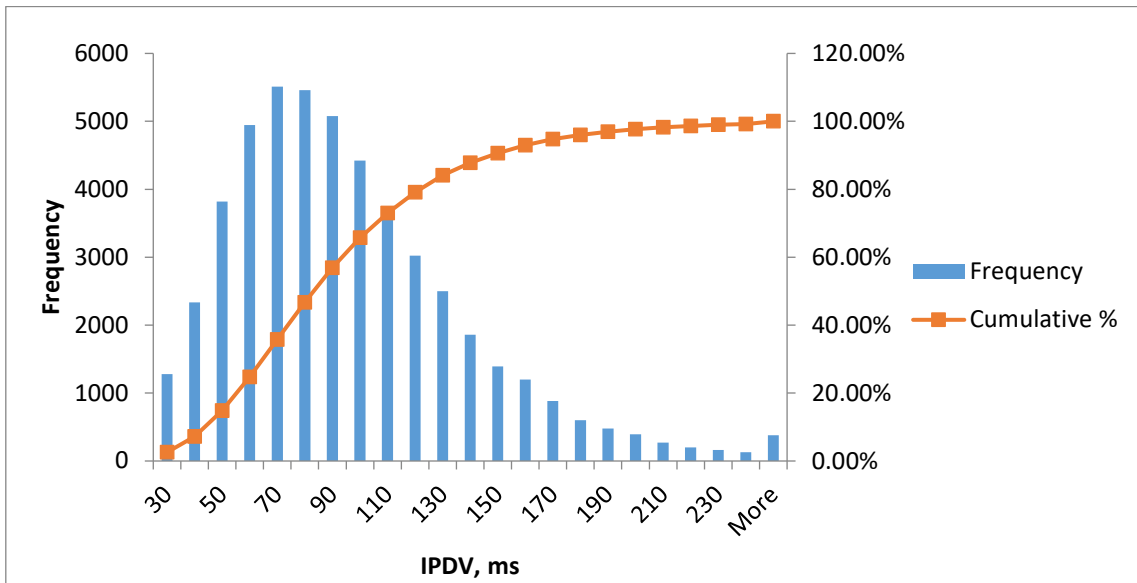

Fig. 2.59 The IPDV of latency (D2D scenario of LTE-to-LTE in the band B20, Tele2-LV).

The experimental data shows that the de-jittering buffer of 310 ms will be sufficient in 99.9 % of times (or 230 ms buffer will be sufficient in 99 % of times). Next, assuming constant length of the de-jittering buffer of 310 ms (that will be sufficient in 99.9% of times, producing 0.1% packet drop) let's define the latencies of different cells. The latencies will be equal to minimum latency plus de-jittering buffer of 310 ms. Since the maximum allowed latency for the FPV is 150 ms, it is clear that all of the resulting latencies will be out of the recommended limit. Therefore, the LTE data transfer service does not satisfy the requirements for the FPV of 150 ms if a constant size 310 ms de-jittering buffer is used.

Now let's assume that the de-jittering buffer is adaptive and is equal to the IPDV value. Since no additional space is considered in the de-jittering buffer, the FPV channel will operate with the constant latency of 0.999 fractal of the latency the given cell.
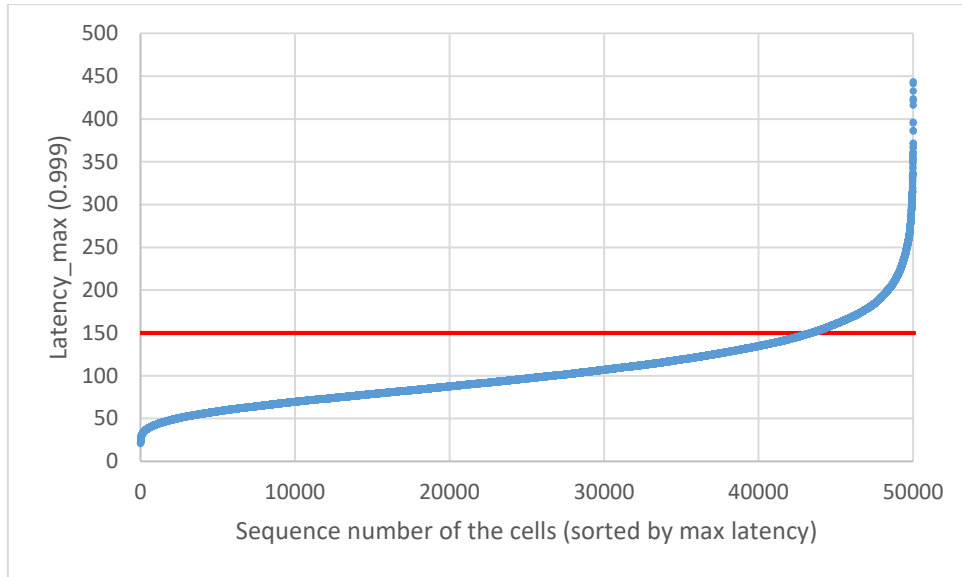
Fig. 2.60 Latencies of different cells, if adaptive de-jittering buffer equal to IPDV is used (D2D scenario of LTE-to-LTE in the band B20, Tele2-LV).

As can be seen from the illustration above, only 86% of LTE cells will satisfy the required latency of <150 ms with the packed drop rate of 0.1%.

Since modern video codecs can accept packet loss up to 1% [66], the upped bound for the IPDV can be set to 0.99. In order to be able to find how many LTE cells can guarantee that the FPV will operate with delays ≤ 150 ms and the packet loss rate 1% (assuming that all packets with the latencies more than 150 ms are discarded), let's show ordered fractals of the 0.99 probability of all LTE cells. The following illustration shows the latencies, if the de-jittering buffer is adaptive and is equal to IPDV with the boundary 0.99, as well as the packet loss can be up to 1 %.
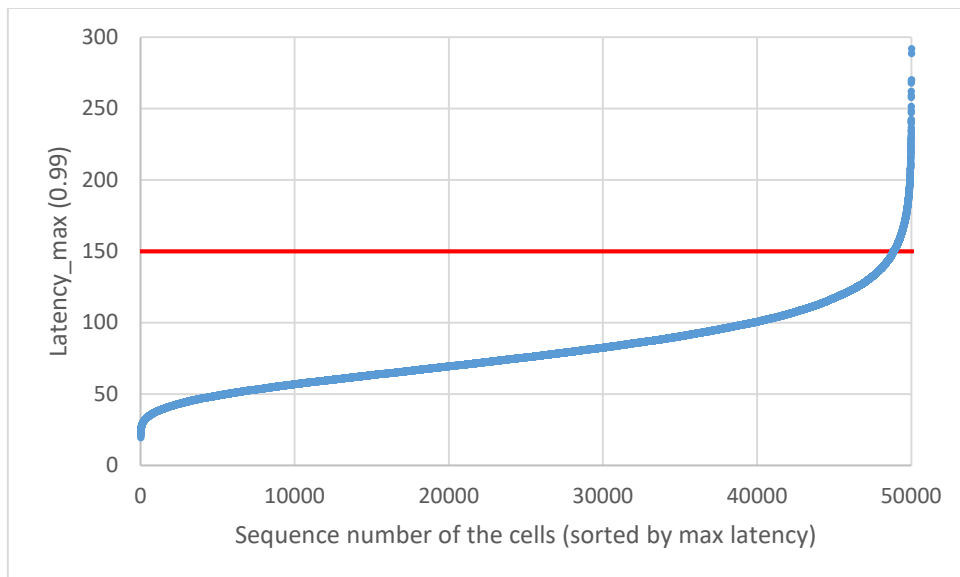

Fig. 2.61 Latencies of different cells, if adaptive de-jittering buffer size is equal to IPDV with the 0.99 boundary (1% packet loss target) (D2D scenario of LTE-to-LTE in the band B20, Tele2-LV).

It can be concluded that 98% of LTE cells will provide satisfactory latencies for the FPV target of < 150 ms latency, if the de-jittering buffer is equal to IPDV, and 1 % packet loss is allowed). This assumption implies zero latency in codecs and camera, as well ideal IPDV estimation for the adaptive de-jittering buffer sizing, as well that the quality of the radio signal is "good" (as per this reference [63]).

Assuming that the pilot receives the feedback through the telemetry, it can be concluded that:
1. Only 25 % of LTE cells provide RTT be below 150 ms and only 53 % of LTE cells provide RTT below 200 ms. Therefore, the delays in LTE networks in many cases are not suitable for the RC operations for a typical pilot.
2. 88 % of LTE cells provide RTT be below 310 ms and 97 % of LTE cells provide RTT below 400 ms. Therefore, the delays in LTE networks in many cases are suitable for the RC operations for an experienced pilot (note that sometimes an experienced pilot will have to provide more mental effort, as RTT will be greater than 310 ms).

Assuming that the pilot receives the feedback through the VPF, it can be concluded that:
1. A constant length de-jittering buffer of 310 ms will be sufficient in 99.9 % of LTE cells (or 230 ms buffer will be sufficient in 99 % of LTE cells).
2. Since the maximum allowed latency for the FPV is 150 ms, the LTE data transfer service does not satisfy the requirements for the FPV if a constant size de-jittering buffer is used.
3. If an adaptive length de-jittering buffer is used and the length of the buffer is set to the IPDV value determined as the difference between the quantile of a maximum delay at the probability 0.999 and minimum delay (0.1% packet loss), only 86% of LTE cells will satisfy the required latency of <150 ms.
4. If an adaptive length de-jittering buffer is used and the length of the buffer is set to the IPDV value determined as the difference between the quantile of a maximum delay at the probability 0.99 and minimum delay (1% packet loss), 98% of LTE cells will satisfy the required latency of <150 ms.

3. ANALYSIS OF THE IMPACT OF FLYING ALTITUDE ON THE PERFORMANCE OF CELLULAR DATA TRANSFER SERVICES

As mentioned in the introduction section, 3G and LTE data transfer services promise a cheap and lightweight solution for the UAV and RCV remote control wireless channel implementation. Available field studies [24], [27] stated that cellular network coverage up to 300 m height above ground level (AGL) is sufficient to promise possible UAV control over cellular data transfer services. However, the all-inclusive field study by Fung Po Tso et al. [61] noted ground moving UE downlink and uplink throughput degradation, even if the signal strength was sufficient. Experimental results, represented in the previous section, also confirm service quality deterioration of 3G networks as soon as the UE starts to move. The data in [61] is statistical representation of throughput, Round Trip Time (RTT) and Energy per chip to Interference plus Noise ratio (Ec/Io) measurements and is not suitable to provide excessive information on degradation problem causes. The field studies performed in Riga also reported poor 3G cellular data transfer service performance during flight even if the signal strength was sufficient [78].

The data transfer service quality considerably depends on UE ability to detect its useful signal against all other signals (considered as interference). This means that the cellular network data transfer service mainly depends on the overall signal strength indicator (RSSI) and useful signal strength indicator (RSCP in 3G or RSRP in LTE networks). In rural area, the regional morphology has a major impact; in urban area, the signal is affected by shadows from buildings and signal multiple reflections (multipath). Consequently, if the UE is placed above the earth surface, the signal strength must be defined by the cell carrier frequency, distance between Base Station and UE, as well as NodeB (or eNodeB) array pattern only (as well antennas gain pattern). At a higher altitude, RSSI and RSCP (RSRP) levels become increased as the UE and the selected Base Station (BS) obtain LOS path without interfering objects at all. However, RSSI also increases because UE obtains LOS with more BSs that were previously shaded. This increases difference between an overall signal strength indicator (RSSI) and a useful signal strength indicator (RSCP in 3G or RSRP in LTE). More BSs at the same band cause higher interference and make signal detection process more complicated. This effect is measured by the UE and indicates via wireless signal performance indicators, such as: Energy per chip to Interference power ratio in 3G networks (Ec/Io, expressed in dB, its value is always below 0 dB) or Reference Signal Received Quality (RSRQ, in dB, always less than 0 dB) and Signal to Interference and Noise Ration) (SINR, in dB, can be negative or positive) in LTE networks.

3.1. Experimental evaluation of the performance of cellular network during real flight with maneuvers

A lot of research papers and field studies are devoted to ground (terrestrial) cellular communications. At present, few research papers are also available for the evaluation of the potential of cellular data transfer service for UAVs. The same problem is stated in all these

papers: high downlink channel interference as flying UAV obtains LOS path with many BSs and other UEs [25], [79], [80]. UE Automatic Modulation and Coding (AMC) mechanism reports increased interference via the Channel Quality Indicator (CQI) to BS to request slower modulation and coding scheme. This leads to slower data rates, but helps to keep BER at 0.1 % [47]. Cellular data transfer services (3G and LTE) at higher altitudes will operate with slower modulation and coding scheme due to increased interference. Interference level values represented in [25] are not below minimum acceptable limits (compared with the cisco requirements [63]) and the data transfer service should be able to operate correctly, keeping BER at 0.1%.

Unfortunately, field studies on real 3G working equipment indicate temporary data packets loss that leads to massive resends made by HARQ mechanism, causing "spikes" in RTT (latency) and jitter. This leads to periodical freeze in UAV telemetry feedback (e.g. real time artificial horizon display) and jittering in video channel.

Let's assume that influence of increased interference can be redoubled by the fact that flying UE antennas have angular position variations, causing antenna polarization variations, as well as Doppler shift variations.

This experiment was performed to check 3G network performance in case of rapid horizontal and vertical speed elevations, as well as tilt and roll changes (UE antenna angular rotations) when UE is flying. This was done by placing UE in lightweight Cessna 172N airplane.
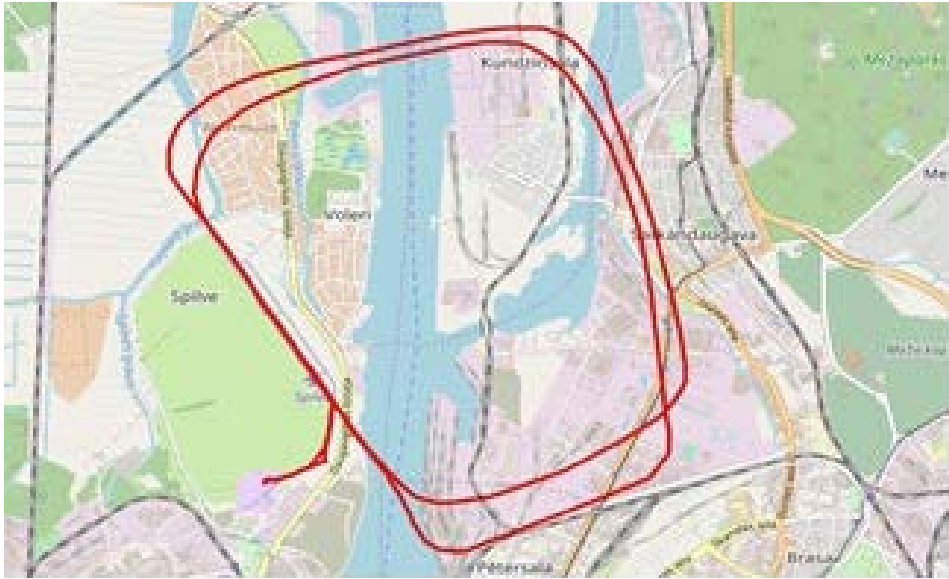

Fig. 3.1 Visualized GPS coordinates of the horizontal flight path.

A ground run, one take-off, one go-around, two flares and one ground roll were performed in Spilve airfield in Riga. GPS data visualization is done by online resource [81].

A strong crosswind at the take-off / landing causes additional complexity for the pilot and causes various types of airplane position and angle elevations. The Meters Above Sea Level (MASL), ground speed and coordinates measurements were reported by GPS receiver once per second. Unfortunately, this results in low gust resolution, whereas angular position (tilt and roll) was not measured at all and not represented here.

The experimental data can be divided into two parts. The first part contains reference data captured from the stationary aircraft, and the experimental results are shown in Fig. 3.2. The first plot shows RTT in time (blue curve); the second plot shows network performance indicators: RSSI (left Y axis, blue curve in dBm); Ec/Io (right Y axis, red curve in dB).
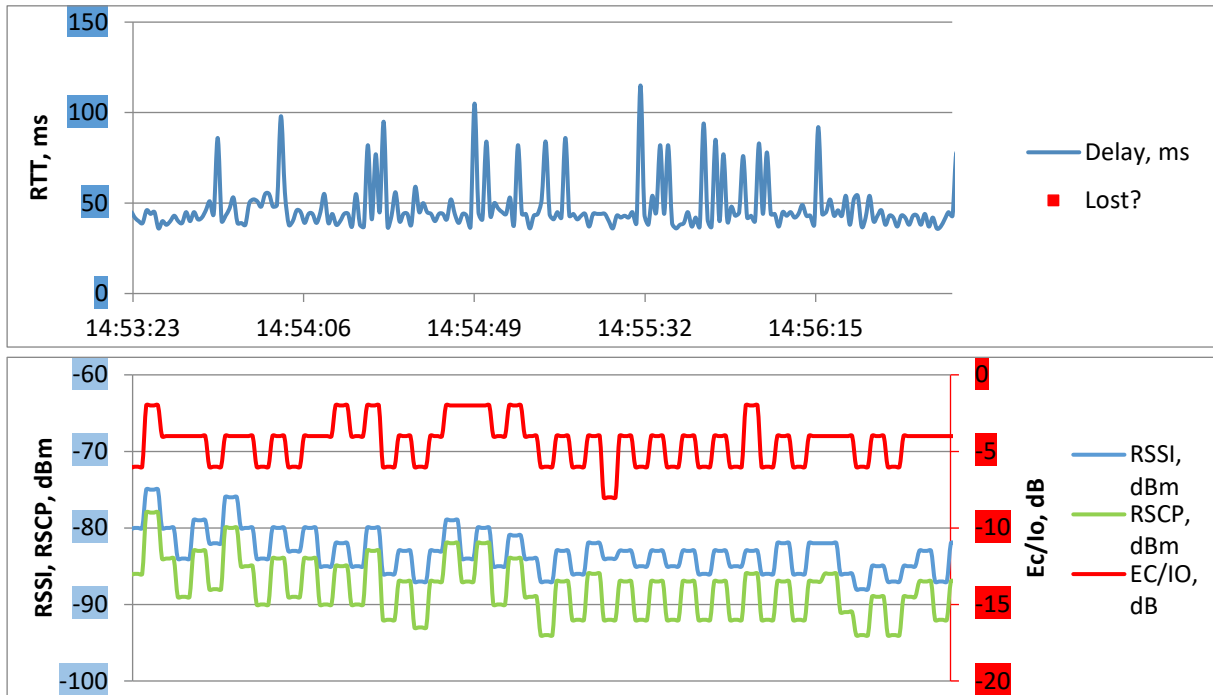

Fig. 3.2 Network performance for the immovable UE placed on the ground.

On the ground RSSI level is satisfactory: −84 dBm. The Ec/Io is in perfect-to-good of −4 … −6 dB limits. RTT values are small and stable: 45 ms in average. None of packets were lost.

The second part contains two paths. The first path (take-off, horizontal flight and approach) was done by inexperienced pilot, while the go-around and further flight was done by the more experienced flight crew and the flight was much more stable.

At the beginning of the ground roll of the airplane, RSSI level is satisfactory: −78 dBm. Then the airplane is accelerated up to 120 kmh. The RSSI and Ec/Io values are not affected, whereas RTT becomes less stable. The take-off takes place at 14:59:56. This results in larger RSSI values: at the top altitude of 300 m the RSSI value increases up to −62 dBm, while the Ec/Io drops down to −10 … −18 dB. The RTT values become unstable and the majority of them exceed 1 sec (are considered as lost) and the data transmission almost failed regardless of high RSSI values and Ec/Io is poor, but still acceptable. Further speed, flight direction and altitude changes have no noticeable effect on almost failed data transfer. A go-around occurs at 15:05:00. The flight path, speed and altitude are almost the same compared with the previous path. The Ec/Io values are in −8 … −22 dB limits, but the data transmission did not fully fail here. The RTT values are unstable again, but the number of lost packets decreased significantly.

Such difference is comprehended as the second flight path was more stable that caused less UE antenna position and angular orientation elevations.

The touch-down and braking take place at 15:09:48. Then the RSSI drops to −70 dBm, the Ec/Io values are again at perfect level of −4 dB and the RTT becomes stable.
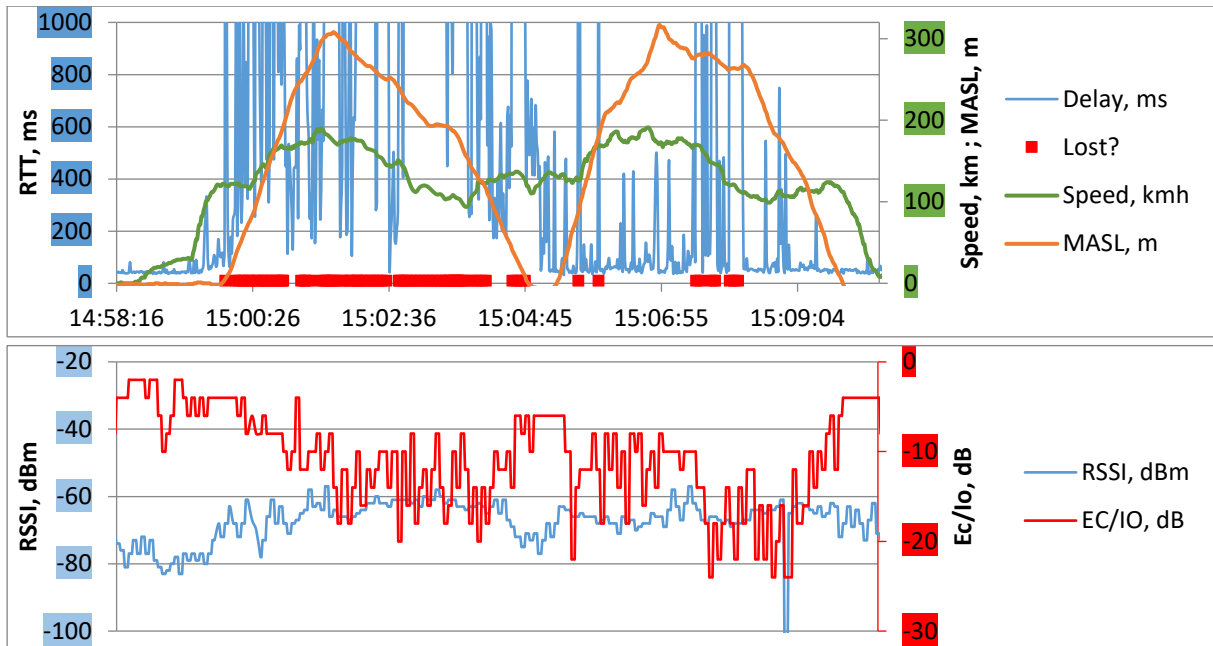
Fig. 3.3 Network performance during ground roll, two laps with one take-off and one go-around, as well as one landing.

The following experiment was made to check cellular network coverage above the ground surface near to Spilve airfield, which was used in field study described above.

All network parameters and network RTT were recorded simultaneously to exclude possible misunderstanding of the obtained experimental results. RTT values are averaged. Measurements were done using firewatch tower. To exclude impact of the UE antennas directivity and possible shadows, the dongle was placed horizontally at 2 m above tower wood floor, keeping the same axial direction for all altitudes. Measurements were obtained both in 3G (DC-HSPA+) and LTE modes.
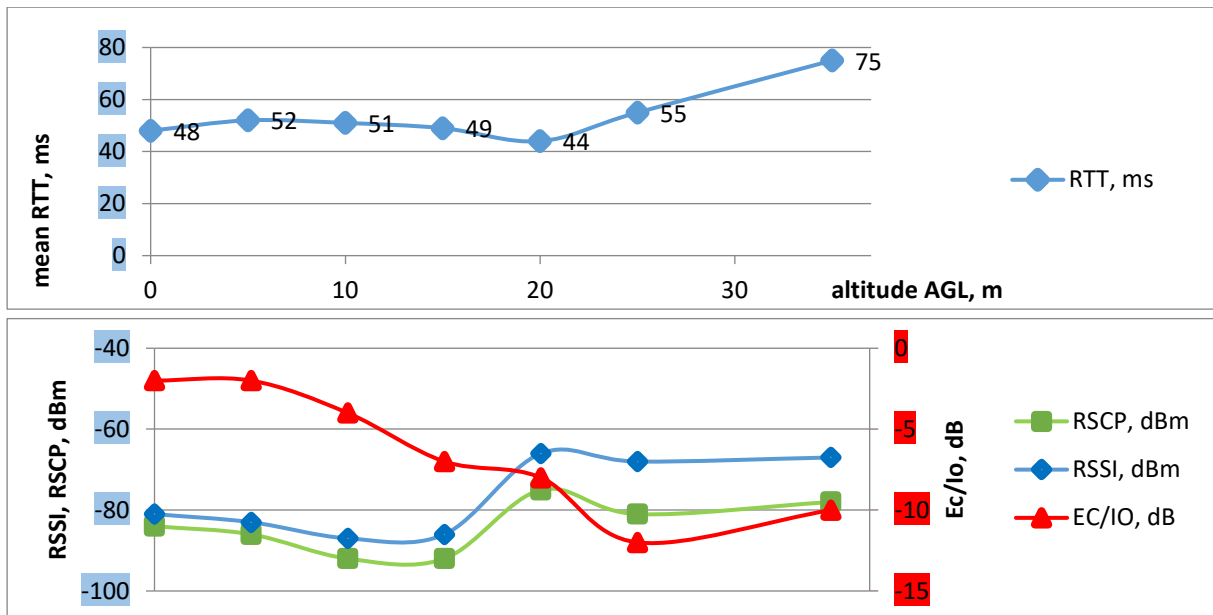

Fig. 3.4 Network performance for the static UE at various altitudes in 3G HSPA+ mode of operation.

Averaged RTT values are shown in the first graph, in milliseconds. Network performance indicators are shown in the second graph: RSSI and RSRP are in the left Y axis, in dBm, Ec/Io is in the right Y axis, in dB. Altitude is in the X axis and represented in meters.

On the ground RSSI is −80 dBm and Ec/Io is −6 dB. At higher altitude Ec/Io monotonically decreases to −12 dB at the 32 m altitude. RSSI and RSCP levels become increased starting from 10 m altitude. True LOS between UE antennas and the base station (NodeB) without interfering objects at all is available when dongle is placed above trees, starting from 13 m. Ec/Io becomes decreased even though RSSI and RSCP increase. RSCP increases as the UE and selected NodeB obtain true LOS path without interfering objects at all. However, RSSI also increases because the UE obtains LOS with more NodeBs that were previously shaded. This causes Ec/Io to decrease. Minimal Ec/Io level during this experiment was −12 dB, which was still enough to operate. None of packets were lost during this experiment.

In the LTE mode, RSSI and RSRP also become increased at higher altitudes because UE obtains LOS communications between its antennas and eNodeBs. Higher altitude causes SINR also to decrease; however, SINR becomes less affected compared to Ec/Io in 3G DC-HSPA+ mode. Such difference is because LTE cell operation in Riga is distributed between 4 bands as well many sectors, whereas all 3G cellular operators operate at the same B1 band and there are at least 7 NodeBs (3G) accessible at the top altitude of 32 m. More BSs at the same band cause higher interference. It should be noted that there is no effect on RTT values in LTE mode.
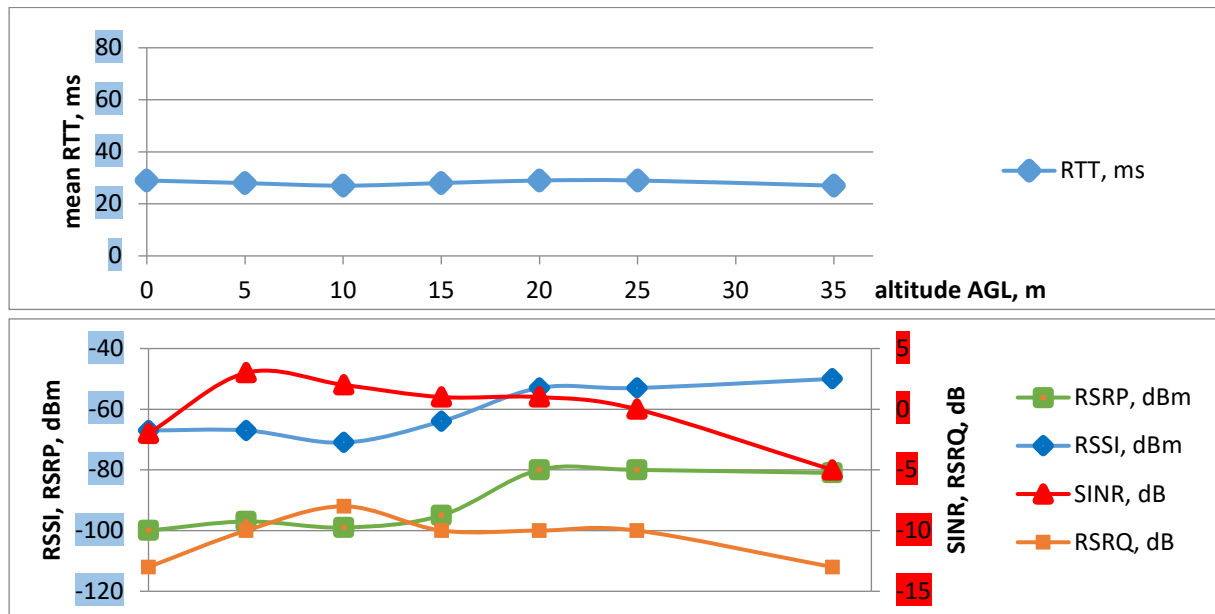
Fig. 3.5 Network performance for the static UE at different altitudes in 3G LTE mode of operation.

Making experiments in the air is too expensive. Also, such experiments do not allow making simultaneous measurements for the stable and not stable flights. The following experiments were done to prove that rapid antenna angular position variation in 3D (for example, during unstable flight) is one of the causes of unreliable data transfer over mobile cellular networks. To consider the impact of possible UE rapid changes in its angular position, two UE USB dongles were used simultaneously. The first dongle was securely fastened to a wood holder 1.5

meter apart from the car body in horizontal position. The second dongle was also fastened to a wood holder and was manually jiggled, tracing out an "8" 0.5 meters long trajectory simultaneously with 180-degree angular rotation. Both dongles were registered within the same cell.

The experimental results for the DC-HSPA+ mode of operation are shown in Fig. 3.6. The first plot shows RTT in time for the first dongle with fixed angular position (left Y axis, in ms and blue crisscross marks); RTT in time for the second shaky dongle (left Y axis, in ms and green square marks); ground speed (right Y axis, in km/h and red curve). The second plot shows network performance indicators. Fixed dongle: RSSI (blue curve, left Y axis, in dBm); Ec/Io (right Y axis, in dB and red curve). Shaky dongle: RSSI (green square marks, left Y axis, in dBm); Ec/Io (orange square marks, right Y axis in dB). During the experiment, the cell was not changed.

The Huawei 3372h dongle approaches its noise floor at RSSI = −90 dBm. In this case, Ec/Io value becomes decreased because the denominator Io also implies spectral density of noise. A lot of retransmissions made by HARQ can be observed here. None of packets were lost during this experiment.
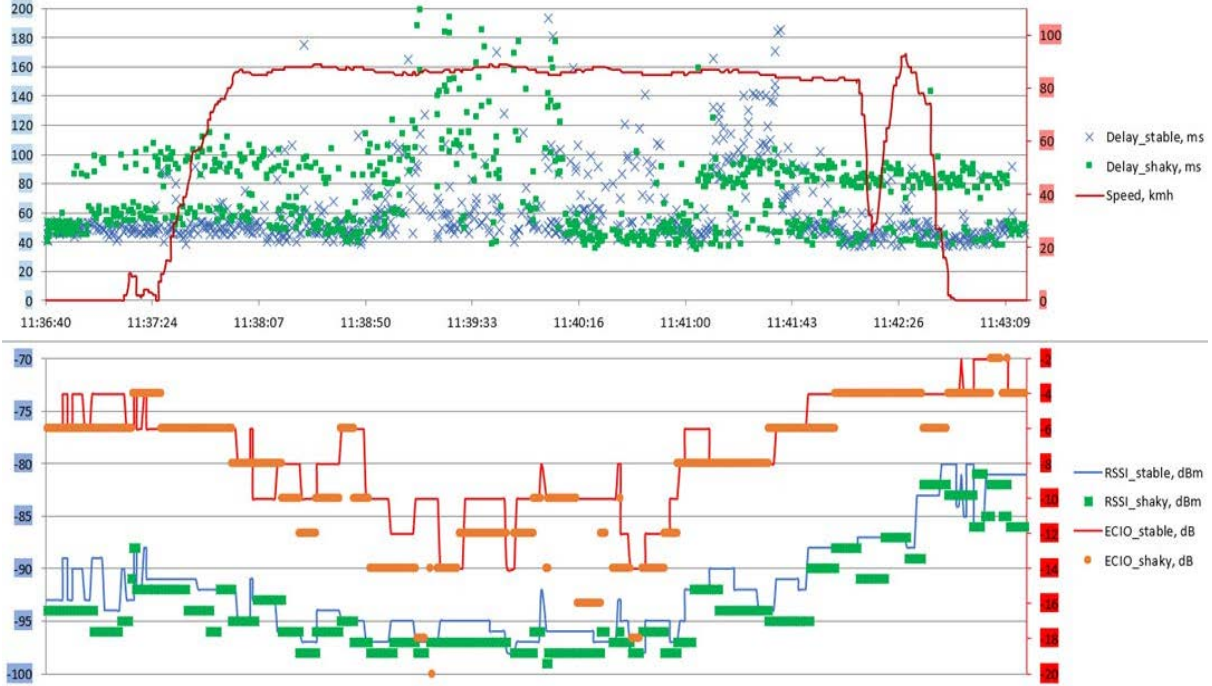
Fig. 3.6 Network performance for the movable UE with fixed and with shaky antennas in 3G HSPA+ mode.

The experimental results for the LTE mode of operation are shown in Fig. 3.7. Both dongles are fastened and the second one is jiggled as described above. The ground speed is 40 km/h. The LTE band is lock to B20 (800 MHz). Operating frequency choice of both dongles was made automatically. Since the LTE typically have many sectors, the dongles have many possible options to select the desired cell. RTT, in milliseconds, is shown in the first part of the plot. The RTT obtained from the fixed dongle is shown via the blue stars; the RTT obtained from the jiggled dongle is shown via the green rhombus, both RTT with respect to the left Y

axis, expressed in milliseconds. The switching to the next cell is shown by the blue and green squares for the stable and jiggled dongle respectively. The speed of the car is shown by the red line, with respect to the right Y axis. The RSSI values are shown on the second part of the plot; the RSCP values are shown on the third part of the plot; the SINR values are shown on the last part of the plot.

Fixed dongle SINR (red curve) and Shaky dongle SINR (orange points) in dB are shown on the 4th plot, RSSI (blue curve for the stable and green dots for the shaky, dBm) are shown on the 2nd plot, RSCP (blue curve for the static and green dots for the shaky, in dB) are shown on the 3rd plot. RTT, in milliseconds, both for the stable and shaky dongles are shown on the first plot. Please note that there is no noticeable difference between RTT of both dongles and no packets were lost during this experiment. To obtain comparable results, switching to the next sell is indicated on the graph too.
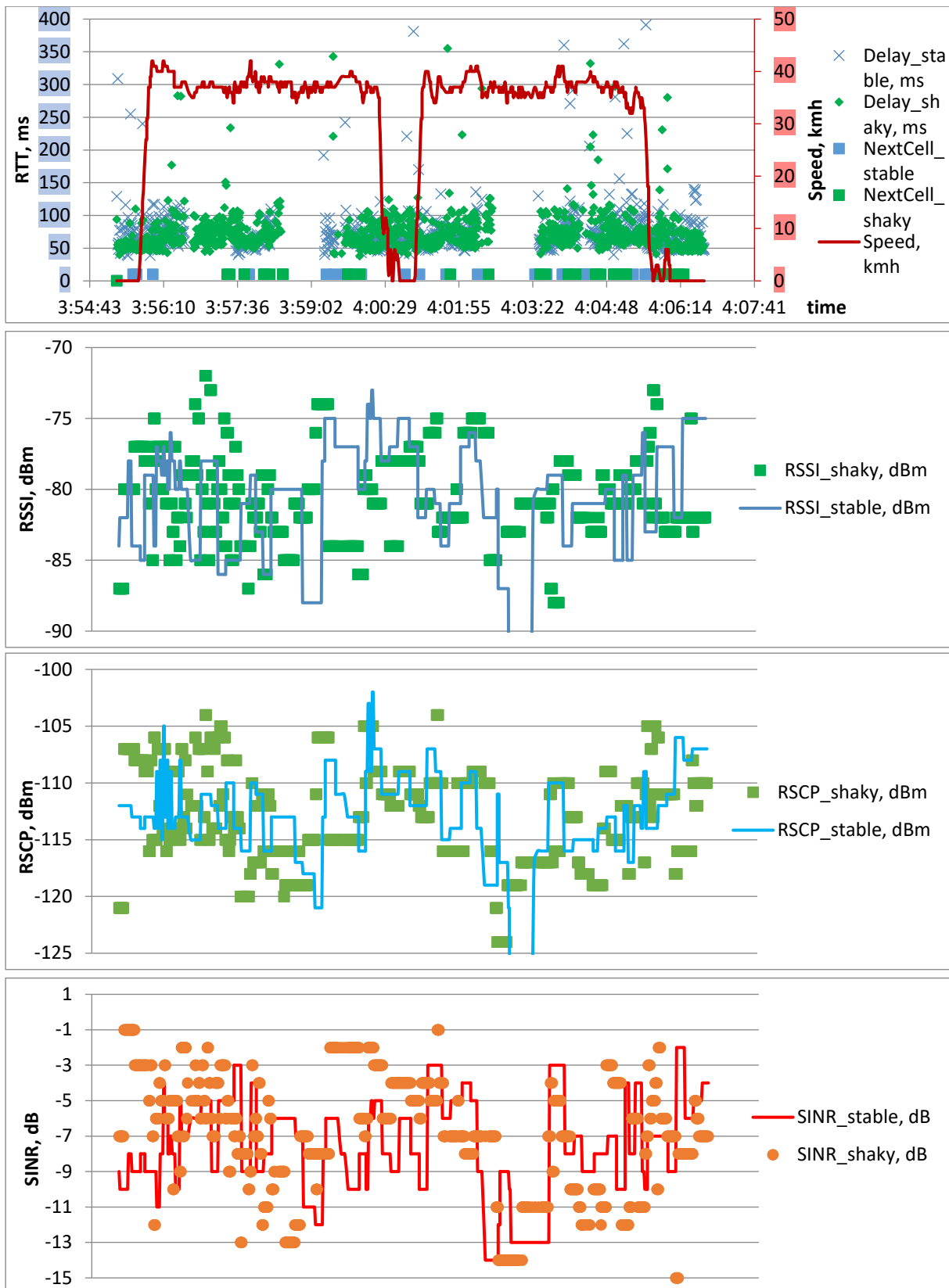
Fig. 3.7 Network performance for the movable UE with fixed and with shaky antennas in LTE mode.

It can be concluded that:

1. Angular position variations of the UE PIFA antennas make the wireless signal prone to negative effects and these effects are not fully compensated by AMC, particularly in 3G HSPA+ mode. This leads to an increased number of resends made by HARQ, which results in an increased jitter and average RTT.

2. The effect of rapid angular position variations of UE built-in PIFA antennas is aggravated at higher altitude due to stronger interference. In this case, 3G HSPA+ data transfer service can be partially interrupted, even if the wireless signal parameters are not below their acceptable limits. This problem is less common for terrestrial vehicles because their antennas typically are securely fixed and have no rapid angular position variations.

3.2. Analysis of the aerial coverage of cellular mobile networks

In the previous chapter it was stated that the performance of a 3G HSPA+ cellular network reduces dramatically as soon as the airplane starts to increase its flight altitude. The following experiment was performed to prove that such condition is not happened occasionally.

3.2.1 Experimental evaluation of the delays in 3G and LTE networks at various altitudes

Making experiments in the air via the airplane is expensive, so further an RPAS copter will be used. The experiments were performed in the middle of Spilve meadows, far away from interfering objects (threes) and metallic objects (like cars, buildings, etc), at 1 km distance from the firewatcher tower, that was mentioned in the previous chapter.

The copter was equipped with the raspberry-pi embedded computer with running gentoo operating system. The Huawei 3372h 3G/LTE dongle was attached to it. It was equipped with the Tele2 SIM card with a fixed IP address and was operating in HiLink (CdcEthernet). The HiLink mode was chosen to simplify network connection setup, as well to be able to specify APN server for the fixed IP address. This, by itself, means that the performance indicators of a radio network were not available. The raspberry-pi received its electrical power from the drone's power supply unit. None of drone's sensors were connected to the raspberry-pi, thus actual position was not logged.

The portable computer was located at the ground (further will be referred as GCS, or Ground Control Station). The GCS computer also was equipped with the Huawei 3372 3G/LTE dongle, running in HiLink mode of operation. The 32 bits echo requests were sent via the ping utility once per second (see introduction section for the motivation), all packets with delay of more than 1 sec are considered as lost. The echo requests were sent to two destinations: to the dongle, located at the copter and to the google free DNS server (IP: 8.8.8.8). The google free DNS server was used to identify which link is failed (in case if there are lost packets): if in case of GSC-to-Drone connection failure google free DNS server still responds, then the cause of the problem is in the link between the drone and the base station; if both responds are not received, then the problem is in the link between the GCS and the base station. RTT values of both

destinations are synchronizes in time and are presented on same graphs. To reduce the number of hops in data traffic, both dongles were equipped with the same cellular provider (Tele2) SIM cards.

All the following experiments were carried as follow:

1. With the drone on the ground, RTT measurement activation for both destinations (GSC-to-Drone and GCS-to-GoogleFreeDNSserver) (typically first 15 seconds)
2. Takeoff of the drone in manual mode up to the altitude of 1,5 meters.
3. Climb of the drone to 120 m altitude and auto mode with the rate of climb of 1 m/s.
4. Hovering in for 15 sec at the top altitude of 120 m.
5. Descent in auto mode with the rate of descend of 1 m/s.
6. Manual landing. Last 15 sec (typically) of RTT measurements were performed at the ground.

It should be noted that the crosswind forces drone to change its angular orientation in order to save its position. This leads to antenna shacking, as well sometimes to reduced rate of climb to 0.8 m/s.

In the first experiment both dongles were locked in 3G mode of operation and B1 (2100 MHz) frequency bands. To bring both dongles from low speed mode (UMTS) into the high-speed mode (HSPA+), initially a burst of ICMP packets was send. This burst is not displayed on the graph. The RTT of GCT-to-drone is referred as GCS2D and is shown in blue color; lost packets are shown by the red squared (28 of 356 packets were lost). The RTT of GCS-to-GoodleFreeDNSserver is referred as GCS2wan and is shown in orange color; none of packets were lost. The takeoff takes place at 15 sec and the hovering at the altitude of 120 m takes place in the period of 125 .. 140 sec. Further a descent takes place and the landing occurs at 300 sec.
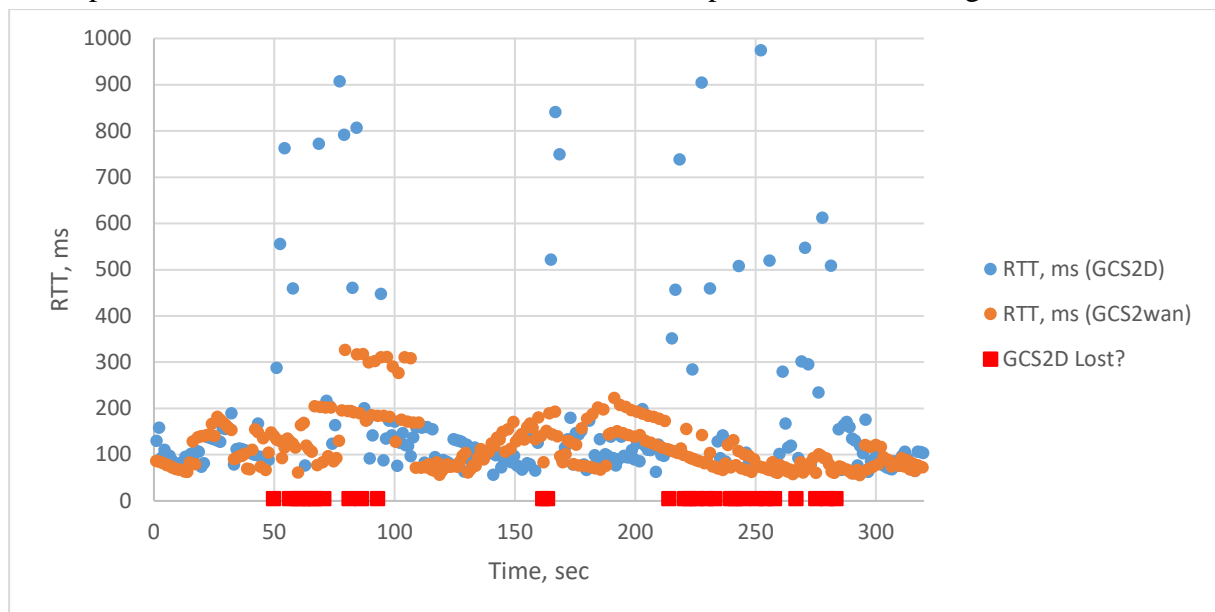

Fig. 3.8 RTT of GSC2D and GCS2 wan connections, in 3G B1 HSPA+.

The experimental results show that the RTT significantly increases as soon as the drone starts to change its altitude (lateral position was hold by using the position feedback, which was obtained via onboard GPS). This leads to increased number of undelivered packets too (28

packets were not delivered during this experiment). The results are similar to those, that were obtained from the light airplane.

In the second experiment both dongles were locked in LTE mode of operation, whereas the band selection was made automatically. The RTT of GCT-to-drone is referred as GCS2D and is shown in blue color; none of packets were lost. The RTT of GCS-to-GoogleFreeDNSserver is referred as GCS2was and is shown in orange color; none of packets were lost. The takeoff takes place at 15 sec and the hovering at the altitude of 120 m takes place in the period of 140 .. 155 sec. Further a descent takes place and the landing occurs at 300 sec.
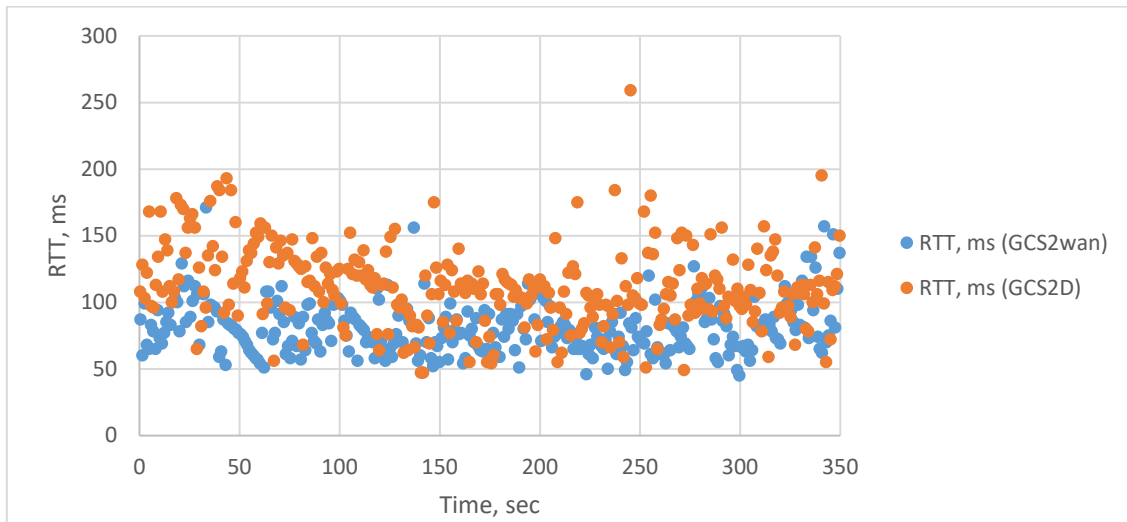

Fig. 3.9 RTT of GSC2D and GCS2wan connections, in LTE (frequency band selection is done automatically).

At higher altitudes the level of interference is higher. However, the experimental results show that the RTT values are lower at the middle of the time scale, where the drone is at maximum altitude. The radio link parameters (as well level of interference) was measured 1 km apart from this location and are shown in the previous chapter. That data also shows increased level of interference at higher altitudes. Thus, the experimental results prove that the AMC is working correctly. However, the impact of adaptation of the modulation and coding schemes (by the AMC) cannot describe why the GSC2D has lower RTT at higher altitudes, whereas GCS2wan has almost constant. It is known that the different cells typically provide different performance (see Chapter 2.6.2 for the numerical data). Also, it is known that low frequency bands (e.g. B20) have greater coverage. However, the LTE dongle will prefer to use higher frequency bands, if these are available with sufficient signal strength.

In the following experiments both dongles will be locked on B3 (1800 MHz) or B20 (800 MHz) bands to exclude possibility to switch between bands.

In the third experiment both dongles were locked in LTE mode B3 band. The RTT of GCT-to-drone is referred as GCS2D and is shown in blue color; lost packets with the red color (4 packets were lost). The RTT of GCS-to-GoodleFreeDNSserver is referred as GCS2was and is shown in orange color; none of packets were lost. The takeoff takes place at 15 sec and the hovering at the altitude of 120 m takes place in the period of 135 .. 150 sec. Further a descent takes place and the landing occurs at 300 sec.
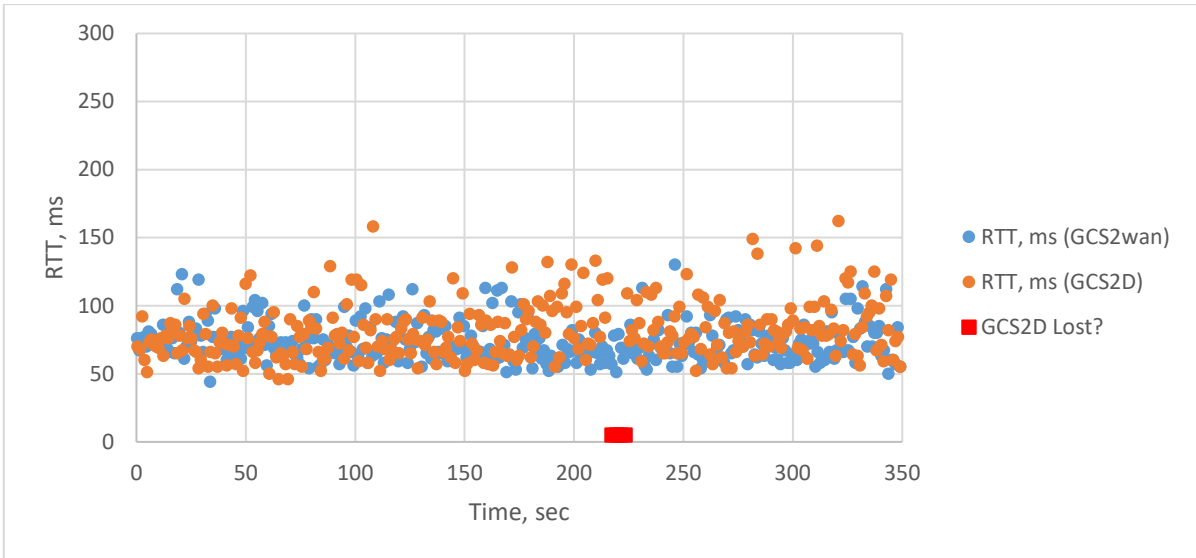
Fig. 3.10 RTT of GSC2D and GCS2wan connections, in LTE B3.

In the fourth experiment both dongles were locked on LTE B20 band. The RTT of GCT-to-drone is referred as GCS2D and is shown in blue color; none of packets were lost. The RTT of GCS-to-GoodleFreeDNSserver is referred as GCS2was and is shown in orange color; none of packets were lost. The takeoff takes place at 15 sec and the hovering at the altitude of 120 m takes place in the period of 145 .. 160 sec. Further a descent takes place and the landing occurs at 300 sec.
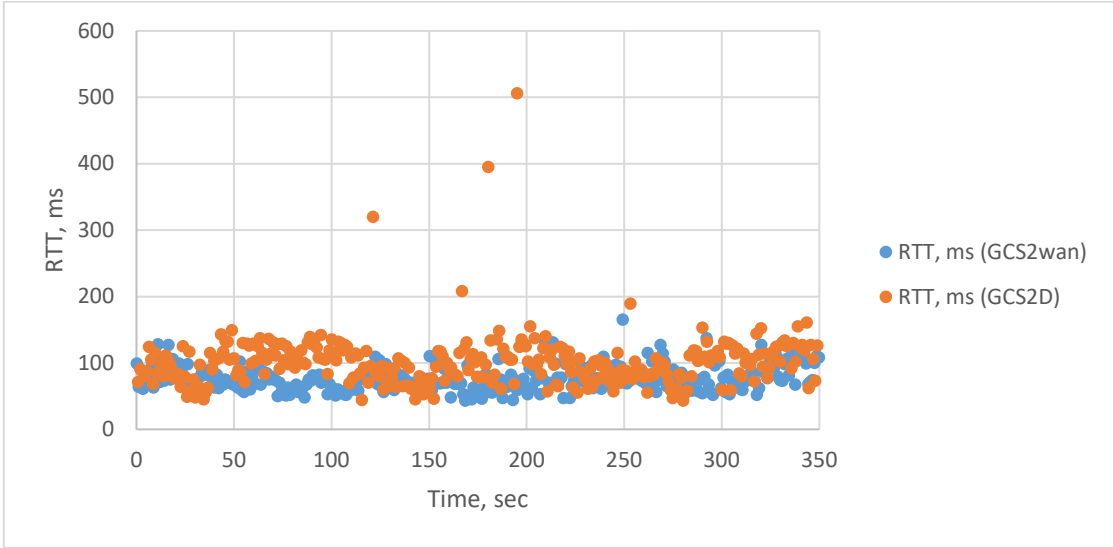
Fig. 3.11 RTT of GSC2D and GCS2wan connections, in LTE B20.

As can be seen, the RTT values does not depends on altitude when different bands cannot be selected. In these experiments B20 band produces slightly increased RTT values compared to B3 band. Hence the reduced RTT, presented in Fig. 3.9 are caused by switching from B20 to B3 band. Such selection can happen if at the ground level B3 eNB has significantly weaker signal strength compared to B20 eNB. This assumption should be checked manually, because it is not possible to make such measurements from the drone.

3.2.2 Evaluation of power level and quality of the signal in the area of experiment

In this experiment a Huawei ME909 with dedicated omnidirectional antenna was used. There are two motivations to use this modem instead of Huawei 3372a. At first, the Huawei ME909 is able to find available cells in 2G, 3G and LTE modes, whereas Huawei 3372h can only search for the 2G and 3G cells. Secondly, the Huawei 3372h utilizes PIFA antennas that are considered as omnidirectional. Actually, these antennas have variations in their directional diagram in all three planes [82]. This means that in order to facilitate repeatability of the measurements, the Huawei 3372h must be aligned in all three dimensions. In a contrast with PIFA antennas, Huawei M909 was equipped with omnidirectional rod antenna. Such antenna should be aligned only in vertical plane (so can be rotated around its axis), that significantly simplify process of measurements.

By default, the Huawei ME909 in Windows 8 and 10 is operating only with enabled MBIM interface (Mobile Broadband mode). In this mode the commands can be sent to the modem thru MBIM interface via the application "MBIM Tool". Such approach makes data logging task complicated. In order to enumerate its serial ports (sometimes called AT command interface), the modem should be switched back to NDIS mode (sometimes called as "debug mode"). This can be done by sending a command "AT^SETMODE=1" via the MBIM Tool. After restart, the device will enumerate the additional serial ports. These ports require additional drivers that are not provided on the Huawei's product page. In our setup a Huawei ME909s-120 LTE Cat. 4 device was used. It was equipped with a single omnidirectional rod antenna; hence the receiver diversity function was not used. The antenna was oriented vertically. The modem was connected to the portable computer with Windows 8.1 and was running under debug drivers version 2.0.6.1.

After finishing above mentioned preparations, the modem is ready to make connections, as well to receive the commands thru the AT port. At first, it should be connected to the desired network. This can be done via the AT^ command:
"AT^SYSCFGEX="02",3FFFFFFF,1,2,7FFFFFFFFFFFFFFF,,", where "02" locks the dongle in 3G mode (WCDMA); "3FFFFFFF" allows to use all 3G bands. This step is very important, because the modem will display cells only in these bands (without any warnings).

Next, the list of cells in the specified mode can be obtained and displayed. This can be done via the AT^NETSCAN command. The commands transcription is the following:
"AT^NETSCAN=<n>,<pow>,<band>,<band>" , where:

<n> is the number of cells to be displayed (sorted by power level), in decimal

<pow> is a minimum power value to scan, dBm

<mode> is the network mode, in decimal

<band> is a 2G, 3G or LTE band, in hex

The following command was used to obtain the list of the 3G cells: "at^netscan=20,-110,1", that means that first 20 (sorted by power level) 3G cells will be displayed, the minimum power threshold is -110 dBm and the modem will search 3G (WCDMA) cells. Since allowed band has been already set to "all bands", then the response of this command will contain 3G cells in all available bands (in Latvia only B1 2100 MHz and B8 900 MHz bands are used).

The response will contain various information about the cell. The response transcription it the following:

^NETSCAN: <arfcn>,,,<lac>,<mcc>,<mnc>,<bsic>,<rxlevel>,<cid>,<band>,<psc>, where:

    arfcn – is a frequency, in decimal

    lac – Location Area Code, 4-digit hexadecimal

    mcc – Mobile Country Code, 3-digit decimal (Latvia = 247) [83]

    mnc – Mobile Network Code, 2-digit decimal (01=LMT, 02=Tele2, 05=Bite) [83]

    bsic GSM base station ID code (GSM only, in 3G and LTE is always 0)

    rxelvel – receive signal level, dBm

    cid – cell identify in the in the SIB3 message, in hexadecimal

    band – band of the cell, in hex (in 3G (WCDMA) 400000 = B1; 2000000000000 = B8).

Example of the response:

at^netscan=20,-110,1

^NETSCAN: 10663,,,A1,247,05,0,-65,259CDD5,400000,438
^NETSCAN: 10787,,,229,247,02,0,-66,19875B,400000,233
^NETSCAN: 10563,,,7532,247,01,0,-80,2649BFC,400000,312
^NETSCAN: 2948,,,A1,247,05,0,-81,259C4F2,2000000000000,449
^NETSCAN: 10812,,,229,247,02,0,-83,1976ED,400000,344
^NETSCAN: 10588,,,7532,247,01,0,-84,2649A2A,400000,359
^NETSCAN: 10837,,,227,247,02,0,-110,197842,400000,89

OK

In this example 7 cells of 3G network were found. The first NB is served by Bite-LV, it is located in Latvia, its CID is 259CDD5, it is operating in B1 band, and its received power is -65 dBm. Now we are ready to perform the experiment.

The experimental evaluations were performed using a drone. The quadrotor copter has a 450 mm frame with typical equipment installed, such as an autopilot module (Pixracer v1.0), a 2.4 GHz transceiver for RC, a 433 MHz transceiver for telemetry feedback as well as a 11.1V 4000 mAh battery pack. In addition to such typical drone's equipment, measuring equipment was also installed. It consists of a companion computer (Raspberry Pi 3B under Gentoo Linux control), a Huawei 3372h modem (for remote control of the Raspberry Pi 3B over an SSH session), a Huawei ME909s-120 (for measurements), as well as its vertically-polarized omnidirectional main antenna (the antenna was attached on the top of the frame; the diversity antenna was not connected). To reduce possible interference from two cellular modems, the Huawei 3372h was locked in 2G (EDGE) mode. The Huawei ME909 was operating in NDIS mode to provide access to its serial interfaces. The preparation of the Huawei ME909 device has already been described in the previous section. The support of the device was ensured via native drivers of the Gentoo Linux operating system.

The field studies were performed in the middle of Spilve meadows, far away from interfering objects (threes) and metallic objects (cars, buildings, etc.), at a distance of 1 km from the firewatcher tower.

The first part of the study was performed to evaluate the coverage of LTE networks (of all cellular operators). The copter was hovering at the desired altitude. During hovering, its altitude was automatically stabilized with respect to altitude information from its barometric altimeter, while its horizontal position was automatically hold with respect to the position, obtained by its GPS receiver, by adjusting thrust of its motors. Please note that this means that if there is a crosswind, the ideal vertical placement of the antenna cannot be achieved. The measurements were performed via the Huawei ME909 modem by sending the AT^NETSCAN command via ssh session. The measurements were performed with the increment of 25 meters of altitude, two times at each altitude. The step-in altitude is so big in order to reduce the required flying time, since the battery lifetime is only 12 minutes.

The following illustrations Fig. 3.12 to Fig. 3.22 show the measurement results, separated by operators and frequency bands (B1=2100MHz; B3=1800MHz; B7=2600MHz; B20=800MHz). The height is shown on the X axis (expressed in meters relative to the earth surface); the received signal level is shown on the Y axis, in dBm; Cellular operator and Band are shown on the graph title; CIDs (Cell IDs) are shown in the legend (in HEX format).

Fig. 3.12 Received signal level, dBm of B1 band of the LMT cellular operator (LTE cells).

Fig. 3.13 Received signal level, dBm vs Altitude AGL, m of B3 band of the LMT cellular operator (LTE cells).

Fig. 3.14 Received signal level, dBm vs Altitude AGL, m of B7 band of the LMT cellular operator (LTE cells).

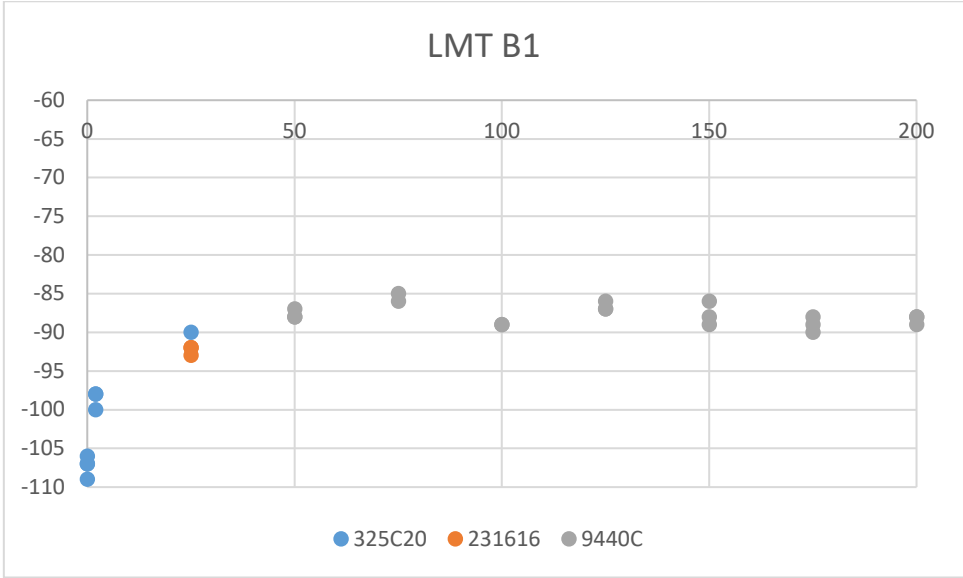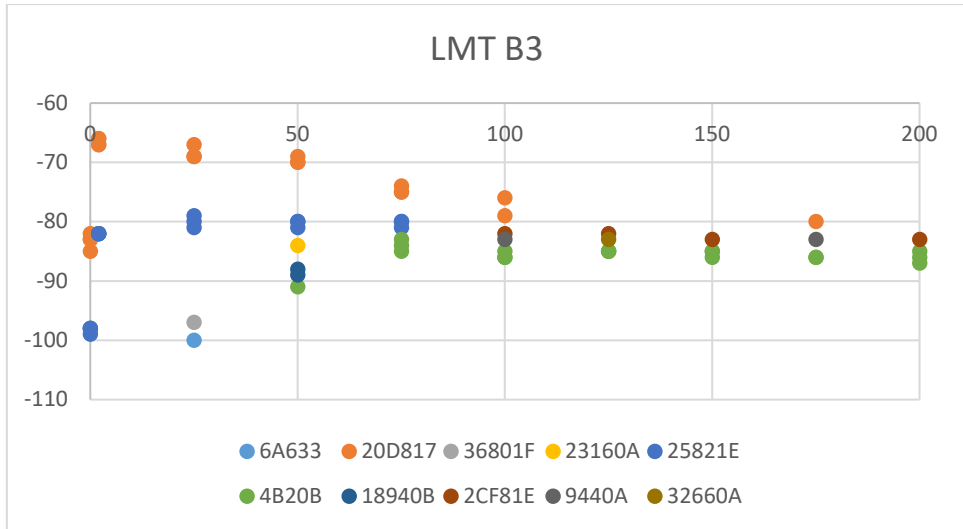Fig. 3.15 Received signal level, dBm vs Altitude AGL, m of B20 band of the LMT cellular operator (LTE cells).

Fig. 3.16 Received signal level, dBm vs Altitude AGL, m of B3 band of the Tele2-LV cellular operator (LTE cells).

Fig. 3.17 Received signal level, dBm vs Altitude AGL, m of B7 band of the Tele2-LV cellular operator (LTE cells).

Fig. 3.18 Received signal level, dBm vs Altitude AGL, m of B20 band of the Tele2-LV cellular operator (LTE cells).

Fig. 3.19 Received signal level, dBm vs Altitude AGL, m of B1 band of the Bite-LV cellular operator (LTE cells).
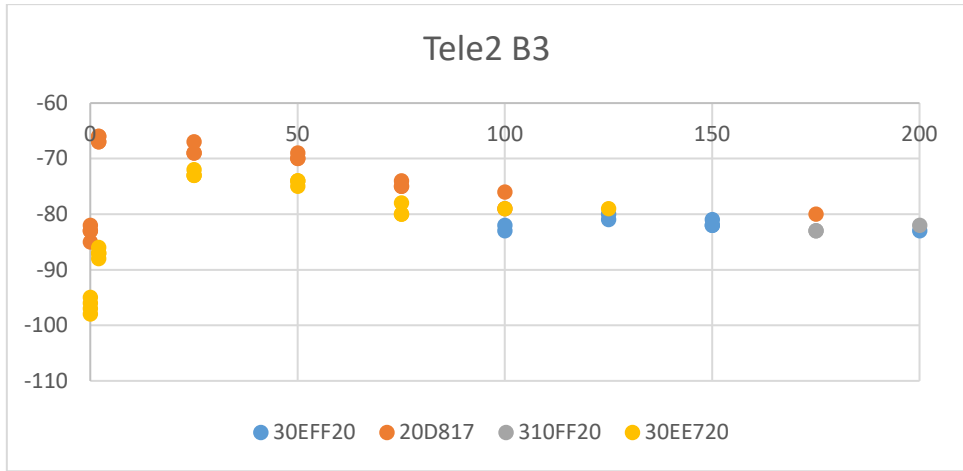

Fig. 3.20 Received signal level, dBm vs Altitude AGL, m of B3 band of the Bite-LV cellular operator (LTE cells).
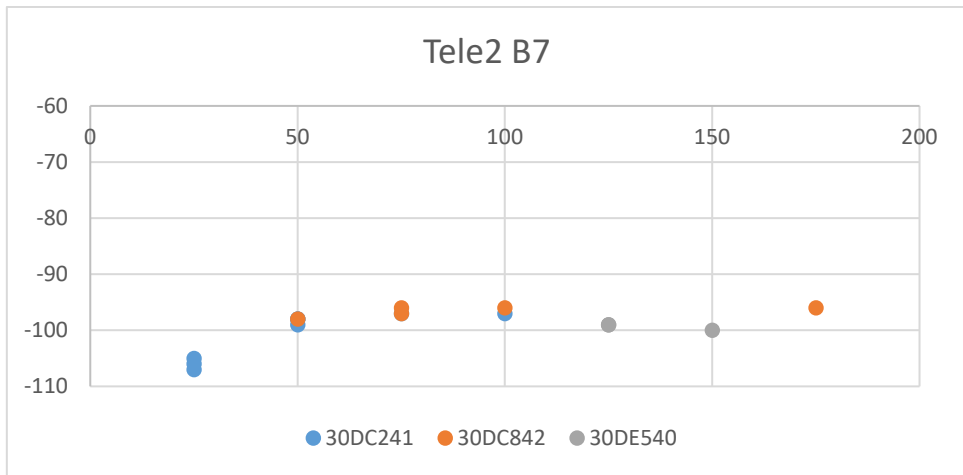

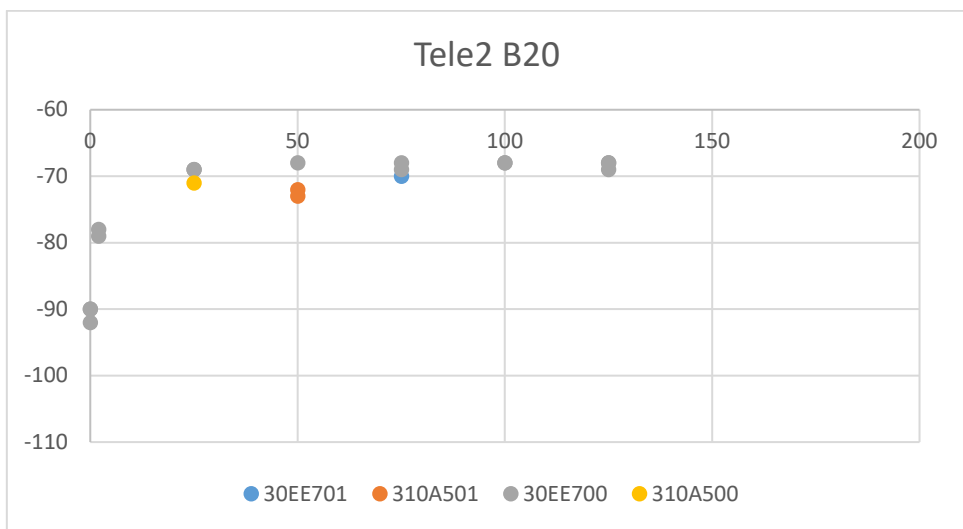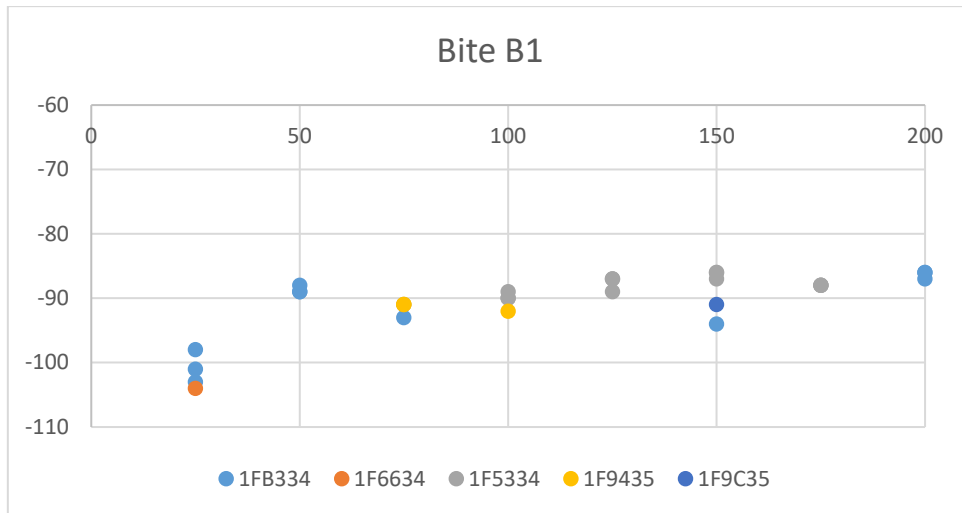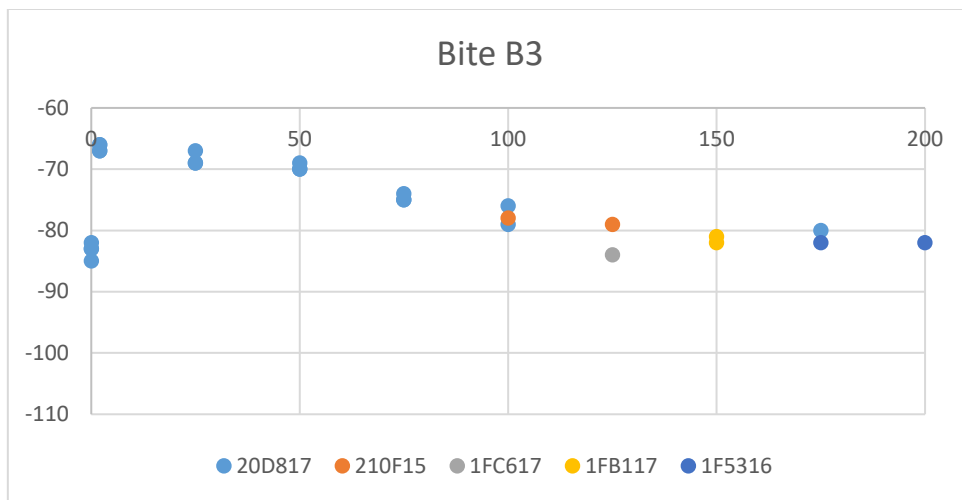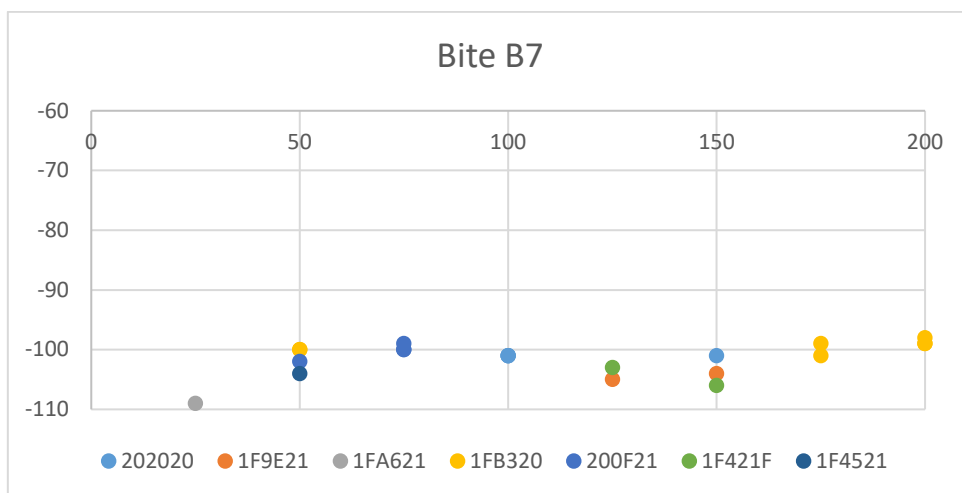Fig. 3.21 Received signal level, dBm vs Altitude AGL, m of B7 band of the Bite-LV cellular operator (LTE cells).
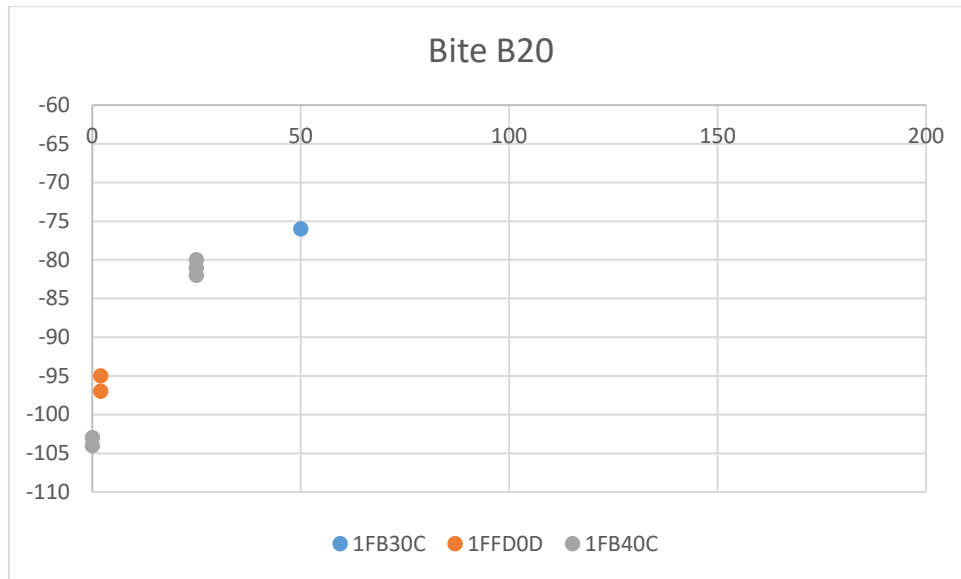
Fig. 3.22 Received signal level, dBm vs Altitude AGL, m of B20 band of the Bite-LV cellular operator (LTE cells).

The experimental results show that the coverage of LTE networks is more than sufficient (- 105 dBm is considered as a "good" signal strength [63]), which promises possibility to operate up to 200 meters. However, in order to ensure that the LTE UE can operate efficiently, not only the signal strength, but also the signal quality should be evaluated.

The second part of the study was performed to evaluate the signal quality indicators (such as SINR and RSRQ). The experiment was performed in the LTE network of the Tele2 cellular operator. The Huawei ME909 was locked in LTE mode, while the band selection was done automatically. First, the drone was sent to 200 m altitude. Then logging was activated, and the drone starts to descent with a rate of 0.75 m/s. All the network parameters (RSSI, RSRP, SINR and RSRQ) as well as the CID of the serving cell were reported by the Huawei ME909 dongle, while the barometric altitude was reported by the altimeter of the drone. Please note that due to wind gusts it was not possible to hold the antenna in a perfectly vertical position!

The following illustrations show the experimental results. On the first illustration the height is shown on the X axis (expressed in meters relative to the earth surface); RSSI and RSRP are shown on the Y axis, in dBm; CID of the serving cell is shown by the colored lines and CIDs colors are shown in the legend (in HEX).

The second illustration shows the interference and quality of the signal with respect to altitude. The height is shown on the X axis (meters, relative to the earth surface); SINR and RSRQ are on the Y axis, in dB.

During the experiment, the modem has lost LTE service at an altitude of 130 m (during climb) and reestablish it at 90 m (during descent). Please note that only the descent is shown here!
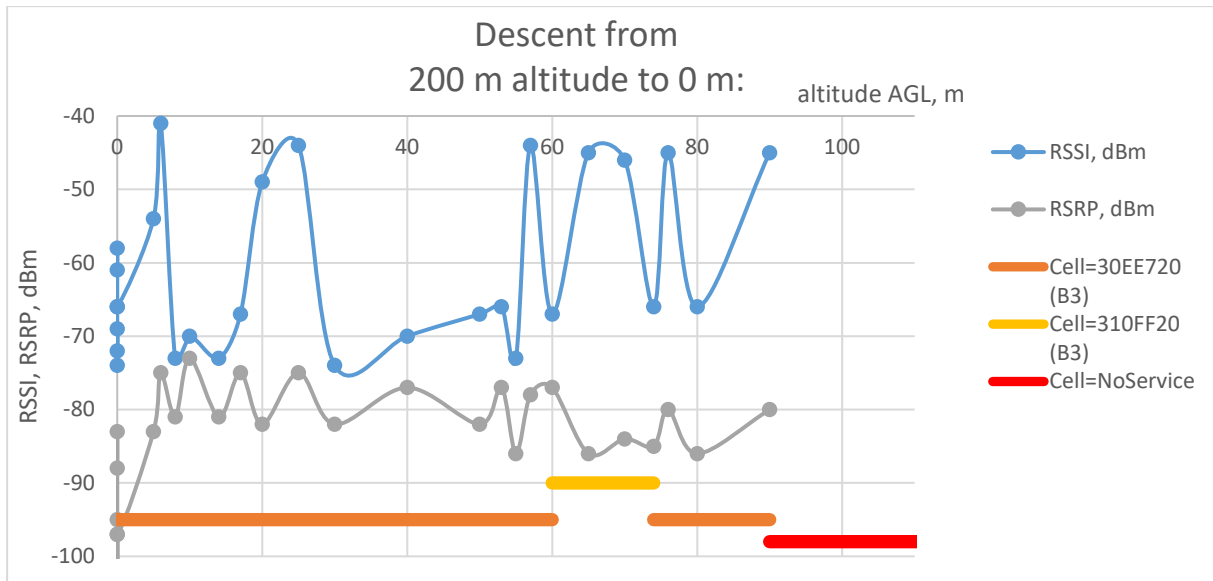
Fig. 3.23 RSSI, RSRP vs Altitude, LTE service of Tele2 cellular operator.
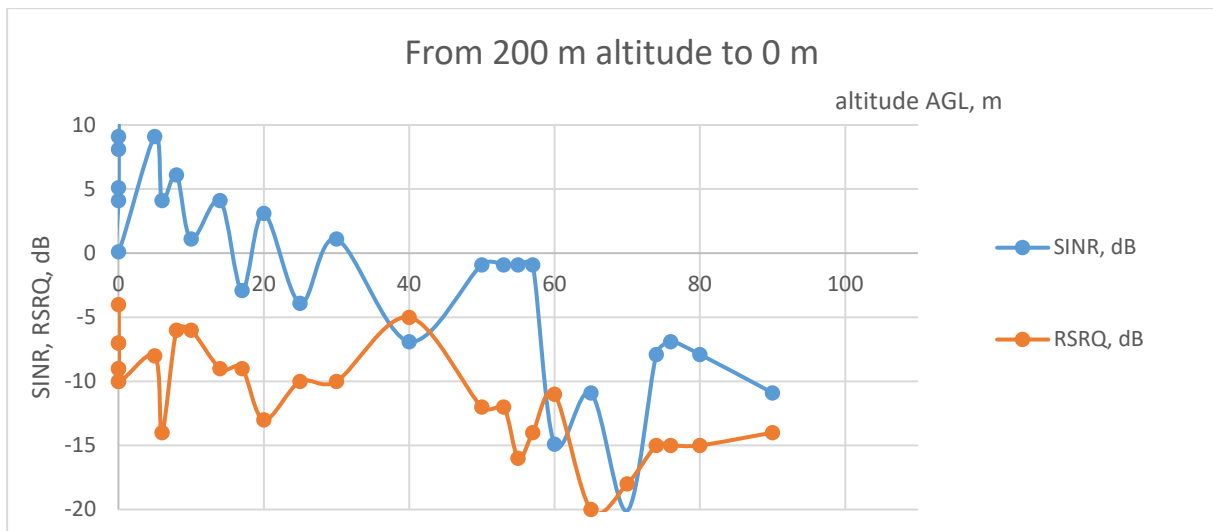
Fig. 3.24 SINR, RSRQ vs Altitude, LTE service of Tele2 cellular operator.

Based on the experimental results, the following can be concluded:

1. With an increase in altitude up to several hundred meters, the signal level from base stations increases. This is due to the fact that BS and UE not only establish LOS visibility, but also because the first Fresnel zone is freed from obstacles. Respectively, a well-known fact that with increasing altitude, interference increases too is confirmed.

2. The proposed method allows not only to display overall signal strength, but also allows to measure the power level of particular BSs.

3. It is proved, that the signal strength in Latvia (at least, in the area of experiment) is sufficient at least up to 200 m AGL.

4. In LTE communication systems, the effect of increased interference is effectively compensated by the HARQ, as demonstrated in experiments of measuring network delays at altitudes up to 120 meters using a drone. The stepwise decrease in the average

value of the delays observed in the experiment using LTE with the possibility of choosing different frequency bands can be explained by switching to another BS. Detailed evaluation of the coverage area of the cellular network showed that, near the earth's surface, the level of the LTE B20 signal of the Tele2 operator's BSs significantly exceeds the level of the signal from the LTE B3 BSs. However, with increasing altitude, the signal level from LTE B3 BSs increases enough so that it can be surely used. Since the UE prioritizes using higher frequency bands, it automatically switches to B3 BSs. This is confirmed by the fact that the average value of the B3 band delays is comparable with that obtained at high altitudes, whereas near the earth's surface the average value of the delays is similar to the average value of the B20 band delays (Fig. 3.10 and Fig. 3.11). Thus, despite the fact that the CID of the BS was not registered, it can be argued that the step decrease in the average value of delays with increasing altitude is caused by switching the UE to BSs operating on the B3 band, which in this region gives less delay. However, further increase in altitude cause loss of LTE service. Despite on more than sufficient RSRP level (with respect recommendations, listed in [63]) the interference becomes too high (SINR < -10 dB) as well as RSRQ drops down to -15 dB. This, by itself, makes impossible to operate in the LTE network in the area of experiment at high altitude.

5. With an increase in flight altitude in 3G networks, a significant increase in delays, as well as a sharp increase in the number of packet losses, are observed. On the one hand, this may be due to the fact that with a decrease in Ec / Io below -12 dB in the presented experiments, an increase in delays is observed (these effects were observed both in measurements with car movement and in measuring delays on the firewatcher tower). It has been experimentally demonstrated that this effect is exacerbated if the angular rotation of PIFA antennas is present, which is quite typical when flying in turbulent air (similar experiments with rod antennas were not performed). Also, experimental data allow us to hypothesize that when the altitude of the flight increases, the UE starts to operate with many BSs due to the use of soft handover (in 3G), as a lot of BSs with almost the same signal level becomes available. Unfortunately, UE is not able to detect switching between BSs when the soft handover is used.

6. The experimental study of vertical coverage also shows that the signal levels from available BSs fluctuate strongly depending on height. This, in turn, leads to the fact that the UE often switches (sometimes several times per 1 meter) from one BS to another. Most probably, this effect is caused not only by the side lobes of the BS antenna patterns, but also by the presence of the multipath radio wave propagation. It should be noted that provided here experiment is insufficient: to confirm the hypothesis measurements should be performed at a smaller step in altitude, whereas the antenna should be gyroscopically stabilized.

7. Handovers between BSs in typical conditions do not cause a significant increase in delays in 3G networks. However, when using these systems in the air, the situation may be completely different. This is due to the fact that in the 3G networks the so-called Soft Handover occurs, in which the UE sends data through two BSs at simultaneously, while

the UE and the RNC select the best packets in real time, which are then sent for processing. This technology allows UE to smoothly move from one BS to another, without breaking the connection. However, at the conditions of a low quality of the radio signal, increased delays of individual packets can be observed (see experiments with driving on a car). In the case of the operation in the air, apparently, constant fluctuations of signal levels at high altitudes, simultaneously with increased interference, do not allow the Soft Handover mechanism to effectively switch between BSs. In LTE networks, this phenomenon is not observed during the testing. The absence of such a phenomenon is explained by the fact that due to the use of OFDMA, simultaneous operation with two BSs is impossible, therefore, only Hard Handover is possible in LTE networks. The presence of X2 terrestrial interfaces allows hard handover with smaller interruptions, as a result without causing a significant increase in delays.

4. METHODS TO MINIMIZE THE IMPACT OF UNSTABLE DATA TRANSFER QUALITY OVER A CELLULAR MOBILE NETWORK

In Chapter 2.8, it was proved that the LTE data transfer service is almost suitable for the implementation of the C2 link if a UE moves on the ground and the signal quality is sufficient. However, at higher altitudes, the performance of both 3G and LTE services become reduced, or even the service becomes completely obstructed. In order to minimize this problem within already existing cellular networks, a parallel redundant solution of C2 link can be used.

4.1. Application of a Parallel Redundant Protocol solution

In order to overcome problems with temporary failed data transfer services two alternate independent active paths should be provided for the same traffic to reach the same destination. A Parallel Redundancy Protocol (PRP) [84] can be used in this implementation.

The PRP uses two independent active paths. The packets are duplicated by a sending node and are transmitted via both paths simultaneously. The first arriving packet is processed, while the second copy is discarded. Therefore, the resulting parallel redundant network latency is equal to minimal value of latency of both networks. In case of a failure of one path, the second path packet backups are processed. In this situation, the parallel redundant network performance is equal to the active path performance.

In the following experiments it is supposed that the GCS will be connected to the wired ethernet. An IEEE Std 802.3 defines that for the 100 Mbit Ethernet BER should not be more than 1e-10 and for the 1000 Mbit Ethernet BER should not be more than 1e-12 [85]. This makes wired Ethernet extremely safe compared with cellular data transmission service with BER of 1e-4 [47].

The cellular network data transfer service BER can be improved by using two cellular operators' services simultaneously. The idea is to send simultaneously two identical packets over two services of different cellular operators to increase air interface availability, while more trusted Ethernet path may not be duplicated.

The Parallel Redundancy Protocol (PRP) [84] is an IEC standard that is used to build redundant industrial ethernet solutions for the critical applications that cannot tolerate with packet losses and require hitless network. The PRP sends identical packets via two independent paths (networks). The key benefits of PRP are the ability to use paths with identical protocol but with different topology, as well as transparent operation for the network equipment. As PRP operation is transparent for both paths, its traffic usually is not blocked by the network equipment [86]. On the receiving side first arriving packet is processed and second (its duplicate) is discarded. As a result, PRP promises fail-safe data transfer with zero-time recovery in case of a single path failure; as well decreased data transfer service latency and jitter values if both paths are in operation.

To implement the PRP, the node must be connected to two different networks with same protocols. Such node name is Dual Attached Node (DAN). Both networks can be still accessible

by other equipment, called Single Attached Nodes (SANs). Simplified PRP network structure is represented in Fig. 4.1.
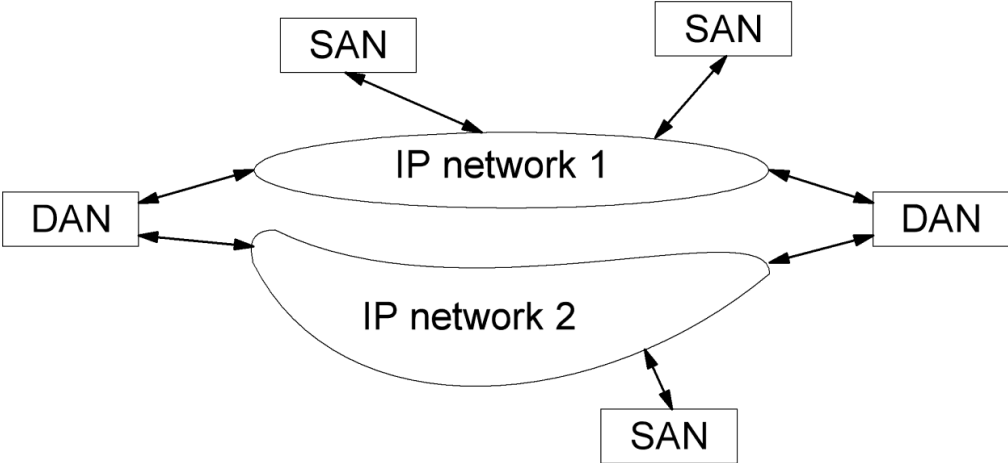
Fig. 4.1 Simplified structure of the PRP network.

The use of PRP protocol enables possibility to send identical packets via two cellular operator services. In the presented solution the DAN should be equipped with two cellular modems (dongles). Both dongles can operate in same or different data transfer modes (eg 2G, 3G, LTE) and in same or different frequency bands. This provides wireless path duplication, while final wired segment duplication depends on cellular operators ground wired segments locations and topologies. Typically ground wired segment will be partially duplicated. Typical cellular networks redundant solution topology is represented on Fig. 4.2.
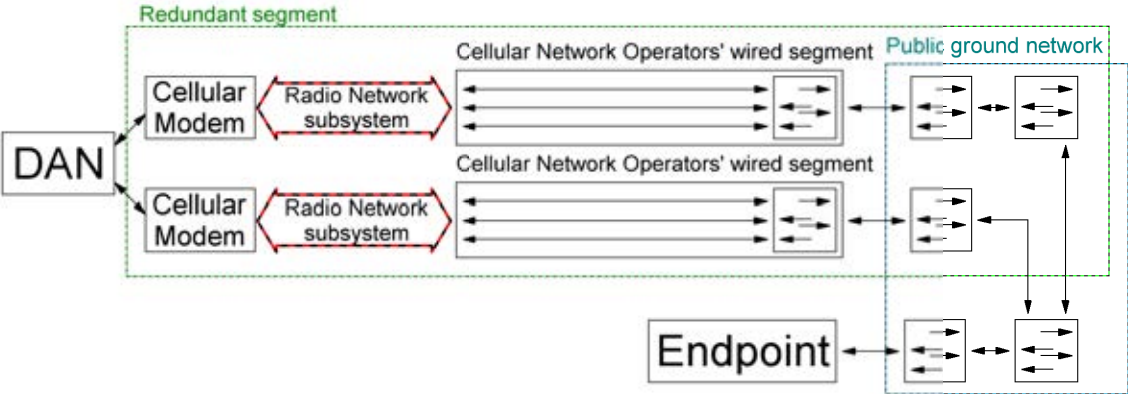
Fig. 4.2 Structure of the redundant network implemented on two different cellular operators' networks.

The testing is performed for the single and double attached nodes (SAN and DAN) simultaneously. The SAN request message is sent by a dedicated computer which is equipped with mobile broadband USB dongle Huawei E3372h. The Huawei E3372h sis operating in Hi-Link (CdcEthernet) mode (firmware 22.200.09.01.161_M_AT_01) to simplify operating system setup. The dongle is equipped with a SIM card of a randomly purchased cellular network operator No.1. The SAN computer runs MS Windows XP professional SP3 with 22.001.26.01.03 Huawei driver.

The DAN is provided by using two dongles which are attached to another dedicated computer. Both dongles are equipped with SIM cards of a randomly purchased operator No.1 and operator No.2. The PRP is implemented as a software sub-layer of the operating system. The solution is entirely transparent to the application and network. A PRP-1 User Mode Stack is used [87]. It requires two independent network cards that should be attached to the computer. The dongles operate in Hi-Link mode and provide the virtual network cards (NDIS) which can be used by the PRP1 User Mode Stack software. The PRP is implemented in PRP-1 User Mode Stack software and provides its virtual network device. The DAN portable computer is running Gentoo Linux with 64 bits kernel version 4.9 assembled in 01.2017 with 22.001.03.01.03 Huawei driver and PRP-1 User Mode Stack 1.0 PRP software solution. To be able to operate with flip-flop device Huawei 3372h an usb_modeswitch version 2.4.0-r1 is used.

At first, the parallel redundant solution performance will be tested for immovable ground-based equipment. The SAN and DAN computers are located in a relatively busy cellular network segment in the building of the institute at 1 Lomonosova, Riga. The test is performed within a 4-day period. It was decided to use 3G mode because the testing results in 2016 shows that the LTE network service quality was not stable. All three dongles are manually locked in 3G mode while B1 / B8 mode selection is done automatically by the dongle operating system. The actual signal parameters are shown in 4.1. table.

4.1. table

Signal parameters of 3G in the place of the experiment for the static SAN and DAN

Operator	Mode of Operation and Band	RSSI, dBm	RSCP, dBm	Ec/Io, dB
Nr.1	DC-HSPA+ , B1	-82	-88	-6
Nr.2	DC-HSPA+ , B1	-79	-83	-4

It should be noted that all cellular network operators switch cellular modems to UMTS mode in the lack of data traffic. The first data packet is always sent in low speed UMTS mode. Once the data traffic has been detected the mobile broadband USB dongle is switched to HSPA+ or DC-HSPA+ mode (depends on the cellular network operator). It is impossible to lock the mobile broadband USB dongle in HSPA+ or DC-HSPA+ modes by the local settings because the mode of operation is defined by the cellular operator. Typically, if there is no traffic in 2 sec period, the mobile broadband USB dongle is switched back to the UMTS mode. As the ping request is sent one per second in 32 kB packets, the dongle should always stay in DC-HSPA+. However, a short - term loss of communication can cause switching back to UMTS mode. UMTS mode RTT typically is 5 times greater than in the HSPA+ or DC-HSPA+ modes.

The RTT values for the SAN during 4 - day testing period are shown in Fig. 4.3. The RTT (an either-direction, in ms) in time is a blue curve; the lost packets are shown by the red vertical lines stemmed from the X axis.

The RTT values for the DAN are shown in Fig. 4.4. The RTT (an either-direction, in ms) in time is a blue curve; no packets are lost.

Summary of the experiment is shown in 4.2. table. The packets with RTT exceeding 1000 ms are considered as lost. The packet jitter is expressed as an average of the deviation from the network mean latency and is calculated according to RFC3550 (RTP) [43].

Fig. 4.3 Static SAN RTT values in 3G.

Fig. 4.4 Static DAN RTT values in 3G (PRP is used).

4.2. table

The results for the static ground equipment (3G)

	Packets sent	Packets lost	Average RTT, ms]	Jitter, ms	Availability, %
SAN	318017	30	86.0254	22.8226	99.990567
DAN	313394	0	74.0388	15.5169	100.000000

The DAN RTT value becomes reduced, because only the first arrived packet is processed, while the second is discarded. The jitter value is also decreased for the same reason.

Next, similar performance testing will be carried out for the moving equipment. The SAN and DAN computers are located in a car. The car average speed is 95 km/h. The experiment is performed far away from busy cellular networks of Riga, so the networks of both cellular

operators No.1 and No.2 are lightly loaded. All three dongles are locked in 3G mode while the B1 / B8 mode selection is done automatically by the dongle operating system. The actual signal parameters depend on the position and cellular operator coverage.

Network operators switch cellular modems in UMTS mode if there is no data traffic. Once the data traffic has been detected, the mobile broadband USB dongle is switched to HSPA+ or DC-HSPA+ mode (depends on the cellular operator). Typically, if there is no traffic in 2 sec period the mobile broadband USB dongle will be switched back to the UMTS mode. As the ping request is sent one per second in a 32 kB packet, the dongle should always stay in DC-HSPA+. However, a short-term loss of communication can cause switching to UMTS mode. UMTS mode RTT typically is 5 times greater than in the HSPA+ or DC-HSPA+.

The RTT values for the SAN are represented in Fig. 4.5. The RTT (in either-direction, in ms) in time is a blue curve; lost packets are shown by the red squares on the X axis. The RTT values for the DAN are represented in Fig. 4.6. The RTT (in either-direction, in ms) in time is a blue curve; there are no lost packets. Summary of the testing is shown in 4.3 table

. The packets with RTT exceeding 1000 ms are considered lost. The packet jitter is expressed as an average of the deviation from the network mean latency and is calculated according to RFC3550 (RTP) [43].
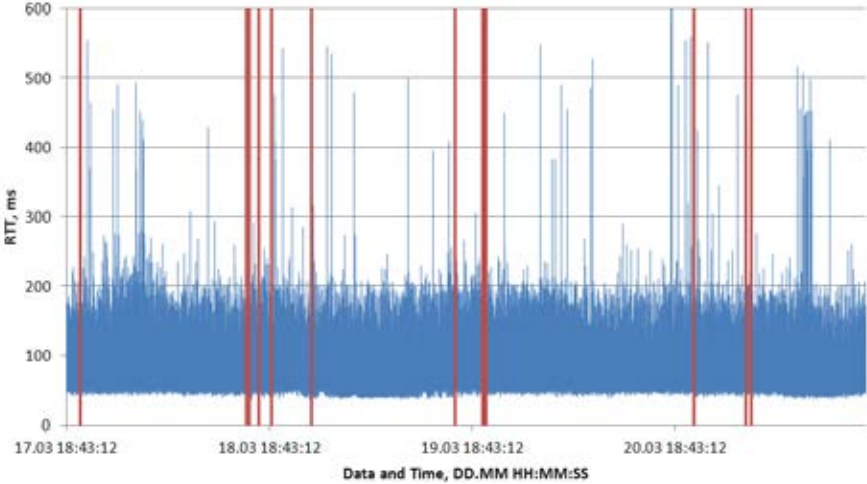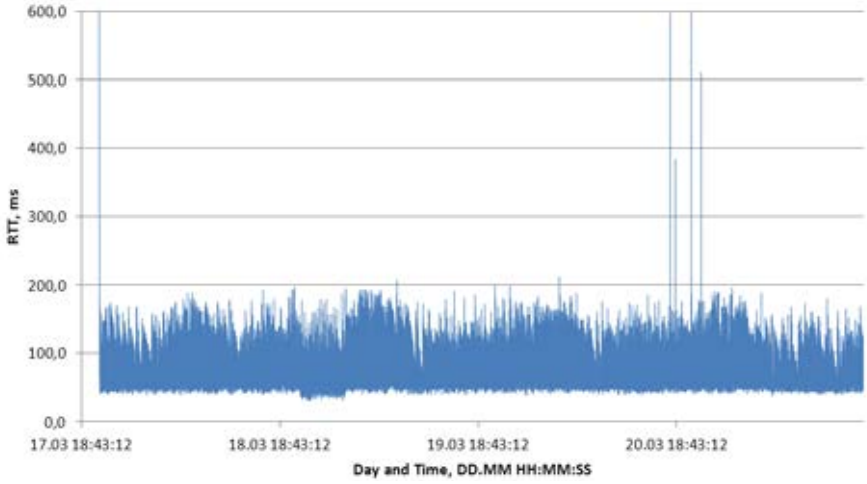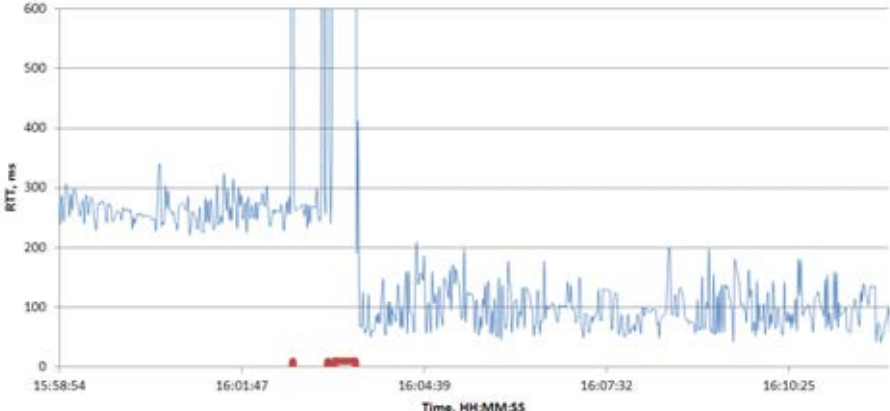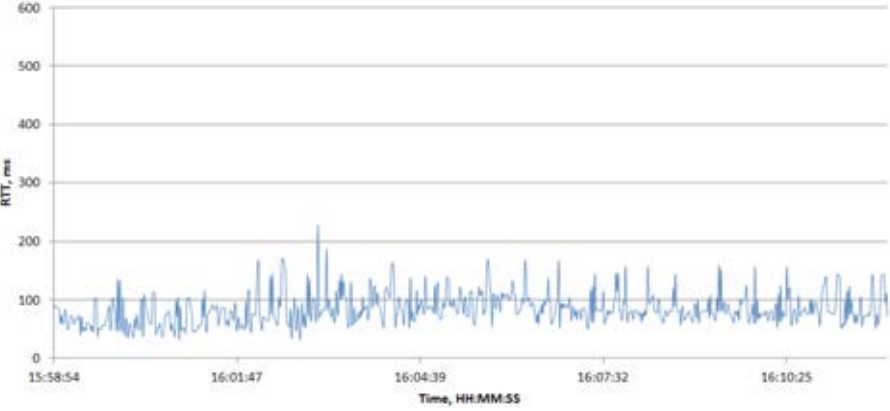
Fig. 4.5 Moving SAN RTT values in 3G

Fig. 4.6 Moving DAN RTT values in 3G (PRP is used).

The results for the moving ground equipment (3G)

	Packets sent	Packets lost	Average RTT, ms	Jitter, ms	Availability, %
SAN	752	13	147.968	29.6875	98.271277
DAN	802	0	85.0711	27.5000	100.000000

The SAN is using SIM card of the cellular operator No.1. Cellular modem does not receive the command from the cellular operator to switch to the DC-HSPA+ and remains in UMTS mode of operation for the first half of the period. This situation happens scarcely ever. Then the coverage by the operator No.1 is not sufficient in the middle of travelling and the data transmission aborts. All further packets are lost. When the second cell with sufficient signal strength is available, the cellular modem reestablishes the data link, receives a command to switch to DC-HSPA+ mode and continues its operation.

The DAN is using both cellular operators No.1 and No.2 3G services. The second operator has sufficient signal strength in the middle of traveling and replaces disconnected service of the operator No.1. For the given period the RTT values become slightly increased, because "the first arrived packet is processed, the second is discarded" does not work here due to the loss of connection of the cellular operator No.1. PRP effectively resolves loss of connection of the cellular operator No.1 and no packets are lost. Hence, the data link recovery time is equal to zero.

A 3G/LTE cellular redundant wireless network with a zero-recovery time can be made by using a PRP.

The 3G network DAN RTT is decreased by 15% approximately compared with SAN. The jitter value is decreased by 30% approximately. A network availability is increased significantly. A combination of two cellular operators' services should be used to build a very stable redundant solution. As cellular operators' output network server infrastructures are replicated one another, the reliability of the system is increased. The use of two different cellular operators helps to separate part of the ground wired segment due to the separate location of the operators' ground wired servers. However, the final wired segment reliability is not increased. This solution is suitable both for static and moving ground-based equipment.

The aim of the second part of experiments is to specify better combination of cellular data transfer services to build redundant link solution for the moving ground equipment both in well-populated and rural areas.

In the following experiment all dongles are locked in 3G mode. In Riga all available cells are operating in B1 (2100 MHz) band. The mode of operation is HSPA+ or DC-HSPA+ (mode selection is done automatically depending on signal quality). The experimental results are represented in Fig. 4.7.
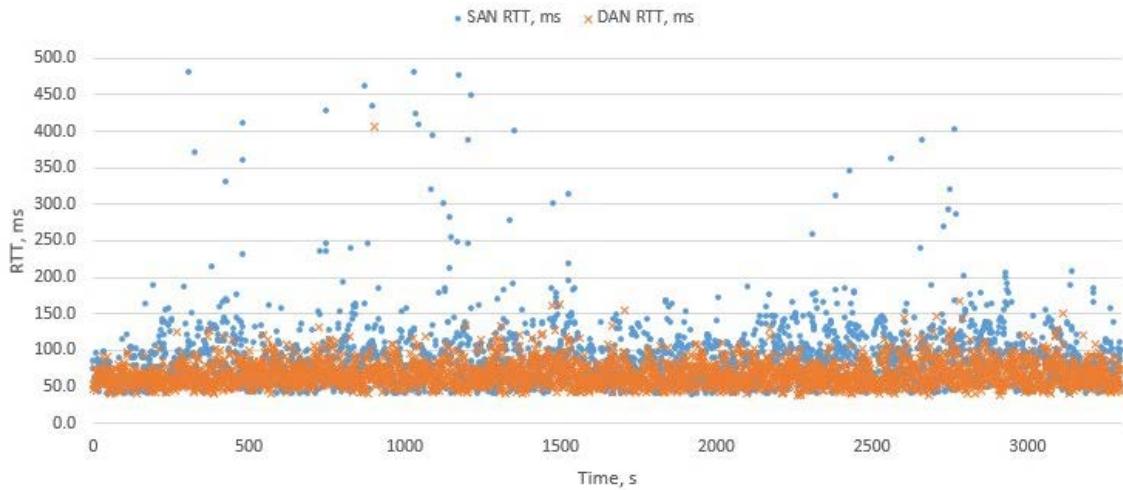
Fig. 4.7 3G SAN and 3G + 3G DAN in the city.

13 packets (0.3831%) are lost in SAN, average RTT is 87.8 ms and average jitter is 32.3 ms. None of packets are lost in DAN, average RTT and jitter are also reduced: 67.3 ms and 13.4 ms respectively.

In the following experiment all dongles are locked in 3G mode, while band selection is done automatically. In populated areas, cells typically operate in band B1 (2100 MHz), in non-populated regions - in band B8 (900 MHz), while in transition between populated and non-populated areas both B1 and B8 are available. The mode of operation is HSPA+ or DC-HSPA+. It should be noted, that 3G networks automatically switches to low speed mode (usually called UMTS) if there is no traffic. As soon traffic is detected, the mode of operation switches to HSPA+ or DC-HSPA+ (depending on signal quality). This means that after short-time data interruption (from 1 to 5 sec, depending on cellular operator settings) network switches to UMTS. Very seldom traffic becomes unrecognized and mode of operation remains UMTS. This situation cannot be fully foreseen and results up to 5 times greater network RTT values. The experimental results are shown in Fig. 4.8.
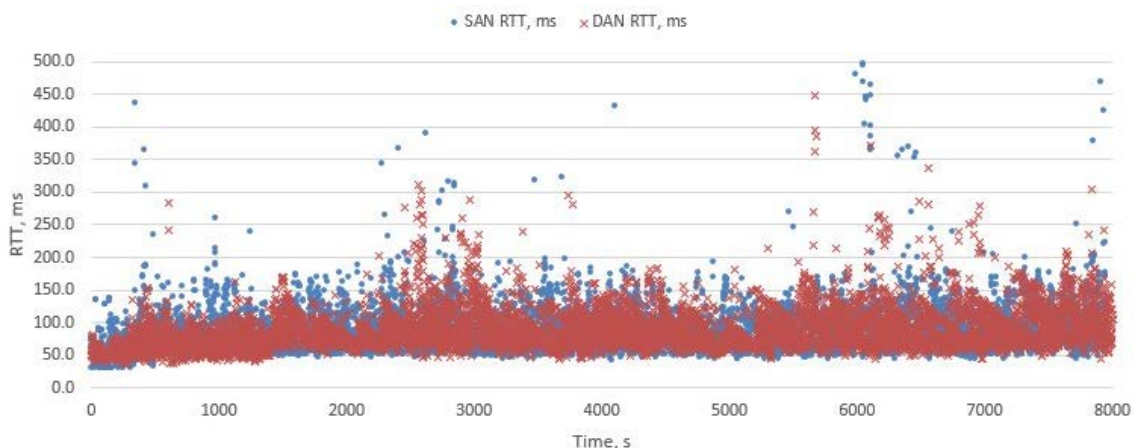
Fig. 4.8 3G SAN and 3G + 3G DAN in rural region.

45 packets (0.5654%) are lost in SAN, averaged RTT and jitter are 91.7 ms and 28.8 ms respectively. In DAN average RTT is 92.1 ms and average jitter is 23.1 ms and none of packets

111

are lost. It should be noted, that RTT in DAN is greater that in SAN. This is explained by the fact, that most of the time DAN second dongle was operating in UMTS mode, while the first DAN dongle and the SAN dongle were operating in HSPA+ and uses same operator Nr.1 service. Thus, second DAN dongle with increased RTT was used only if first dongle packet was lost or significantly delayed. All lost packets were successfully delivered by the second dongle with 5 times higher RTT, resulting higher overall DAN RTT.

LTE networks offer higher throughput, lower RTT and jitter, as well as reduced starting time. However, as LTE cells are UEs' prime choice, these cells are more loaded compared with 3G cells. Due to LTE cells overload in dense cities, sometimes conventional 3G provide better availability and performance. In the following experiment SAN dongle is locked in 3G LTE mode while DAN comprises 3G LTE and 3G services. All dongles band selection is done automatically.
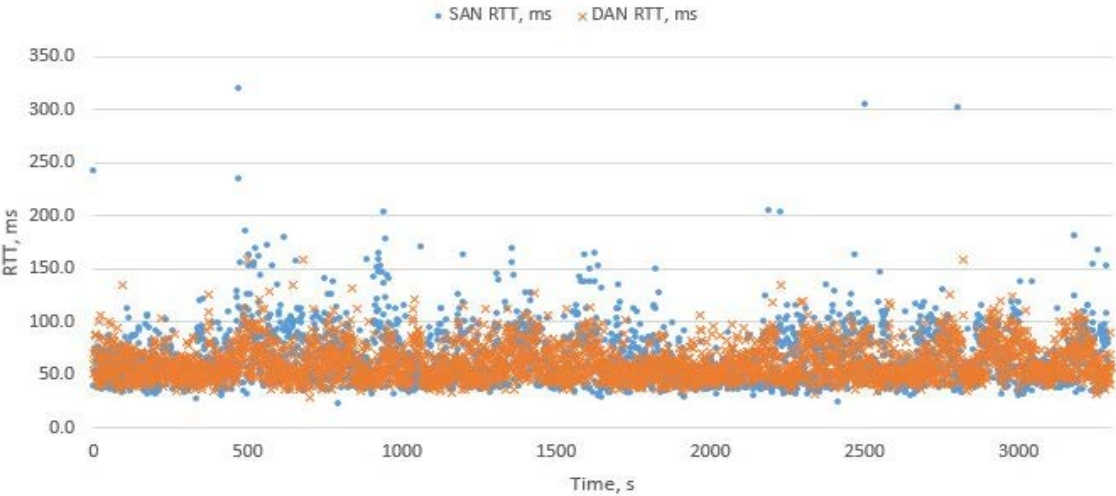


Fig. 4.9 LTE SAN and LTE + 3G DAN in the city.

1 packet (0.0303%) is lost in SAN, average RTT is 64.8 ms and average jitter is 20.9 ms. DAN have no lost packets, averaged RTT and jitter are 61.0 ms and 14.5 ms respectively. It can be concluded that LTE cells were not overloaded in Riga and, since LTE provides smaller RTT, most packets were processed from LTE service.

LTE cells are low loaded in rural regions, thus should provide better performance compared with 3G HSPA+ cells. Also, it should be noted, that 3G in rural regions operates in B8 (900 MHZ) band, that results in higher delays. As 3G requires NodeB and LTE requires eNodeB and these are usually, operating in different bands hence its coverage must be different by default. This is the main motivation to use 3G as a second node for the DAN in rural regions.
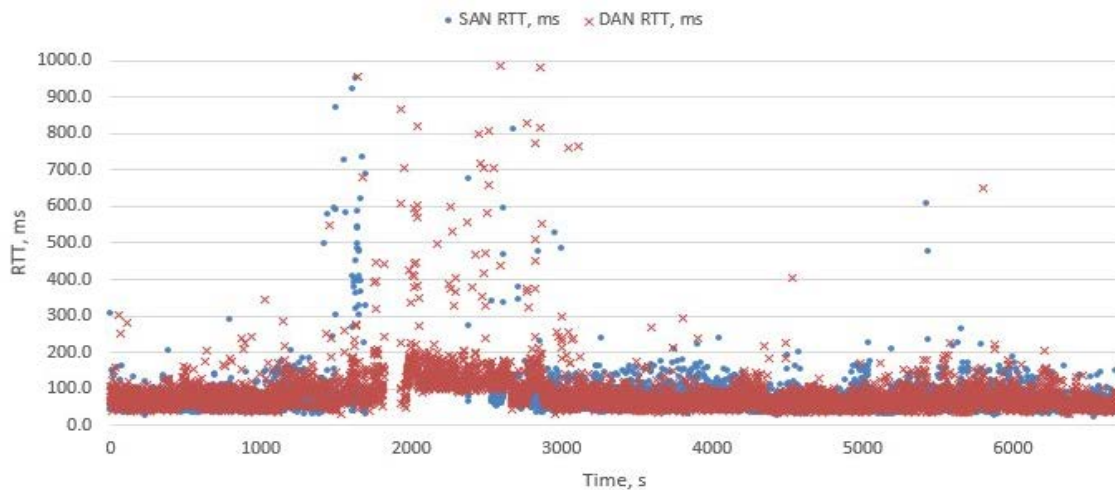
Fig. 4.10 LTE SAN and LTE + 3G DAN in rural region.

1038 packets (15,53%) are lost in SAN, RTT and jitter averaged values are 73.2 ms and 28.4 ms respectively, DAN number of lost packets is 218 (3.249%), averaged RTT is 85.0 ms and averaged jitter is 28.1 ms. Despite different 3G and LTE cells coverage, deep rural valley coverage is problematic for all existing cellular technologies. This results in both service failures or near to miss operation in the region of 1700 .. 2800 sec of the experiment, resulting in DAN data transfer interruption.

If there is no problem with LTE cells overload, a combination of different cellular operator LTE services can be used to build DAN to improve network reliability. In the following experiment all three dongles are locked in LTE mode. In Riga more than one band is available for simultaneous operation. As dongle band selection is done automatically, it is not possible to foresee does whether dongles are operating in same or in different in bands.
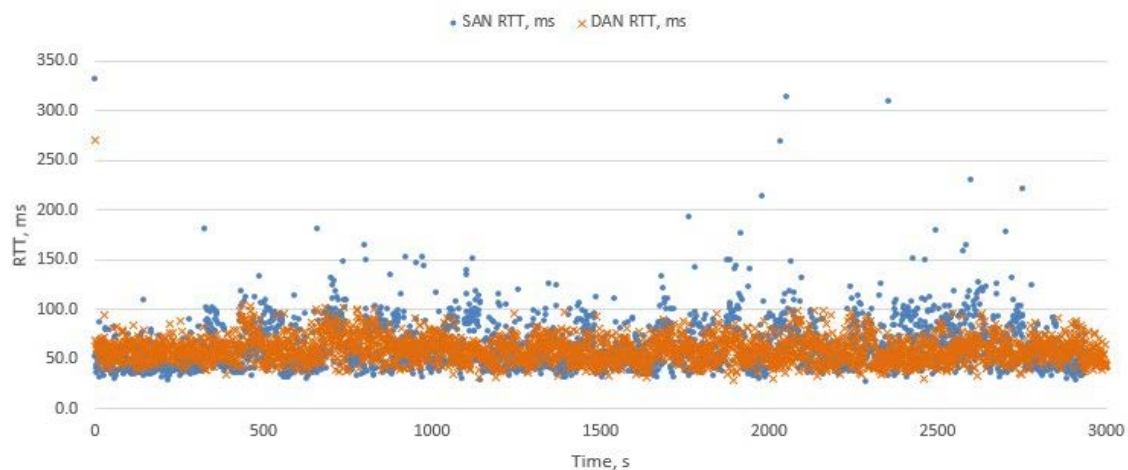
Fig. 4.11 LTE SAN and LTE + LTE DAN in the city.

3 packets (0.1022%) are lost in SAN, RTT and jitter averaged values are 62.6 ms and 18.9 ms respectively. There are no lost packets in DAN, its RTT and jitter averaged values are 59.6 ms and 11.5 ms respectively.

Over recent years LTE coverage in rural regions in Latvia was significantly improved. This makes possible to use different cellular network operators' LTE services combination to build

113

stable DAN solution with reduced RTT and jitter also in rural areas. In the following experiment all three dongles are locked in LTE mode, while band selection is done automatically.
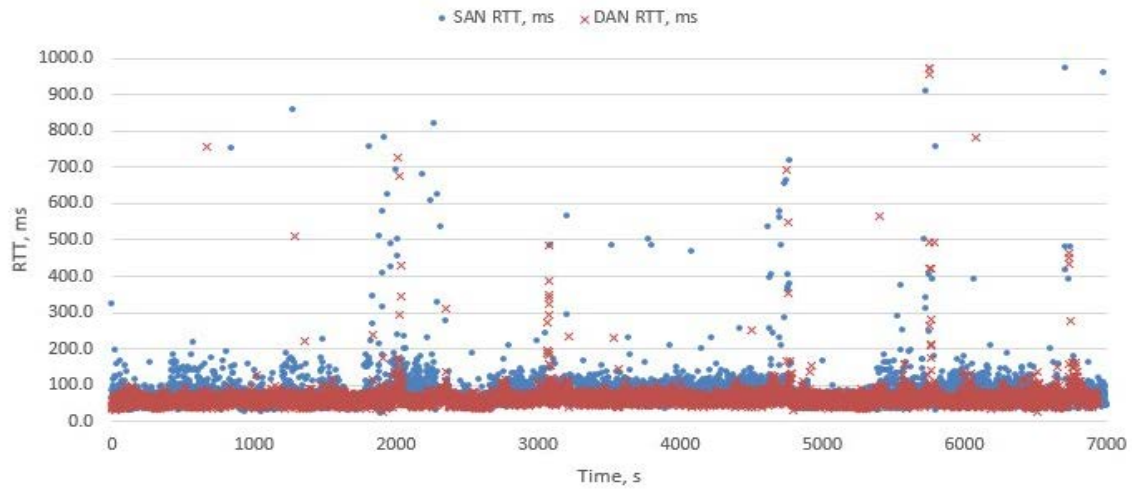
Fig. 4.12 LTE SAN and LTE + LTE DAN in rural region.

The number of lost packets in SAN is 186 (2.648%), RTT and jitter averaged values are 77.9 ms and 29.5 ms respectively. Only 11 packets (0.1586 ms) are lost in DAN, while RTT and jitter averaged values are 64.7 ms and 14.6 ms respectively.

The experimental results are summarized in 4.4. table. Improvement calculation results are inverted to get positive improvement values when RTT and Jitter values are reduced.

4.4. table

Summarized results

	SAN	DAN	Improvement	
RTT, ms	87.8	67.3	23.3%	3G SAN vs 3G+3G DAN in the city
Jitter, ms	32.3	13.4	58.5%	
Number of lost packets, %	0.3831%	none	100.0%	
RTT, ms	91.7	92.1	-0.4%	3G SAN vs 3G+3G DAN in rural region
Jitter, ms	28.8	23.1	19.8%	
Number of lost packets, %	0.5654%	none	100.0%	
RTT, ms	64.8	61.0	5.9%	LTE SAN vs LTE+3G DAN in the city
Jitter, ms	20.9	14.5	30.6%	
Number of lost packets, %	0.0303%	none	100.0%	
RTT, ms	73.2	85	-16.1%	LTE SAN vs LTE+3G DAN in rural region
Jitter, ms	28.4	28.1	1.1%	
Number of lost packets, %	15.530%	3.249%	79.1%	
RTT, ms	62.6	59.6	4.8%	LTE SAN vs LTE+LTE DAN in the city
Jitter, ms	18.9	11.5	39.2%	
Number of lost packets, %	0.1022%	none	100.0%	
RTT, ms	77.9	64.7	16.9%	LTE SAN vs LTE+LTE DAN in rural region
Jitter, ms	29.5	14.6	50.5%	
Number of lost packets, %	2.6480%	0.1586%	94.0%	

Experimental results graphical representation is shown in Fig. 4.13. Network RTT and Jitter averaged values are represented in ms (left Y axis); number of lost packets, as well as RTT and jitter improvements are in % (right Y axis).
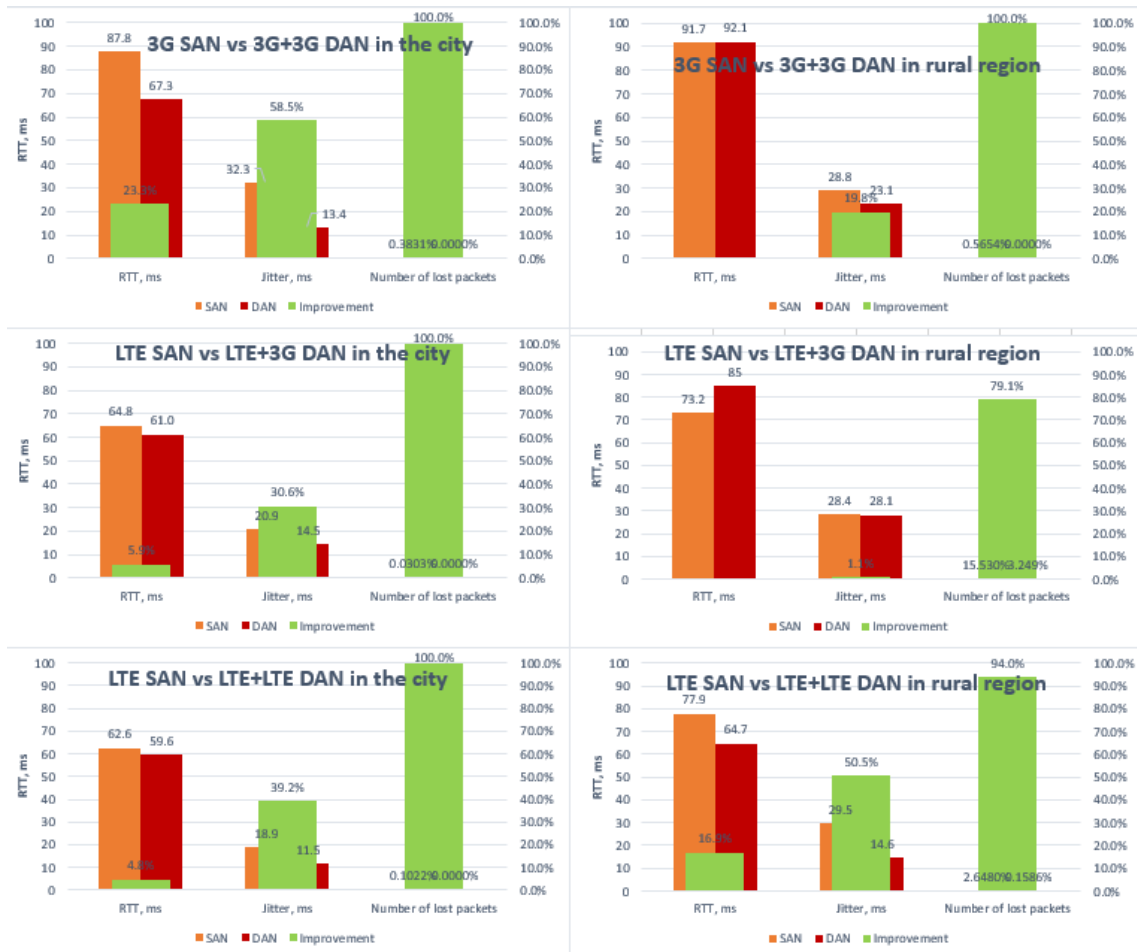
Fig. 4.13 Summarized results

It is possible to conclude, that:

1. Packet duplicates of redundant data flows are not discarded in 3G and LTE networks, thus it is possible to use parallel redundant data flows in 3G and LTE cellular networks.
2. The PRP-1 User Mode Stack [87] is an efficient solution to protect data flow over cellular network.
3. Although LTE is preferred service compared to 3G, sometimes the combination of LTE and 3G in dense areas is more profitable than the combination of LTE and LTE (of different cellular operators) since 3G networks are much less loaded in such areas.
4. In rural regions of Latvia, the combination of LTE and LTE (of different cellular operators) is recommended.
5. It should be noted, that in a case of a rugged topography in rural regions, parallel redundancy cannot provide fully reliable data transfer service, since in deep valleys can be no coverage of both cellular networks.

4.2. Application of a Multipath TCP redundant solution

Parallel redundancy can be used to improve the service quality of data transmission services of a mobile cellular network. In such a solution, each data/control packet is sent in parallel by two cellular data transfer services simultaneously. However, the implementation of such a solution is sometimes impractical, since PRP requires two data transmission channels, and both receiving and transmitting parties must be equipped with two network adapters with different real IP addresses.

The solution described in this part is also based on the use of two cellular network data transfer services. The use of the two services helps improve network availability and can also improve RTT and the maximum possible data rate, depending on the applied parameters of the congestion control scheduler. The implemented solution is flexible for network topology and allows simultaneous protection of transmitting or transmitting and receiving parties. In the experimental setup, it was decided to protect only part of the cellular data transmission, since 100 Mbit Ethernet BER should not be more than 1e -10 (defined in IEEE Std 802.3 [85]) compared to the BER 1e-4 cellular data service [47] (or even more if the service is overloaded [88]).

In the experimental setup, two computers are used: one acts as a wireless remote-controlled equipment, and the second - as a wired GCS.

The laptop is used to implement remote-controlled equipment. It runs the 64-bit Gentoo Linux operating system (based on stable kernel version 4.9) and is equipped with two cellular data transfer USB dongles Huawei 3372h. During all subsequent experiments, the dongles were equipped with randomly purchased different cellular operators SIM cards, and the modes of operation were locked at LTE mode. The simultaneous use of two dongles is provided by the implementation of Multipath TCP version 0.94 [89] in the Gentoo kernel.

Multipath TCP allows to use more than one network interface for a single TCP data flow. Multipath TCP provides TCP data subflows, creating regular TCP connections over available network interfaces. To maintain the integrity of each subflow and prevent it from being blocked by network equipment, each TCP subflow is started with a 0 packets sequence number, so the transmission of the subflow is completely transparent to the network. Further, the original data is restored in the receiving side using the sequence number of the data that is transmitted in the MPTCP subdivision of the TCP packet header. This means that the receiving party must also be compatible with Multipath TCP. Therefore, Multipath TCP always sends the MP_CAPABLE flag during a three-way handshake (initial creation of a TCP subflow) and waits for MP_CAPABLE confirmation. If the use of Multipath TCP is not confirmed by the receiver, Multipath TCP will use only one TCP flow. This makes it capable of operating with both MPTCP and conventional TCP receiving parties. For those interested, more detailed information about the operating principle of Multipath TCP can be found in [90].

If the receiver is Multipath TCP capable, then the use of subflows depends on the selected congestion control Scheduler. There are three schedulers available starting from Multipath TCP version 0.92. If "Default" scheduler is used, then TCP packets are sent over the subflow with the lowest RTT. Further, when the subflow congestion window is full, it will start transmitting

on the next subflow. This approach promises summarized bandwidth of both subflows [89]. If the "Redundant" scheduler is used, TCP packets are sent in parallel via both subflows simultaneously. This approach promises the lowest RTT [89], since the first arriving packet is processed by the receiver. The "Roundrobin" scheduler sends packets in cyclic mode and can work efficiently only with equal bandwidth links. This scheduler is not recommended by developers [89]. For those interested, additional information about the schedulers can be found in [91].

Multipath TCP have a number of aspects in the lost packets delivery in 3G and LTE cellular data transfer networks. In regular TCP connection, packets sequence numbers are ACKnowledged by the receiving party. In the absence of an ACK, the transmitter will resend lost data. Each Multipath TCP subflow is responsible for retransmitting lost packets based on a regular TCP retransmission mechanism. However, if the link of the subflow fails completely, then its data will not be delivered at all. Because Multipath TCP uses more than one subflow, it is possible to retransmit the lost packets thru the remaining subflow(s). However, mobile cellular network data transfer services (starting from 3GPP release 5) automatically acknowledges all packets before they are actually acknowledged by the receiving party and the HARQ mechanism is responsible for retransmission of data over the radio link. This means that if HARQ cannot deliver data, the sender will not be able to use absence of the ACK packet as a trigger for retransmitting data. As described in Section 2.2, a typical loss of data over a 3G or LTE network is 0.1% (1e-4).

To solve this problem, a Data Acknowledgement is implemented in the Multipath TCP [92]. It uses Data ACK to facilitate cumulative acknowledgment for the entire connection. Now, if Multipath TCP detects the absence of data ACK, the data will be retransmitted. The retransmission will be performed in accordance with the selected congestion scheduler. The use of Data ACK makes Multipath TCP extremely suitable for trusted data transmission over mobile data services of a cellular network.

Since the receiving party must be Multipath TCP capable of operating in Multipath TCP mode, the wired remote-control terminal was implemented in Raspberry PI 3B (RPI3) running Gentoo Linux. Since the trusted 4.9 kernel does not support RPI3, the 64-bit Gentoo 4.10 kernel was used. Here, to resolve conflict in *tcp_output.c* the string *void __pskb_trim_head(struct sk_buff *skb, int len)* was replaced by the *int __pskb_trim_head(struct sk_buff *skb, int len)* .

Hewlett Packard (HP) software for testing "netperf" was used in tests of the experimental setup. Netperf runs in client-server mode and provides tests for unidirectional bandwidth and RTT. Since the Multipath TCP only operates with TCP packets, the UDP testing was not performed. The experimental setup is presented in 4.5 table and the Multipath TCP settings are shown in 4.6 table.

Experimental setup

	Wireless remote-controlled equipment	Wired remote control terminal
Hardware	Portable 64 bits computer	Raspberry PI 3B (RPI3)
Operating System	Gentoo Linux 64 bits Kernel 4.9 with MPTCP v.0.94 implementation	Gentoo Linux 64 bits Kernel 4.10 with MPTCP v.0.94 implementation
Network facilities	Two Huawei 3372h dongles, locked in LTE mode; different cellular operators SIM cards	Single wired Ethernet 100 Mbit
Testing software	Netperf 2.7.0-r2 server	Netperf 2.7.0-r2 client

4.6. table

Multipath TCP settings

Settings Option	Meaning
Default MPTCP Path-Manage	Full mesh
MPTCP advanced scheduler	Default, roundrobin or redundant
Default TCP congestion control	Linked Increase Algorithm (LIA)

Since the Multipath TCP is operating with TCP only, the benchmarking was done by running two netperf tests:

1. Stream (to measure the throughput of the connection in the uplink); the syntax of the command is: *netperf -P 0 -t TCP_STREAM -H dest.ip.addr - - o THROUGHPUT*
2. RR (to measure the Request/Response rate (how many TCP transactions per 1 byte can be made per second)); command syntax: *netperf -P 0 -t TCP_RR -H dest.ip.addr -- -r 1,1 -o THROUGHPUT, MEAN_LATENCY , P99_LATENCY*

Statistical data for the average RTT, maximum RTT for 99% threshold of the probability, as well as 1 Byte TCP packet transactions per second rate is from the RR tests. Average throughput statistics are taken from the Stream tests. The duration of each test is 10 seconds, and each test is repeated 10 times (except for comparison in motion).

At first, the remote-controlled equipment is stationary. The radio channel performance indicator's averaged values are shown in 4.7. table. The experimental results are shown in Fig. 4.14. The results are combined in four groups:

- average RTT of 1 byte transfer (in milliseconds),
- maximum RTT with 99% threshold probability of 1 byte transfer (in milliseconds),
- number of 1 byte transfers per second,
- average uplink throughput (in megabits per second).

Each group contains five columns:

- standalone operation of the eth1,
- standalone operation of the eth2,
- Multipath TCP operation over eth1 and eth2 with "default" congestion scheduler enabled,
- Multipath TCP operation over eth1 and eth2 with "RoundRobin" congestion scheduler enabled,
- Multipath TCP operation over eth1 and eth2 with "redundant" congestion scheduler enabled.
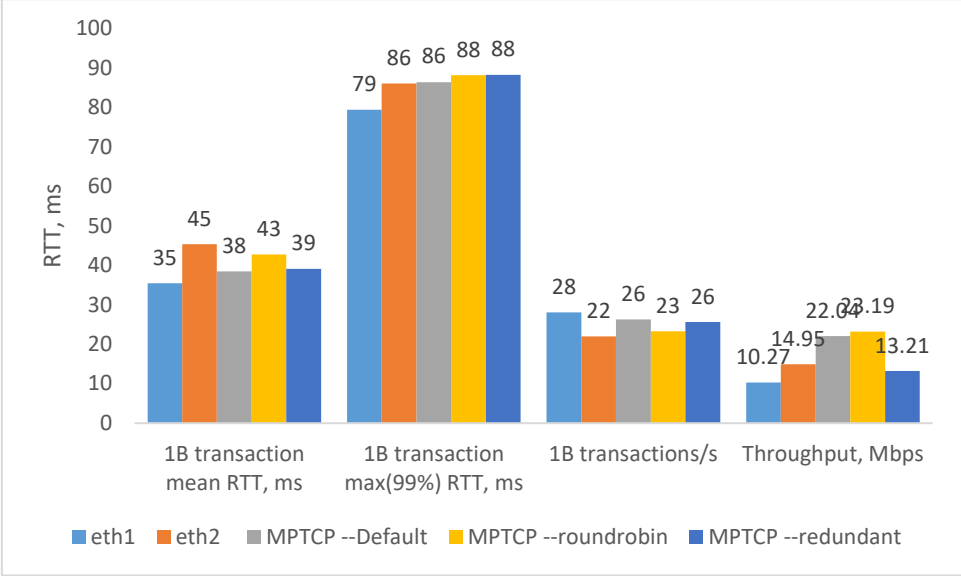
Fig. 4.14 Results of the network performance for the stationary remote equipment.

4.7. table

Signal parameters (LTE)

Dongle	RSSI, dBm	RSRP, dBm	RSRQ, dB	SINR, dB
eth1	-75	-107	-9	8
eth2	-75	-101	-9	-1

The next test is performed to check the Multipath TCP network response for eth2 failure. First, both eth1 and eth2 are operating, and then the SIM card is removed from the second dongle, called eth2. This keeps the eth2 interface "up", but it blocks any data transfer through the radio interface, which leads to failed TCP subflow. Further Multipath TCP congestion control is responsible for retransmission of failed data. The experimental results are shown in Fig. 4.15. The Fig. 4.15 layout is similar with Fig. 4.14. Please note that the standalone operations of eth1 and eth2 are shown here for comparison. The SIM card is not removed during testing standalone operation of the eth2.
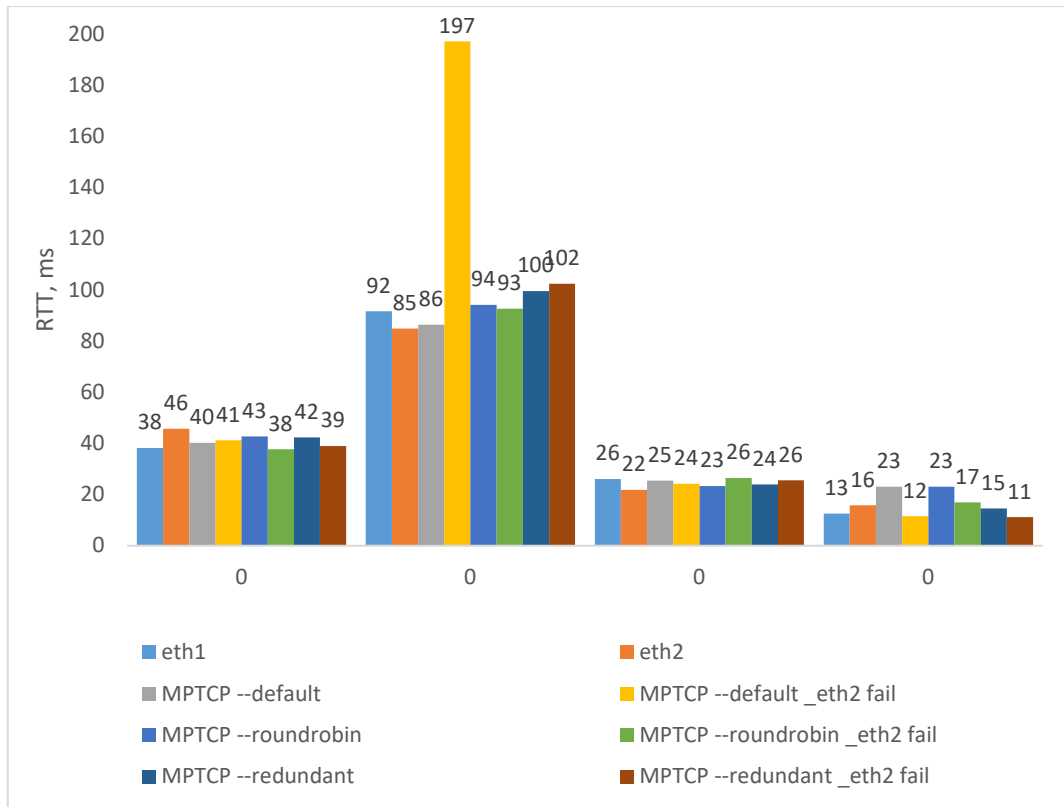
Fig. 4.15 Results of the network performance for the stationary remote equipment with and without failed eth2.

Fig. 3.15 provides only statistical representation of two conditions: before and after failure of the TCP subflow through the eth2. The represented data is averaged. A more detailed representations of the effect of TCP subflow failure through eth2 with "default" congestion control scheduler are shown in Fig. 4.16 and Fig. 4.17. The TCP flow over eth2 fails between 6th and 7th measurements, that leads to significantly increased maximum RTT values during 30 sec period (each measurement duration is 10 sec).

Fig. 4.16 Maximum RTT values for the stationary remote equipment with failed TCP subflow over eth2 after 6th measurement and "default" congestion scheduler applied.

The "default" congestion scheduler allows to combine both uplink subflows. This leads to summarized uplink throughput if both TCP subflows are operational. Failure of the TCP subflow through eth2 leads to decreased uplink throughput down to remaining eth1 throughput.

Fig. 4.17 Uplink throughput for the stationary remote equipment with failed TCP subflow over eth2 after 6th measurement and "default" congestion scheduler applied.

Use of a "redundant" congestion control scheduler does not allows to summarize both TCP subflows throughput but helps to avoid delays in packets delivery if one TCP subflow is failed. Both these effects are shown on Fig. 4.18 and Fig. 4.19. In this experiment, a TCP subflow failure through the eth2 occurs between 4th and 5th measurements.
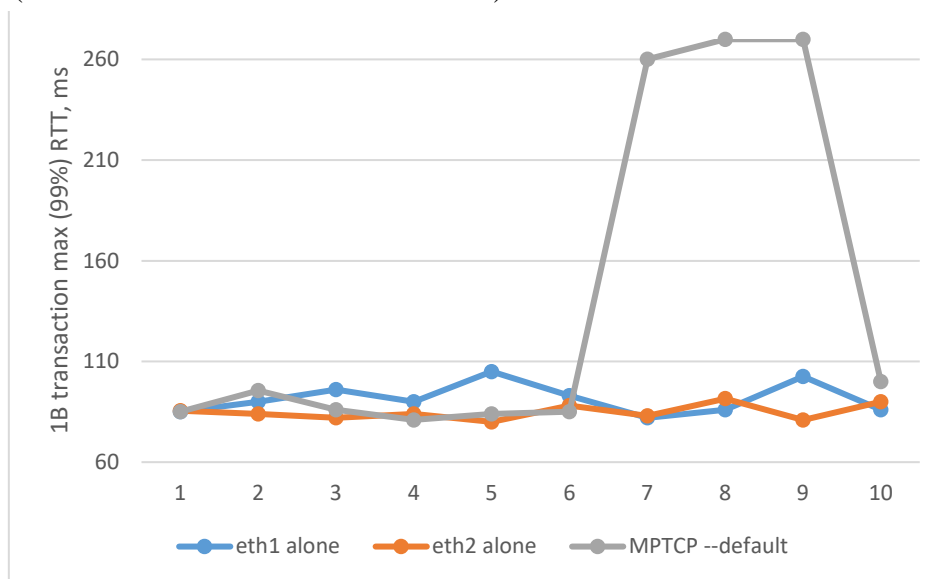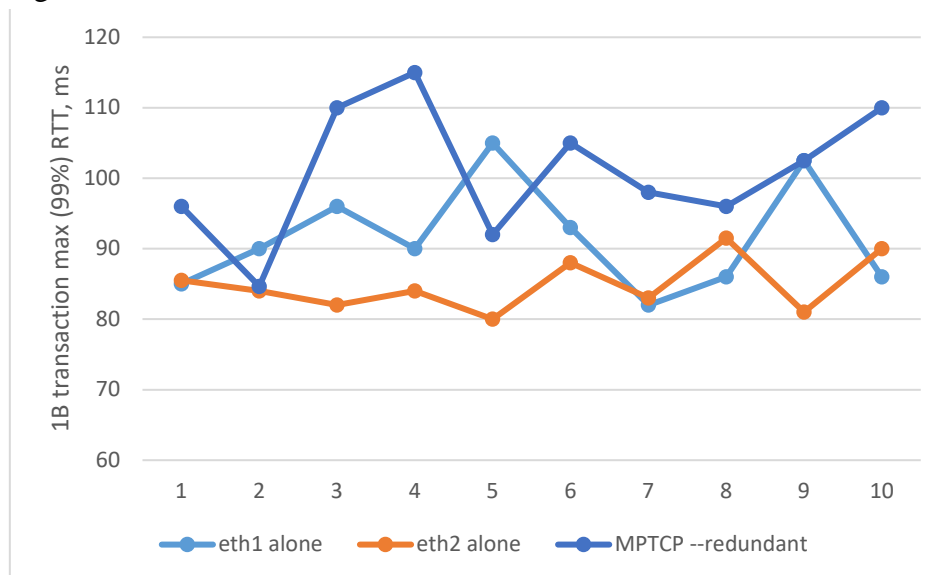

Fig. 4.18 Maximum RTT values for the stationary remote equipment with failed TCP subflow over eth2 after 4th measurement and "redundant" congestion scheduler applied.

The "redundant" congestion scheduler allows to obtain the resulting throughput equal to the best throughput of two subflows (in this experiment it is throughput through the eth2). Failure

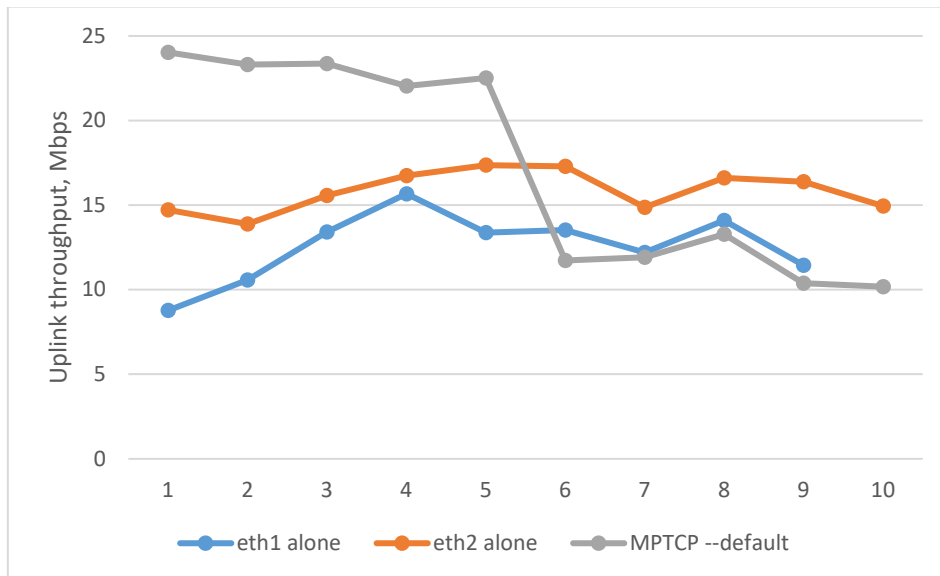of the TCP subflow through eth2 leads to decreased uplink throughput down to remaining eth1 throughput.
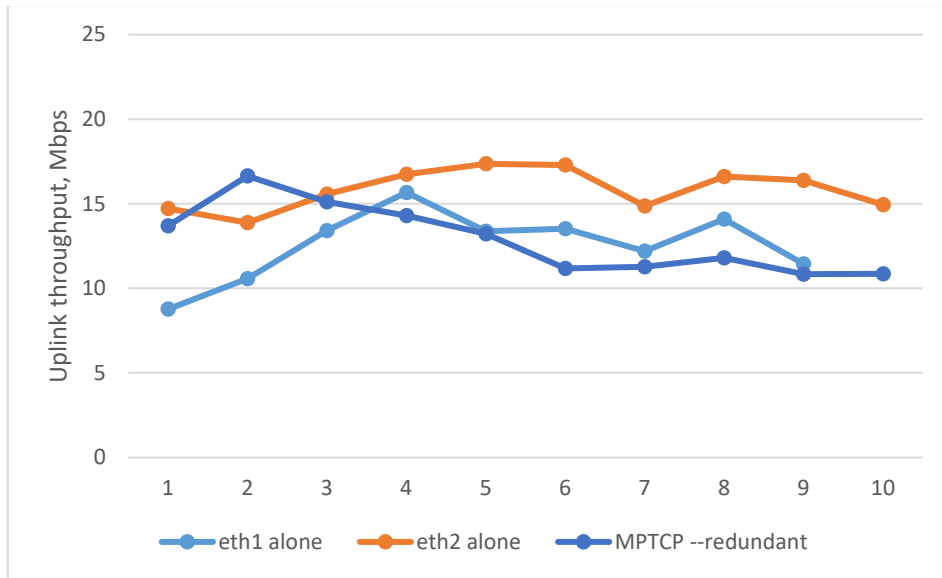
Fig. 4.19 Uplink throughput for the stationary remote equipment with failed TCP subflow over eth2 after 4th measurement and "redundant" congestion scheduler applied.

One of the key features of cellular mobile networks is the support of UE mobility. In the next benchmark the remote-controlled equipment is moved by car in the city. Since each test should be performed separately, testing was carried out sequentially, following the same path several times. The experimental results are shown in Fig. 4.20. In this experiment, average uplink throughput measurements were not performed due to limited amount of allowed data traffic.
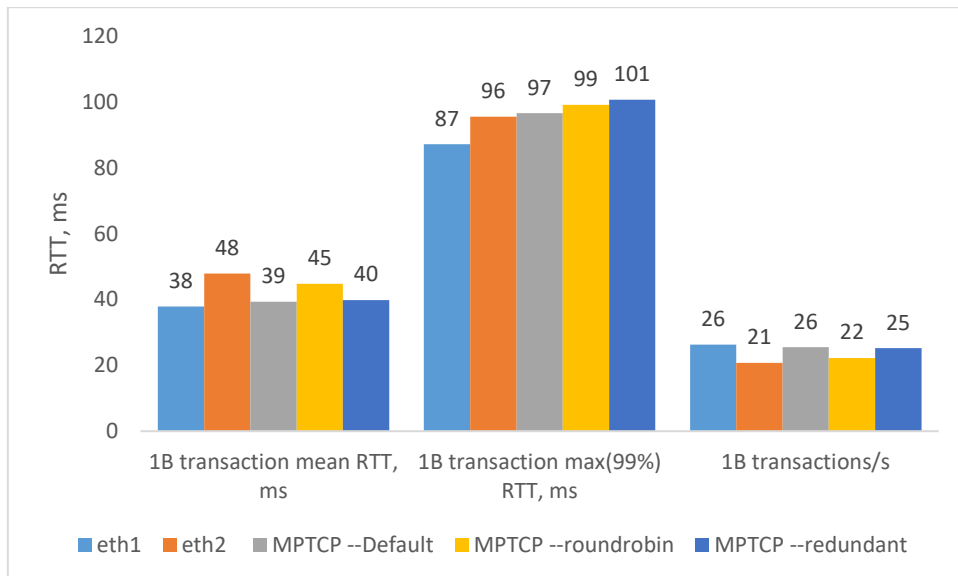
Fig. 4.20 Network performance results for the moving remote equipment.

Finally, it should to especially noted, that MPTCP solution operates with TCP packets only. It can be concluded, that:

1. The resulting performance of a multi-path data network highly depends on the selected congestion control scheduler.
2. The "default" congestion control scheduler allows to effectively summarize throughput of both subflows. However, its usage can be recommended only if the goal is to obtain maximum data rate over wired networks with low data loss by itself, because lost (undelivered) packets leads to increased delays by approximately 3 times, because there is a deadtime before the MPTCP will try to resend a packet over another interface. This makes "default" congestion control schedules unfitted for moving equipment due to a lot of temporary interruptions of cellular data transfer services.
3. The "redundant" congestion control scheduler does not allow to summarize throughput of both subflows but makes no increased RTT if undelivered packets occurs over partially or fully failed subflow. This makes "redundant" congestion control scheduler more suitable for portable or moving ground equipment's wireless control channel implementation.
4. The "Round-robin" scheduler is only suitable for networks with an equal cost, its use is not recommended by the developer, therefore it will not be discussed here.

4.3. Unified method of prediction the delays in parallel redundant channels

Modern cellular data transfer services like 3G (Cat 15 3GPP Release 7 HSPA+ devices and above) as well as LTE (LTE Cat 4 devices and above) provide well-deployed, mature and cheap terrestrial wireless data transfer solutions. The goal for the modern cellular data transfer services is the highest possible data rate and reduced latencies by the cost of increased packet loss and packet jitter. Increased jitter and relatively high BER makes cellular data transfer service unacceptable for near to real time control applications. The situation can be improved by applying well known diversity, namely parallel redundancy.

Parallel redundancy typically is used in industrial or in highly available wired data networks. Generally, such networks utilize parallel redundancy to increase reliability and availability [93]. Resultant redundant network availability and reliability typically are estimated with Markov chain approach [94]. The results of the availability improvements can be found in [95]. Despite typical application of the parallel redundancy in the wired networks, some scientific papers for parallel redundant WLANs are available too. In [96], [97] authors utilizes OPNET simulation tool to estimate not only network reliability, but also parameters of the resultant redundant channel, such as Latency and Jitter. More detailed simulation via OMNet++ for various wireless standards can be found in [98]. In the [99], [100] authors demonstrate real working examples of the IEEE 802.11 redundant networks, based on Parallel Redundancy Protocol (PRP) (according to IEC 62439-3). Resultant networks parameters in both papers has been measured directly and both papers have no mathematical model for estimating. Further, in the [101] authors apply Markov chain approach (which is described in [94]) to estimate network parameters. Results are experimentally verified. Such approach allows availability estimation of the resultant network (if failure probabilities are known). Unfortunately, resultant

network parameters, such as latency and jitter, are not estimated and are measured only during experimental verification.

At the time of this writing, author is familiar of two software solutions for parallel redundancy implementation. These are: ZHAW university implementation of the Parallel Redundancy Protocol (PRP according to IEC 62439‑3 / 2012) as a VHDL IP core [87] and Icteam' MultiPath TCP (MPTCP) kernel implementation with the "redundant" MPTCP scheduler enabled (version v0.91 and above) [89]. Both solutions are applicable to Linux systems only and facilitate a good software platform for parallel redundant network experiments. The results of the parallel redundant network implementation via cellular 3G / LTE mobile services has been discussed in previous chapters and were published in [102] and [103] for the ZHAW PRP and Multipath TCP implementations respectively.

The resultant redundant network availability and reliability parameters can be easily calculated by using recommendation [94]. The resultant redundant network performance parameters, such as latency (or Round Trip Time (RTT)) and Jitter typically are estimated via simulation software, e.g. OPNET, OMNet++, etc.

This chapter presents generalized method based on mathematical statistics to estimate redundant network delays. This chapter is focused on this method applicability and experimental verification in the cellular LTE networks only. As already stated in the Chapter 2.3, at least 90% of RTT values of the LTE network obeys the lognormal distribution.

4.3.1 Applying a definition of a new random value of delays

In the following section a parallel redundancy of two parallel data transfer services is consider, because the use of three or more parallel redundant lines is impractical. Since it is wise to utilize different cellular operators' services to build robust parallel redundant system, both data transfer services RTT values are considered as independent random variables. Let's denote random variables of RTT of the first data transfer service as T_1 and random variables of RTT of the second data transfer service as T_2. Hence T_1 and T_2 are independent random variables with continuous probability functions $F_{T1}(t_1)$ and $F_{T1}(t_2)$ respectively.

Since in parallel redundant system only first arriving packet is processed, while the second is discarded, the resulting random variable Z of a parallel redundant system can be expressed as a minimum of two independent random variables:

$$Z = \min(T_1, T_2) \tag{4.1}$$

Hence:

$$F_Z(z) = P(Z \leq z) = P(min(T_1, T_2) \leq z) \tag{4.2}$$

The use of inverse probability allows to find a lower boundary of the minimum, so:

$$F_Z(z) = 1 - P(Z > z) = 1 - P\big(min(T_1, T_2 > z)\big) \tag{4.3}$$

And since T_1 and T_2 are independent random variables, then:

$$F_Z(z) = 1 - P(Z > z) = 1 - \big(1 - F_1(z)\big) \cdot \big(1 - F_2(z)\big) \tag{4.4}$$

This is a standard approach of finding a minimum of two random variables. However, in case of real working data transfer service, some packets can be lost (undelivered). The lost packet has RTT equal to infinity. This makes it impossible to represent network performance as a probability function of a minimum.

Let's define probability of packet loss for the first data transfer service as q_1 and the probability of packet loss for the second data transfer service as q_2. Since it is assumed that different cellular operators' services are utilized, the packet loss values will be independent too. Next, let's denote T_1^* as a conditional random variable of T_1, when $T_1 < \infty$ (packet was delivered) as well T_2^* as a conditional random variable of T_2, when $T_2 < \infty$. Hence, T_1^* and T_2^* are independent random variables with corresponding specific random continuous distribution functions, which with probability $(1-q_1)$ and $(1-q_2)$ respectively are equal to $F_{T1}(t_1)$ and $F_{T1}(t_2)$ respectively if packet was delivered or equal to infinity ∞ if packet is lost. Now, let's define conditional distribution function of T_i^* where i=1,2:

$$F_{T_1}(t) = P\langle T_1^* < t | T_1^* < \infty \rangle \tag{4.5}$$

$$F_{T_2}(t) = P\langle T_2^* < t | T_2^* < \infty \rangle \tag{4.6}$$

Now, let's denote Z^* as a conditional random variable of Z, when $Z < \infty$ (at least one packet from the redundant system has been delivered). Then the conditional distribution function of the parallel redundant system with n=2 parallel data transfer services can be defined as:

$$Z^* = min(T_1^*, T_2^*) \tag{4.7}$$

Here the conditional random variable $T_i^* = T_i$ with the probability of $1-q_i$ and $T_i^* = \infty$ with the probability q_i, where i=1,2.

Thus, we have the following exhaustive events (for $Z^* < \infty$):

$$\begin{cases} T_1^* = T_1, T_2^* = T_2 \\ T_1^* = T_1, T_2^* = \infty \\ T_1^* = \infty, T_2^* = T_2 \end{cases} \tag{4.8}$$

Next, let's find the probability when $Z^* < \infty$. To do this, it is necessary to utilize exhaustive events:

$$P(Z^* < z)$$
$$= \begin{cases} P(T_1 < z | T_1^* < z) \cdot P(T_2 < z | T_2^* < z) \cdot P(T_1^* = T_1) \cdot P(T_2^* = T_2) \\ P(T_1 < z | T_1^* < z) \cdot P(T_1^* = T_1) \cdot P(T_2^* = \infty) \\ P(T_2 < z | T_2^* < z) \cdot P(T_1^* = \infty) \cdot P(T_2^* = T_2) \end{cases} = \tag{4.9}$$
$$= F_{T_1}(z) \cdot F_{T_2}(z) \cdot (1 - q_1) \cdot (1 - q_2) + F_{T_1}(z) \cdot (1 - q_1) \cdot q_2 + F_{T_2}(z) \cdot q_1 \cdot (1 - q_2)$$

Hence, the conditional distribution function of Z^*, providing that at least one T_i (i=1,2) has real value ($Z^* < \infty$), will be defined as:

$$F_Z(z) = P(Z^* < z | Z^* < \infty) = \frac{P(Z^* < z)}{1 - P(T_1^* = \infty) \cdot P(T_2^* = \infty)} = \frac{P(Z^* < z)}{1 - q_1 q_2} \tag{4.10}$$

The same conditional distribution function of Z^* can be expressed in generic form (for i = 1, 2, ..., n):

$$F_Z(z) = P(Z^* < z | Z^* < \infty) = \frac{P(Z^* < z)}{1 - \prod_{i=1}^{n} q_1} \tag{4.11}$$

The use of inverse probability allows to find a lower boundary of the minimum, so the inverse probability for the channel i of the redundant system can be expressed as:

$$P(T_i^* > z) = P(T_i > z) \cdot P(T_i^* < \infty) + P(T_i^* = \infty)) \tag{4.12}$$
$$= (1 - F_{T_i}) \cdot (1 - q_i) + q_i$$

Then the probability of Z*, when Z* < ∞, can be expressed by finding a minimum, as follow:

$$P(Z^* < z) = 1 - \prod_{i=1}^{n} \{P(T_i^* > z | T_i^* < \infty) + P(T_i^* = \infty)\}$$

$$= 1 - \prod_{i=1}^{n} \{(1 - F_{T_i}(z)) \cdot (1 - q_i) + q_i\}$$

(4.13)

Now let's solve this equation assuming that the number of parallel data transfer services is n=2. Then:

$$P(Z^* < z) = 1 - P(T_1^* > z) \cdot P(T_2^* > z) = P(T_i^* > z)$$
$$= P(T_i > z) \cdot P(T_i^* = T_i) + P(T_i^* = \infty)$$
$$= (1 - F_{Ti}(z)) \cdot (1 - q_i) + q_i, where\ i = 1,2.$$

(4.14)

So:

$$P(T_i^* > z) = 1 - \prod_{i=1}^{2} \{P(1 - F_{T_i}(z)) \cdot (1 - q_i) + q_i\} =$$

$$= 1$$
$$- \{(1 - F_{T_1}(z)) \cdot (1 - q_1) + q_1 \cdot (1 - F_{T_2}(z)) \cdot (1 - q_2) + q_2 \cdot$$
$$\cdot (1 - F_{T_1}(z)) \cdot (1 - q_1) + q_1 q_2\} =$$
$$= (1 - q_1) \cdot F_{T_1}(z) + (1 - q_2) \cdot F_{T_2}(z) - F_{T1}(z) \cdot F_{T2}(z) \cdot (1 - q_1)$$
$$\cdot (1 - q_2)$$

(4.15)

Now the conditional random variable Z* (when Z ≤ ∞) can be defined, in general form, as:
$$F_Z(z) = 1 - P(Z > z | Z < \infty) = P(Z^* < z | Z^* < \infty) =$$

$$= \frac{P(Z^* < z)}{1 - P(Z_1^* < z) \cdot P(Z_2^* < z) \cdot ... \cdot P(Z_n^* < z)} = \frac{P(Z^* < z)}{1 - \prod_{i=1}^{n} q_i}$$

(4.16)

Hence the conditional distribution function of the parallel redundant system with two parallel data transfer services (n = 2) is defined by:

$$F_Z(z) = 1 - P(Z > z | Z < \infty) =$$

$$= \frac{1 - \left((1 - F_1(z)) \cdot (1 - q_1) + q_1\right) \cdot \left((1 - F_2(z)) \cdot (1 - q_2) + q_2\right)}{(1 - q_1 q_2)}$$

(4.17)

Since T_1 and T_2 are independent random variables, as well F_{T1}^* and F_{T2}^* are logarithmically normal distribution functions, the resultant F_Z^* also can be considered as a logarithmically normal distribution function (this is a unique property of the multiplication of several lognormal functions).

4.3.2 Experimental verification of the calculations of delays in the parallel redundant networks

In the following section a parallel redundancy of two parallel data transfer services is consider, because the use of three or more parallel redundant lines is impractical.

During this experiment, two LTE data transfer services were used via two Huawei 3372h USB dongles. A google free DNS server (ip: 8.8.8.8) was selected as the destination. RTT values of both LTE data transfer services were measured using ICMP packets (the motivation

is explained in section 2.2). The first LTE service's RTTs CDF is shown in Fig. 4.21 ("RTT-1st_Network", blue color); the second LTE service's RTTs CDF is shown in Fig. 4.21 ("RTT-2nd_Network", red color). The first LTE service's average values of RTT = 87.83 ms and Jitter =21.64 ms; 2nd LTE service's average values of RTT = 75.89 ms and Jitter = 13.37 ms; packet loss rates are 0.022 % and 0.027 % respectively.

Next, parallel redundant network RTT is estimated by taking minimum from pair of RTT values of 1st and 2nd LTE channels. Redundant network RTT values estimation is done in this way to exclude additional delays, caused by processing time of the redundancy boxes (RedBox). Its average RTT = 71.1 ms and average Jitter = 10.28 ms. The resulting RTT's CDF of the "ideal" redundant system is shown in Fig. 4.21 ("RTT-Estimated_via_min.f._Paral.Red.Netw").

Further, parallel redundant network performance is calculated via equation (4.17). 1st and 2nd networks losses are set to 0.022% and 0.027% respectively. Calculated redundant network RTT CDF is shown in Fig. 4.21 ("RTT-Calculated_paral.Red.Netw").
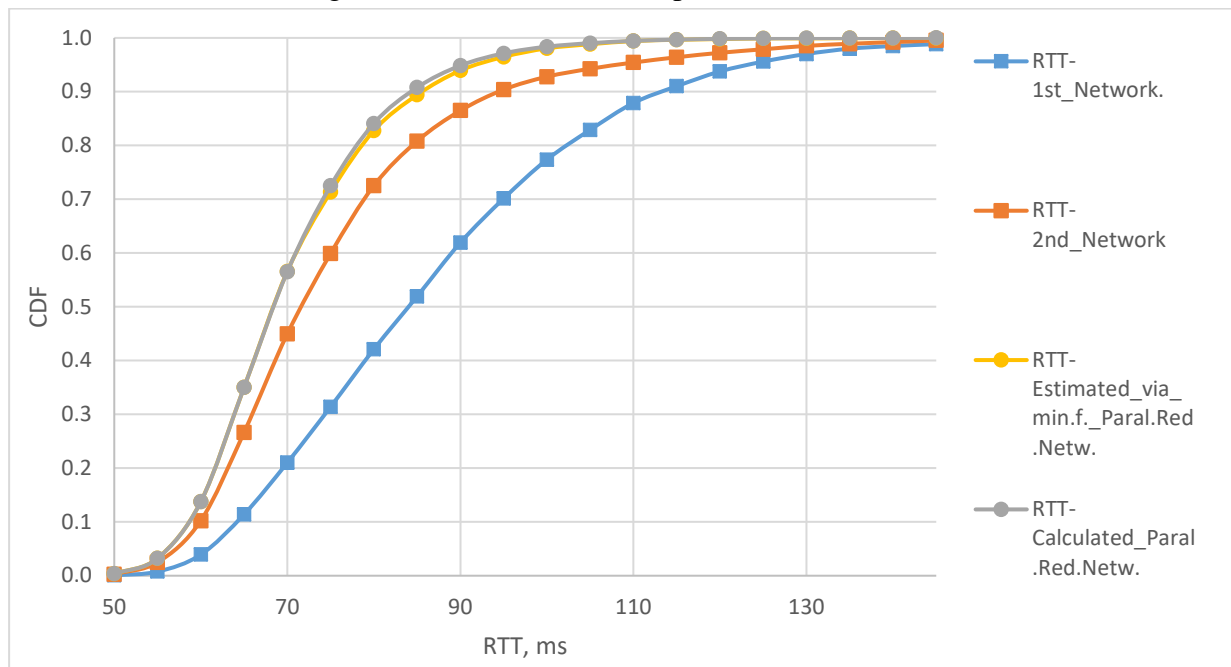
Fig. 4.21 RTT of 1st and 2nd LTE networks; RTT of calculated and estimated redundant solution.

Fig. 4.21 shows that estimated and calculated redundant network CDFs are not exactly matched: calculated results propose slightly better (lowest) delays. This can be explained by the fact, that both LTE services utilize same destination. This means that the final wired segment for both networks is same. This, by itself, leads to small correlation between 1st and 2nd networks RTT values. In this experiment the correlation is equal to 7%.

Resultant redundant solution expected values E(t_red), as well Correlation Coefficient Deviation (CCD) of the calculated redundant network CDF are calculated to compare both estimated and calculated redundant network CDFs. Estimated by minimum redundant network CDF expected value is E(t_red_est)=70.3865, whereas calculated redundant network CDF expected value is E(t_red_calc)=70.1517 (0.33% difference). Calculated redundant network

CDF CCD (for 99% confidence interval) with respect to estimated redundant network is CCD_red.calc = 0.0112%.

4.3.3 Experimental verification of the calculations of delays if lognormal distribution function is used

In Chapter 2.4 it was proved that at least 9% of the LTE network RTT values are logarithmically normal distributed. This assertion allows not to build CDFs from the experimental data, since these can be built for lognormal distribution function with parameters $\theta_0=\mu$ =median and $\theta_1=\sigma$=STDEV. The distribution function parameters estimation can be done via various methods, but the maximum likelihood method is recommended here because it is more applicable for censored observations processing. However, the "ping" application returns only statistical values of minimum (Tmin), average (Tavrg) and maximum (Tmax) RTT values, as well as the amount of sent and lost packets. The method for the parameter's estimation for the lognormal distribution function from known minimum and average RTT values is presented in Chapter 0. Definition of the required number of measurements n is given in Chapter 2.4.2.1.

In Fig. 4.22 the resultant redundant network CDF functions are shown. The first one is calculated from two CDF functions that are built from experimental data. The second one is calculated from two CDF functions that are built as lognormal functions with parameters θ_0 and θ_1, calculated via the equations (2.9) and (2.10). The third one is calculated from two CDF functions, that are built as lognormal functions with parameters θ_0 and θ_1, that are calculated via approximate formulas (2.19).

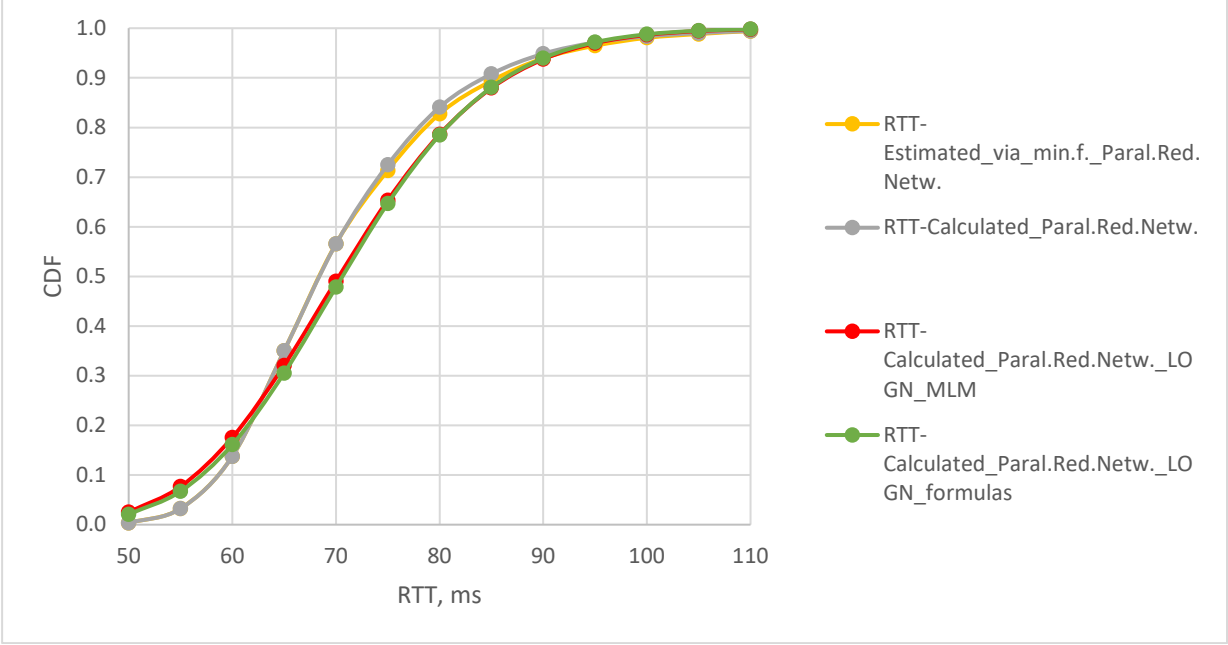Fig. 4.22 CDF of RTT of the resultant redundant solution, calculated from experimental data, as well estimated via MLM and approximate equations.

Estimated by minimum redundant network CDF expected value is E(t_red_est)=70.3865, whereas calculated from experimental data redundant network CDF expected value is E(t_red_calc)=70.1517 (0.33% difference) as well CCD (for 99% confidence interval) with

respect to estimated redundant network is CCD_red.calc = 0.0112%); calculated from lognormal distributed data (θ_0 and θ_1, are calculated via the MLM) E(t_red_logn_mlm)=74.7892 (6.26% difference) as well CCD_ red_lnorm_mlm=0.4904%; calculated from lognormal distributed data (θ_0 and θ_1, are calculated via the approximate equations (2.9) and (2.10)   E(t_red_logn_form)=75.3695 (7.08% difference) as well CCD_red_lnorm_form=0.5378%.

4.3.4   Improvements of the delays in the resultant redundant network solution

The following 4.8. table shows the comparison of the results calculated from the experimental data. The experimental setup has same destination for both redundant networks, as well common final line, which leads to correlation of 7% for T_1 and T_2 values (RTT values of 1st and 2nd LTE data transfer service). The difference in average RTT values is calculated with respect to expected value of the "ideal redundant channel". The CCD is calculated for 99% confidence interval of the resultant CDF with respect to ideal redundant channel's CDF. The "ideal redundant channel" is estimated by taking minimum from pair of two channels RTT values.

4.8. table

Averaged RTT values and relative errors of the redundant network (based on two LTE services with 7% correlation of their RTTs)

Results	Average RTT, ms	Error, %	CCD$_{99\%}$, %
Real redundant network	70.3865	-	-
Redundant network, calculated via equation (4.17) from CDFs based on experimental data	70.1517	0.33	0.0112
Redundant network, calculated via (4.17) from two lognormal CDFs, (θ_0 and θ_1 are estimated via MLM)	74.7892	6.26	0.4904
Redundant network, calculated via (4.17) from two lognormal CDFs, (θ_0 and θ_1 are estimated via (2.20)	75.3695	7.08	0.5378

Higher deviation of T_1 and T_2 random variables (RTT values of 1st and 2nd data transfer services) results lower average and maximum delays of the redundant system. The Fig. 4.23 shows the dependence of the relative improvement in the average delay (T1_avrg / Tred_avrg) and maximum delay (T1_max / Tred_max) depending on the distribution parameter θ_1 (σ). The maximum delays are specified at the level of 0.99. The results are provided for two identical data transfer channels with parameters $\mu 1 = \mu 2 = 4.0$; whereas θ_1 for both channels lies between 0 and 0.3 ($\sigma_1 = \sigma_2 = [0 : 0.3]$).
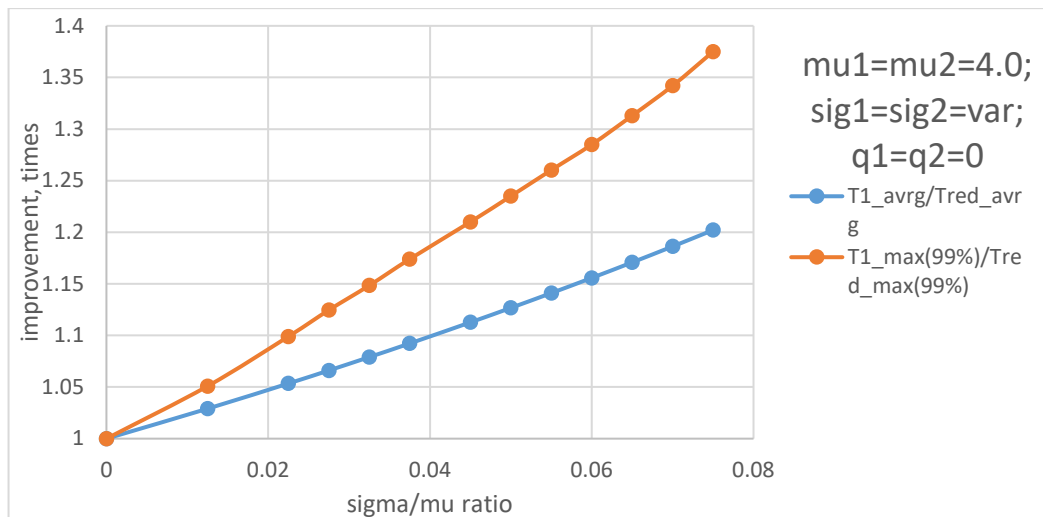
Fig. 4.23 Improvement in average and maximum (at 99%) RTT in the redundant solution, depending on standard deviation to median ratio (σ/μ), assuming that similar data transfer services are used.

The difference in median values θ_0 (μ) of T1 and T2 random variables (RTT values of 1st and 2nd data transfer services) results different improvement in average and maximum delays of the redundant system. Fig. 4.24 shows the dependence of the relative improvement in the average delay (T1_avrg / Tred_avrg) and maximum delay (T1_max / Tred_max) depending on the distribution parameters θ_0 (median) ratio μ_1 / μ_2. The maximum delays are specified at the level of 0.99. The results are provided for two data transfer channels with parameters $\sigma_1 = \sigma_2 = 0.2$, $\mu_2 = 4.0$; whereas μ_1 is in range from 3.4 to 4.6 ($\mu_1 = [3.4 – 4.6]$).
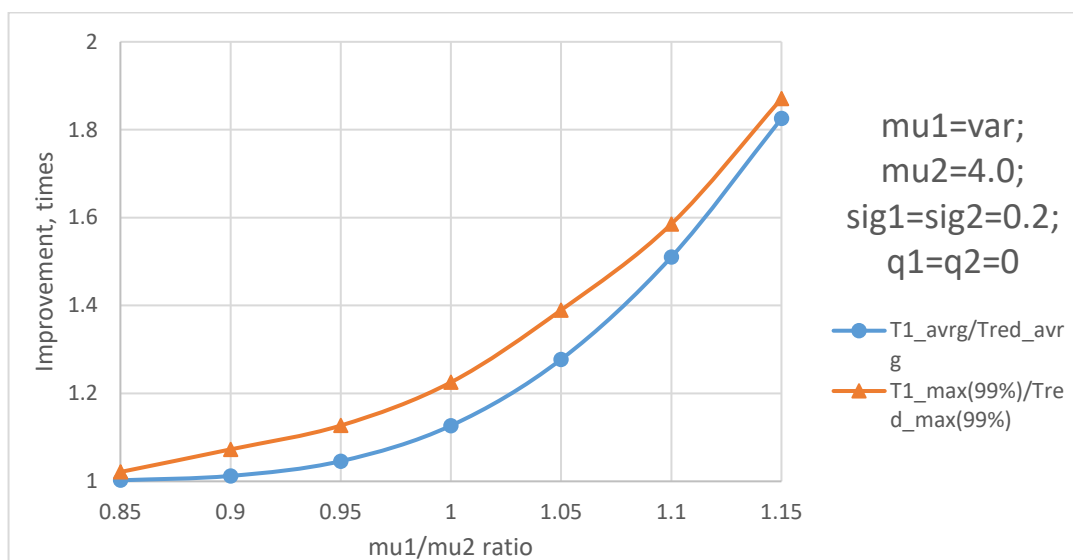
Fig. 4.24 Improvement in average and maximum (at 99%) RTT in the redundant solution, depending on 1st channel median to 2nd channel median ratio (μ_1 / μ_2), assuming that $\sigma_1 = \sigma_2$.

Higher packet loss of the channel reduces its impact on the resulting performance of the redundant system. Fig. 4.25 shows the dependence of the improvement in the average delay (T1_avrg / Tred_avrg) depending on the packet loss q1 in the first data transfer channel, if the

second channel has no lost packets (q2=0). Next, the dependence of the improvement in the average delay is shown with assumption that both data transfer channels have similar packet loss rates (q1=q2). The results are shown for µ1 = µ2 = 4.0; and three θ_1 values ($\sigma1 = \sigma2 = [0.15, 0.2, 0.25]$).
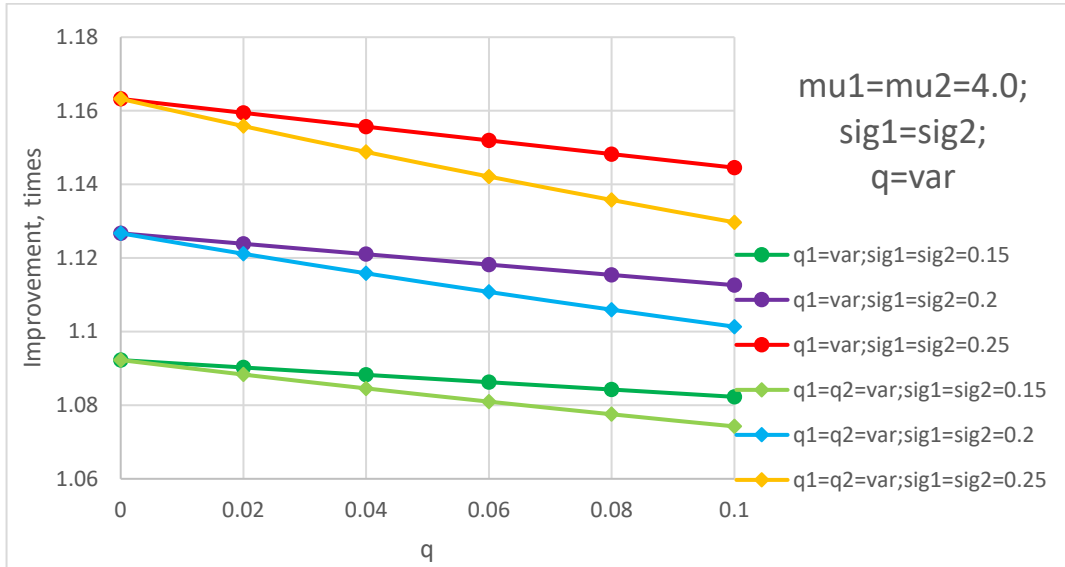
Fig. 4.25 Improvement in average RTT in the redundant solution, depending on packet loss (q1=var, q2=0 ; q1=q2=var), assuming that µ1= µ2=4.0 and for σ1=σ2=0.15, σ1=σ2=0.2, σ1=σ2=0.25.

It can be concluded, that

1. The author suppose that this method is more instructive for small redundant networks than typical calculations that are based on the Markov chain model, recommended by ITU.
2. The proposed method requires known latency (or RTT) CDFs as well as known packet loss rate of all parallel networks. The CDFs can be obtained from experimental data, or experimental data can be approximated according to a known distribution law (for example, a lognormal distribution can be used in the LTE networks).
3. The method assumes that all parallel networks are independent to each other (otherwise the result will be more optimistic than it will be in the real network).
4. The method is applicable to various number of parallel networks (e.g. more than 2).

CONCLUSIONS

The purpose of the thesis is to evaluate the possibility to implement wireless Command and Control link of low-flying UAVs via existing mobile data transfer services. According to the obtained experimental data it can be concluded that, in general, the existing LTE network allows to create an RC and FPV channels, suitable for experienced pilots, considering sufficient quality of a radio signal. Since the coverage of existing cellular mobile networks is optimized for terrestrial users, special attention is payed to evaluation methods and experimental results, associated with the high maneuverability and flight altitude of UAVs. The results presented are intended to supplement the theory and practice of remote control of UAVs using cellular networks. The research results of independent significance are the following:

1. The performance requirements for the wireless "Command and Control Link" of lightweight UAVs has been developed based on review of available scientific papers. An experimental evaluation of the defined KPIs has not been performed.

    a. It was found that the recommended value of the two-way delay in the RC channel for a typical pilot should be ≤ 150 ms, with a limit of 200 ms; for an experienced pilot the recommended value of the two-way delay should be ≤ 310 ms, with a limit of 400 ms.

    b. It was found that the one-way delay in the FPV video channel should be ≤ 150 ms.

2. The type of distribution law of delay values of LTE cells has been defined. The applicability of the Log-Normal distribution law and quick estimation method were experimentally proved. It should be highly noted that since delays in different cells generally differ, the analysis should be carried out for each cell separately.

    a. If was proved that the delays of a real-working LTE cell mostly fit to Log-Normal distribution (compared to Gamma, Normal and Weibull). In order to obtain the average delay and delay jitter with satisfactory accuracy, it is possible to accept that the delays in LTE cells obey the logarithmically normal distribution law.

    b. In addition, a quick estimation method for the parameters of Log-Normal distribution has been provided. The method is based on known minimum and average RTT values, that are available from the ping utility's report.

    c. The recommendations of the required number of RTT measurements to be used in the quick estimation method are also provided.

3. The delay values in the LTE network of the Tele2-LV cellular operator has been experimentally estimated. In contrast to the available scientific papers, delays of LTE cells were estimated separately for each specific cell. This allows to build the CDF of the delays in a cell without using weighting factors (considering the time spent in each specific cell), as well as with a given probability to predict delays in those cells, that were not evaluated during the experimental study.

    a. Assuming that the delays of an LTE cell obey the lognormal distribution law, the delays in each LTE cell can be described by estimates of two parameters $\acute{\theta}_0 = \hat{\mu}$ and $\acute{\theta}_1 = \hat{\sigma}$ of logarithmically normal distribution.

b. It has been experimentally confirmed that the cells of a cellular operator have different delays due to differences in terrestrial backhaul of BSs. Therefore, when evaluating the delays of overall LTE network, the delays of each LTE cell should be evaluated separately.

c. Considering the above mentioned, the delays of the LTE network of a particular cellular operator can be described using a system of two random variables *parameter* $\hat{\mu}$ and *parameter* $\hat{\sigma}$ of logarithmically normal distribution of each LTE cell. To exclude the influence of a weak signal due to lack of the coverage of the cellular network on the delay values, only those data were processed that were obtained at the signal level RSSI $\geq$ -80dBm (for the given UE it has been experimentally proved, that there are no impact onto the delays of small packets if the RSSI $\geq$ -80dBm).

d. Approximating the above system of two random variables $\hat{\mu}$ and $\hat{\sigma}$ according to the normal distribution law and taking into account that the values of variables $\hat{\mu}$ and $\hat{\sigma}$ are independent, it is possible to obtain unbiased estimates of mathematical expectation $\hat{m}_{\hat{\mu}}$ and $\hat{m}_{\hat{\sigma}}$, standard deviation $\hat{\sigma}_{\hat{\mu}}$ and $\hat{\sigma}_{\hat{\sigma}}$ and correlation coefficient $\hat{r}_{\hat{\mu}\hat{\sigma}}$. The numerical values of these parameters for the D2D and D2WAN connections are provided in Chapter 2.6.2.

4. The analysis of the compliance of the delays of LTE network to the requirements of a "Command and Control Link" of low-flying, lightweight UAVs has been performed. In a contrast to the averaged experimental results provided in the available scientific papers, the proposed conclusions are based on the delays analysis of individual LTE cells. The experimental results were obtained from LTE B20 band of the Tele2-LV cellular operator. The RTT of LTE cells was expressed as the 0.999 fractals (with the aim to show that the RTT in 99.9% will not be greater). Note that the proposed results assume "good" signal quality specified in the recommendation [63]).

a. It was found that only 25 % of LTE cells guarantee that at least 99.9% of RTT will be below 150 ms and only 53 % of LTE cells guarantee that at least 99.9% of RTT will be below 200 ms. Therefore, the delays of LTE networks are not suitable for the RC operations for a typical pilot.

b. It was found that 88 % of LTE cells guarantee that at least 99.9% of RTT will be below 310 ms and 97 % of LTE cells guarantee that at least 99.9% of RTT will be below 400 ms Therefore, an experienced pilot can perform RC operations via the LTE network (note that sometimes an experienced pilot will have to provide more mental effort, as RTT will be greater than 310 ms).

c. If was found that in the video channel, the constant size de-jittering buffer of 310 ms will be sufficient in 99.9 % of times (thus providing 0.1% packet loss in LTE cells with worth performance); 230 ms buffer will be sufficient in 99 % of times (thus providing 1% loss in LTE cells with worth performance).

d. Taking into account previously stated, the LTE data transfer service does not satisfy the requirements for the FPV of 150 ms latency if a constant size de-jittering buffer is used.

e. If was found that in the video channel, if the size of de-jittering buffer is adaptive and is equal to the IPDV, only 86 % of LTE cells will satisfy the requirements for the FPV of 150 ms latency. Since modern video codecs can accept packet loss up to 1%, the upped bound for the IPDV can be set to 0.99. In this case 98 % of LTE cells will provide satisfactory latencies for the FPV.

5. Experimental evaluation of the impact of terrestrial user mobility on the delays of mobile data transfer services has been performed. It was found that in 3G (HSPA+ and above) delays becomes increased if UE PIFA antennas have angular rotations as well as that spikes in latency may occur during sharp turns or ground altitude changes. These phenomena have not been previously mentioned in the available scientific papers. However, such behavior in LTE was not observed. Therefore, it can be concluded, that the performance of LTE (LTE-A was not tested) network does not depend on the travelling speed (proved up to 100 km/h), as well acceleration/deceleration and other attitude changes at the reasonable rate (typical car acceleration / deceleration rates).

6. Experimental evaluation of the impact of flying altitude on the performance of mobile data transfer services has been performed. It has been found that:
   a. The interference increases with the increase of altitude, because the UE got direct visibility with many BS. Strong interference leads to the selection of slower modulation and coding scheme or even to blocked service of 3G/LTE networks at higher altitudes. However, this conclusion has no scientific novelty, because a lot of research papers in this field were published in 2018.
   b. The effect of rapid angular position variations of PIFA antennas is aggravated at higher altitude due to stronger interference. In this case, the 3G data transfer service can be partially interrupted even if the wireless signal parameters are not below their acceptable limits.
   c. A lot of handovers are observed due to complex aerial coverage of cells. In this situation the use of soft handovers (like in 3G HSPA+ and above) leads to high amount of delayed packets/reordered packets even if the wireless signal parameters are not below their acceptable limits. This finding has not been previously published in the scientific papers.
   d. The LTE technology utilizes hard handovers only, therefore, there are no lost/reordered packets due to soft handover in the complex aerial coverage. However, massive handovers were observed in LTE too. Therefore, it is advisable to pay more attention to the operation of handover mechanism if the cellular network is planned to be used for aerial users.

7. The approach of detailed evaluation of the aerial coverage has been proposed. It allows to measure signal levels from all surrounding BS of all cellular operators simultaneously. The proposed method is based on the legacy search function and doesn't require expensive equipment. Such method was not previously published in scientific papers.

8. The parallel redundant communication solutions to increase the reliability and performance of a "Command and Control Link" were applied and tested.

a. Two redundant solution implementations (PRP and MPTCP), that previously were not used in cellular mobile data transfer services, were experimentally evaluated. It can be concluded that it is possible to utilize the PRP and MPTCP (with the "redundant" scheduler) solutions in LTE networks.

b. The thesis contains the method of calculations, which helps to foresee the delays of the redundant network solution based on the available delays and packet loss rates of the proposed redundant networks. The proposed method previously was not published and, in a contrast to existing ITU methodology, is less complicated and requires fewer initial data. However, it is not suitable for very complex redundant solutions.

REFERENCES

[1] International Civil Aviation Organization (ICAO), "Remotely Piloted Aircraft System (RPAS) Concept of Operations (CONOPS) for International IFR," p. 22, 2014.

[2] J. Stanczak, D. Koziol, I. Z. Kovacs, J. Wigard, M. Wimmer, and R. Amorim, "Enhanced Unmanned Aerial Vehicle Communication Support in LTE-Advanced," in *2018 IEEE Conference on Standards for Communications and Networking, CSCN 2018*, 2018.

[3] ITU, "ITU-T Y.1541 - Network performance objectives for IP-based services," 2011.

[4] E. W. Frew and T. X. Brown, "Airborne Communication Networks for Small Unmanned Aircraft Systems," *Proc. IEEE*, vol. 96, no. 12, pp. 2008–2027, 2008.

[5] N. Goddemeier, S. Rohde, and C. Wietfeld, "Experimental validation of RSS driven UAV mobility behaviors in IEEE 802.11s networks," in *2012 IEEE Globecom Workshops, GC Wkshps 2012*, 2012, pp. 1550–1555.

[6] E. Yanmaz, R. Kuschnig, and C. Bettstetter, "Achieving air-ground communications in 802.11 networks with three-dimensional aerial mobility," in *Proceedings - IEEE INFOCOM*, 2013, pp. 120–124.

[7] E. Yanmaz, R. Kuschnig, and C. Bettstetter, "Channel measurements over 802.11a-based UAV-to-ground links," in *2011 IEEE GLOBECOM Workshops, GC Wkshps 2011*, 2011, pp. 1280–1284.

[8] C. Cheng and P. Hsiao, "Performance Measurement of 802 . 11a Wireless Links from UAV to Ground Nodes with Various Antenna Orientations," *Int. Conf. Comput. Commun. Networks (ICCCN 2006)*, 2006.

[9] D. Hague, H. T. Kung, and B. Suter, "Field experimentation of cots-based UAV networking," in *Proceedings - IEEE Military Communications Conference MILCOM*, 2007.

[10] N. Goddemeier and C. Wietfeld, "Investigation of Air-to-Air Channel Characteristics and a UAV Specific Extension to the Rice Model," in *IEEE Globecom Workshops*, 2015, pp. 1–5.

[11] S. Hayat, E. Yanmaz, and C. Bettstetter, "Experimental analysis of multipoint-to-point UAV communications with IEEE 802.11n and 802.11ac," in *IEEE International Symposium on Personal, Indoor and Mobile Radio Communications, PIMRC*, 2015.

[12] T. Brown, B. Argrow, C. Dixon, S. Doshi, R.-G. Thekkekunnel, and D. Henkel, "Ad Hoc UAV Ground Network (AUGNet)," 2012.

[13] N. Ahmed, S. S. Kanhere, and S. Jha, "On the importance of link characterization for aerial wireless sensor networks," *IEEE Commun. Mag.*, vol. 54, no. 5, pp. 52–57, May 2016.

[14] J. P. Bodanese, G. M. De Araujo, C. Steup, G. V. Raffo, and L. B. Becker, "Wireless communication infrastructure for a short-range unmanned aerial," in *Proceedings - 2014 IEEE 28th International Conference on Advanced Information Networking and Applications Workshops, IEEE WAINA 2014*, 2014, pp. 492–497.

[15] J. Allred *et al.*, "SensorFlock: An Airborne Wireless Sensor Network of Micro-air Vehicles," *ACM 5th Int'l Conf. Embed. Networked Sens. Syst. (SENSYS '07)*, pp. 117–129, 2007.

[16] F. Dimc and T. Magister, "Mini UAV communication link systems," *Promet Glob. Zb. Ref. Conf. Proc.*, p. 9, 2006.

[17] D. Stojcsics and L. Somlyai, "Improvement methods of short range and low bandwidth communication for small range UAVs," in *SIISY 2010 - 8th IEEE International Symposium on Intelligent Systems and Informatics*, 2010.

[18] J. Chen *et al.*, "Long-range and broadband aerial communication using directional

antennas (ACDA): Design and implementation," *IEEE Trans. Veh. Technol.*, 2017.

[19]   J. A. Godoy, F. Cabrera, V. Arana, D. Sanchez, I. Alonso, and N. Molina, "A new Approach of V2X Communications for Long Range Applications in UAVs," in *2018 2nd URSI Atlantic Radio Science Meeting (AT-RASC)*, 2018, pp. 1–4.

[20]   F. Adelantado, X. Vilajosana, P. Tuset-Peiro, B. Martinez, J. Melia-Segui, and T. Watteyne, "Understanding the Limits of LoRaWAN," *IEEE Commun. Mag.*, 2017.

[21]   A. Lewandowski and J. Modelski, "The use of troposcatter communications to increase the range of unmanned aerial vehicle - UAV," in *2018 Baltic URSI Symposium (URSI)*, 2018, pp. 171–173.

[22]   I. H. Lu, J. Y. Hsueh, Y. Y. Lin, and H. C. Hsu, "Development of an instant relay communication system via quadcopter (drone)," in *Proceedings of the 2017 IEEE International Conference on Information, Communication and Engineering: Information and Innovation for Modern Technology, ICICE 2017*, 2018.

[23]   W. Shi *et al.*, "Multiple drone-cell deployment analyses and optimization in drone assisted radio access networks," *IEEE Access*, 2018.

[24]   N. Goddemeier, K. Daniel, and C. Wietfeld, "Coverage evaluation of wireless networks for unmanned aerial systems," in *2010 IEEE Globecom Workshops, GC'10*, 2010, pp. 1760–1765.

[25]   B. Van Der Bergh, A. Chiumento, and S. Pollin, "LTE in the sky: Trading off propagation benefits with interference costs for aerial nodes," *IEEE Commun. Mag.*, 2016.

[26]   L. Afonso, N. Souto, P. Sebastião, M. Ribeiro, T. Tavares, and R. Marinheiro, "Cellular for the skies: Exploiting mobile network infrastructure for low altitude air-to-ground communications," *IEEE Aerosp. Electron. Syst. Mag.*, vol. 31, no. 8, pp. 4–11, 2016.

[27]   J. A. Romo, G. Aranguren, J. Bilbao, I. Odriozola, J. Gómez, and L. Serrano, "GSM / GPRS Signal Strength Measurements in aircraft flights under 3,000 meters of altitude," *WSEAS Trans. Signal Process.*, vol. 5, no. 6, pp. 219–228, 2009.

[28]   N. Santos, A. Raimundo, D. Peres, P. Sebastião, and N. Souto, "Development of a software platform to control squads of unmanned vehicles in real-time," in *2017 International Conference on Unmanned Aircraft Systems, ICUAS 2017*, 2017, pp. 1–5.

[29]   H. Choi, M. Geeves, B. Alsalam, and F. Gonzalez, "Open source computer-vision based guidance system for UAVs on-board decision making," in *IEEE Aerospace Conference Proceedings*, 2016.

[30]   Minla-RC, "Minla HDW." [Online]. Available: http://minlarc.com/. [Accessed: 08-Jun-2018].

[31]   Virt2real-ltd, "Virt2Real." [Online]. Available: http://virt2real.com/. [Accessed: 08-Jun-2018].

[32]   Emlid, "Navio2." [Online]. Available: https://emlid.com/navio/. [Accessed: 08-Jun-2018].

[33]   Ardupilot, "APSync." [Online]. Available: http://firmware.ap.ardupilot.org/Companion/apsync/. [Accessed: 08-Jun-2018].

[34]   Tele2.lv, "Tele2: 4G coverage in Latvia," 2016. [Online]. Available: https://www.tele2.lv/ru/4ginternets/. [Accessed: 28-Sep-2016].

[35]   Bite.lv, "BITE: coverage in Latvia," 2016. [Online]. Available: https://www.bite.lv/parklajums/atrs-internets-visa-latvija/ar-4g-internetu-viss-dzive-ir-iespejams-daudz-atrak. [Accessed: 28-Sep-2016].

[36]   Lmt.lv, "LMT: 4G coverage in Latvia," 2016. [Online]. Available: https://www.lmt.lv/ru/vozmozhnosti-interneta-4g. [Accessed: 28-Sep-2016].

[37]   G. Almes, S. Kalidindi, and M. Zekauskas, "RFC 7679: A One-way Delay Metric for

IPPM," *Internet Eng. Task Force*, Sep. 1999.

[38] V. Paxson, J. Mahdavi, M. Mathis, and G. Almes, "RFC 2330: Framework for IP Performance Metrics."

[39] M. J. Zekauskas, S. Kalidindi, and G. Almes, "RFC 2681: A Round-trip Delay Metric for IPPM," *Internet Eng. Task Force*, 1999.

[40] V. Paxson, J. Mahdavi, M. Mathis, and G. Almes, "RFC 2330: Framework for IP Performance Metrics."

[41] Aristóteles *et al.*, "RFC 3393 - IP packet Delay variation metric for IP Performance Metrics (IPPM)," *Internet Eng. Task Force*, vol. 52, 2002.

[42] V. Firoiu, W. Courtney, B. Davie, and A. Charny, "RFC 3246 - An Expedited Forwarding PHB (Per-Hop Behavior)," *Internet Eng. Task Force*, 2002.

[43] IETF, "Request for Comments RFC3550 - RTP: A Transport Protocol for Real-Time Applications," 2003.

[44] A. T. H.Holma, *HSDPA/HSUPA for UMTS: High Speed Radio Access for Mobile Communications*. Wiley, 2006.

[45] M. Jurvansuu, J. Prokkola, M. Hanski, and P. Perala, "HSDPA performance in live networks," in *IEEE International Conference on Communications*, 2007, pp. 467–471.

[46] M. Kottkamp, "HSPA + Technology Introduction," *Rohde Schwarz White Pap.*, 2012.

[47] R. Stuhlfauth, *High Speed Packet Access*, First Edit. Munchen: Rohde&Schwarz GmbH&Co. KG2012, 2012.

[48] H. Holma, A. Toskala, K. Ranta-aho, and J. Pirskanen, "High-speed packet access evolution in 3GPP release 7," *IEEE Commun. Mag.*, vol. 45, no. 12, pp. 29–35, 2007.

[49] D. Astély, E. Dahlman, A. Furuskär, Y. Jading, M. Lindström, and S. Parkvall, "LTE: The evolution of mobile broadband," *IEEE Communications Magazine*, vol. 47, no. 4. pp. 44–51, 2009.

[50] A. Roessler, M. Kottkamp, and J. Schlienz, "LTE- Advanced (3GPP Rel.11) Technology Introduction," *Rohde Schwarz White Pap.*, pp. 1–38, 2013.

[51] E. Metsala and J. Salmelin, *Mobile Backhaul*. Wiley, 2012.

[52] H. Holma and J. Reunanen, "3GPP release 5 HSDPA measurements," *IEEE Int. Symp. Pers. Indoor Mob. Radio Commun. PIMRC*, pp. 2–6, 2006.

[53] HUAWEI, "HUAWEI Dongles E3372h." [Online]. Available: http://consumer.huawei.com/en/mobile-broadband/dongles/tech-specs/e3372.htm. [Accessed: 28-Sep-2016].

[54] Bite-LV, "BITE data plans." [Online]. Available: http://www.bite.lv/tarifu-plani/bite-1. [Accessed: 02-Aug-2016].

[55] Tele2-LV, "Tele2 data plans." [Online]. Available: https://www.tele2.lv/datu-plani/. [Accessed: 02-Aug-2016].

[56] LMT, "LMT data plans." [Online]. Available: http://www.lmt.lv/lv/prieksapmaksas-mobilais-internets. [Accessed: 02-Aug-2016].

[57] Y. Paramonov, M. Kleinhofs, and A. Kuznetsov, *Reliability of fatigue prone airframes and composite materials*. Riga: RTU Publishing House, 2011.

[58] G. Almes, S. Kalidindi, and M. Zekauskas, "RFC 7679: A One-way Delay Metric for IPPM," *Internet Eng. Task Force*, Sep. 1999.

[59] L. Walter and L. Emlyn, *Handbook of Applicable Mathematics - Statistics*, A & B edit. Wiley, 1984.

[60] Van Der Waerden, *Mathematische statistik*. Berlin-Gottingen-Heidelberg: Springer-Verlag, 1957.

[61] F. P. Tso, J. Teng, W. Jia, and D. Xuan, "Mobility: A double-edged sword for HSPA networks: A large-scale test on hong kong mobile HSPA networks," *IEEE Trans. Parallel Distrib. Syst.*, vol. 23, no. 10, pp. 1895–1907, 2012.

[62] S. Sesia, I. Toufik, and M. Baker, "The LTE Network Architecture," *Strateg. White Pap.*, no. Wiley, p. 26, 2009.

[63] Cisco and/or its affiliates, "LTE Antenna Guide. Cisco Integrated Services Router (ISR G2) and Connected Grid Router," pp. 1–23, 2016.

[64] 3GPP, "TS 123 207 - End-to-end Quality of Service (QoS) concept and architecture," vol. 0, pp. 0–40, 2018.

[65] ITU, "ITU-T G.114 General Recomendations on the transmission quality for an entire international telephone connection," 2003.

[66] ITU, "ITU-T G.1010 - End-user multimedia QoS categories," 2001.

[67] M. Dusi, S. Napolitano, S. Niccolini, and S. Longo, "A closer look at thin-client connections: Statistical application identification for QoE detection," *IEEE Commun. Mag.*, 2012.

[68] E. Vinogradov, H. Sallouha, S. De Bast, M. M. Azari, and S. Pollin, "Tutorial on UAV: A Blue Sky View on Wireless Communication," pp. 1–43, 2019.

[69] M. Claypool and K. Claypool, "Latency and player actions in online games," *Commun. ACM*, 2006.

[70] M. Ries, P. Svoboda, and M. Rupp, "Empirical study of subjective quality for massive multiplayer games," in *Proceedings of IWSSIP 2008 - 15th International Conference on Systems, Signals and Image Processing*, 2008.

[71] F. Wang, S. Qi, and L. Jing, "An Analysis of Time-delay for Remote Piloted Vehicle," 2017, pp. 1–6.

[72] V. Casas and A. Mitschele-thiel, "On the impact of communication delays on UAVs flocking behavior," in *2018 IEEE Wireless Communications and Networking Conference Workshops (WCNCW)*, 2018, pp. 67–72.

[73] National Instruments, "3GPP Release 15 Overview," *IEEE Commun. Soc. White Pap.*, 2018.

[74] S. D. Muruganathan, X. Lin, H.-L. Maattanen, Z. Zou, W. A. Hapsari, and S. Yasukawa, "An Overview of 3GPP Release-15 Study on Enhanced LTE Support for Connected Drones," pp. 1–7, 2018.

[75] C. Huang, C. Yeh, A. Kandhalu, A. Rowe, and R. R. Rajkumar, "Real-Time Video Surveillance over IEEE 802 . 11 Mesh Networks," *15th IEEE Real-Time Embed. Technol. Appl. Symp.*, pp. 205–214, 2009.

[76] A. Detti, P. Loreti, N. Blefari-Melazzi, and F. Fedi, "Streaming H.264 scalable video over data distribution service in a wireless environment," in *2010 IEEE International Symposium on "A World of Wireless, Mobile and Multimedia Networks", WoWMoM 2010 - Digital Proceedings*, 2010.

[77] M. Laner, P. Svoboda, P. Romirer-Maierhofer, N. Nikaein, F. Ricciato, and M. Rupp, "A Comparison Between One-way Delays in Operating HSPA and LTE Networks," *Proc. 8th Int. Work. Wirel. Netw. Meas. (WiNMee 2012)*, no. May, pp. 14–18, 2012.

[78] J. Jans, B. Roberts, and P. Jelinskis, "Mobile Application Based Traffic Advisory System for General Aviation – Is It Possible ?," in *2015 Advances in Wireless and Optical Communications (RTUWO)*, 2015, pp. 155–158.

[79] X. Lin *et al.*, "The Sky is Not the Limit: LTE for Unmanned Aerial Vehicles," *IEEE Commun. Mag.*, vol. 56, no. 4, pp. 204–210, 2018.

[80] DOCOMO and Ericsson, "RP-170779: Study on Enhanced LTE support for Aerial Vehicles," 2017. [Online]. Available: http://www.3gpp.org/ftp/tsg_ran/tsg_ran/TSGR_75/Docs/.

[81] Schneider Adam, "GPS Visualizer," 2016. [Online]. Available: http://www.gpsvisualizer.com/. [Accessed: 23-Oct-2017].

[82] I. Heydarov and D. Brodnevs, "Experimental Evaluation of the Shadowing of a Planar

Antenna Caused by a Quadcopter Frame," *Electr. Control Commun. Eng.*, vol. 16, no. 1, pp. 37–43, 2020.

[83]   ITU, "E.212 : The international identification plan for public networks and subscriptions," *Telecommun. Stardartization Sect. ITU*, 2016.

[84]   IEC, "International Standart 62439-3:2016 Industrial communication networks – High availability automation networks," 2016.

[85]   IEEE Computer Society, "IEEE Standard for Ethernet 802.3," in *IEEE Standard for Ethernet*, vol. 2012, no. December, 2012, pp. 1–400.

[86]   M. Rentschler and H. Heine, "The Parallel Redundancy Protocol for industrial IP networks," in *Proceedings of the IEEE International Conference on Industrial Technology*, 2013, pp. 1404–1409.

[87]   ZHAW Institute of Embedded Systems InES, "PRP-1 Software Stack." [Online]. Available: https://www.zhaw.ch/en/engineering/institutes-centres/ines/products-and-services/high-availability/prp-1-software-stack/#%2Fc46689. [Accessed: 15-Jan-2017].

[88]   D. Brodnevs and A. Kutins, "An Experimental Study of Ground-Based Equipment Real Time Data Transfer Possibility by Using Cellular Networks," *Electr. Control Commun. Eng.*, vol. 12, no. 1, pp. 11–19, Jul. 2017.

[89]   C. Paasch and S. Barre, "Multipath TCP in the Linux Kernel," 2018. [Online]. Available: multipath-tcp.org. [Accessed: 02-Apr-2018].

[90]   C. Paasch and O. Bonaventure, "Multipath TCP," *Commun. ACM*, vol. 57, no. 4, pp. 51–57, 2014.

[91]   C. Paasch, S. Ferlin, O. Alay, and O. Bonaventure, "Experimental evaluation of multipath TCP schedulers," in *Proc.2014 ACM SIGCOMM workshop on Capacity sharing workshop - CSWS '14*, 2014, pp. 27–32.

[92]   A. Ford, C. Raiciu, M. Handley, and O. Bonaventure, "RFC 6824: TCP Extensions for Multipath Operation with Multiple Addresses," *Internet Eng. Task Force*, pp. 1–64, 2013.

[93]   M. Graham, "Applying High Availability Design and Parallel Redundancy Protocol (PRP) in Safety Critical Wide Area Networks," *J. Telecommun. Syst. Manag.*, vol. 04, no. 01, pp. 1–7, 2015.

[94]   ITU, "ITU-T G.911 Parameters and calculation methodologies for reliability and availability of fibre optic systems," *ITU Telecommun. Stand. Sect.*, 1997.

[95]   E. Molina, E. Jacob, J. Matias, N. Moreira, and A. Astarloa, "Availability improvement of layer 2 seamless networks using openflow," *Sci. World J.*, vol. 2015, no. v, 2015.

[96]   M. Rentschler *et al.*, "Simulation of parallel redundant WLAN with OPNET," *IEEE Int. Conf. Emerg. Technol. Fact. Autom. ETFA*, pp. 1–8, 2013.

[97]   M. Hendawy *et al.*, "Application of parallel redundancy in a Wi-Fi-based WNCS using OPNET," *Can. Conf. Electr. Comput. Eng.*, vol. 1, pp. 1–6, 2014.

[98]   M. Rentschler *et al.*, "Simulative comparison of parallel redundant wireless systems with OMNet++," in *IEEE International Symposium on Industrial Electronics*, 2014.

[99]   M. Rentschler and P. Laukemann, "Towards a reliable parallel redundant WLAN black channel," *IEEE Int. Work. Fact. Commun. Syst. - Proceedings, WFCS*, pp. 255–263, 2012.

[100]   G. Cena, S. Scanzio, and A. Valenzano, "Experimental evaluation of seamless redundancy applied to industrial Wi-Fi networks," *IEEE Trans. Ind. Informatics*, vol. 13, no. 2, pp. 856–865, 2017.

[101]   M. Rentschler and P. Laukemann, "Performance analysis of parallel redundant WLAN," *IEEE Int. Conf. Emerg. Technol. Fact. Autom. ETFA*, no. September 2012, 2012.

[102]   D. Brodnevs and A. Bezdel, "High - Reliability low - Latency cellular network

communication solution for static or moving ground equipment control," in *Proc. IEEE 58th Annual International Scientific Conference on Power and Electrical Engineering of Riga Technical University (RTUCON)*, 2017, pp. 1–6.

[103] D. Brodnevs and A. Kutins, "Reliable data communication link implementation via cellular LTE services for static or moving ground equipment control," in *Proc. IEEE 59th Annual International Scientific Conference on Power and Electrical Engineering of Riga Technical University (RTUCON)*, 2018, pp. 1–6.